UNIVERSITY OF Southampton

University of Southampton Research Repository
ePrints Soton

http://eprints.soton.ac.uk

University of Southampton

FACULTY OF SCIENCE

School of Medicine

Acquired Abnormalities of Chromosome 21
in
Acute Lymphoblastic Leukaemia

By

Hazel M Robinson

Thesis for the degree of Doctor of Philosophy

June 2008

UNIVERSITY OF SOUTHAMPTON

ABSTRACT

FACULTY OF SCIENCE

SCHOOL OF MEDICINE

Doctor of Philosophy

ACQUIRED ABNOMALITIES OF CHROMOSOME 21 IN ACUTE

LYMPHOBLASTIC LEUKAEMIA

by Hazel M Robinson

The intrachromosomal amplification of chromosome 21 (iAMP21) was identified as a novel and prognositically important acquired chromosomal abnormality in childhood acute lymphoblastic leukaemia (ALL). It is defined by multiple copies of the *RUNX1* gene, as seen by fluorescence *in situ* hybridisation (FISH), localised to a single abnormal duplicated chromosome 21 [dup(21)]. The morphological form of this chromosome is highly variable between patients and currently the only reliable method of detection is FISH with probes to *RUNX1*. Studies of 48 iAMP21 patients using detailed FISH techniques and array-based comparative genomic hybridisation highlighted an extensive region of chromosome 21 involvement. A minimum common region of amplification, between 33.19 and 39.80Mb, including *RUNX1* was identified, together with a minimum common region of deletion, between 46.54 and 46.92Mb, in 100% and 77% of patients, respectively. This study established that there were unique patterns of imbalance, with evidence of deletions, inversions and amplification, displayed on the dup(21), between individual patients. This provided evidence of an abnormality that may have arisen from a breakage-fusion-bridge mechanism, possibly initiated by loss of a telomere. Results indicated that iAMP21 represents a distinct genetic subgroup of childhood ALL and is not secondary to a cryptic abnormality of chromosome 21. Two possible variant cases were identified both involving chromosome 15. The abnormality can be distinguished from other numerical abnormalities of chromosome 21 by exploiting the unique pattern of gain, amplification and deletion seen in these patients. This allowed for the development of diagnostic tests based on copy number using either FISH or multiplex ligation dependent probe amplification (MLPA), both of which successfully identified iAMP21 patients.

DECLARATION OF AUTHORSHIP

I, Hazel Robinson

declare that the thesis entitled

Acquired abnormalities of chromosome 21 in acute lymphoblastic leukaemia.

and the work presented in it are my own. I confirm that:

- this work was done wholly or mainly while in candidature for a research degree at this University;
- where any part of this thesis has previously been submitted for a degree or any other qualification at this University or any other institution, this has been clearly stated;
- where I have consulted the published work of others, this is always clearly attributed;
- where I have quoted from the work of others, the source is always given. With the exception of such quotations, this thesis is entirely my own work;
- I have acknowledged all main sources of help;
- where the thesis is based on work done by myself jointly with others, I have made clear exactly what was done by others and what I have contributed myself;
- parts of this work has been published as;

Strefford,J.C., van Delft,F.W., Robinson,H.M., Worley,H., Yiannikouris,O., Selzer,R., Richmond,T., Hann,I., Bellotti,T., Raghavan,M., Young,B.D., Saha,V., & Harrison,C.J. (2006) Complex genomic alterations and gene expression in acute lymphoblastic leukemia with intrachromosomal amplification of chromosome 21. *Proc.Natl.Acad.Sci.U.S.A*, **103**, 8167-8172.

Robinson,H.M., Harrison,C.J., Moorman,A.V., Chudoba,I., & Strefford,J.C. (2007) Intrachromosomal amplification of chromosome 21 (iAMP21) may arise from a breakage-fusion-bridge cycle. *Genes Chromosomes.Cancer*, **46**, 318-326.

Signed………………………

Date…………………………

TABLE OF CONTENTS

List of Figures

List of Tables

Acknowledgements

Abbreviations

aCGH	Array comparative genomic hybridisation
A	Adenine
ALL	Acute lymphoblastic leukaemia
AML	Acute myeloid leukaemia
ATP	Adenosine triphosphate
BAC	Bacterial artificial chromosome
B-cell	Bursa dependant lymphocyte
BCP-ALL	Precursor B-cell acute lymphoblastic leukaemia
BCR	Breakpoint cluster region
BFB	Breakage-Fusion-Bridge
BFM	Berlin Franfurt Münster
BIR	Breakage induced replications
CCD	Charge-coupled device
CD	Cluster of differentiation
CML	Chronic myeloid leukaemia
CNNLOH	Copy number neutral LOH
CRA	Common region of amplification
CRD	Common region of deletion
CTSU	Clinical Trial Service Unit
DAPI	4',6-diamidino-2-phenylindole
dH2O	Distilled water
DSB	Double stranded break
dup(21)(q)	Duplicated chromosome 21q
FAB	French-American-British
FE	Feature extraction
FISH	Fluorescence *in situ* hybridization
FITC	Fluorescein

G-banded	Giemsa banded
gDNA	Genomic DNA
HeH	Hyperdiploidy
Ho	Hypodiploidy
HSC	Haematopoietic stem cells
HSR	Homogeneously staining regions
iAMP21	Intra chromosomal amplification of chromosome 21
INK4	Inhibitor of the cyclin-dependent kinase 4
ISCN	International System for Human Cytogenetic Nomenclature
LA	Large acrocentric
LB	Luria-bertani
LM	Large metacentric
LOH	Loss of heterozygosity
LPO	Left side probe oligo
LRCG	Leukaemia Research Cytogenetics Group
LRF	Leukaemia Research Fund
LSI	Locus specific probes
LRUKD	LRF UKCCG karyotype database in acute leukaemia
M-bcr	Major breakpoint cluster region
m-bcr	Minor breakpoint cluster region
MDS	Myelodysplastic syndrome
MIC	Molecular Immunophenotypic and Cytogenetic
MIC-M	Morphology, immunophenotype, cytogenetic and molecular analysis
MLPA	Multiplex ligation probe amplification
MRC	Medical research council
MRD	Minimal residual disease
NCRI	National Cancer Research Institute
NK	Not Known

NRT	Nonreciprocal translocation
PAC	Plasmid artificial chromosome
PBS	Phosphate buffered Saline
PCR	Polymerase chain reaction
Ph	Philadelphia chromosome
PNA	Peptide Nucleic Acid
Q-PCR	Quantative PCR
R	Ring
Rb	Retinoblastoma
RPO	Right side probe oligo
RT	Real Time
SA	Small acrocentric
SHC	Src homologue
SM	Sub-metacentric
SNP	Single-Nucleotide-polymorphism
SSC	Saline Sodium Citrate
T	Thymine
T-ALL	Thymus cell acute lymphoblastic leukaemia
TCR	T-cell receptor
UCSC	University of California Santa Cruz
UK	United Kingdom
UKCCG	United Kingdom Cancer Cytogenetic group
UPD	Uniparental disomy
WBC	White blood cell count
WCP	Whole chromosome paint
WHO	World Health Organisation
WRGI	Wessex regional genetic institute

Gene abbreviations

BCL11A	B-cell CLL/lymphoma 11A (zinc finger protein)
E2A	TCF3 (E2A) fusion partner (in childhood Leukaemia)
PAX5	Paired box 5
ABL1	v-abl Abelson murine leukaemia viral oncogene
APP	Amyloid beta (A4) precursor protein
ATM	Ataxia telangiectasia mutated
BCR	Breakpoint cluster region homolog
C/EBP-a	CCAAT/enhancer binding protein (C/EBP), alpha
CYP27C1	Cytochrome P450, family 27, subfamily C, polypeptide 1
CBF-β	Core-binding factor, beta subunit
CDKN2A	Cyclin-dependent kinase inhibitor 2A
CDKN2B	Cyclin-dependent kinase inhibitor 2B
EBF	Early B-cell factor 1
ERG	v-ets erythroblastosis virus E26 oncogene homolog
ETS2	v-ets erythroblastosis virus E26 oncogene homolog 2
ETV6	ets variant gene 6 (TEL oncogene)
FLT3	fms-related tyrosine kinase 3
FOXP1	Forkhead box P1
GRB-2	Growth factor receptor-bound protein 2
HER2/ERBB2	v-erb-b2 erythroblastic leukemia viral oncogene homolog 2
IGH	Immunoglobulin heavy locus
IGK	Immunoglobulin kappa locus
IGL	Immunoglobulin lambda locus
IL-7R	Interleukin 7 receptor
INK4	Inhibitor of the cyclin-dependent kinase 4
MET	Met proto-oncogene (hepatocyte growth factor receptor)
MLL	Myeloid/lymphoid or mixed-lineage leukemia
MYB	v-myb myeloblastosis viral oncogene homolog (avian)

MYC	v-myc myelocytomatosis viral oncogene
PIP	Prolactin-induced protein
PRMT2	Protein arginine methyltransferase 2
PRSS7	Protease, serine, 7 (enterokinase)
PU.1 SPIC	Spi-C transcription factor
RAS CDK1	Cyclin-dependent kinase inhibitor
RUNX1/AML1	Runt-related transcription factor 1 / Acute myeloid leukemia 1 oncogene
SHC	Src homology 2 domain containing
SLC19A1	Solute carrier family 19 (folate transporter), member 1
STCH	Stress 70 protein chaperone, microsome-associated, 60kDa

Chapter One – Introduction

1 Introduction

1.1   Cancer is an acquired genetic disorder

Recurrent chromosomal abnormalities are one of the hallmarks of malignancy. The detailed analysis of these abnormalities and their molecular characterisation has provided significant information regarding the biology of neoplastic disorders and frequently their clinical outcome. As a consequence, it is generally accepted that at the cellular level cancer is an acquired genetic disorder (Mitelman *et al*, 2007). The biology of cancer cells, in relation to the functions of cell division, differentiation, proliferation and apoptosis is similar to that of their normal counterparts. However, interference in the regulation of these functions leads to an altered phenotype resulting in malignancy. Thus it follows, that it is the disruption of the genes that control these regulatory pathways, which is crucial to the development of cancer.

There are two main types of gene involved in the development of a malignancy - active proto-oncogenes (oncogenes) and inactive tumour suppressor genes (Pierotti *et al*, 2003). The activation of proto-oncogenes usually occurs via one of three main mechanisms: mutation, amplification and/or chromosomal rearrangement such as translocation. The resulting oncogenes then play a direct role in the development of cancer due to their functional characteristics as either growth factors, growth factor receptors, signal transducers, transcription factors or regulators of apoptosis (Pierotti *et al*, 2003).

The normal role of tumour suppressor genes is to inhibit cell growth and differentiation when the conditions for division and proliferation are changed. Thus, their inactivation, promotes cell proliferation and differentiation of "damaged" cells. The inactivation of tumour suppressor genes usually occurs as a result of mutation and/or deletion (Pierotti *et al*, 2003). A further class of cancer

genes also exists, known as DNA repair genes, whose function is to recognise aberrations in the DNA repair pathways (Wood *et al*, 2005). Unlike tumour suppressor and oncogenes the activation of these genes results in an increased rate of mutations in proto-oncogenes and tumour suppressors.

The majority of malignancies occur as a result of the acquisition of several mutations, which arise in a sequential manner rather than a single event. Studies of haematological malignancies have shown that tumours arise from a single ancestor cell and are thus, clonal in nature. Following an initial genetic event, the cell may attain a slight growth advantage. Progeny of this cell then acquire further mutations, which provide them with a selective advantage. By the continuation of this process the abnormal clone expands, in a multi-step fashion, until it eventually results in overt clinical disease (Figure 1.1). As the acquired mutations are random, it follows that some will be deleterious to the cell resulting in loss of that particular subclone. Within a tumour cell population many different subclones, all of which are derived from a single ancestral cell will exist. Evan and Vousden (2001) proposed that a minimum number of critical events are required to drive uncontrolled expansion and invasion. They hypothesised that these minimal requirements involve deregulation in cell proliferation and suppression of apoptosis.
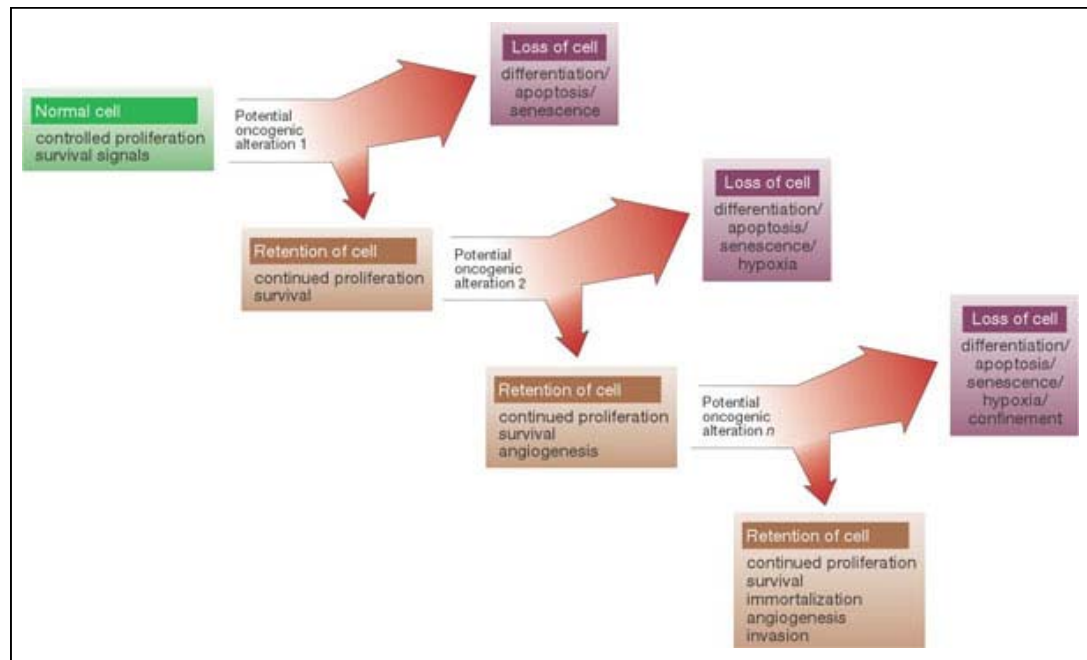
Figure 1.1 Schematic diagram showing the development of cancer driven by the accumulation of genetic aberrations. Adapted from Evans (2001).

1.2   Haematopoiesis

Normal adult peripheral blood contains a substantial number of highly specialized cells, all of which are generated via haematopoiesis, in the bone marrow from a common pluripotent progenitor cell, known as the haematopoietic stem cell (HSC). These cells have the most important function within the haematopoietic system, as they are responsible for the life long production of all circulating blood cells. It has been estimated that for every one stem cell there are 20 million nucleated cells in adult bone marrow (Hoffbrand & Pettit, 1993).

During haematopoiesis, HSC undergo cell division to produce two daughter cells, one of which retains its stem cell properties, and so maintains the stem cell pool, whilst the other undergoes a step wise process of division and differentiation to produce mature haematopoietic cells (Hoffbrand *et al*, 2005). Those cells committed to differentiation go on to divide and mature into cells

from one of two main lineages: myeloid and lymphoid (Figure 1.2). Lineage specification is achieved by precise activation of individual genes controlling differentiation. External factors bring about alterations to specific growth factors. These in turn initiate changes to transcription factors resulting in the activation of the genes controlling differentiation and proliferation.
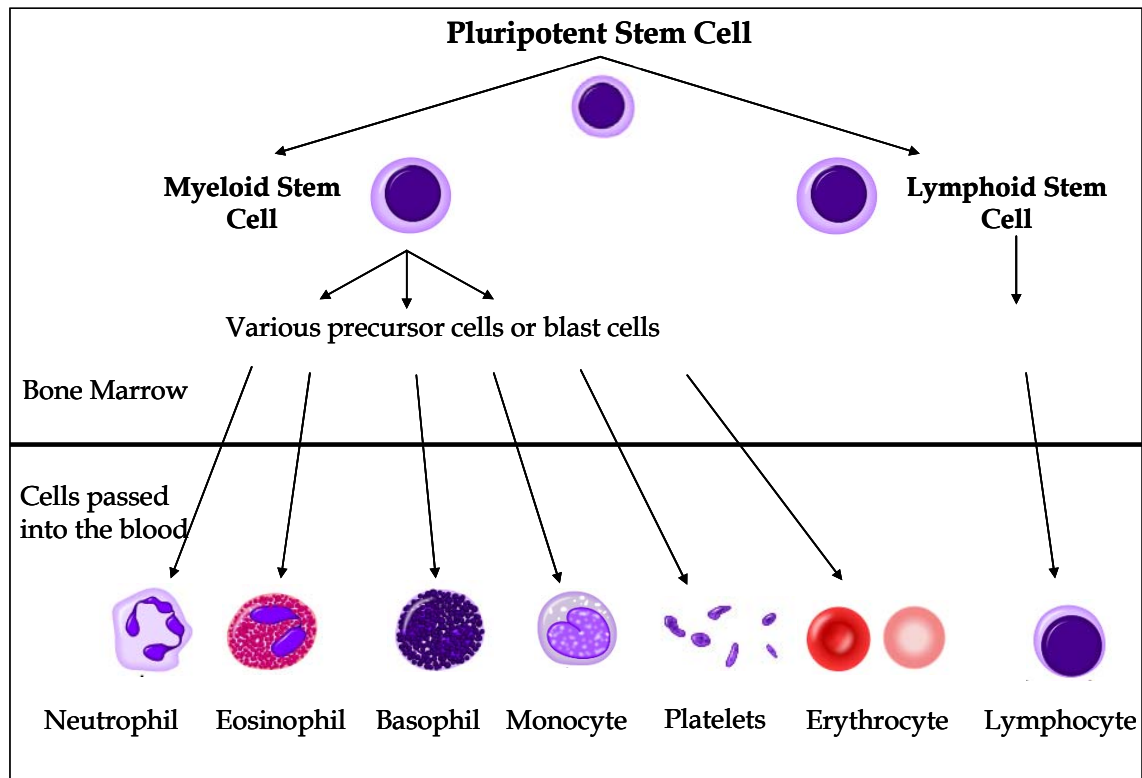
Figure 1.2 Diagrammatic representation of haematopoiesis. Pluripotent stem cell in the bone marrow gives rise via cell division and differentiation to circulating peripheral blood cells. Immature cells remain in the bone marrow environment whilst mature cells are passed into the blood.

The process of maturation consists of a number of stages and, as the stem cells differentiate into progenitor cells, they lose the ability to self renew, until finally, as mature haematopoietic cells, they have a limited life span. This process, which involves the rapid production of mature circulating blood cells, is controlled by the constant need to replace those cells undergoing apoptosis.

Disruption of those genes involved in the regulation of haematopoiesis results in the development of leukaemia (Byrne & Russell, 2005).

1.3   Leukaemia

Leukaemia is defined as a neoplastic disorder, characterised by the uncontrolled proliferation of malignant haematopoietic cells, usually leucocytes. The disease can originate from any cell, blocked at a particular stage of development, including primitive cells with a multilineage potential, as well as more mature cells. The resulting abnormal cells exhibit a number of features common to all cancers:

- Clonal generation from a single precursor cell
- Unchecked growth, frequently of immature cells
- Evasion of programmed cell death

There are two main clinical forms of leukaemia: acute and chronic. Acute leukaemia is characterized by the rapid growth and accumulation of malignant cells, typically undifferentiated immature cells, which if left untreated will lead to death within weeks or months (Bain, 1999). Chronic leukaemia, which may be asymptomatic for a number of years, is distinguished by the slow accumulation of cells frequently involving more mature cell types and, if left untreated, may lead to death within months or years (Bain, 1999). It is possible to further classify these two groups into myeloid and lymphoid lineages depending on the progenitor cell of their origin.
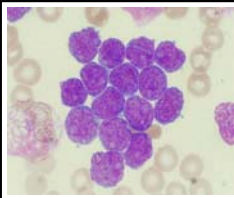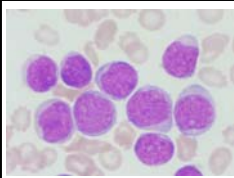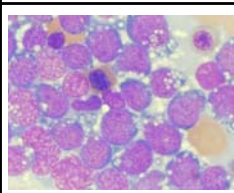
FAB category	Blast appearance	Diagnostic criteria
L1		Small blasts with scanty cytoplasm, smooth-variable indented nuclear outline, condensed chromatin, and discrete nucleoli.
L2		Large heterogeneous blasts with moderately abundant cytoplasm, irregularly shaped nuclei, variable chromatin, and prominent nucleoli.
L3		Large, generally homogeneous blasts with finely stippled chromatin, round nuclei, prominent nucleoli and moderate basophilic cytoplasm with vacuolization

Table 1.1 French-American-British (FAB) classification of acute lymphoblastic leukaemia.

In adults, acute myeloid leukaemia (AML) is the most frequently occurring acute subtype with an incidence of approximately 10 in 100,000. Almost 1,950 new cases are diagnosed annually in the United Kingdom (Leukaemia Research, 2008a). In children, acute lymphoblastic leukaemia (ALL) is the most common acute subtype, accounting for 85% of all cases (Greaves, 2002;Spector *et al*, 2006). It has an incidence of 4 in 100,000 and approximately 400-450 new cases are diagnosed each year in the United Kingdom (Leukaemia Research, 2008b).

1.4 Acute lymphoblastic leukaemia

ALL is a disease typically characterised, by the accumulation of immature abnormal lymphoid progenitor cells (lymphoblasts) in the bone marrow, which have abnormal proliferation and differentiation. It is a heterogeneous disease

which can be divided into a number of distinct biological and prognostic subtypes. The classification and accurate diagnosis of ALL involves a stepwise process, which has improved over the past 20 years with the development of new techniques. Originally it was classified solely using the French-American-British (FAB) classification system (Bennett *et al*, 1976;Bennett *et al*, 1981). This scheme based on the simple morphological appearance of the blast cells, subdivides ALL into three main subgroups L1, L2 and L3 (Table 1.1). Due to the limited morphological variation between blast cells in ALL, the use of this classification system alone was restricted, as it included no correlation with specific immunophenotype or karyotype features which provided valuable prognostic information. Despite the limited variability in the appearance of leukaemic cells from one patient to another, there is significant variability in the underlying molecular pathology with a number of distinct subtypes of ALL now described (Downing & Mullighan, 2006).

ALL can develop from any lymphoid cell, blocked at a particular stage of development, including both primitive cells with a multilineage potential, as well as more mature cells. As reviewed by Downing and Mullighan (2006;2007), the differentiation of lymphoid progenitors into mature B cells is a tightly regulated process coordinated by a network of transcription factors and cytokines. The process is closely associated with the sequential rearrangement of immunoglobulin receptor genes. The initial rearrangement of the immunoglobulin heavy chain enables expression of the pre-B cell receptor required for survival of the B-cell precursors, whilst subsequent immunoglobulin light chain rearrangement permits expression of the mature B-cell receptors. At least seven transcription factors (*PU.1, Ikaros, E2A, BCL11A, EBF, PAX5* and *FOXP1*) and two cytokines (*FLT3* and *IL-7R*) are known to be involved (Figure1.3).

	Stem cell	Lymphoid precursor	Pro-B	Pre-BI	Pre-BII		Immature B	Mature B	Plasma cell
IgH	GL		DJ	VDJ	VDJ	VDJ	VDJ	VDJ	VDJ
IgL	GL		GL	GL	GL	VJ	VJ	VJ	VJ
B220	+		+	+	+	+	+	+	-
CD43	+		+	+	-	-	-	-	-
CD25	-		-	+	+	-	-	-	-
λ5/VpreB	±		+	+	-	-	-	-	-
CD19	-		+	+	+	+	+	+	-
mb-1/Igα	±		+	+	+	+	+	+	-
B29/Igβ	±		+	+	+	+	+	+	+
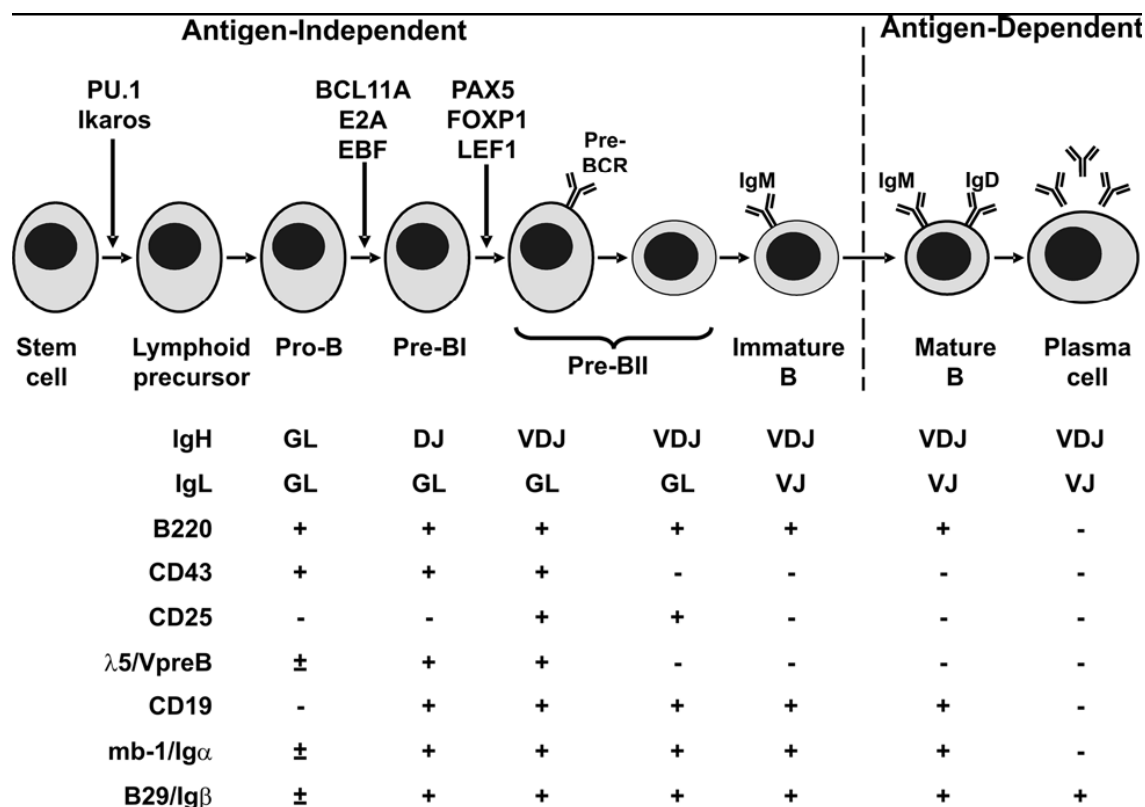
Figure 1.3 Transcription factors involved in the development of normal B cell lymphocytes. Large arrows denote the stage that each factor influences. Adapted from Downing and Mullighan (2006).

During haematopoiesis, as the cells differentiate and mature, the expression of their surface antigens alters, so making it possible to subdivide them into groups based on the stage of their development. Analysis of these immunological features led to the development of a comprehensive classification system using immunophenotyping (the process used to identify cells according to their cell lineage). The current World Health Organisation (WHO) classification of acute leukaemia (Harris *et al*, 1999;2001) identifies three main subtypes of ALL based on immunophenotype: precursor B-cell lymphoblastic leukaemia (BCP-ALL), precursor T lymphoblastic leukaemia (T-ALL), and mature B-cell leukaemia. Within BCP-ALL it is possible to further subdivide the

cases into three main divisions depending on the expression of their cluster of differentiation (CD) antigens (Table 1.2).

B- ALL			T- ALL	
Subgroup		CD Antigens	Subgroup	CD Antigens
Precursor B cell ALL	Pre-pre- B-cell ALL	CD19,CD79a,CD22 CD10 -	Pre-T-cell ALL	CD1a, CD2, CD5, CD7, CD8, cCD3
	Common ALL	CD10 (CALLA)		
	Pre-B – cell ALL	Cytoplasmic IgM + / – CD10		
	Mature B-cell	Cytoplasmic surface Ig λ or κ chains	Mature T- cell ALL	Surface CD3 (plus any other T-cell markers)

Table 1.2 Basic immunological classification of acute lymphoblastic leukaemia.

1.5 Acquired genetic aberrations in ALL

Since the discovery of the Philadelphia chromosome (Ph) by Nowell and Hungerford (1961), standard cytogenetic analysis has proved to be an essential tool in the identification of chromosomal changes in cancer, particularly leukaemia. A number of acquired chromosomal abnormalities arising from translocations, deletions, duplications and inversions have been identified which are often associated with deregulated gene expression. Over 50,000 cases of cancer with clonal cytogenetic abnormalities have been reported to the Mitelman Database of Chromosomal Abnormalities in Cancer, (2008) with approximately 7000 being attributed to childhood and adult ALL (Johansson *et al*, 2004).

The development of sensitive molecular techniques, has improved the level of detection of these genetic aberrations, in addition to identifying novel alterations not visible cytogenetically. Characterisation of the genes involved has led to the definition of distinct genetic subgroups of prognostic significance, which have been adopted for risk stratification with regard to treatment.

Currently an abnormal karyotype is detected in more than 80% of childhood (Harrison, 2000) and 79% of adult ALL patients (Moorman *et al*, 2007a). The chromosomal abnormalities may be either numerical or structural in nature, with many karyotypes containing both types of aberration.

1.5.1 Numerical chromosomal abnormalities

Aneuploidy, defined as having more or less than the normal diploid number of chromosomes, is a significant feature of ALL. A high hyperdiploid karyotype, with 51-65 chromosomes, is found in approximately 30% of childhood and 5% of adult patients. It was the first to be associated with a good prognosis in childhood ALL (Secker-Walker *et al*, 1978), in which an event free survival of greater than 80% at five years has since been observed (Moorman *et al*, 2003). The chromosomal gains in the form of trisomies are restricted to certain chromosomes. Chromosomes X, 4, 6, 10, 14, 17, 18 and 21 (frequently the gain of chromosome 21 is tetrasomic) were gained more often than expected (Moorman *et al*, 1996).

A second significant numerical abnormality in childhood ALL is hypodiploidy (Ho), where the modal number of chromosomes is ≤ 45 chromosomes. It is rare, with an overall reported incidence of approximately 6% (Harrison *et al*, 2004). In the majority of reported cases patients have 45 chromosomes (Raimondi *et al*, 2003;Harrison *et al*, 2004).

Overall, hypodiploidy has been linked to a poor prognosis (Heerema *et al*, 1999a;Harrison *et al*, 2004;Raimondi *et al*, 2003). However, Harrison *et al* (2004) showed that it was possible to subdivide hypodiploidy into three distinct

subgroups based on chromosome number, other cytogenetic features and clinical features: near-haploidy (23-29 chromosomes), low hypodiploidy (33-39 chromosomes) and high hypodiploidy (42-45 chromosomes). Near–haploidy (which is restricted to childhood ALL) and low hypodiploidy have a poor overall survival in comparison to those cases with high hypodiploidy. Karyotypic analysis of the near-haploid group showed chromosomal gains onto the haploid chromosome set in common with high hyperdiploidy (X, Y, 14, 18 and 21). They showed rare structural abnormalities and a co-incident doubled hypodiploid clone. Doubling of the hypodiploid clone was also found in patients with low hypodiploidy.

1.5.2 Structural chromosomal abnormalities

Structural chromosomal rearrangements occur in approximately 50% of childhood ALL (Harrison, 2000) patients. These rearrangements arise from translocations, deletions, duplications and inversions, resulting in the disruption of genes frequently encoding transcription factors. There are two main mechanisms in ALL which are responsible for activation of transcription factors:

1. Gene fusion, which occurs following the joining of discrete regions of two separate genes to form a novel fusion gene with oncogenic properties
2. Deregulation of intact transcription factor genes by juxtaposition with transcriptionally active promoter genes which are usually lineage specific

1.5.2.1 The *BCR-ABL1* fusion gene

The *BCR-ABL1* fusion gene is a characteristic example of the formation of a novel oncogene resulting from a translocation. This gene, usually located on the Ph (derived chromosome 22), arises from a reciprocal translocation between chromosomes 9 and 22 at breakpoints 9q34 and 22q11, respectively. The t(9;22)(q34;q11), results in the fusion of the 3′ segment of the tyrosine kinase *ABL1* proto-oncogene to the 5′ segment of *BCR* on chromosome 22 (Figure 1.4). Although this rearrangement is the hallmark of chronic myeloid leukaemia

(CML), it occurs in 3-5% of children (Pui & Evans, 1998) and 25% of adults (Secker-Walker, 1997) with ALL. The incidence increases exponentially with age (Secker-Walker, 1997). It is associated with an extremely poor prognosis in adults (Secker-Walker, 1997) and children alike (Hann *et al*, 2001). In ALL, expression of the fusion gene results in two types of chimaeric mRNA. This is dependent upon the location of the breakpoint within the breakpoint cluster region (bcr) of the *BCR* gene. In two thirds of childhood patients, the breakpoint arises in *BCR* between exons e2′ and e2, known as the minor breakpoint cluster region (m-bcr). The translocation involving this breakpoint produces a p^{190} *BCR-ABL* protein (Deininger *et al*, 2000). In the remaining third of *BCR-ABL1* positive ALL patients, the breakpoint occurs within a 5.8 kb region spanning *BCR* exons 12-16 (exons b1-b5), known as the major breakpoint cluster region (M-bcr). The translocation involving this breakpoint results in the production of a p^{210} *BCR-ABL* protein (Deininger *et al*, 2000). Studies in *BCR-ABL1* transformed cells showed that there was increased activation in a number of signal transduction pathways, leading to increased proliferation, reduced growth-factor dependence and apoptosis, and an altered interaction with the extracellular matrix (Deininger *et al*, 2005). These observations implied that the expression of *BCR-ABL1* provides a survival advantage to leukaemic cells over the normal cells. The resultant fusion proteins have increased tyrosine kinase activity. These tyrosine kinase proteins are enzymes that catalyse the phosphorylation of the terminal phosphate from adenosine triphosphate (ATP) to tyrosine residues.

Targeting the activity of the tyrosine kinase *BCR-ABL1* fusion protein has been effective in the development of the tyrosine kinase inhibitor, Imatinib®. This therapy is an effective treatment for chronic phase CML, with patients having an estimated overall survival of 89% at 60 months (Druker *et al*, 2006). In Ph positive ALL, initial haematological response to Imatinib® therapy was good, however development of relapse and subsequent disease progression were rapid (Ottmann *et al*, 2002). On the current UK treatment trials for ALL, virtually all

patients with a *BCR-ABL1* fusion are treated on a high risk protocol, emphasising the importance of their accurate detection.
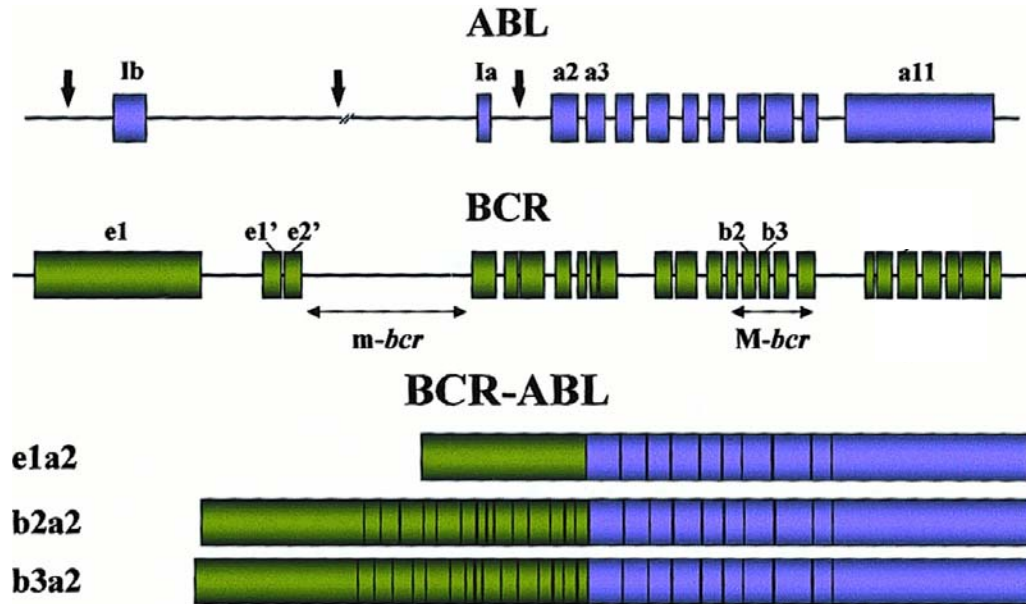
Figure 1.4 Locations of the molecular breakpoints in the t(9;22) and the resulting mRNA structure. Adapted from Deininger *et al* (2000).

1.5.2.2 The t(8;14)(q24;q32) translocation

The translocation, t(8;14)(q24;q32), is an example of a rearrangement resulting in the deregulation of intact transcription factor genes by juxtaposition to a transcriptionally active promoter gene. It was the first immunophenotype specific abnormality to be identified and is found in Burkitt's lymphoma and mature B-cell or Burkitt's type ALL (L3). It is highly specific for these disease subtypes, occurring in 85-90% of cases (Figure 1.5) (Hecht & Aster, 2000). The translocation has two variants, t(2;8)(p13;q24) and t(8;22)(q24;q11). In all three translocations the *MYC* oncogene, located at 8q24, is juxtaposed to either the immunoglobulin heavy chain (*IGH*) or one of the immunoglobulin light chain loci, kappa (*IGK*) or lambda (*IGL*), at 14q32, 2p11 and 22q11, respectively. Although the cytogenetic breakpoint on chromosome 8 is the same in all three

translocations, they differ at the molecular level. In the t(8;14), *MYC* breaks 5′ of the second exon, resulting in translocation of the entire coding sequence to chromosome 14. The orientation of the *IGH* and *MYC* on the derivative chromosome 14 is 5′ to 5′. In the two variant translocations, the breakpoint occurs 3′ of *MYC*, leaving the structure of *MYC* intact on the derivative chromosome 8. In these translocations the orientation of the *IGK* and *IGL* is 5′ to 3′ (Harrison, 2001). In all three circumstances *MYC* is placed under the transcriptional influence of an immunoglobulin enhancer. This results in deregulation, increased transcription and overexpression of *MYC*, leading to increased cellular proliferation. This subtype of ALL (Burkitt's type, mature B, L3) is particularly aggressive and its treatment differs from that of other forms of ALL, with patients responding well to short-term intensive treatment.
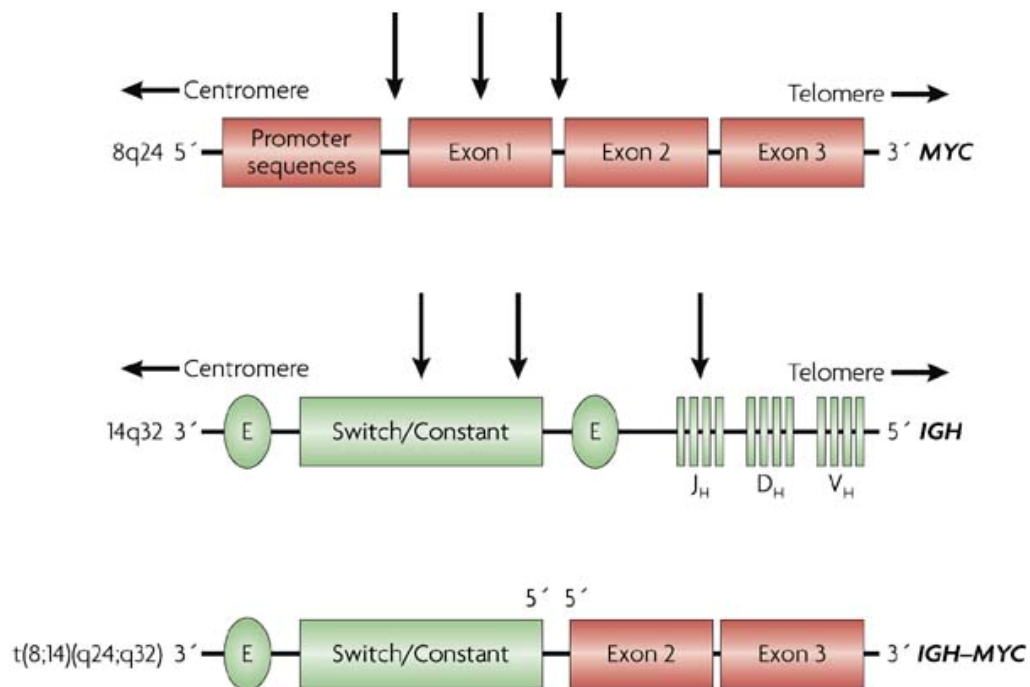
Figure 1.5 Locations of the molecular breakpoints in the t(8;14) and the resulting mRNA structure. Adapted from Mitelman (2007).

1.5.2.3 Structural abnormalities specific to T-cell ALL

T-ALL is also associated with a number of specific genetic aberrations, which alter gene expression in a similar way to the t(8;14). Rearrangements of the T-cell receptor (TCR) genes result in their promoter/enhancer elements being placed adjacent to various oncogenes. This in turn leads to their deregulation and subsequent overexpression. The gene loci encoding the *TCR ά* and δ genes are located on the long arm of chromosome 14 at 14q11, whilst those encoding β and γ chains are located to chromosome 7 at 7q34 and 7p15, respectively. Cytogenetic analysis of T-ALL patients reveals recurrent translocations in 25-50% of patients (Graux *et al*, 2006). However a large proportion of patients have a normal karyotype with cryptic abnormalities which require more sophisticated molecular techniques for their detection (Ferrando & Look, 2003).

1.5.3 Deletions

Deletions involving different chromosome arms are common abnormalities in ALL. Those involving the short arm of chromosomes 9 and 12 and the long arm of chromosome 6 are among the most frequent recurrent abnormalities reported in ALL. There is some evidence that these deletions result in the loss of tumour suppressor genes. Deletion of the short arm of chromosome 9 occurs in both T- and B-lineage ALL, with 80% of childhood T-ALL having a deletion of 9p compared to 20% in B-ALL. This deletion frequently involves the 9p21~22 region, with loss of *p16INKa* (*CDKN2A*) and *p15INKb* (*CDKN2B*) (Heerema *et al*, 1999b;Andreasson *et al*, 2000;Harrison, 2000). These genes, members of the inhibitor of the cyclin-dependent kinase 4 (*INK4*) family, are an important class of tumour suppressors. Their main function is to act as negative regulators of cell cycle control by binding to and inhibiting cyclin-dependant kinase 4, thus preventing the phosphorylation of the retinoblastoma (Rb) protein.

Both homozygous and hemizygous deletions have been detected, with loss of material from the maternal chromosome being preferential (Morison *et al*,

2002). It has been suggested that loss of *p16* and *p15* expression may occur through methylation in the remaining allele in some patients (Chim *et al*, 2001). The prognostic significance of these deletions remains debatable with some reports indicating an association with a poor prognosis (Heerema *et al*, 1999b; Harrison, 2000) whilst other reports indicate no prognostic significance (Takeuchi *et al*, 1995).

1.5.4 Amplification

Gene amplification, defined as the gain of additional copies of a gene, resulting from the duplication of a DNA segment (Myllykangas & Knuutila, 2006) is another mechanism that can lead to the activation of a proto-oncogene. It frequently occurs in solid tumours but is rarely described in acute leukaemia. At the cytogenetic level, gene amplification is typically seen extrachromosomally as double minute chromosomes or intrachromosomally in the form of homogeneously staining regions (HSR). In T-ALL, the extrachromosomal amplification of the *NUP214-ABL1* fusion in the form of episomes, has been reported at an incidence of ~2-5% (Barber *et al*, 2004;Graux *et al*, 2004). The intrachromosomal amplification of *RUNX1* (see section 1.6.3) and *MLL* (Cuthbert *et al*, 2000) have also been reported as recurrent abnormalities in BCP-ALL, where they are associated with a poor prognosis.

1.6   Abnormalities of chromosome 21

Abnormalities of chromosome 21 are frequently observed acquired genetic changes in ALL. Individuals with Down syndrome and constitutional trisomy 21 have a 10-20 fold increased risk of developing acute leukaemia of both myeloid and lymphoid origin. Acquired abnormalities of chromosome 21 can be either numerical or structural, which together account for > 50% of the acquired abnormalities detected in the abnormal karyotypes of ALL patients. Trisomy 21 as a sole change has been reported in 1.8% of childhood ALL (Raimondi *et al*, 1992), whilst extra copies are observed within hyperdiploid and hypodiploid

karyotypes. In hyperdiploid karyotypes gain of chromosome 21 is observed in all cases. The functional significance of a high hyperdiploid karyotype in ALL is not known. A study by Gruszka-Westwood *et al* (2004) used comparative expressed sequence hybridization to investigate if increased chromosome copy number in hyperdiploid ALL led to increased overexpression. They found a number of common regions of overexpression, including one on chromosome 21 at band q21, which they concluded was consistent with copy number gain.

Acquired structural rearrangements involving a number of breakpoints on chromosome 21 have been reported in ALL (Jeandidier *et al*, 2006), with the most frequent rearrangement being the translocation, t(12;21)(p13;q22) (section 1.6.2). This occurs at an incidence of approximately 25% in childhood ALL. Such findings clearly indicate that this chromosome plays a key role in the regulation of haematopoiesis. Detailed analysis of the abnormalities involving chromosome 21 have provided insight into the importance of the *RUNX1* gene in leukaemogenesis, which is known to be one of the most frequently targeted and rearranged genes in a variety of leukaemias (Mikhail *et al*, 2006).

1.6.1 *RUNX1* abnormalities

The *RUNX1* gene, located at 21q22, is one of the main regulators of definitive HSC formation. Niebuhr *et al* (2008) proposed that *RUNX1* is a "gatekeeper"of the pathway responsible for maintaining haemopoietic cell numbers by regulating differentiation and proliferation. As reviewed by Mikhail (2005), it is one of the most frequently deregulated genes in leukaemia. It was originally identified by cloning the breakpoint of the translocation, t(8;21)(q22;q22), associated with AML (Miyoshi *et al*, 1991). It is a nuclear protein with two large functional domains, a proximal DNA-binding region, known as the Runt homology domain, and a distal transactivation domain. Together with its heterodimeric transcription co factor, core-binding factor (CBF-β), it functions as a transcription regulator of haematopoiesis by allowing for the assembly of a

number of transcriptional activation complexes. It can act as either an activator or repressor of transcription. This dual function is dependant on its interaction with a number of different lineage-specific transcription factors and co-regulators (Figure 1.6)
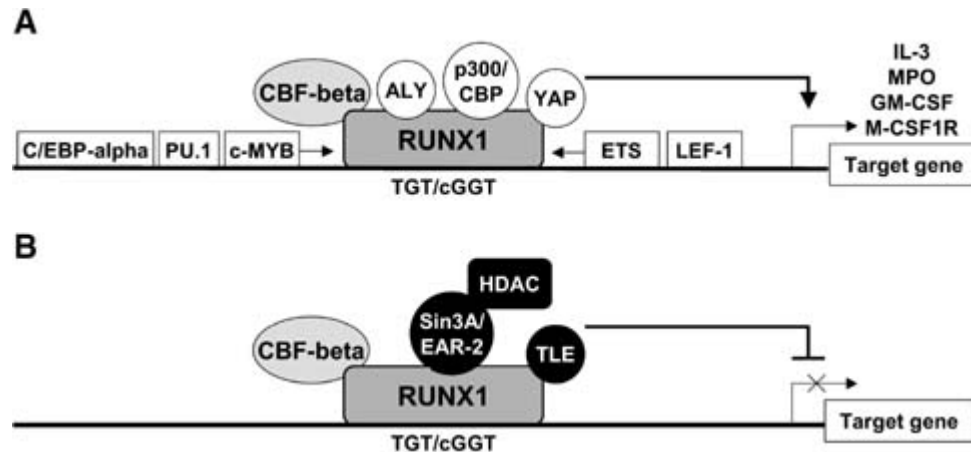
Figure 1.6 The model of transcription activation and repression mediated by RUNX1. *RUNX1*, in association with its cofactor CBF-beta, has an enhanced binding affinity to the DNA sequence present in the regulatory region of genes. These sites are often adjacent to those of *RUNX1*-associated transcription factors including *C/EBP-alpha, PU.1, MYB, ETS, LEF-1. RUNX1* can mediate transcription activation (A) or repression (B) by recruitment of non-DNA-binding transcription co-activators or co-repressor. Adapted from Mikhail (Mikhail *et al*, 2006).

RUNX1 is rearranged through a variety of mechanisms including translocations, mutations and amplification, in a range of haematological disorders, providing evidence of its fundamental importance in haematopoiesis. A number of translocations involving *RUNX1* have been found in different lineage specific subtypes of leukaemia. These include *RUNX1-RUNX1T1* from t(8;21)(q22;q22), in AML (Miyoshi *et al*, 1991); *ETV6-RUNX1* from t(12;21)(p13;q22) in ALL (Romana *et al*, 1994) and *RUNX1-MDS1* from the t(3;21)(q26;q22) in myelodysplastic syndrome (MDS) and blast phase CML (Nucifora *et al*, 1993). The molecular consequence of these fusion genes is the

generation of fusion proteins that act as negative inhibitors of the normal *RUNX1* allele.

Acquired and inherited point mutations of *RUNX1*, have been detected in both AML and MDS (Osato *et al*, 1999;Roumier *et al*, 2003;Cameron & Neil, 2004;Niebuhr *et al*, 2008;Owen *et al*, 2008;Mikhail *et al*, 2006). The majority of mutations occur in the Runt domain and result in the impairment of *RUNX1* through loss of DNA binding. Studies in *RUNX1* +/- haploinsufficient mice have shown that haploinsufficiency resulted in a decrease in the number of HSC and a reduction in their capacity to expand and differentiate (Sun & Downing, 2004). This led to speculation that the function of *RUNX1* is dose dependant and that haploinsufficiency may lead to leukaemia. Coupled with this mutations have been identified in familial platelet disorder. Such individuals have a predisposition to AML (Song *et al*, 1999;Owen *et al*, 2008).

Amplification of *RUNX1* has also been reported as a potential mechanism of deregulation of this gene. In ALL amplification may occur from the gain of intact copies of chromosome 21 as seen in high hyperdiploidy, or through intrachromosomal amplification (section 1.6.3).

1.6.2 *ETV6-RUNX1* fusion gene

One of the most common translocations in childhood ALL is the t(12;21)(p12;q22). This cytogenetically cryptic translocation was first reported by Romana *et al* (1994) as a chance finding when investigating patients with deletions in the short arm of chromosome 12. It has subsequently been shown to result in the fusion of two transcription factor genes - *ETV6* and *RUNX1*. The resulting chimeric fusion gene includes the 5' portion of *ETV6*, a member of the *ETS* family of transcription factors and almost the entire coding region of *RUNX1* (Pui *et al*, 2004). The *ETV6-RUNX1* fusion protein inhibits transcriptional activity by recruiting histone deacetylase, which induces the closure of the chromatin

structure leading to inhibition of transcription (Figure 1.7). The consequence of these changes is alteration in both the self- renewal and differentiation pathways.
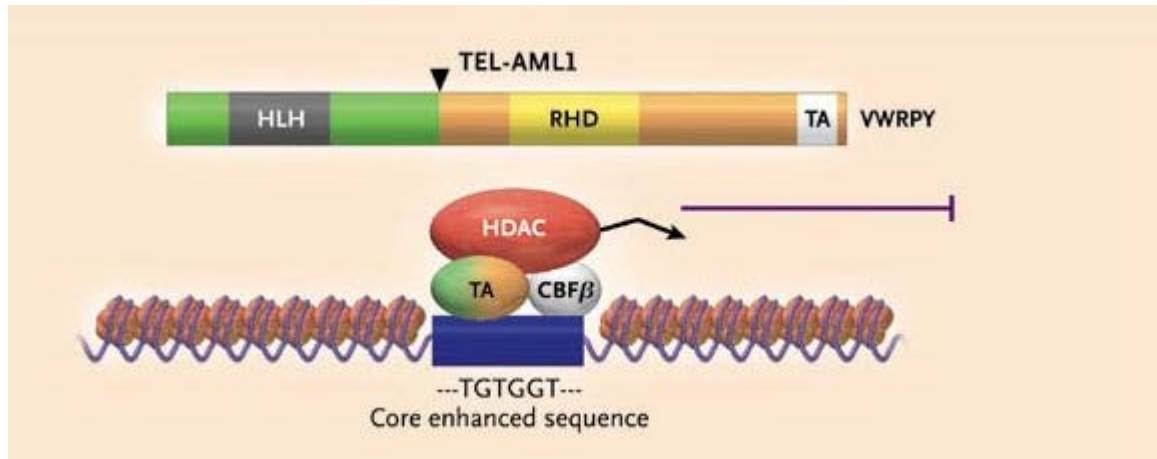
Figure 1.7 The *ETV6-RUNX1* fusion. The *ETV6-RUNX1* recruits histone deactylase, resulting in the closure of the chromatin structure and so inhibiting transcription. Adapted from Pui (2004).

The *ETV6-RUNX1* fusion alone is insufficient for the development of leukaemia. A number of studies have demonstrated that the fusion arises in utero (Gale *et al*, 1997;Ford *et al*, 1998; Greaves *et al*, 2003). This is followed by a postnatal pre-leukaemia phase, which requires a further secondary genetic event in order to develop overt leukaemia (Greaves *et al*, 2003). Loss of the non rearranged *ETV6* allele has been implicated as an important secondary event in transformation of the pre-leukaemic cells to leukaemia.

The t(12;21) translocation occurs almost solely in childhood BCP-ALL at an incidence of ~25% and a median age of 4 years (Mitelman *et al*, 2007). It has rarely been reported in adult ALL (Jabber Al-Obaidi *et al*, 2002), and has only been described in a single case of T-ALL (Ma *et al*, 2001). It is generally associated with a favourable outcome (Rubnitz *et al*, 1997;Borkhardt *et al*, 1997;Romana *et al*, 1995), however late relapse as well as the incidence of the fusion gene in diagnosis and relapse suggest that the *ETV6-RUNX1* fusion may not be an

independent good–risk marker (Harbott *et al*, 1997). Further studies are required to fully characterise the genotype of those patients who relapse in order to determine the true prognostic significance of this rearrangement in relation to its associated genetic changes.

1.6.3 Intrachromosomal amplification of chromosome 21 (iAMP21)

Gene amplification is a mechanism that may lead to altered gene expression. In 2003, two groups Harewood *et al* (2003) and Soulier *et al* (2003), defined a new molecular cytogenetic subgroup in ALL. The abnormality had an apparent amplification of the *RUNX1* gene located to band 21q22, on a duplicated chromosome 21. It was described by both groups as the presence of multiple copies of apparently un-rearranged *RUNX1* genes, which were detected using FISH. The signals appeared as clusters of ≥ 4- 5 signals in interphase cells. In metaphases ≥ 3-4 signals appeared in a ladder like fashion on a single marker chromosome, which was shown by chromosome painting to be composed entirely of chromosome 21 material (Figure 3.1). In both studies the *RUNX1* copy number ranged from 4-≥ 10, in the majority of patients. Conventional cytogenetic analysis of those patients with an abnormal karyotype, found that one copy of a normal chromosome 21 was replaced by the marker/duplicated chromosome 21[dup(21)]). However, both groups noted that the chromosomal morphology of the marker as determined by G-banded analysis was highly variable between patients. Harewood *et al* (2003) subdivided the dup(21) into five distinct morphological groups; small acrocentric (SA), large acrocentric (LA), large metacentric (M) resembling an isochromosome, sub-metacentric (SM) and ring (R) chromosomes (Table 1.3).

G-Banded form of normal chromosome 21 (Left) and dup(21)(q?) (Right)	ISCN description
	dup(21)(q?) Small acrocentric
	dup(21)(q?) Large acrocentric
	der(21)(q10)dup(21q?) Large metacentric
	der(21)dup(21)(q?) Sub-metacentric
	der(21)r(21)(q?)dup(21)(q?) Ring

Table 1.3 Morphological forms and ISCN description of dup(21) as described by Harewood *et al* (2003).

The abnormality has been associated with distinctive clinical features. It occurs in childhood ALL, with a higher incidence in older children. The combined median age of patients from the two studies was 11 years (range 5-20 years). This is outside the usual distribution for childhood ALL, which is 2-5 years. The peripheral blood white cell count (WBC) at presentation was low (mean $6x10^9$/l; range $1-19x10^9$/l). All patients had a precursor B-cell immunophenotype, with distinct immunophenotypic features (Soulier *et al*, 2003). Of note was that no other previously described, established recurrent genetic abnormalities were detected in association with dup(21), for example patients were all negative for *ETV6-RUNX1* and *BCR-ABL1* fusions, *MLL* rearrangements, high hyperdiploidy and near-haploidy (Harrison *et al*, 2005).

Although these two studies were the first to establish this aberration as an emerging subgroup in childhood ALL, sporadic cases had been previously reported. One of the first was described by Le Coniat and Berger in 1995 (1995). They reported a case of an 11 year girl with ALL whose G-banded analysis

showed the presence of an abnormal clone, in which there appeared to be a single copy of chromosome 21 and a marker: 46,XX,-21,+mar. Using FISH, they showed that the metacentric marker chromosome was composed entirely of chromosome 21 material, and involved the uneven amplification of a region of chromosome 21, at band 21q22. They proposed that the mechanism of formation may have been from a secondary breakage of a ring chromosome. From the literature reviewed by Harewood *et al*, Soulier *et al* and a more recent study by Perez- Vera *et al* (2008;2003;2003), a total number of 86 cases with *RUNX1* amplification have been identified. Comparison of all cases published to date in relation to karyotypes, age and WBC at presentation, established that these characteristics were consistent (Appendix 1). All patients had been identified using similar FISH techniques, with all having multiple copies of the *RUNX1* gene arranged on a dup(21) chromosome.

It was noted that in the initial studies follow up time was too short to draw any conclusions regarding the prognostic significance of this cytogenetic abnormality. However, a subsequent study by Robinson *et al* (2003), combining a further eight cases with the initial 20 described by Harwood *et al* (2003), showed that for children with this abnormality entered to the UK Medical Research Council (MRC) ALL97 treatment trial, relapse rate was high. This report also demonstrated that the estimated incidence was low at 1.5%. This finding was confirmed in a later report by Garcia-Casado *et al* (2006), who screened 110 consecutive paediatric ALL cases and identified two with *RUNX1* amplification.

Although previous studies had described this abnormality as "*RUNX1* amplification", it was established that the involvement of chromosome 21 extended beyond the *RUNX1* gene. Consequently, this abnormality was renamed in order to more accurately reflect this, as the intrachromosomal amplification of chromosome 21 (iAMP21) (Strefford *et al*, 2006).

Following the initial observation that iAMP21 was associated with a low event-free survival, outcome data has since been closely monitored in these

patients. A recent report of those patients (Moorman *et al*, 2007b) identified with iAMP21, treated on the UKALL97 treatment protocol, has conclusively established that these patients had a significantly inferior event-free and reduced overall survival at 5 years compared with other ALL patients of 29% verses 78% and 71% versus 87%, respectively. Consequently, childhood patients entered to the current UK ALL 2003 treatment trial are being treated on the high risk arm (Moorman *et al*, 2007b).

1.7 The morphological, immunological and cytogenetic (MIC) classification system

The incidences of different chromosomal rearrangements vary, with some abnormalities being more common than others and some being associated with specific morphological or phenotypic subtypes. In 1981, the Third International Workshop on Chromosomes in Leukaemia demonstrated for the first time that cytogenetics had an impact on the biology, diagnosis and the prognosis of ALL (1981). Since that time, cytogenetic abnormalities have been further elucidated and their molecular and biological significance better understood. The impact of such genetic rearrangements and the development of improved cytogenetic techniques for their detection resulted in the development of a system of classification, which categorizes patients according to their acquired genetic/molecular aberrations. This system, the MIC classification, includes morphological, immunological and cytogenetic data (1986).

Further development of sophisticated molecular techniques including FISH and the polymerase chain reaction (PCR) has allowed the detection of genetic rearrangements at the molecular level. This resulted in an improved classification system being proposed that incorporated morphology, immunophenotype, cytogenetic and molecular analysis - MIC-M (Bain, 1998). Currently the WHO system (2001) includes a number of specific chromosomal aberrations in its classification of acute leukaemia. As newly characterised

abnormalities become associated with distinct biological groups it is likely that further aberrations will be added to the classification system.

1.8   Prognosis

The clinical outcome of patients with acute leukaemia is dependent upon a number of factors, including WBC count at diagnosis, age, gender and genetic subgroup. A number of recurrent genetic rearrangements have been identified and characterised in ALL, of variable incidence and prognostic value (Table 1.3). The impact of these genetic rearrangements on prognosis has influenced the development of current treatment regimes providing a risk–stratified approach to therapy. Consequently the accurate identification of genetic abnormalities is paramount to the success of treatment. In ALL chromosomal and molecular abnormalities often correlate with other clinical and haematological factors of prognosis, as well as having independent prognostic value.

The overall survival rate in ALL is lower in adults compared to children, 40% versus ≥ 80% respectively (Pui & Evans, 2006). This is often attributed to the higher incidence of poor risk genetic factors in adults (Table 1.3). For example, the *BCR-ABL1* fusion gene, associated with a poor prognosis irrespective of age, has a lower incidence in childhood compared to adult ALL.

Genetic abnormality	Adults		Childhood	
	Incidence (%)	Prognosis	Incidence (%)	Prognosis
< 45 chromosomes	4-9	Poor	6	Poor
> 50 chromosomes	2-5	Good	25-30	Good
t(9;22)(q34;q11.2)	25-30	Poor	3-5	Poor
t(4;11)(q21;q23)	3-5	Poor	2	Poor
t(1;19)(q23;p13.3)	3	Poor	5-6	Good
t(12;21)(p13;q22)	<1	NK	20-25	Good
t(17;19)(q22;p13)	<1	Poor	<1	Poor
t(11q23;V)	3-6	Intermediate	3-5	Poor
t/del (9p)	10-15	Intermediate	7-12	NK
t/del (12p)	5	NK	10-12	NK
del(6q)	5-6	NK	4-13	NK

Table 1.4 Overall incidences of recurrent genetic abnormalities in acute lymphoblastic leukaemia. Adapted from Ramondi (Raimondi, 2006). (NK = not known).

The impact of primary genetic changes on prognosis in ALL is unequivocal. Rigorous classification systems based on risk of relapse is essential in selection of therapy that will maintain a high cure rate, whilst avoiding excessive toxicity. With the development of more sophisticated technologies, it has been possible to define new genetic subgroups. In turn, the characterisation of such abnormalities may provide further insights into their biology, so leading to the development of novel drug treatments and possible disease prevention.

1.9 Aims of research

The precise classification and diagnosis of patient groups at high-risk of relapse is essential. This project focuses on one newly described chromosomal

abnormality, iAMP21. Although the studies outlined above have demonstrated that the *RUNX1* copy number was over represented in patients with this abnormality, it has not been established that this is the underlying mechanism. Consequently this study was proposed to further characterise iAMP21, to identify the potential causative mechanism driving the leukaemia in these patients, which in turn will lead to the development of the most accurate method for diagnosis.

This study has involved the detailed investigation of a number of previously identified iAMP21 cases using a combination of techniques including:

- An investigation into copy number changes along chromosome 21, using a combination of array based comparative genomic hybridisation (aCGH) and FISH on a small group of iAMP21 patients

- An interphase FISH profiling study, to screen a large group of iAMP21 patients to establish if they all have an identical profile in relation to the copy number changes

- Metaphase FISH mapping with clones located along the length of chromosome 21 and mBAND to investigate the types and extent of the intrachromosomal rearrangements

- G-banded analysis of all cases to establish whether the morphology of the dup(21) chromosome is indicative of distinct subgroups among iAMP21 patients, as suggested by Harewood *et al* (2003)

- Detailed analysis of additional chromosomal abnormalities detected by G-banding, to establish whether there are specific genetic aberrations associated with iAMP21

- An investigation to determine whether iAMP21 represents a distinct subgroup of patients or it is a secondary chromosomal change

- The development of a diagnostic test that would allow this genetic
  subgroup to be detected using FISH, PCR or Multiplex ligation probe
  amplification (MLPA)

Chapter Two –
Materials and Methods

2 Materials and Methods

2.1 Patients

Patients with a confirmed diagnosis of ALL and registered to one of the UK Medical Research Council (MRC)/National Cancer Research Institute (NCRI) treatment trials: ALL 97, MRD pilot, ALL 2003 for children aged 1-18 years, or UKALLXII for adults aged 15-55 years, were included in this study. Ethical approval and patient consent were obtained on entry to the clinical trial by the Clinical Trial Service Unit & Epidemiological Studies Unit (CTSU, 2008). All patients were entered to the LRF UKCCG Karyotype Database in Acute Leukaemia (LRUKD) database (Harrison *et al*, 2001) and selected for inclusion in this study by searching this database (Section 3.1). The demographic and clinical data were collected from the CTSU (Oxford, UK).

2.2 Patient Material

Fixed cell suspensions prepared from diagnostic bone marrow and/or peripheral blood, for routine cytogenetic analysis, were obtained from the UK regional cytogenetic laboratories. The karyotypes from standard G-banded cytogenetic analysis, undertaken by the same laboratories, were obtained on all patients. For those patients with an abnormal karyotype, G-banded slides were requested for review through the LRUKD. Where available, genomic DNA (gDNA) from matched diagnostic samples were obtained from the same laboratories.

2.3 Fluorescence in situ hybridisation (FISH)

FISH is a molecular cytogenetic technique that allows detection of a specific DNA sequence *in situ*. It relies on the principle that a fluorescently labelled single stranded DNA probe will anneal (hybridise) to a complementary

single stranded target DNA. The target DNA from either metaphase chromosomes or non-dividing interphase nuclei can be visualised using a fluorescent microscope (Czepulkowski, 2001) (Figure 2.1).
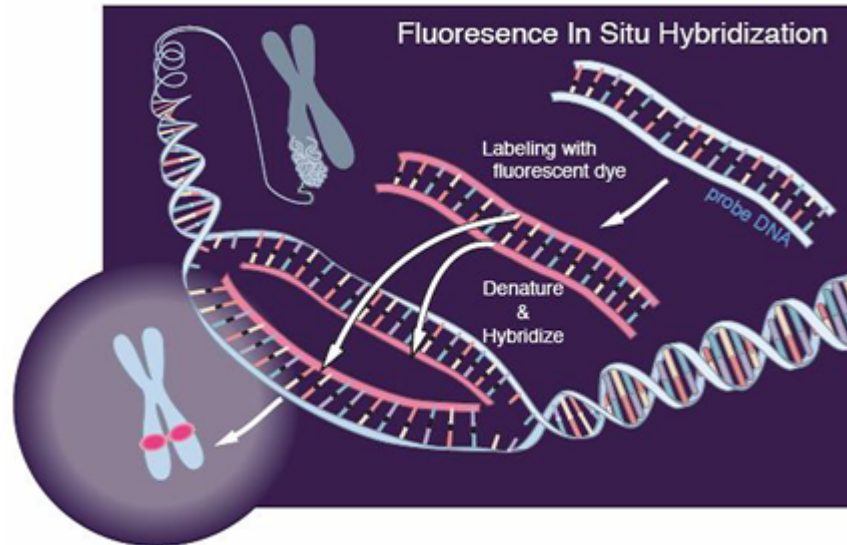
Figure 2.1 Diagrammatic representation of the principle of FISH.

There are a number of different designs of FISH probe available, making use of either DNA or RNA. For the purpose of this study six different DNA probe types were used:

- Locus specific probes: unique sequence probes that are designed to detect specific regions of a chromosome or gene.
- Whole chromosome paints (WCP): a library of sequence probes specific for individual chromosome pairs which hybridise or 'paint' the length of the chromosome.
- Subtelomeric probes: unique repetitive DNA sequences specific for the subtelomeric regions of each chromosome.
- Alpha satellite probes: repetitive DNA sequences specific for the alpha satellite centromeric regions of the chromosomes. These probes are

usually chromosome specific; however chromosomes 13 and 21 share the same sequences.

- Peptide nucleic acid (PNA) telomeric probes: composed of PNA, which is a short synthetic DNA/RNA like molecule which can be used to generate probes capable of binding to target DNA. Telomeric PNA probes are composed of dye labelled oligomers comprising the common tandem repeat sequence (TTAGGG) found in all human chromosome telomeres.
- mBAND probe, Xcyte 21 (Section 2.3.7).

2.3.1 Probe selection

Plasmid artificial chromosome (PAC) (from libraries RCP1) and bacterial artificial chromosome (BAC) (from libraries RCP11) clones, positioned to specific chromosomal bands on chromosome 21 were identified using the following websites:

- Ensemble: http//www.ensemble.org/index.html
- UCSC: http://genome.ucsc.edu/cgi-bin/hgGateway
- NCBI: http//www.ncbi.nlm.nih.gov/

The selected clones were obtained on request through the Wellcome Trust Sanger Institute (Cambridge, UK) or Wessex Regional Genetics Laboratory (Salisbury, UK).

2.3.2 Probe preparation

Clones were streaked onto pre-prepared Luria-Bertani (LB) (Appendix 2) agar plates containing the appropriate antibiotic and placed in a 37°C incubator for 16-20 hours. Following incubation, a single colony was picked out and grown at 37°C overnight in 100ml of LB (Appendix 2) broth in a shaking incubator.

The following morning a glycerol stock consisting of 850µl of the overnight culture in 150µl glycerol (BDH Laboratory Supplies, UK) was produced and stored at -80°C.

2.3.2.1 DNA extraction

DNA was extracted using a midi Qiagen plasmid purification kit (Qiagen, USA). The principle of this technique is based on a modified alkaline lysis procedure, followed by binding of plasmid DNA to an anion-exchange resin under low-salt and pH conditions. Impurities, RNA, and proteins are removed by a medium-salt wash and the DNA is eluted in a high-salt buffer. DNA is then concentrated and desalted by isopropanol precipitation and ethanol washes. The overnight culture was spun in a Stovall centrifuge at 5000 rpm for 5 minutes at 4°C. The supernatant was discarded and cell pellet resuspended by vortexing in 4ml of P1 Buffer. The cells were lysed by the addition of the P1 buffer and the chromosomal and plasmid DNA denatured by the presence of sodium hydroxide in the buffer. 4mls of Buffer P2, previously warmed to 37°C was added to the lysate and mixed by inversion. This was followed by 5 minutes incubation at room temperature (RT). After incubation, 3ml of chilled P3 buffer was added and the lysate gently mixed by inversion. The P3 buffer neutralizes the lysate by precipitating the denatured bacterial DNA, proteins and lipids. The plasmid DNA remains in solution. The lysate was placed directly onto a QIAfilter cartridge and incubated at RT for 10 minutes to collect the supernatant.

Qiagen tips were equilibrated using 4ml of Buffer QBT prior to addition of the collected supernatant. The tips were allowed to drain and the supernatant discarded. Flow of buffer begins automatically by reduction in surface tension due to the presence of detergent in the buffer. Contaminants are removed from the column by washing with 10ml of buffer QC. This step was repeated twice with the supernatant being discarded each time. The DNA was eluted from the column by adding 5ml of buffer QF previously warmed to 65°C. The eluate was collected and 3.5ml of isopropanol added to precipitate the DNA. This sample was centrifuged at 14000 rpm at 4°C for 30 minutes. The supernatant was discarded and 2mls of 70% ethanol added to remove any remaining precipitated salt. The sample was then spun at 14000 rpm at 4°C for 10 minutes. The ethanol

replaces the isopropanol making it easier for the DNA to dissolve. The DNA pellet was left to air dry before resuspending in 2ml of distilled water (dH$_2$O). The quality of the extracted DNA was determined by running 8µl on a 1% agarose gel (Section 2.4.2).

2.3.2.2   Preparation of fluorescence labelled DNA probe

Probes are fluorescently labelled by one of two methods:

Indirect labelling: The probe is attached to a reporter molecule, either digoxigenin or biotin. A fluorochrome, conjugated to a molecule, such as avidin, is added. This combines with the labelled reporter molecule. Further fluorescent layers may be added if the signals are weak, by adding an antibody to this conjugated molecule. For example, biotin labelled probe is hybridised to the target DNA. Fluorescently labelled avidin (which has a strong affinity for biotin) is then added, which binds to the biotin. By subsequently adding a biotinylated anti-avidin molecule it is then possible to repeat the process, building up layers of fluorescence.

Direct labelling: The probe DNA is directly joined to the fluorochrome and can thus be visualised without any further detection steps.

Following detection, a counterstain is added so that the chromosomes and interphase cells can be visualised and the relative positions of the fluorescent probes noted. Analysis is then carried out using an epifluorescence microscope.

Probes were labelled using Nick translation. The principal behind this technique is the cleaving of DNA ('nick') and the synthesis of new DNA with the incorporation of fluorochrome–conjugated or hapten-conjugated nucleotides. It relies on the activity of two enzymes working simultaneously: DNase1 which cleaves the DNA and DNA polymerase1 which both removes and adds nucleotides.

To allow for dual colour FISH experiments, probes were labelled with either Spectrum Red or Spectrum Green conjugated d-UTP (Abbott Diagnostics, US) using a nick translation kit (Abbott Diagnostics, US).

Individual labelling reactions containing 2.5µl dUTP (0.2 Mmol Spectrum Red or Spectrum Green), 10µl dNTP mix (0.1Mmol each of dATP, dCTP, and dGTP), 5µl 0.1mM dTTP and 5µl nick translation buffer were added to a 1.5ml microcentrifuge tube and gently mixed together. 17.5µl of extracted DNA was added followed by 10µl of nick translation enzyme (a mixture of DNase1 and DNA polymerase 1). The samples were incubated at 15˚C for 3 hours. 3µl 0.5M EDTA was added to stop the reaction. To remove unbound probe, samples were run through a Sephadex G-50 column (Amersham, UK). The Sephadex column was flick mixed to resuspend the granules, opened, and placed in a collection tube. The column was spun at 4000 rpm at 4˚C for 1 minute, the supernatant was discarded, and 50µl of TE buffer (Appendix 2) was added to the column. The column was centrifuged as before and the supernatant discarded. The column was then placed in a clean collection tube and the nick translated DNA sample pipetted into the centre of the column. The column was spun as before and the eluate collected. To confirm that the DNA probe had been cleaved and labelled the sample was run on an agrose gel (section 2.4.2).

To remove repetitive sequences, 10µl labelled DNA probe was co-precipitated by adding 10µl human Cot1-DNA (1mg/ml) (Invitrogen, UK) in 40µl 100% ethanol and 2µl 3M sodium acetate (pH 5.2), at -20˚C for 1-2 hours. The DNA was then pelleted by centrifugation at 13000 rpm at 4˚C for 30 minutes, air dried and resuspended in nuclease free water. Fluorescent probes are photosensitive and so care was taken to minimise their exposure to light.

2.3.3 Slide Preparation

Fixed cells were centrifuged and the pellet re-suspended in fresh fixative (3:1 Methanol: Acetic acid) until the cloudy suspension became almost clear in

appearance. Using a pipette 2- 3µl of this suspension was dropped onto a clean previously labelled glass slide. Cell density and metaphase spreading were checked using a phase contrast microscope. Cell concentration should be such that the cells do not overlap, are flat and have no visible cytoplasm. Slides were then air dried slowly to allow the chromosomes time to spread (adding a drop of fix to the slide immediately after spreading can slow down the drying process and so aid metaphase spreading). Slides were aged on a hotplate at 60°C for 15 minutes.

2.3.4 Hybridisation

In order to incorporate the probe DNA into the target DNA, double stranded probe and target DNA were denatured by heating in order to render them single stranded. As DNA needs temperatures of >90°C to denature, mixing the probe with formamide (an organic solvent) and salt solutions lowers the temperature at which denaturation occurs. Hybridisation buffer contains a mixture of formamide, saline sodium citrate (SSC), dextran sulphate, salt-dextran solution and a blocking DNA. Together these components optimise the conditions for hybridisation to take place. Both probe and target DNA may be denatured simultaneously (by co-denaturing) on a hotplate, or they can be denatured separately using heated formamide solutions. Some probes are single stranded and do not require denaturation.

Following denaturation, the probe DNA was left to hybridise to the target at 37°C. A 1:10 dilution of probe was prepared using hybridisation buffer (Abbott Diagnostics, US). The total volume of probe used is dependent upon the size of the coverslip. For 10 or 13mm coverslips a total volume of 3µl was used whilst for 22 x 22mm coverslips a total volume of 5µl was used. The probe solution is spotted on to the cover slip and the slide inverted over it, aligning the coverslip with the sample spot. This upside down approach reduces the formation of air bubbles between the slide and the coverslip. The coverslip was sealed with

rubber solution and the slide placed on a Hybrite (Abbott Diagnostics, US) a temperature controlled hotplate. Probe and patient DNA was co-denatured at 72°C for 2 minutes and hybridised overnight at 37°C. For commercial probes, the manufacturers' protocols were followed with regard to hybridisation, temperatures and timing.

2.3.5 Post hybridisation washing

During the process of hybridisation, some probe will bind to non specific sequences in addition to binding to the target DNA. This background hybridisation is removed by stringent washes to break the weaker bonds of the non-specifically bound DNA. The stringency of the wash solution required is dependent on the level of background. At higher stringency, there is a greater disassociation of the less specific DNA, making the resulting signals cleaner but faint. The stringency is adjusted by altering the temperature and salt concentration of the washes.

The rubber sealant and coverslip were removed (to aid the removal of the coverslip, slides may be soaked in 2x SSC solution (Appendix 2) for 30 seconds and slides placed in Wash 1: 0.4 x SSC +0.3% Nonidet P40 (NP40) (Roche, Germany); pre heated to 73°C for 2 minutes. Slides were transferred to Wash 2: 2 x SSC + 0.01% NP40; at RT for 2 minutes.

2.3.6 Detection and counterstaining

Probes are detected by one of two methods depending on the initial labelling. For indirectly labelled probes following post hybridisation Wash 2, 10μl blocking agent (Appendix 2) was pipetted onto the areas of slide requiring detection. This area was covered with a parafilm coverslip and incubated in a humidified chamber at RT for 10 minutes. Following incubation, the excess block was drained from the slide and 10μl detection reagent applied: Avid-Fluorescein for biotin labelled probes (Roche, Uk) and Anti-Digoxigenin-Rhodamine Fab

fragments for digoxigenin labelled probes (Roche, UK), The area was covered with a parafilm coverslip and incubated for 10 minutes in a humid chamber. The slide was then placed in Wash 3 (Appendix 2) for 1-2 minutes to remove the unbound detection reagent. Directly labelled probes require no detection.

The counter stain, 4',6-diamidino-2-phenylindole (DAPI), is required for visualisation of metaphase and interphase cells. The stain is preferentially taken up by the adenine (A)-thymine (T) rich chromosomal regions which produces a staining pattern similar to that seen with G-banding. As both the fluorochromes and DAPI are light sensitive, an antifade solution is added to reduce the rate of photo bleaching that occurs on exposure to light. Slides were mounted in 7μl Vectorshield antifade solution (Vector Laboratories, UK) containing DAPI (Vector Laboratories, UK) and sealed with nail varnish. The slides were kept in the dark until required.

2.3.7 Analysis

Visualisation of the FISH signals was undertaken using an Axioplan fluorescent microscope (Karl Zeiss, Germany) and images were captured using a charge-coupled device (CCD) camera and MAC probe software (Applied Imaging International, UK). Copy number changes were determined by counting either the number of signals for specific probes in 200 interphase cells; or the number of signals in 100 abnormal (*RUNX1* amplified) interphase cells. The locations of specific probes on metaphase chromosomes were noted and where possible images were captured and stored. For scoring purposes, the signals on the normal chromosome 21 served as internal positive controls.

2.3.8 mBAND

mBAND is a high resolution multicolour banding technique based on region-specific chromosome paints combined with quantitative colour ratio analysis. Following micro-dissection of a specific chromosome, partial

chromosome paints are generated by labelling each individual chromosomal region with a unique combination of fluorochromes, which partly overlaps with its neighbouring one. The resulting fluorescence intensity pattern along the chromosome axis shows a continuous change of fluorochrome ratios. This allows for the assignment of pseudo colours to each of the chromosome sections with similar ratios, producing a reproducible colour banding pattern that does not depend on chromosome condensation (Figure 2.2). This quantitative ratio analysis effectively multiplies the resolution of the region specific probes.
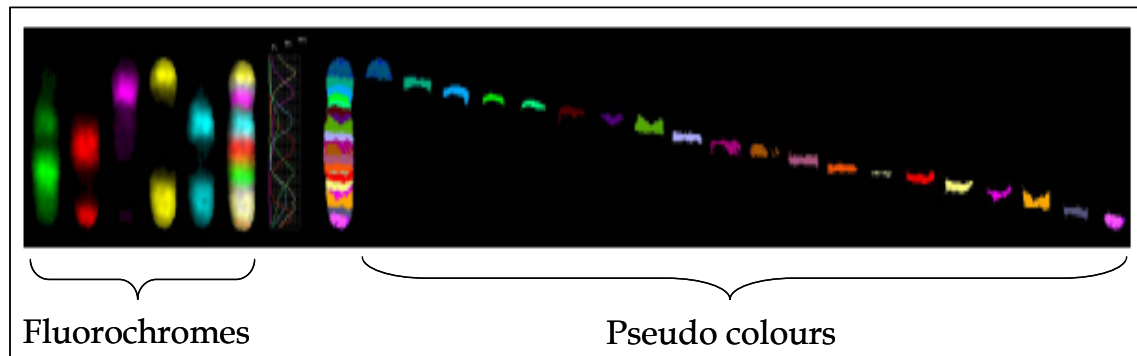
Figure 2.2 High resolution mBAND of chromosome 6. Using five different fluorochromes, 20 pseudo colour bands are generated (the ratio analysis multiplies the initial resolution of the probe kit by a factor of 3 to 4).

The Xcyte 21 mBAND probe (Metasystems®, Germany) is a mixture of two region specific areas of chromosome 21, generated by micro-dissection. The two regions are labelled with two different fluorochromes, Fluorescein (FITC) and Texas red. The partial overlap of adjacent banding probes results in seven pseudo colour regions along the chromosome. This produces a higher level of precision banding within one chromosome and improves the detection of intrachromosomal rearrangements.

This probe was chosen to specifically analyse chromosome 21 rearrangements in metaphases. Slide preparation was carried out as outlined in section 2.3.3. Hybridisation and post hybridisation washes were carried out

according to the manufacturer's instructions. Analysis of XCyte 21 mBAND probe was undertaken using a Zeiss Axioplan 2 microscope (Karl Zeiss®, Germany) and Isis capture software (MetaSystems®, Germany).

2.3.9 Sequential FISH

Rehybridisation of the same metaphase with different probes can be undertaken several times to allow for direct comparison of location of probes relative to each other in the same chromosome, as well as to confirm chromosome identification (Pinson *et al*, 2000).

Following initial hybridisation and analysis, the coverslip was gently removed and the slide immersed in 2xSSC for 1 hour. The slide was then placed in Wash 2 for 20 minutes at RT. It was then dehydrated by passing through a 70%, 85% and 100% ethanol series for 1 minute in each solution and left to air dry. The slide was then rehybridised with a new probe following the same hybridisation procedure as previously outlined (Section 2.3.4). Although this procedure may be repeated several times, the quality of the preparation deteriorates with each hybridisation.

2.4   DNA Extraction

For those samples with no DNA provided from the referral laboratory, DNA was extracted from the fixed cell suspensions using the Qiagen DNeasy tissue extraction kit (Qiagen, USA). The basic principle is; following lysis with proteinase K, the lysate is loaded onto the DNeasy Mini spin column where buffering conditions are adjusted to provide optimal DNA binding. During centrifugation, DNA selectively binds to the DNeasy membrane as contaminants pass through. Remaining contaminants and enzyme inhibitors are removed in two efficient wash steps and DNA is then eluted in water or buffer, ready for use.

Fixed cell suspensions were spun at 13000 rpm for 5 minutes, the supernatant was discarded and the pellet resuspended in 1ml of phosphate

buffered saline (PBS) (Sigma, UK). This step was repeated to ensure that all the fixative was removed. The resulting pellet was resuspended in 200 µl PBS, 20µl proteinase K followed by 200µl Buffer AL were added to the sample which was thoroughly mixed by vortexing and incubated at 56˚C for 10 minutes. After incubation, 200µl 100% ethanol was added to the sample and mixed.

The mixture was pipetted into a DNeasy Mini spin column placed in a 2ml collection tube and centrifuged at 8000 rpm for 1 minute. The collection tube and flow were discarded. The column was placed into a second collection tube and 500µl buffer AW1 added, followed by centrifugation at 8000 rpm for 1 minute. The collection tube and flow through were discarded. The column was placed into a new collection tube and 500µl AW2 added. It was then centrifuged at 14000 rpm for 3 minutes. The collection tube and flow through were discarded and the column placed into a clean microcentrifuge tube and 200µl Buffer AE was pipetted into the column. This was left for 1 minute before spinning at 8000 rpm. The eluted DNA was collected, placed onto the column and the elution stage repeated.

2.4.1 DNA concentration

The quality and concentration of the DNA was determined using a Nanodrop spectrophotometer. The quality of extracted DNA, as measured by the ratio of the absorbance values at A260nm/A280nm, should be between 1.7-1.9 and the absorbance scans should show a symmetric peak at 260 nm, confirming high purity.

2.4.2 Gel electrophoresis

The quality of DNA can alternatively be assessed using gel electrophoresis. The principle of the technique relies on DNA being separated by differential migration through agrose gel. When an electric current is applied to the gel, the negatively charged DNA will migrate towards the cathode. The smaller molecules migrate faster through the polymer than the larger ones. To

visualise the DNA, ethidium bromide is added, which fluoresces under UV light. A 1% agarose gel was prepared by heating 0.5gm agarose (Sigma, UK) in 50ml 1x Tris-borate buffer (Sigma, UK) in a microwave. Following cooling 0.4mls Ethidium bromide (Sigma, UK) was added and the liquid gel poured into a gel tank fitted with an appropriate sized comb. Once set, the gel was immersed in TBE buffer (Appendix 2) and the comb removed. 8μl test DNA mixed with 2μl of loading dye was loaded into the appropriate lane. To allow for a quantitative comparison, a 1kb DNA ladder was loaded into a lane at the end of the comb. The gel was run at approximately 80 volts for 20 minutes and the bands were visualised using a UV transilluminator. Good quality DNA will have a sharp band whilst poor quality degraded DNA will produce bands that appear smeared.

2.5   Array-based Comparative Genomic Hybridisation

Array-based comparative genomic hybridisation (aCGH) is a sophisticated molecular technique that is used to identify and characterise DNA copy number alterations at the genome level. Two samples of genomic DNA, a test DNA and a reference DNA, are differentially labelled with fluorescent dyes and hybridised to known mapped genetic sequences spotted onto a glass slide (Figure 2.3) (Pinkel *et al*, 1998). The intensity of the different fluorochromes is measured and a CGH profile of each chromosome generated from the log2 fluorescent ratios. Regions in which there is no deviation from the normal will have a ratio of 0, whilst those regions with duplications will have positive ratio values. Conversely those with deletions will have negative ratio values. The signal intensity is not a direct measure of copy number, rather an arbitrary value, thus an alternative method, for example FISH, is required to confirm the actual DNA copy number. The resolution of the array platform is variable depending upon the design. Initial designs were based on BAC clones. The clones in these platforms were approximately 200kb long and usually each platform contained

on average 3000 clones, spaced approximately 1Mb apart. Although they provided precise identification of the chromosomal regions involved in the copy number change, their resolution was insufficient to identify aberrations within specific genes. To overcome this limitation, oligonucleotide probes have been developed, which have a higher resolution to the level of 6kb. Agilent oligonucleotide Human Genome CGH Microarray Kits 185A and 244A (Agilent, UK) were chosen for the study of two patients with amplification involving both chromosomes 15 and 21.
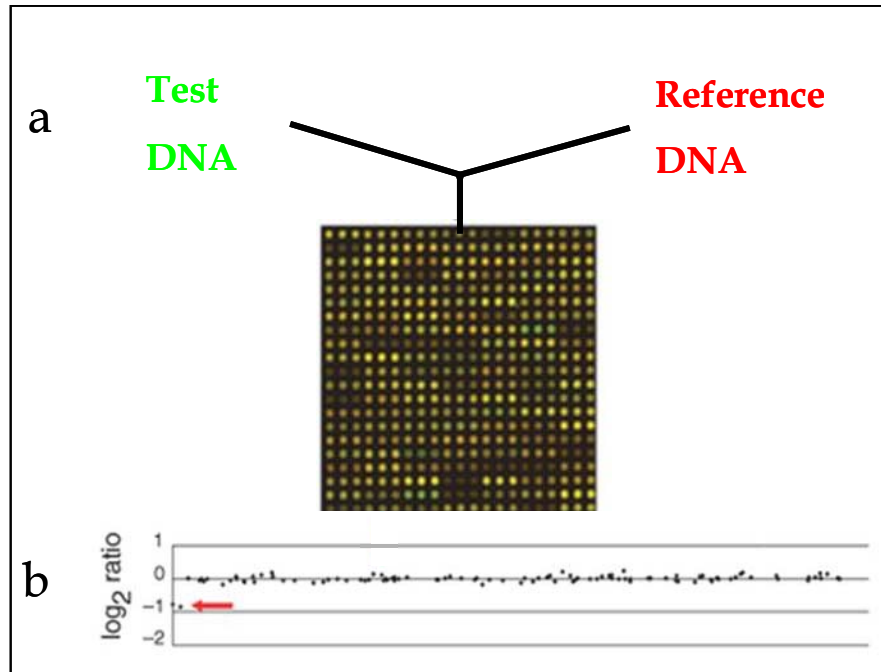
Figure 2.3 An overview of aCGH. a) Genomic DNA from test and control are differentially labelled and hybridised to a microarray. The fluorescent ratios of each array spot are calculated and normalised so that the median log2 ratio is 0.b) Plotting of the data for chromosome 9 shows that most spots have a ratio near 0. However, the spots nearest pter (red arrow) have a ratio of -1, indicating a deletion. Adapted from Pinkel (2005).

2.5.1 Sample Preparation

2.5.1.1   Restriction Digestion

Using the Agilent Human Genome CGH Microarray Kit (Agilent,UK) patient gDNA and sex matched commercial reference gDNA (Promega, UK) at a concentration of 1.5ug were made up to a total volume of 20.2µl with nuclease-free water, in separate microcentrifuge tubes. The tubes were placed on ice and to each 2.6µl 10xBuffer C, 0.2µl Acylated BSA, 0.5µl each of *Alu1* and *Rsa 1* enzymes and 2µl nuclease-free water (digestion master mix) were added. Samples were incubated in a 37°C water bath for 2 hours. The tubes were transferred to 65°C for 20 minutes to stop the reaction by inactivating the enzymes. 5µl 10x Random Primers were added to each reaction tube. Tubes were

transferred to 95°C hot block for 3 minutes then moved to ice for a further 5 minutes.

2.5.1.2   Sample Labelling

The Agilent gDNA kit uses random primers and an exonuclease free Klenow fragment (a genetically engineered enzyme in which the 3′ to 5′ exonuclease activity has been removed) to differentially label the gDNA with fluorescently labelled nucleotides. The test sample is labelled with one dye whilst the reference is labelled with another. To each tube, 10µL 5x Buffer, 5µL 10x dNTP and 1µL Exo-Klenow (labelling master mix) (Agilent, UK) were added followed by: to the test gDNA 3µL Cy5-dUTP and to the reference gDNA 3µL Cy3-dUTP. The fluorescent labelled dyes are light sensitive, thus should have minimum exposure to light. The samples were mixed well by gentle pipetting, incubated at 37°C for 2 hours and the reaction stopped by transferring to a water bath at 65°C for 10 minutes. Following incubation samples were transferred to ice.

The samples were purified using Micron centrifugal filter devices. To each tube 430µl 1xTE Buffer (Appendix 2) was added and mixed using gentle pipetting. A Micron YM-30 filter was placed into a pre labelled 1.5ml microcentrifuge tube and loaded with either the test gDNA or reference gDNA. The tubes were spun at 6.5 rpm for 10 minutes and the flow through discarded. This step was repeated with the flow through again being discarded. The columns were inverted and placed into fresh microcon tubes. Tubes were spun at 6.5 rpm for 1 minute. The volume of each eluate was determined, if it was ≤ 80.5µl, sufficient nuclease free water was added to make the final volume 80.5µl. If the volume was ≥ 80.5µl the eluate was returned to the column and spun at 6.5 rpm for 1 minute as previously described. The two samples were combined to give a total volume of 161µl.

2.5.2 Array processing

2.5.2.1 Hybridisation

To the combined sample, 50µl Cot-1-DNA, 52µl 10x Blocking Agent and 260µl Agilent 2x Hybridization buffer (Agilent, UK), was added and the sample gently mixed. The tubes were pulse spun before being placed on a hot block at 95°C for 3 minutes. Immediately the tubes were transferred to 37°C water bath for 30 minutes. Following incubation, the samples were removed from the water bath and spun at 13000 rpm for 1 minute. A pre-labelled gasket slide was loaded into the Agilent SureHyb chamber with the gasket label face up. Slowly 490µl suspension was dispensed onto the slide. The slide was placed onto the SureHyb chamber, ensuring that the active side was face down. The chamber cover was positioned over the slide and secured in place. The assembled chamber was rotated to wet the slide and ensure that no stationary air locks were present. This was then placed into the hybridisation oven at 65 °C and rotated at 20 rpm for 40 hours.

2.5.2.2 Post-hybridisation washes

Excess unbound test and reference gDNA is removed by post hybridisation washes. At the same time it is important to stabilise and dry the hybridised array slide. As Cyanine 5 is sensitive to ozone degradation, stabilisation and drying solutions have been designed to minimize the ozone induced degradation.

The required volume of Wash Buffer 2 (Agilent, UK) was pre-warmed in a 37°C water bath overnight. If the stabilisation and drying solution showed a visible precipitation, this too required pre-warming at 37°C overnight. Five slide staining tanks were filled with the following solutions;

- Tank 1 - Wash Buffer 1

- Tank 2 - Wash Buffer 1 filled to a sufficient level to cover a slide rack

- Tank 3 - Wash Buffer 2 at 37 ˚C

- Tank 4 - Acetonitrile (Sigma, UK)

- Tank 5 - Stabilisation and Drying Solution (Aglilent, UK)

In addition to the solutions, tanks 2-5 contained a magnetic flea and all four tanks were placed on a magnetic stir plate which was set at a speed of level 3. The slide was removed from the SureHyb chamber and placed in tank 1. Whilst submerged in the wash, the slides were gently prised apart, and placed into the slide rack before being quickly transferred to tank 2. The slides were left for 5 minutes before being transferred to tank 3, where they were left for 1 minute. The rack was transferred to tank 4 and left for 1 minute. Finally the rack was transferred to tank 5 for 30 seconds. Very slowly the slides were removed from the tank, taking care to ensure that there were no droplets on the slide. The slides were than scanned on an Agilent scanner using the default scan settings. The scan resolution was set to 5μm as recommended for 244k density arrays.

2.5.3 Data Extraction

The Feature Extraction (FE) software version 9.1 (Agilent, UK) converts the tiff images obtained from the scanner into a reduced representative set of features, which are required to describe a large set of data accurately. The arrays were then analyzed using the Agilent CGH Analytics 3.4.27 software, which is based on the UCSC May 2004 assembly (HG17). The ratio of the fluorescent intensity of the test gDNA compared to the reference gDNA was calculated and averaged for each replicate before being converted to a log ratio, which was then normalised using z-scoring, with the modal ratio of the array being set to zero. Aberrant regions were identified for each point in the data by calculating the

moving average within a 2Mb window. Outliers were classified using a cut off of +/- 0.25.

Following the initial identification of a deviation, the data was then subjected to an aberration detection method 1 (ADM-1) algorithm (which takes into account the number of probes in an aberrant region as well as the extent of their deviation from zero) to give a true estimation of the aberrant section. Five consecutive deviant spots were required for an aberrant call.

2.6   Quantitative PCR (Q-PCR)

The standard polymerase chain reaction (PCR) is a method for amplifying in vitro a specific target DNA sequence present within a heterogenic DNA sample. Two oligonucleotide primers (one forward and one reverse), specific for a target sequence, are added to a denatured template DNA. They bind to complementary DNA sequences at the target site and in the presence of a heat-stable DNA polymerase (Taq) and DNA precursors, initiate the synthesis of new DNA strands, complementary to the target DNA segment. This newly synthesized DNA strand then acts as a template for further DNA synthesis in subsequent cycles, so allowing for the exponential amplification of the target DNA. The reaction consists of three main steps:

- Denaturation, typically at about 93–95˚C for human genomic DNA.
- Reannealing at temperatures usually from about 50˚C to 70˚C.
- DNA synthesis, typically at about 70–75˚C.

PCR techniques can be used to quantify DNA in an optimised reaction as the quantity of target DNA will approximately double during each amplification cycle. By linking the amount of amplified product to a fluorescent reporter molecule and measuring the subsequent fluorescence intensity, it is possible to calculate the quantity of the initial DNA. The florescence signal can be measured

either at the end of the reaction (endpoint PCR) or during the reaction real time (RT-PCR).
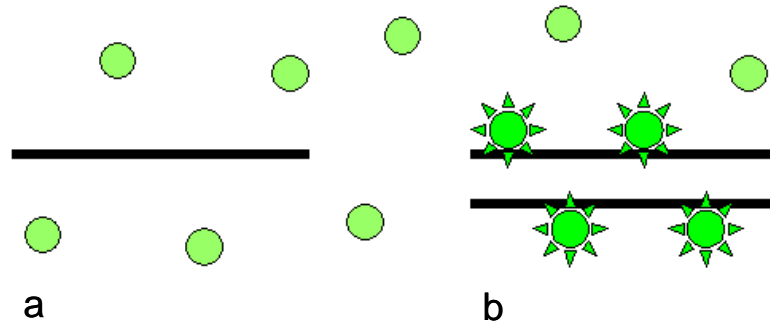
Figure 2.4 SYBR® Green detection mechanism. Double-stranded DNA (dsDNA) in the reaction is bound by the dye. In the bound state (b), SYBR® Green is 1000fold more fluorescent than in the unbound state (a) As PCR amplification increases the amount of dsDNA present, the fluorescence signal increases proportionately.

2.6.1 Relative quantitative PCR (Q-PCR)

Real time quantitative PCR (Q-PCR) measures the fluorescence level at each cycle of the PCR amplification phase. Using the double stranded DNA binding dye SYBR® Green as a fluorescent reporter molecule, it is possible to monitor the progress of each PCR cycle, as the intensity of the fluorescence increases proportionally to the increased target DNA concentration. The first cycle at which the fluorescence intensity is above that of the background (threshold cycle "Ct") can be directly correlated to the starting concentration of the sample.

Often the absolute value of the target DNA is not required, rather the amount of target DNA relative to a reference DNA sequence. Relative quantitative RT-PCR compares the ratio of a target DNA to a reference DNA sequence in an unknown sample and the ratio of the same two sequences in a

standard sample. The results are expressed as the fold-change of the target DNA relative to the standard.

Using relative quantification Q-PCR it is possible to generate reliable results that can be compared between different samples and different experimental systems. Q-PCR was chosen to establish the relative amounts of three genes, *STCH*, *RUNX1* and *PRMT2* located on chromosome 21. *CYP27C1* was used as the house keeping gene located to the long arm of chromosome 2. All primers used in the relative quantification RT-PCR are presented in Appendix 2.

2.6.1.1   Q-PCR method

The following master mix was prepared (volumes given for a single reaction):

- 0.4 µl 10x Buffer (Invitrogen, UK)
- 0.4 µl dNTP mix (Promega, UK)
- 0.3 µl MgCL2 (50mM) (Invitrogen, UK)
- 0.5 µl primer mix (0.5 µM; MWG, Germany)
- µl SYTO 9 (5µM; Invitrogen, UK)
- 75 µl PCR grade H_2O
- 0.05 µl Taq (Invitrogen, UK)

For each reaction, 2µl of sample DNA at a concentration of 5ng/µl was added to the master mix. For the negative control, an equal volume of PCR grade H_2O was added to the master mix in place of the sample DNA.

The PCR reactions were performed on a Roche Light Cycler 480 system. A 96-well plate was designed to include six patient samples, a negative control and a normal male genomic DNA (Promega, UK). Each sample was run in triplicate and the plate design was such that for each sample all four primers were run on a single plate.

10μl PCR mix was added to each well. The plate was sealed with a clear plastic film to prevent evaporation and pulse spun to ensure that the reaction mix was positioned at the bottom of the plate. Plates were loaded into the analyser and the cycling conditions were set as follows:

1 cycle:

95˚C 10 mins to activate the Taq enzyme followed by 40 cycles:

- 95˚C 15 seconds
- 60˚C 30 seconds
- 72˚C 30 seconds
- 4˚C hold

Results were analysed using the LightCycler 480 Relative quantification Software.

2.7   Multiplex Ligation-dependent Probe Amplification

Multiplex Ligation-dependent Probe Amplification (MLPA) (Figure 2.5) is a novel molecular technique able to detect copy number changes of up to 45 different target nucleic acid sequences in a single PCR reaction (Schouten *et al*, 2002). For each specific DNA target sequence, a complementary MLPA probe is designed, consisting of two oligonucleotides that hybridise to sites immediately adjacent to each other. Attached to the 5′ end of one of the short synthetic oligonucleotides is the forward PCR primer, whilst at its 3′ end is the target DNA hybridizing sequence. The second oligonucleotide has a hybridizing sequence at its 5′ end and the complementary (reverse) PCR primer at its 3′ end.
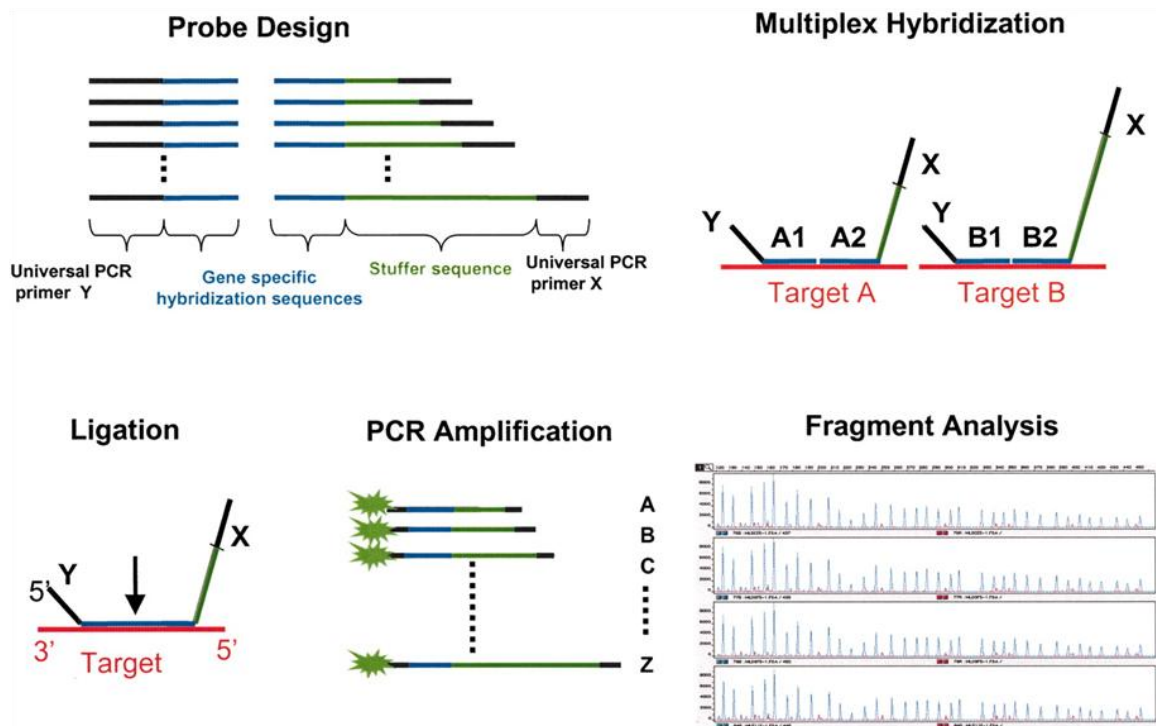
Figure 2.5 Schematic outline of MLPA reaction. Adapted from Hogervorst *et al* (2003).

Following hybridisation of the MLPA oligonucleotides with the target, the two parts of the probe are ligated by a specific ligase enzyme. This reaction is precise and only those probes that are directly adjacent to one another will ligate (this allows for the detection of sequences that differ from one another by only a single nucleotide at the site of ligation). After the ligation reaction, the resulting fragment contains both PCR primer sequences which amplify exponentially during the subsequent PCR reaction. Any oligonucleotides that are not ligated contain only a single PCR primer sequence and so will not be exponentially amplified.

Each MLPA probe is designed to give rise to an amplification product of a unique size, with the total size range between 120-480 nucleotides for each of the different target sequences. This is achieved by the addition of a sequence which does not hybridise to the target sequence known as a 'stuffer' sequence (Figure

2.6). This sequence usually increases in length by 6 - 9 nucleotides between probes. The size range of the probes is optimal for fragment separation and low background levels. These fragments are detected and quantified by capillary gel electrophoresis. By comparing the profiles obtained from the test sample to a control, it is possible to calculate the relative copy number of a specific target sequence.

2.7.1 Synthetic Probe Design

Commercial MLPA kits are available from MRC-Holland for a wide range of disorders and specific gene characterisations. These kits can be enhanced by the addition of home designed probes in order to tailor the target areas to a specific query. The process involved in designing a synthetic probe follows a number of stages:

The region of interest is determined and a specific target selected using one of the following websites:

http://www.ncbi.nlm.nih.gov

http://www.ensembl.org/index.html

For each target DNA area of interest, a 48 base pair region is selected.

This sequence is checked for single nucleotide polymorphisms (SNPs) to rule out polymorphisms and run through a Blast program to ensure that it is unique in the genome.

The probe is then designed using the following criteria:

The total length should be evenly spread over right side probe oligo (RPO) and the left side probe oligo (LPO) to avoid too long oligonucleotides (Figure 2.6). Each hybridising sequence should be 24 base pairs in length and approximately 50% GC rich. When synthetic probes are used with an existing MRC-Holland kit, they are usually designed to fit into the gap at the start of the kit. The total probe length (LPO + RPO, plus a 42 base pair of primers) is between 96-130 bp, with a minimum length difference between probes of 4 base pairs. In order to achieve

the correct length a stuffer sequence may be inserted between the hybridising sequence and the PCR primer sequence. This stuffer sequence is inserted into the RPO and is uncomplimentary to the sequence following the 48 bp target (by swapping A with C and G with T this part of the sequence will not bind as the purines will be opposite purines and pyrimidines opposite pyrimidines).

The RPO requires a 5′ phosphate group added to its 3′ end to allow for ligation. For each target DNA a 5′ and 3′ primer sequence is required;

LPO GGGTTCCCTAAGGGTTGGA

RPO TCTAGATTGGATCTTGCTGGCAC

These are the binding sites for the MRC- Holland primers which are supplied with the SALSA MLPA kit. One of the PCR primers in the MLPA kit has a fluorescent label in order to allow for detection of the PCR products.
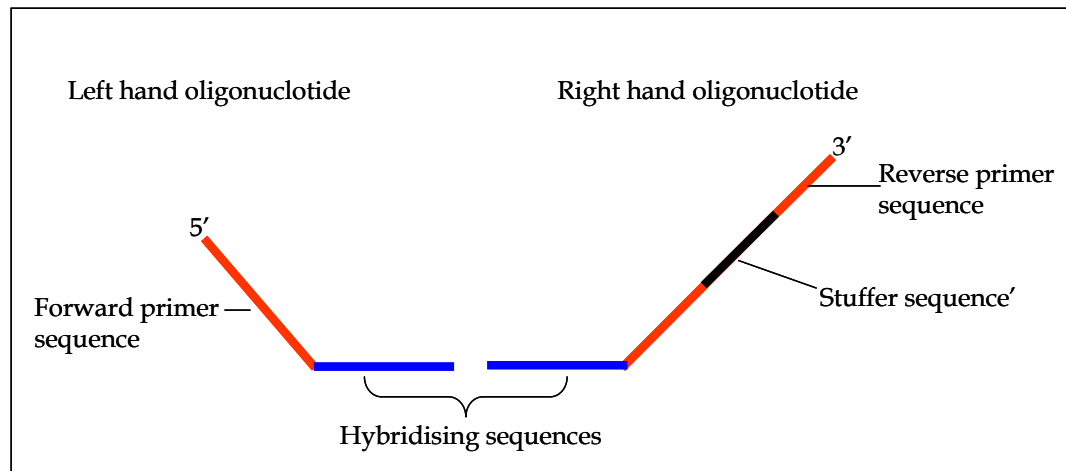
Figure 2.6 MPA probe design. Red lines indicate the forward and reverse primer sequences; blue lines = hybridisation sequences and black = stuffer sequence.

The self design probe oligonucleotides were obtained from Thermo-Hybaid (Germany). These probes were diluted with TE buffer to give a

71

concentration 0.00133µM and denatured in a total volume of 3.5µl as outlined in section 2.7.2. When making up the probe mix for the overnight hybridisation (Section 2.7.2) a master mix containing 1.5µl each of MLPA buffer, the commercial MRC probe mix and the synthetic probe was prepared. 4.5µl of this was added to the denatured DNA. The protocol as outlined in section 2.7.2. was then followed.

2.7.2 Sample Denaturation and hybridisation

3.5µl of test gDNA diluted with TE (Appendix 2) to a concentration of 30ng/ml was added to a 200 µl PCR tube. The tubes were briefly spun to collect DNA in the bottom of the tube and a drop of mineral oil placed on the top to prevent evaporation and condensation during denaturation and hybridisation. The tubes were placed in a PCR thermal cycler and denatured at 98˚C for 7 minutes. The samples were then cooled to 25˚C and 4.5µl master mix containing 1.5µl MLPA buffer, 1.5µl commercial MLPA probe mix (to provide control probes for comparison) and 1.5µl homemade probe mix (section 2.7.1) was added to each reaction tube. The samples were mixed well by pipetting up and down. The reaction tubes were heated to 95˚C for 1 minute cooled to 60˚C and left to hybridise over night (a minimum of four hours is required).

2.7.3 Ligation reaction

Ligase buffer master mix was prepared by mixing 3µl Ligase buffer A with 3µl Ligase buffer B and 25µl dH$_2$O. Mixed by vortexing and prior to use 1µl of Ligase-65 added (Ligation-65 mix can be made 1 hour prior to use and stored on ice). The temperature of the thermal cycler was reduced to 54˚C and 32µl Ligase-65 mix added to each sample, mixed well by pipetting up and down. The sample was incubated for 23 minutes at 54˚C, then heated for 5 minutes at 98˚C to denature the ligase, before cooling to 4˚C. The two MLPA probes were then ligated and at this point the ligate can be stored at -20˚C for one week.

2.7.4 PCR reaction

On ice the following master mix was prepared (volumes given for a single reaction):

1μl of SALSA PCR-primers

- 2μl of SALSA buffer
- 1μl l of Enzyme buffer
- 15.75μl of dH$_2$O

Mixed well before adding 0.25μl of SALSA polymerase.

To a clean pre labelled PCR tube 20μl of the above master mix was added together with 5μl of ligate and mixed gently. The tubes were placed in the PCR thermal cycler and the cycling conditions set as follows:

33 cycles:

- 95˚C 30 seconds
- 60˚C 30 seconds
- 72˚C 60 seconds

Followed by

- 72˚C for 20 minutes
- 4˚C hold

2.7.5 Separation of amplification products by electrophoresis

Following PCR, the products were separated on an ABI 3100 genetic analyzer. For each sample 1μl PCR product was mixed with 9μl deionized formamide and 0.1μl Genescan-500 ROX standard (Applied Biosystems, USA). The samples were run using the GeneScan POP 3100 module.

2.7.6 MLPA Data Analysis

Peak areas were exported to an Excel spreadsheet (Microsoft, USA), designed to assess the ratios of each test peak relative to all other peaks for that individual. Ratios of target peaks to other peaks in each patient sample were compared with the same ratios obtained for 2 healthy individuals, included in each run. For normal sequences, a dosage quotient of 1.0 is expected; if a single deletion or duplication is present the dosage quotient should be 0.5 and 1.5, respectively. For multiple duplications, each extra copy will increase the ratio by 0.5, e.g. a triplication will have a relative ratio of 2.

2.8 G-Banded review

The principle behind G-banding is that following enzymatic treatment or denaturation of metaphase chromosomes, application of Giemsa (a DNA specific dye) stains the chromosomes in such a way as to produce crossways patterns of light and dark bands. These bands are unique to each chromosome pair. They are thought to reflect the differences in base composition, replication time, chromatin conformation and gene density within the chromosome. The dark G-bands are rich in condensed heterochromatin, have a higher concentration of adenine-thymine (AT) base pairs and are late replicating, whilst the pale or light bands have fewer condensed structures, a higher concentration of cytosine-guanine (CG) base pairs and are early-replicating. The pale areas are gene rich and so are transitionally more active than the dark bands (Czepulkowski, 2001).

Conventional cytogenetic analysis of the diagnostic bone marrow samples was carried out by the UK regional cytogenetic laboratories. Karyotypes, written according to the International System of Human Cytogenetic Nomenclature, were collected through the LRUKD and entered into the LRUKD database (ISCN, 2005). G-banded slides from iAMP21 patients with an abnormal karyotype were requested, and the morphology of the dup(21) reviewed. Where possible the appearance of the dup(21) chromosome was observed in ≥ 5 abnormal

metaphases and classified into one of five groups (Table 1.3) based on their morphology. Karyograms were generated using MacKtype® software (Applied Imaging International, UK). Karyotypes of all iAMP21 patients were collected from the LRUKD database.

Chapter Three - Results
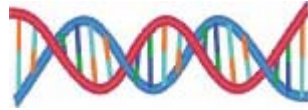
3 Results

3.1   Identification of Patients to Include in Study

3.1.1 Introduction

A review of the literature in which patients with iAMP21 were described (section 1.6.3) disclosed, that in the majority of studies, patients had been identified by chance, during screening for the *ETV6-RUNX1* fusion using FISH probes specifically designed for this purpose. In those cases where *RUNX1* copy number had been established, the number of signals was ≥ 5, with three or more of the signals being localised to a dup(21) chromosome composed entirely of chromosome 21 material (Harewood *et al*, 2003;Soulier *et al*, 2003). In those patients with no metaphases available to confirm the presence of a dup(21), the *RUNX1* copy number by interphase FISH was used to define the abnormality (Najfeld *et al*, 1998;Mikhail *et al*, 2002). In these cases it was usual to see the signals displayed in a characteristic cluster together with a single signal, assumed to represent the normal 21, located apart (Figure 3.1). To date, there are no reports of patients with ALL and amplification or over representation of chromosome 21 on a single marker chromosome, which do not involve amplification of the *RUNX1* gene. However, it has not been clearly established if these were accurate findings or a reflection of selection bias, incurred by only selecting cases based on *RUNX1* copy number. Therefore, before using these criteria to select the patients to be included in this research, it was important to determine that selection would not be biased by the use of FISH to select iAMP21, when there may be other cases with dup(21)/iAMP21 involving other regions of chromosome 21 amplification. To address this problem, patients not previously identified as iAMP21 were selected by their cytogenetic result, having

a distinctive marker chromosome and the associated loss of one copy of a normal chromosome 21. Their *RUNX1* copy number was determined using FISH.
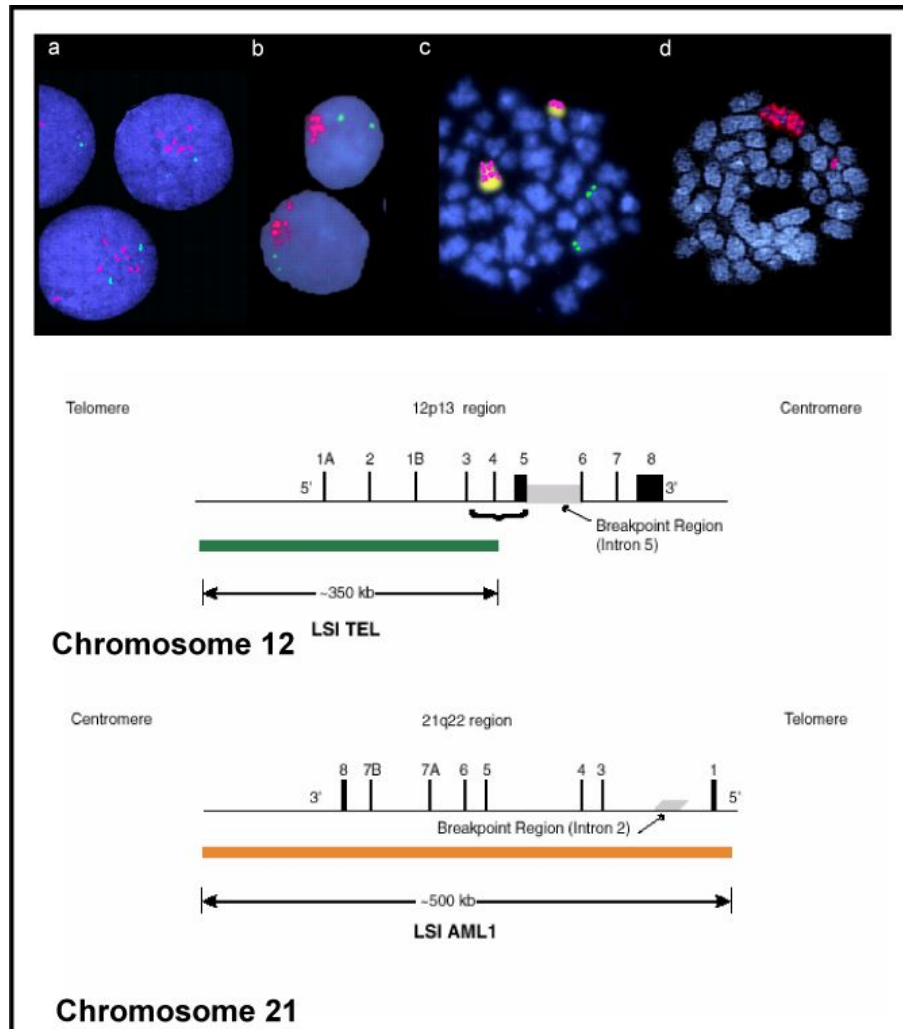
Figure 3.1. Vysis LSI TEL-AML ES®. (a,b) Vysis LSI TEL-AML ES® hybridised to interphase nuclei from patients 4623 and 3956, respectively. The *RUNX1* (AML1) signals are red and the TEL (*ETV6*) green). The *RUNX1* signals cluster in a distinct pattern with the normal chromosome 21 represented by a single red signal located apart from the cluster. (c) Probe on metaphase from patient 3368. The dup(21) and normal 21 are painted (yellow) with WCP 21. (d) Cosmid probes to *RUNX1* exons 1-5 (ICRF C0664) and exons 5-7 (ICRF HO8116) on patient 7980. The *RUNX1* exon signals (labelled red) are arranged in tandem along the dup(21). (e) Vysis LSI TEL-AML ES® probe design. Adapted from Robinson *et al.*(2007)

One important consideration is that, although currently iAMP21 is defined by the presence ≥ 5 *RUNX1* signals in interphase, not all patients with this copy number have iAMP21. Previous studies have shown (Moorman *et al*, 2003;Sutcliffe *et al*, 2005;Heerema *et al*; 2007) that pentasomy of chromosome 21 may occur in high hyperdiploid ALL, although to a much lesser extent than tri- or tetrasomy 21. Isochromosome 21 [i(21)(q10)] has been described in BCP-ALL at an incidence of 1.4% (Martineau *et al*, 1996). In these cases one copy of a normal chromosome 21 is replaced by an i(21)(q10) involving a duplication of the whole long arm of chromosome 21. Occasionally, the isochromosome is duplicated, resulting in pentasomy for 21q. In both of these cytogenetic subgroups, FISH with the *RUNX1* probe will result in a copy number of 5 signals. This raised the question: if cases with high hyperdiploidy, i(21)(q10) and those with additional copies of intact chromosome 21 with a *RUNX1* copy number of ≥ 5 are excluded from the selection, are the remaining cases exclusively iAMP21? To address this issue, a number of cases previously screened with the Vysis LSI TEL-AML ES® probe were reviewed to establish the incidence of those cases with ≥ 5 *RUNX1* signals and determine their karyotypic origin.

3.1.2 Method

A retrospective search of the LRUKD cytogenetic database was undertaken in order to identify potential iAMP21 cases for study. As this abnormality has previously been associated with childhood ALL (Harewood *et al*, 2003;Soulier *et al*, 2003) , the search was initially restricted to patients registered to the childhood UKALL97 treatment trial. As none of the previously reported cases had included known recurrent chromosomal abnormalities, this was taken into consideration when designing the selection criteria. To ensure that cases were accurately identified, irrespective of their *RUNX1* copy number, the search was divided into two phases:

1. To identify patients with chromosome 21 abnormalities based on their G-banded karyotype.
   - They were selected if their karyotypes contained one of the following abnormalities:
     - -21, +mar
     - add(21)
     - dup(21)
     - der(21)
   - They were excluded if they were:
     - high hyperdiploid
     - near haploid/low hypodiploid
     - i(21)(q10) positive by cytogenetics
     - *ETV6-RUNX1* fusion positive
     - *BCR-ABL1* fusion positive
     - Positive for a *MLL* gene rearrangement

2. To identify patients with additional copies of *RUNX1* detected by FISH:
   - Cases were selected if their interphase cells had ≥ 5 *RUNX1* signals by FISH as well as having a successful karyotype.
   - They were excluded if:
     - The *RUNX1* copy number corresponded to the number of copies of chromosome 21, which would include high hyperdiploidy, near-haploidy, low hypodiploidy
     - The karyotype included an i(21)(q10)
     - They were
       - *ETV6-RUNX1* fusion positive
       - *BCR-ABL1* fusion positive
       - Positive for a *MLL* gene rearrangement

Cases identified from Search 1 were further investigated by FISH with the LSI TEL-AML ES® (Vysis, UK) probe and chromosome 21 WCP to establish the copy number and chromosome location of the *RUNX1* gene.

Prospective screening, using the selection criteria applied to Searches 1 and 2, was carried out on new cases entered to the LRUKD database to increase the number of patients available for study.

3.1.3 Results

Of 2094 cases registered to the childhood ALL treatment trial, UKALL97, and the LRUKD database, 2083 had a successful result from either G-banded analysis and/or FISH. Among these cases, 1205 had abnormalities of chromosome 21. Twelve patients were identified (Appendix 3, Table A3.1) with a marker associated with the loss of one copy of a normal chromosome 21. In six of these patients the description of the marker chromosome morphology in the karyotype was similar to that previously used to define iAMP21 (Table 3.1). In three of these patients (2647, 2904, and 3767), material was available to test for *RUNX1* involvement. No slides were available for review on one case (5661) in which an add(21) had been described. In another patient (2647) two copies of a derivative chromosome 21 were present which had replaced the two normal copies of chromosome 21. In case 2848, previous studies had confirmed that the add(21) was composed entirely of chromosome 21 material using WCP 21; however insufficient material was available to test for the involvement of *RUNX1*. In case 5661, FISH confirmed *RUNX1* amplification in interphase cells, although no metaphases were seen. In two cases (2848 and 2752) the involvement of *RUNX1* could not be established.

FISH with the LSI TEL-AML ES® (Vysis, UK) probe indicated *RUNX1* involvement with ≥ 5 copies scored for all four patients.

Patient ID	RUNX1 copy No	dup(21) morphology	Abnormal Karyotype
2647	7	SA	47,XY,+X,dup(21)(q11q22),dup(21)(q11q22)[7]
2752	NM	LM	46,XX,add(9)(q34),del(11)(q23),der(18),t(18;20) (q25;p1?1),der(20)t(11;20)(q?;p?),add(21)(q22)[3]
2848	NM	SA	46,XY,add(21)(q11)[7]
2904	9	LA	46,XX,del(7)(q22q32),add(21)(q22)[16]
3767	5	LM	46,XX,+X,dup(21)(q?)[2]
5661	5	NA	47,XX,+X,del(11)(q?),add(17)(q?),add(21)(q?),inc[cp10]
4746	5	rea(21)*	50,XY,+X,+14,der(20)t(20;21)(q13;q?),rea(21), +rea(21)x2[16]
5047	5	add(21)	47,XX,+X,-8,-17,-17,add(21)(q?2),+3mars[cp5]

Table 3.1 Karyotype, marker chromosome 21 morphology and *RUNX1* FISH copy number of patients identified as being potential iAMP21 patients from the G-banded review. NM: no material. *Although rea is not a currently accepted ISCN abbreviation, it is used here as there is no other appropriate description for these chromosomes.

In the six patients not listed in Table 3.1, the morphology resembled a standard duplicated chromosome 21 in three patients, loss of chromosome 21 in two, and in a single case no slides or material were available to review.

Search 2 identified a total of 32 patients, of which 30 had been previously defined as iAMP21. In the two additional cases (4746 and 5057, Table 3.1), although the *RUNX1* copy number was consistent with iAMP21, the signal location and the karyotype, in relation to chromosome 21, was not. These cases are described in more detail in section 3.3.2.

3.1.4 Conclusion

Searching for patients with iAMP21 based on their G-banded morphology identified six patients. In four of these cases with material available, FISH detected *RUNX1* amplification. In partial support of the abnormality being iAMP21 in one case with no available material, WCP 21 had previously shown

that the marker was composed entirely of chromosome 21 material. Although it was not possible to test all six cases by FISH, this study did not detect a marker chromosome 21 without *RUNX1* amplification. These results, coupled with those of previous studies (Niini *et al*, 2000), established that *RUNX1* is always amplified in iAMP21. Thus, we were able to conclude that selection of patients on the basis of *RUNX1* copy number, using the criteria outlined above, was appropriate to identify cases in an unbiased fashion for inclusion in this study.

Screening for cases with ≥ 5 *RUNX1* signals identified 30 patients previously defined as iAMP21 and two additional cases. These may represent morphological variants, as discussed under a separate heading (Section 3.3.2).

3.2   Characterisation of the iAMP21 chromosomal abnormality

3.2.1 Introduction

The characterisation of high-risk cytogenetic groups in ALL is important in order to ensure their correct classification and appropriate risk group stratification. Although the involvement of *RUNX1* in iAMP21 patients has been clearly demonstrated by a number of studies (Section 1.6.3), the contribution of other genes located within the amplified region of the abnormal chromosome 21 is unclear. Thus iAMP21 remains unclassified at the molecular level and the initiating mechanism is unknown. Previous reports (Le Coniat *et al*, 1997; Niini *et al*, 2000;Busson-Le Coniat *et al*, 2001) have demonstrated that regions both centromeric and telomeric of *RUNX1* were also amplified. To investigate the extent of the chromosome 21 involvement in iAMP21, a profiling study was designed to screen a number of patients with probes spanning the length of chromosome 21 using a combination of FISH and BAC array comparative genomic hybridisation (BAC aCGH). The FISH profiles were qualitatively compared to those derived from complementary BAC aCGH.

3.2.2 Method

Ten patients, previously identified as iAMP21 with the commercial LSI TEL-AML1 ES® probes were selected. A further two BCP-ALL patients, one with tetrasomy of chromosome 21 in a high hyperdiploid karyotype and one with an apparently normal karyotype (6899, 6009, respectively) were included as control samples. BAC clones were selected to use as FISH probes which corresponded to those covering chromosome 21 in the 32k BAC aCGH system (Spectral Genomics, Genosystems®, France). This BAC array comprises twenty six clones located along chromosome 21q, starting at the centromeric genomic position of 15.1Mb, terminating at the telomeric genomic position of 46.9Mb and spanning the chromosome bands 21q21-q22. The clones were positioned approximately 1Mb apart. To allow direct comparison, 21 of the same BAC clones as spotted onto the arrays were used as locus specific FISH probes (Genosystems®, France) (Appendix 3, Table A3.2) to determine copy number changes along the length of chromosome 21. Two additional probes were included: a commercial chromosome 21q subtelomeric probe, Tel21q (D21S1446) (Molecular cytogenetics, Qbiogene®, UK), and the LSI TEL-AML1 ES® probe (Vysis, UK). These probes were selected to detect copy number changes in the subtelomeric region and at the *RUNX1* locus of the derivative chromosome 21. The number of signals in interphase cells was recorded for each clone. Amplification was defined as ≥ 5 signals, whilst gain was defined as 3 or 4 copies. Where a range of signals was observed at any one clone position, the modal number was recorded and the range of signals noted. DNA was available to carry out BAC aCGH on seven patients. The BAC array work was carried out by Dr Jon Strefford, (Leukaemia Research Cytogenetic Group [LRCG]) as part of an ongoing molecular investigation of iAMP21 patients. A qualitative comparison of the profiles obtained from the two techniques was made.

3.2.3 Results

3.2.3.1 Interphase FISH results

The results, recorded as the modal number of signals seen for each clone are displayed in Table 3.2. In all cases the most highly amplified region, referred to as the amplicon, included the *RUNX1* locus. A minimal common region of amplification (CRA) of ~3Mb in size located to band 21q22 was defined for all patients, which included RP11-79A12 and the *RUNX1* locus (genomic positions 32.3 and 35.3Mb, respectively). In four patients (4405, 6788, 7219, 7255), the amplicon extended upstream and downstream to include, the BAC probes RP11-80N20 and AF121782, (genomic positions 23.8 and 40.0Mb, respectively). Two amplicons were identified in patient 6092, positioned between the BAC probes RP11-97F14 and RP11-15H6, (genomic positions 22.9 to 31.4Mb) and RP11-191I6 and AF121782, (genomic position 31.4 to 40.0Mb), respectively. Patient 6957 also had two amplicons positioned between RP11-88D18 and RP11-191I6, (genomic position 25.5 to 31.4Mb), RP11-79D9 and RP11-120C17, (genomic position 33.2 to 41.7Mb). In patient 4134 three amplicons were detected positioned between RP11-15E10 and RP11-49B5 (genomic position 18.7 to 20.3Mb), RP11-97F14 to RP11-191I6, (genomic position 22.9 to 31.4Mb) and RP11-79D9 and *RUNX1* (genomic position 33.2 to 35.3). Within each of these three patients the amplicons were separated from each other by the gain or loss of one signal.

Bac Probe	Clone Position Mb	FISH										Control patients	
		4405	4134	4279	5898	6092	6783	6788	6957	7219	7255	6009	6899
AF127936	15.1	2	3	2	1	2	4	2	2	4	3	4	2
RP11-15E10	18.7	3	5	Fail	1	2	2	2	2	4	1	4	2
RP11-375O2	19.3	3	5	3	1	2	2	2	2	3	1	4	2
RP11-49B5	20.3	3	5	4	1	2	2	3	2	5	3	4	2
RP11-64I12	22.1	5	4	4	2	4	2	3	3	2	3	4	2
RP11-97F14	22.9	5	5	4	3	6	2	3	3	3	3	4	2
RP11-80N20	23.8	7	7	3	3	6	3	5	4	6	5	4	2
RP11-13J15	24.1	7	7	3	3	5	3	5	4	5	6	4	2
RP11-88D18	25.5	7	5	4	3	5	2	5	5	5	5	4	2
RP11-15H6	26.7	8	5	4	3	6	3	5	5	6	7	4	2
RP11-90A17	27.7	10	8	4	4	4	3	7	6	8	6	4	2
RP11-79G23	29.3	9	5	5	5	4	2	6	5	6	7	4	2
RP11-30N6	29.7	8	5	5	5	4	2	5	5	6	6	4	2
RP11-191I6	31.4	8	5	5	5	6	3	5	5	7	7	4	2
RP11-147H1	32.3	10	4	5	5	6	5	5	4	6	7	4	2
RP11-79D9	33.2	10	5	5	5	5	4	5	5	7	6	4	2
RP11-79A12	34.7	9	8	5	5	6	5	5	5	6	7	4	2
RUNX1	35.3	10	8	5	5	6	5	5	5	8	10	4	2
AF121782	40.0	5	3	5	5	6	3	5	5	4	8	4	2
RP11-114H1	41.2	1	1	5	4	2	4	5	5	1	2	4	2
RP11-120C17	41.7	1	5	4	5	2	4	5	5	1	2	4	2
RP11-88N2	43.7	1	3	1	1	2	4	5	4	1	2	4	2
21qtel D21S1575	46.9	1	1	1	1	2	2	3	1	1	2	4	2

Key   **Deletion :1**   **Normal : 2**   **Gain : 3-4**   **Amplification : >5**

Table 3.2 Copy number changes detected by interphase FISH screening along the length of chromosome 21 in ten iAMP21 patients and two control patients (6899, 6009). Columns represent patients and rows represent the individual probes. Probes run from top to bottom in a centromeric to telomeric direction. Copy number is expressed as the modal number for each location.

The largest amplicon (~22.5Mb) was seen in patient 6788, where it extended from BAC probe RP11-80N20 (genomic position of 23.8Mb) downstream to RP11-88N2 (genomic position 43.7Mb). The smallest amplicon (~1Mb) was seen in patient 6783, running from clone RP11-79A12 (genomic position of 34.7Mb) downstream to the *RUNX1* locus (genomic position 35.3Mb).

The control patients 6009 and 6899 showed a consistent copy number change at each BAC clone location. In patient 6899, two copies of each clone were found, whilst in the patient with high hyperdiploidy (6009), the copy number observed was 4. In both patients the results were consistent with the number of chromosomes 21 observed in their diagnostic karyotype (Table 3.5).

When the signals were numerous their distribution in interphase was such that they were often in close association making accurate enumeration difficult. In a number of cells the signals appeared as doublets, if the distance between these two signals was smaller than the estimated diameter of an individual signal, they were counted as one. For the 12 patients tested, FISH was successful for 23 probes. One clone, RP11-15E10, failed in one patient (4279). The range of signal numbers (excluding the normal copy number of 2) was recorded for the probes that corresponded to those areas defined as amplified. At the locations where a gain was noted, the range was substantially lower, whilst in those regions with a deletion, in only two patients (6783 and 7219) was a range of signals (1-3) noted (Appendix 3, Table A3.3).

Gain of signals was seen within the region centromeric to the amplicon in all patients. Deletions in this region were also recorded for patients 5898 and 7255. In three patients (4279, 6957 and 6783) a gain of signals was seen downstream of the amplicon.

A deletion of the 21q22.3 subtelomeric region was observed in seven of the ten cases (4405, 4134, 4279, 5898, 6783, 6957, and 7219). Although the size of the deletion was variable between patients, it was possible to define a minimum common region of deletion (CRD) at the site of the subtelomeric probe. In three

patients (4134, 4279, 5898), the deletion extended upstream to include the RP11-88N2 clone, at genomic position 43.7Mb, providing evidence of a deletion of ~3.5Mb in size. In two patients (4405, 7219) the deletion was further extended and included clones RP11-120C17 and RP11-114H1, at genomic positions 41.2 and 41.7Mb, respectively. The smallest deletions in this region were seen in patients 4134, 6783 and 6957, with only the subtelomeric clone missing. Patients 6783 and 7219 had mixed populations of cells with some appearing to harbour a deletion, whilst others showed gain of the subtelomeric probe indicating the presence of different populations.

The degree of amplification, as established by signal copy number, was variable both within and between patients. The highest frequency of amplification was consistently observed in the minimal CRA for all patients, which encompassed the *RUNX1* locus, with copy numbers ranging from 5 to 14.

3.2.3.2   BAC array CGH results

The results obtained from BAC aCGH are displayed in Table 3.3. Successful array profiles were obtained for all samples tested (Appendix 3, Figures A3.1). Control samples 6009 and 6899 showed consistent copy number changes at each location. In sample 6009, (high hyperdiploidy) a ratio of 1.5-2.0 was recorded for each clone, whilst in the sample from the patient with a normal karyotype (6899), a ratio of 1 was recorded at each location. Imbalances were observed for all seven iAMP21 patients, with each one showing a unique profile. A minimal CRA (defined as an area with the highest level of gain) was recorded at the genomic position of 35.5 Mb, corresponding to the *RUNX1* locus in all patients.

Clone Position Mb	iAMP21 Patients								Control patients	
	4279	5898	6783	6788	6957	7219	7255		6009	6899
15.1	2	1	4	2	2	4	3		4	2
15.7									4	2
18.7		1	2	2	2	4	1		4	2
19.3	3	1	2	2	2	3	1		4	2
20.3	4	1	2	3	2	5	3		4	2
21									4	2
22.1	4	2	2	3	3	2	3		4	2
22.9	4	3	2	3	3	3	3		4	2
23.8	3	3	3	5	4	6	5		4	2
24.1	3	3	3	5	4	5	6		4	2
25.5	4	3	2	5	5	5	5		4	2
26.7	4	3	3	5	5	6	7		4	2
27.7	4	4	5	7	6	8	6		4	2
29.3	5	5	2	6	5	6	7		4	2
29.7	5	5	2	5	5	6	6		4	2
31.4	5	5	3	5	5	7	7		4	2
32.3	5	5	5	5	4	6	7		4	2
33.2	5	5	4	5	5	7	6		4	2
34.7	5	5	5	5	5	6	7		4	2
35.3									4	2
40	5	5	3	5	5	4	8		4	2
41.2	5	4	4	5	5	1	2		4	2
41.7	4	5	4	5	5	1	2		4	2
43.7	1	1	4	5	4	1	2		4	2
46.7									4	2
46.9	1	1	2	3	1	1	2		4	2

Table 3.3 Combined BAC aCGH and interphase FISH data. Columns represent patients and rows represent BAC clones with their genomic positions indicated from centromere to telomere. For clone names refer to Appendix 3, Table A3.2. BAC array data are represented by coloured boxes (see key). FISH copy number data, expressed as a mode are shown as a numeric within the boxes.

Key	Fail	Deletion	Normal	Gain	Amplification	High Amplification
Ratio		< 1	1	1-1.5	1.5-2.0	2.0-4.0

A further two common regions of gain were recorded at genomic positions 23.8 Mb and 26.7 to 27.7Mb, which were seen in all patients. The overall level of gain was less in these two areas than the minimal CRA (ratio values of 1-<1.5 and 1.5->2.0).

Deletions in the telomeric region were found in three patients, whilst in a further three patients the array failed to produce a result for this locus. The size of the amplicon was variable between patients. The largest amplicon was found in patient 6788 and extended from genomic position of 23.8Mb through to the telomere, whilst the smallest amplicon was detected in 6783 where the areas of highest amplification was found at genomic position 35.3-43.7Mb. The profiles from the FISH and BAC aCGH were compared. The variation in copy number observed by FISH along the length of 21q in all seven patients reflected the BAC aCGH profiles at locations distal to and including the clone at 23.8Mb. Both techniques detected the same copy number imbalances, demonstrating a high concordance between the two methods, as demonstrated in Figure 3.2.

Discrepant results were noted at 22.1Mb and 22.9Mb for four patients (4279, 6783, 6788 and 6957). In all four patients the copy number recorded by FISH was greater than that seen with BAC aCGH. In patient 5898 discrepant results were seen at clone positions 22.1Mb and 24.1Mb with FISH recording a normal copy number change in comparison to a BAC aCGH gain and a gain of copy number in comparison to a BAC aCGH normal, respectively.
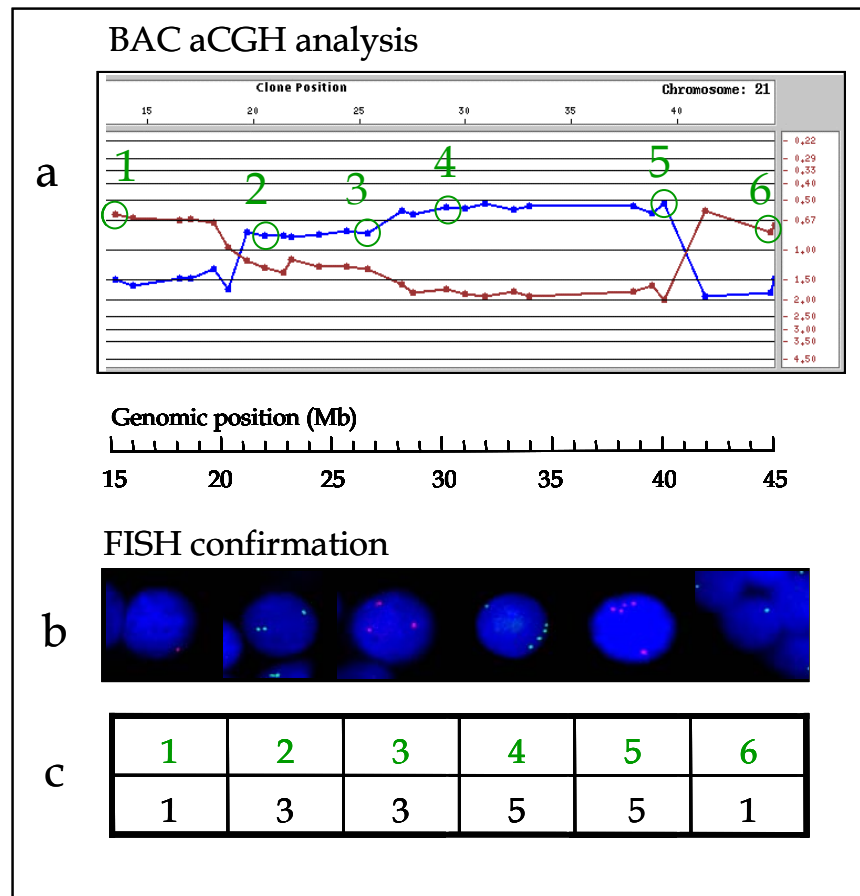
Figure 3.2 Combined BAC aCGH and interphase FISH from patient 5898. (a) BAC aCGH result with BACs positioned from left to right, centromere to telomere. Dye swap experiments are shown by red and blue lines. A deviation of >1 shows loss or gain of material. FISH confirmation of each circled area using interphase FISH is illustrated in (b), with the corresponding copy number found at each site shown in (c). Adapted from Strefford *et al* (2006)

3.2.4 Conclusion

In this direct comparison between FISH and aCGH, the relative advantages of these techniques in the investigation of iAMP21 became apparent. As aCGH employs a whole genome approach, the full extent of the chromosome 21 involvement was revealed. Although conventional cytogenetic and FISH techniques had originally identified iAMP21, they had failed to precisely define the level and extent of the intrachromosomal imbalances within iAMP21. FISH

and aCGH are able to detect copy number change, but one disadvantage of FISH is that it is time consuming, especially in terms of whole genome coverage.

Array CGH has been successfully employed in a number of studies of haematological malignancies to identify disease specific copy number changes. There are a number of different platforms available and each one is able to provide different levels of performance depending on its application (Pinkel & Albertson, 2005;Parker *et al*, 2008). The 32K BAC array employed in this investigation successfully identified regions of gain and loss, but was limited in providing precise data with regards to boundaries of deletion or amplification. High resolution arrays, such as the Agilent 244K Oligonucleotide array subsequently used to further characterise iAMP21, identified the distinct pattern of 'step wise' gain seen along 21q in these patients (Strefford *et al*, 2006). It is known that smaller array elements can provide higher genomic resolution when looking at multiple copy aberrations, however they are more sensitive to background noise (Pinkel & Albertson, 2005). Discrepant results were recorded at a number of sites when compared directly to the FISH result. Interphase FISH screening provides an accurate reflection of copy number for any one specific probe providing that the region of interest has not been rearranged in such a way as to cause the probe to split. It is the current gold standard employed to detect copy number change at individual loci.

The discrepancies seen in this study may be due to poor hybridisation of the aCGH slides, or a reflection of the difficulty in the interpretation of the fluorescence ratios, when considering deviation from the expected values by loss or gain of a single copy. It may be a reflection that the two probes sourced from different laboratories do not cover complementary regions. Lastly, it may be that the contaminating normal cells within the bone marrow sample from which the DNA was extracted may reduce the overall level of amplification, which would have more effect on small genomic regions.

3.2.5 Combined FISH and G-banded Study

3.2.5.1 Introduction

The combined results of interphase FISH and BAC aCGH on a series of iAMP21 patients pointed to a highly complex chromosome 21 abnormality in these patients with each case having a unique genomic profile. A region of gain/amplification between genomic position 24.1 (band 21q21) - 40Mb (band 21q22) and a region of deletion located at the subtelomeric region of chromosome 21, were identified. Regions with high copy number changes often harbour genes of interest, consequently it was important to establish whether this region was common to a larger group of patients.

An earlier study (Harewood *et al*, 2003) grouped patients according to the morphological form of the dup(21) using conventional cytogenetics, implying common chromosomal features between patients. This appeared to contradict the findings from FISH and BAC aCGH showing unique patient profiles. Although the interpretation of marker chromosomes from G-banded analysis is limited due to both low resolution and the lack of recognition of specific chromosomal landmarks, it seemed unlikely that each patient within any one morphological group would have a unique profile. As the initial FISH and aCGH study was carried out on only ten patients, it could not be ruled out that the findings were a reflection of the differences in the G-banded form of the dup(21) chromosome rather than each patient having a truly unique profile.

In order to further investigate these observations as well as to characterise this abnormality in a larger group of patients, an expanded FISH study was undertaken. This was appropriate as the only material available was fixed cells. The aims of this second FISH investigation were to:

- Determine whether the minimal CRA established from the preliminary study was consistent among iAMP21 patients

- Establish the incidence and extent of the deletion involving the subtelomeric region of the dup(21)

- Investigate the relationship between the amplicon size and G-banded morphology

3.2.5.2 Method

A combinatorial approach, using both interphase and metaphase FISH together with conventional G-banded cytogenetics of the same sample, was considered to be the most suitable method of investigation. Rather than screening all patients with each of the BAC clones used in the previous study, five of these probes (BAC LSI probes, Genosystems®, France) were selected together with the Vysis LSI TEL-AML1-ES® probe and the 21q subtelomeric probe-Tel21q (D21S1446) (Molecular cytogenetics, Q-BIOgene®, UK). The BAC clones were located along 21q, with three clones positioned centromeric to *RUNX1* and two clones telomeric (Figure 3.3). They were chosen to represent those areas, either side of the previously identified minimal CRA, which had been shown in the preceding study to be gained/amplified or lost. As with the initial study, dual probe, dual colour experiments were carried out, with the same probe combinations being used on all patients. Probes RP11-147H1 (C), RP11-30N6 (B) and AF121782 (E) labelled with Spectrum red were combined with RP11-13J15 (A), RP11-88N2 (F) and Tel21q (D21S1446) (G) labelled with Spectrum green, respectively. The Vysis LSI TEL-AML1-ES® (D) probe was hybridised as a single experiment. Copy number was determined by counting, where possible, the number of signals in 50 abnormal interphase cells. In addition to the ten patients initially screened a further 38 iAMP21 patients were selected based on the criteria outlined in section 3.1.
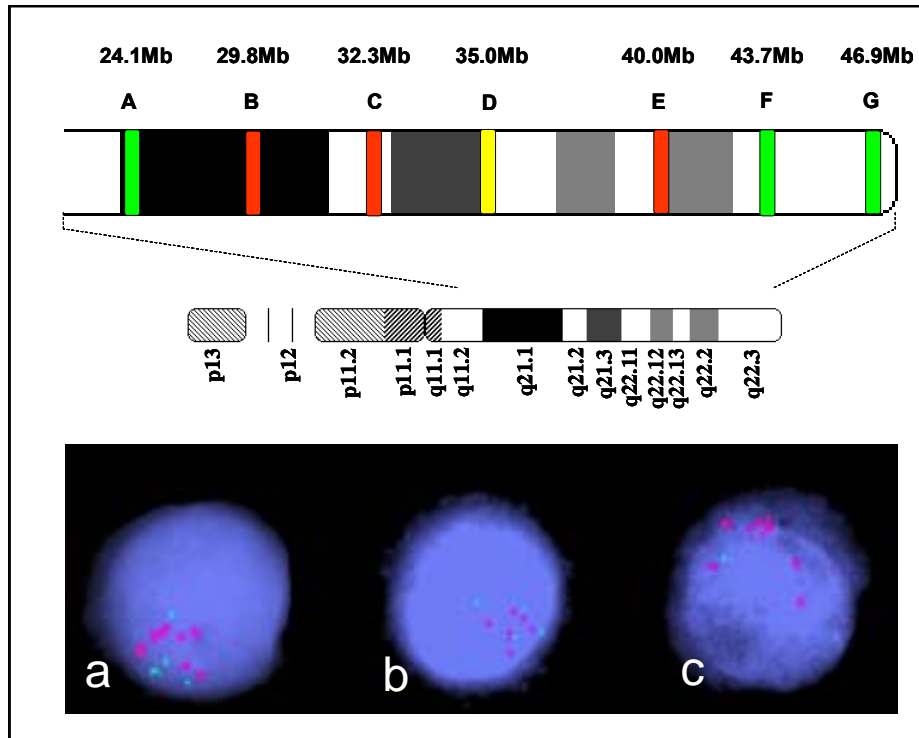
Figure 3.3 The chromosomal band locations and genomic positions of the LSI BAC FISH probes. The red and green boxes on the chromosome 21 ideogram indicate the labelling of the probes with either Spectrum red or green. Interphase nuclei from patient 4444 displaying the BAC probe signals are shown for (a) probes A and C, (b) B and F, (c) E and G.
Key to probes: A = RP11-13J15, B = RP11-30N6, C= RP11-147H1, D= *RUNX1*, E= AF121782, F = RP11-88N2, G= Tel21q (D21S1446). Adapted from Robinson *et al*(2007).

The previous FISH study had demonstrated that in the majority of patients the amplicon appeared to be continuous. So for the purpose of this study, if amplification was noted at two consecutive sites, it was assumed that the area between these points was also amplified.

3.2.5.3 Results

Patients	dup(21)	24.1 A RP11-13J15	29.8 B RP11-30N6	32.3 C RP11-147H1	35.5 D RUNX1	40.0 E AF121782	43.7 F RP11-88N2	46.9 G 21qtel
3131	LM	5	3.5	6.5	5.5	4.5	5	3.5
5754	LM	3	6.5	5.5	5.5	5	6.5	1
5898	LM	3	5	5	5	4	1	1
6020	LM	3	4.5	7	6	4	1	1
6788	LM	4.5	4	4.5	4	5	4.5	4
6957	LM	4	4.5	5	6.5	5	5	1
7045	LM	5	6	6.5	6.5	6	6	1
7829	LM	FAIL	6.5	FAIL	7.5	7.5	1	1
3956	LA	5	6.5	6.5	8	7	6	1
4134	LA	6.5	5	5	5.5	3.5	3	1
4178	LA	4.5	6.5	7	7	7.5	1	1
4623	LA	2	4	7	7	7.5	1	1
6008	LA	5	5	5	7.5	6.5	1	1
6783	LA	3	2	5	5	3	4	2
6937	LA	2	4.5	7.5	8.5	8	1	1
7219	LA	6	6	6	7	4.5	1	1
7255	LA	6	3.5	9	7.5	6.5	3	2
8743	LA	4	5	4	4	4.5	4.5	1
2776	R	3	3	3	5	7	6.5	1
3743	R	2	2	4.5	5.5	4.5	5	3
3970	R	FAIL	3.5	FAIL	4.5	6.5	1	1
4405	R	6	8	8	6.5	6.5	1	1
4444	R	5	5	5	5.5	7	6.5	1
5607	R	6	2.5	6	5	FAIL	5.5	FAIL
5674	R	1	5	FAIL	7	6.5	1	1
5809	R	3	4	6.5	7	6	1	1
7583	R	3	3	4.5	5	4	4.5	1
7650	R	4.5	5	7	7	6	1	1
3527	SA	3	3.5	4.5	4.5	3	2	2
4780	SA	2	4	4.5	5	2.5	2	2
3745	SM	6.5	4.5	7	7	5	6	1
4135	SM	7	6	6	7.5	6.5	4.5	1
4237	SM	7	6	6.5	6.5	6.5	6	1
4279	SM	3.5	4.5	5.5	6.5	4	1	1
5655	SM	5	3	1	5.5	4.5	1	1
6868	SM	FAIL	7	FAIL	7	FAIL	7	FAIL
4316	n/a	FAIL	3	FAIL	4	4.5	3	3
5858	n/a	3.5	6	6	6	6.5	4	4
6092	n/a	5	3.5	6	6.5	5	2	2
6111	n/a	FAIL	FAIL	FAIL	7	FAIL	FAIL	1
6996	n/a	7	FAIL	9	10.5	8.5	1	1
7024	n/a	3.5	1	4.5	6	7.5	1	1
7093	n/a	4	6	6	7	6	1	1
7100	n/a	3	3.5	4.5	5	3	3	2
7732	n/a	3	4	FAIL	5.5	6	5	1
7828	n/a	5	6.5	8	6	6.5	1	1
8767	n/a	3	5	5	5.5	6	1	1
8983	n/a	6	1	FAIL	6.5	FAIL	1	1
	Key	Fail	Deletion	Normal	Gain	Amplification		

Table 3.4 Interphase FISH screen of 48 iAMP21patients. Columns represent probes and rows represent patients. The results are grouped according to the morphology of the dup(21) (column 2). The boxes relate to the results from individual probe hybridisations for each patient (columns A-G). The numbers indicates the mean copy number for each probe.
Key: LM= large metacentric; LA=large acrocentric; R=ring; SA=small acrocentric; SM= small metacentric; n/a= not available.
F=Fail; D=deletion (1 copy); N= Normal (2 copies), G=Gain (3-4 copies); A= Amplification (> 5 copies).

3.2.5.3.1 Interphase FISH

The FISH screening results for all 48 iAMP21 patients are displayed in Table 3.4. Patients previously defined as iAMP21 are ordered according to the morphology of the dup(21) (section 1.6.3) and the number of signals in 50 abnormal cells is recorded as a mean. FISH for at least two probes was successful on all patients, with 38 patients having a successful result with all seven probes. The size of the amplicon (extent of dark green in Table 3.4) and the degree of amplification (number of signals) was highly variable, with each patient exhibiting a unique pattern of imbalance (Appendix 3, Table A3.4). In 25 (66%) of those patients with successful FISH, the size of the amplicon was comparatively large (≥ 10.2Mb), in agreement with the results of the initial study. In every case the amplicon included the *RUNX1* locus and, in the majority of cases, extended ~2Mb proximally to include the BAC probe RP11-147H1, genomic position 32.2Mb, and ~5Mb distally, to include AFA121782, at genomic position 40.0 Mb (Table 3.4). This confirmed the location of the minimal CRA to band 21q22.1.

The level of amplification as determined by copy number was variable. A comparison between the level of amplification (as measured by mean copy number) and probe position showed that for all patients the highest levels were recorded for the *RUNX1* locus. In two patients (5858, 6996) interphase FISH showed two clusters of signals together with a single signal at a different location in the cell. This indicated that there might be two copies of the dup(21) and a

normal chromosome 21 present. No metaphases were available to confirm these findings.

A deletion of the subtelomeric clone was observed in 35 (76%) of the 46 iAMP21 patients with a successful FISH result for this probe. In 20 (59%) of these patients the deletion extended proximally to include BAC RP11-88N2, genomic position 43.0Mb, so confirming the minimal CRD of 3.5Mb, found in the previous study. In six patients normal copy number was noted for this region, whilst in four (3743, 3131, 4316, 5809) a gain was observed.

In four patients (5655, 5674, 7024, 8983) deletions were noted at sites centromeric to *RUNX1*. There was no common region of deletion in these areas.

3.2.5.3.2 Amplicon Size and dup(21) morphology

A comparison between the size and location of the amplicon and the dup(21) morphology is shown in Figure 3.4. Apart from the small acrocentric, group it was not possible to associate a particular dup(21) morphology with a particular level or region of amplification. Patients with large acrocentric (LA) marker chromosomes had amplicons that spanned large regions of 21q (Appendix 3, Table A3.5). The exception to this was patient 6783, for which the G-banded morphology of the chromosome resembled that described as a large metacentric (LM), although the FISH amplicon size was small. Detailed results from karyotyping studies on this patient are given in section 3.5.3.

The size of the amplicon in the other morphological groups was also extensive, reflecting the substantial size of the G-banded forms of the dup(21) in comparison to a normal chromosome 21. The level of amplification and the size of the amplified region in the two patients with a small acrocentric morphology (SA) were similar to each other, and smaller than seen in other patients. Neither case had a deletion of the subtelomeric probe. Among the group of patients with a failed G-banded cytogenetic result, FISH profiles similar to those seen for all of the subgroups were noted.
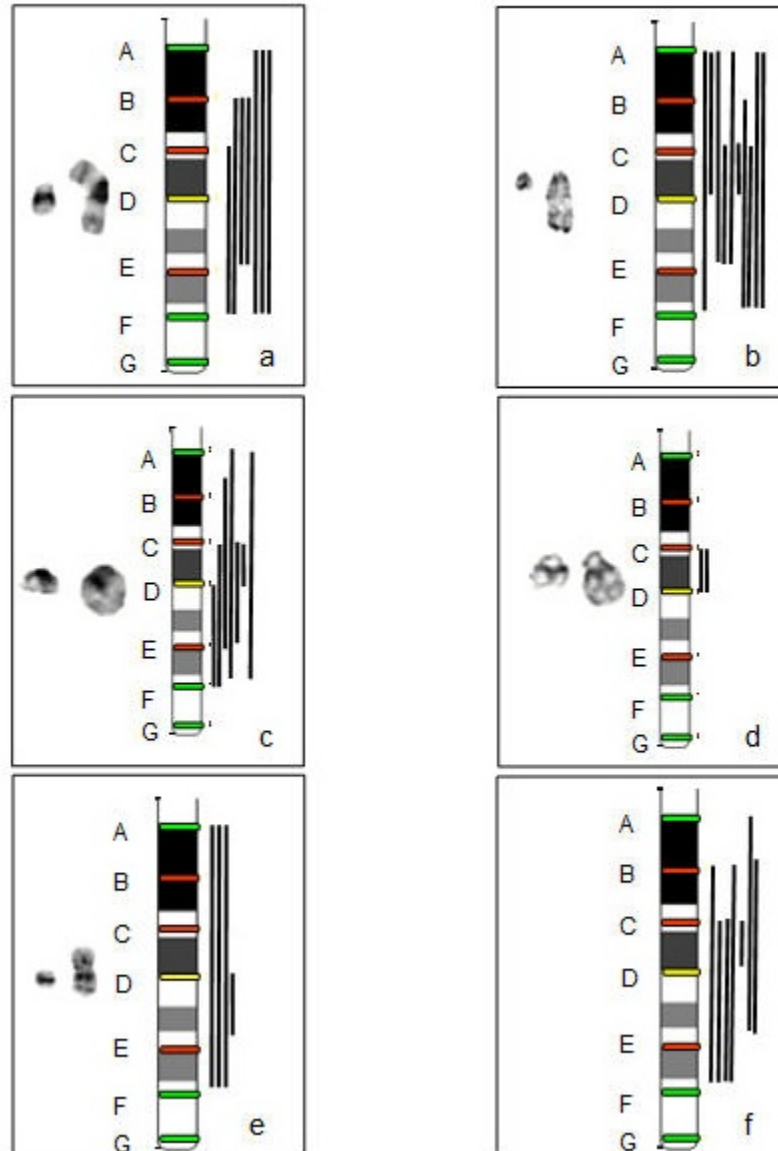
Figure 3.4 Amplicon size as determined by FISH compared to the G-banded morphology of the dup(21). Vertical lines to the right hand side of the ideogram represent the size and location of individual patient amplicons. Coloured bars on chromosome 21 ideogram represent the probe location, which is the same as shown in Figure 3.3.

3.2.5.3.3 dup(21) G-banded review

A direct comparison of the G-banded morphology of the dup(21) chromosomes within each of the morphological subgroups is shown in Figure 3.5. Although the morphological description was correctly assigned, it was obvious from this visual comparison that the dup(21) morphology was also different between patients in each group so providing further support for a unique profile.
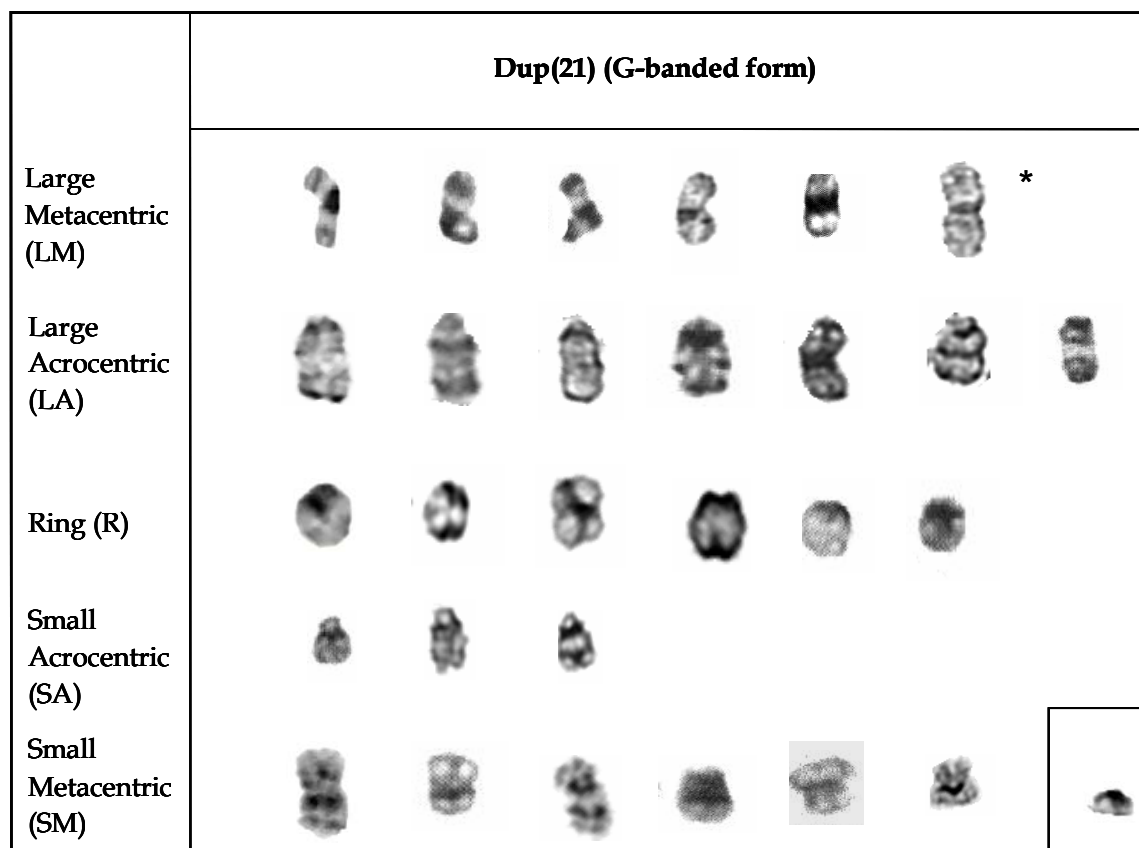
Figure 3.5 G-banded morphology of dup(21) chromosomes from 28 iAMP21 patients. The chromosomes are ordered in rows according to the G-banded morphology group to which they were assigned. A normal chromosome 21 is shown in the box in the bottom right. *G-banded form of dup(21)(q) from patient 6783, identified as a der(15;21)dup(15;21) (Section 3.5.3).

3.2.5.4   Conclusion

Analysis of a large group of iAMP21 patients using interphase FISH and conventional cytogenetics has confirmed the variability seen by more detailed FISH and aCGH as described in the previous section. Each patient was found to have a unique genomic profile by FISH. Detailed analysis of the G-banded forms of the dup(21) chromosomes in any one morphological group concurred with this observation. The size of the amplicon was relatively large in most patients and the region with the highest levels of amplification was located to band 21q22, which included the *RUNX1* locus in all patients. Deletions of the subtelomeric region were found in 76% of the patients analysed. G banded review illustrated the morphological form of the dup(21) chromosome was variable within any one morphological group. This provided supporting evidence of the unique profiles observed by FISH and BAC aCGH.

3.2.6 Metaphase FISH

3.2.6.1   Introduction

Although interphase FISH and BAC aCGH are able to provide sensitive and reliable information for the analysis of copy number changes at the molecular level, neither technique is able to provide information about structural rearrangements at the chromosomal level in relation to these changes. Interphase FISH and aCGH indicated that each iAMP patient had a unique profile and review of the G-banded morphology of the dup(21) supported these findings. The results implicated that this abnormality was highly complex and may have arisen from mechanisms other than straight forward duplication and deletion. Metaphase FISH mapping was undertaken in five cases, using the same probes as described in section 3.3.2, to determine the complexity of the rearrangements giving rise to the dup(21) chromosome. In 76% of patients a deletion of the subtelomeric region had been found by interphase FISH. Studies in animal models have shown that the shortening of telomeric DNA repeats (Gisselsson *et*

al, 2001) can lead to loss of the protective proteins from the chromosome ends, which in turn can lead to the formation of ring chromosomes. In order to establish whether the loss of subtelomeres resulted in the formation of ring chromosomes in iAMP21 patients, further FISH investigations were undertaken using probes to span the telomeric repeat sequences found in all chromosomes.

3.2.6.2 Method

In five cases (3131, 3956, 4623, 6937, and 6788), metaphase FISH with seven LSI probes as shown in Figure 3.3, was carried out. For each probe, different chromosomes were analysed, as sequential FISH with probes located too close together was difficult to interpret. For each patient, a comparison of the location of each probe was made in relation to the other probes. This was limited to a certain extent by the low resolution resulting from the contracted morphology of chromosomes in the leukaemic cells. Dual probe, dual colour experiments were carried out, with the same probe combinations being used, as previously described in Section 3.3.2 : probes RP11-147H1 (C), RP11-30N6 (B) and AF121782 (E) labelled with Spectrum red were combined with RP11-13J15 (A), RP11-88N2 (F) and Tel21q (D21S1446) (G) labelled with Spectrum green, respectively. The Vysis LSI TEL-AML1 ES® (D) probe was hybridised as a single experiment. The same five cases were screened with PNA telomeric probes to detect common telomeric sequence found on all chromosomes. This was then followed by sequential FISH using WCP21 to confirm the dup(21).

3.2.6.3 Results
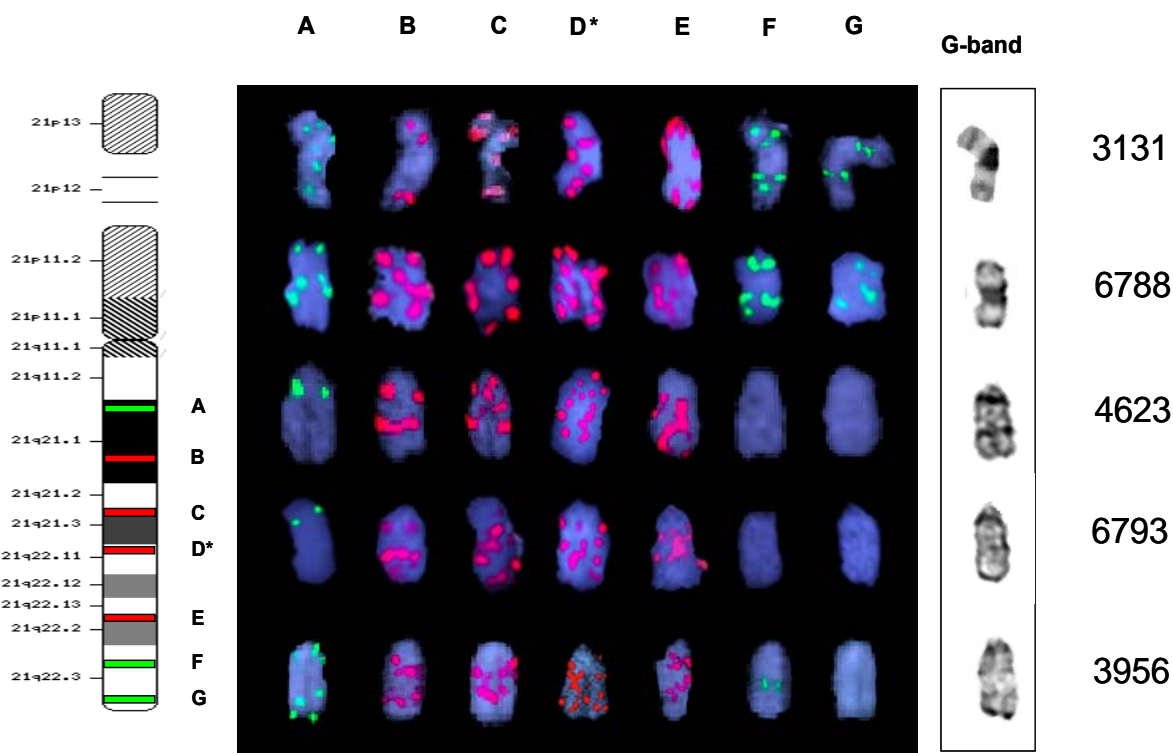
Figure 3.6 Metaphase FISH and G-banded appearance of the dup(21) from five iAMP21 patients. The chromosomal band locations and genomic positions of the LSI probes, A-G is shown in the chromosome 21 ideogram (as Figure 3.3). The red and green boxes indicate the labelling of the probes with Spectrum red and green, respectively. The patients are arranged in rows, whilst the probes are arranged in columns: LSI probes A-G, and G-banded morphology. (Key Probe: as for Figure 3.3)

In all patients the location of the probe signals confirmed that they were restricted to the normal and dup(21) chromosomes and not translocated to other regions of the genome. The normal chromosome 21 showed a single copy of each probe in the appropriate location. There was extensive heterogeneity with regard to number, location, size and intensity of probe signal on the dup(21). This variability was further emphasised when comparisons were made between patients, with no two patients displaying the same profile. A significant finding,

was that in all patients the signals were located in unexpected patterns on the dup(21), indicating that complex rearrangements involving a number of chromosomal breaks must have occurred.

In case 3131 (Figure 3.6), the dup(21) morphology was that of a large metacentric chromosome. Detailed FISH mapping showed that there were four copies of probe A (RP11-13J15), but only two copies of probe B (RP11-30N6). The orientation of these probes relative to each other provided evidence of an inversion in each arm of this chromosome, with probe B being located between the two copies of probe A. Multiple copies of probes C, D, and E (RP11-147H1, *RUNX1*, AF121782) were distributed in a ladder like fashion along the length of the dup(21), signifying numerous breaks had also occurred within these regions. In case 3131, there was evidence of an inversion, the location of probe C (RP11-147H1) was proximal to probe A (RP11-13J15) when it should have been in a distal position. The two copies of the subtelomeric probe G, were located to the centre of each arm of the dup(21), whilst probe F (RP11-88N2) was located in a position distal to this, providing evidence of another inversion. In case 6788, also described as a large metacentric chromosome, the distribution of the probes was uneven between the two chromosome arms. The signal distribution pattern in the large acrocentric chromosomes from cases 4623 and 6793 were similar to each other. In both cases, it was noted that the size and signal intensity of one of the two copies of probe B (RP11-30N6) was larger and more intense than the same probe located at a position proximal to this, suggesting localised amplification of this region. In both cases deletions of probes F (RP11-88N2) and G (subtelomeric probe) were found. Detailed analysis of the large acrocentric case 3956 showed that the dup(21) composition was different from the two other large acrocentric cases. Probe F was positioned in the centre of the dup(21), the size of the signal was larger than that seen on the normal 21, providing evidence of amplification at this site. In all five patients the probes within the amplicon, as defined by interphase FISH (Section 3.3.3.1) probes C,D and E (RP11-147H1, *RUNX1*,

AF121782, respectively) were distributed along the length of the chromosome in a ladder like fashion. Studies with PNA telomere probes (Appendix 3, Figure A3.2) showed that in all patients, investigated telomeric sequences were present on the dup(21) chromosome.

3.2.6.4 Conclusion

The signal pattern arrangement in all five cases was highly complex, indicating that the dup(21) chromosomes resulted from complex intrachromosomal rearrangements, involving multiple chromosome breaks, duplications and inversions. In all patients investigated evidence of telomeric sequence was present indicating that in these patients the dup(21) chromosome was not a ring chromosome.

3.2.7 mBAND

3.2.7.1 Introduction

Previous studies carried out on solid tumours have shown that recurrent chromosomal breaks on amplified chromosomes can highlight the genes involved at these locations and so provide information with regards to the pathogenic event leading to malignancy (Albertson, 2006). Although metaphase FISH mapping indicated the presence of inversions, duplications and deletions along the dup(21), the approach was limited as it was difficult to visualize accurately the location of all probes relative to each other. It was anticipated that the use of multicolour banding (mBAND), which provides simultaneous visualisation of all regions of the dup(21), may reveal aberrations not visible by other methods and allow further investigation of common regions of interest on the dup(21). mBAND FISH was undertaken on the same five iAMP21 cases as the FISH mapping (Section 3.3.5.2).

3.2.7.2   Method

XCyte 21 chromosome paint was hybridised to the five patients previously studied in section 3.3.5.2 and compared to the G-banded morphology and metaphase FISH with the locus specific probes.
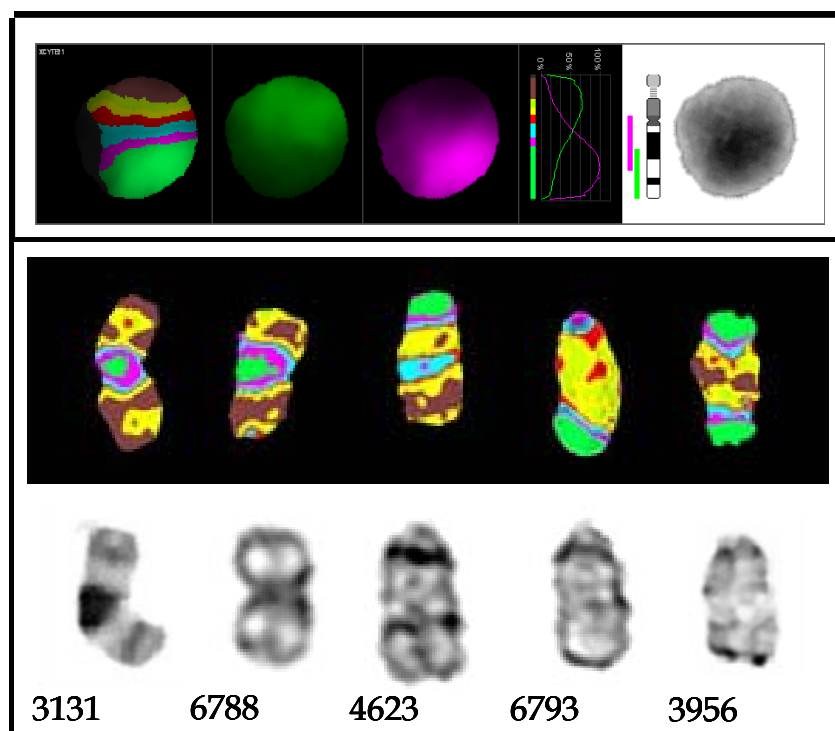
Figure 3.7 mBAND and G-banding patterns from five iAMP21 patients. a) Normal **chromosome 21 mBAND and G-banding.** b) dup(21) mBAND pattern and G-banded morphology of five iAMP21 cases.

3.2.7.3   Results

mBAND FISH with the XCyte21 chromosome paint (Figure 3.7) showed considerable variation in the mBAND pattern between dup(21) chromosomes from the five different cases. The banding pattern along the length of the dup(21), indicated by the size of the coloured bands and their distribution, confirmed the presence of some of the complex intrachromosomal exchanges seen also by the LSI probe mapping (Section 3.3.5). In all cases the mBAND

indicated amplification within band 21q22, genomic position ~29-40Mb, represented by the yellow/green colour. There was evidence of large inversions with the banding patterns indicating telomeric regions (green) located to the centromeric areas (case 6788).

A comparison between the mBAND patterns of chromosomes within the same G-banded morphological group showed different patterns. Cases 4623, 6793 and 3956 were all classified as having a large acrocentric (LA) morphology by G-banding, but in all three cases their mBAND patterns were different.

3.2.7.4   Conclusion

The use of mBAND FISH verified the complexity of the dup(21) chromosome in iAMP21 patients. Clear evidence of large inversions, duplications and amplification were observed. However, the resolution of the banding was limited, making breakpoint assignment impossible. This is likely a reflection of the design of the Xcyte 21 paint. As chromosome 21 is very small, the paint is composed of only two probes. Consequently the location of a fluorochrome to a specific region may result from a duplication/amplification of the region where the fluorochromes overlap, or an inversion of one fluorochrome into a different region so making precise interpretation difficult. Nevertheless, comparison between different cases provided further evidence for the unique structure of the dup(21) chromosomes, confirming the results of the FISH and aCGH.

3.2.8 Karyotype Review

3.2.8.1   Introduction

Conventional chromosomal analysis remains the method of choice for the initial detection of cytogenetic abnormalities in leukaemic samples. The most relevant abnormalities are considered to be the primary events and are thought to reflect the initiation of tumour development, whilst secondary changes reflect karyotypic evolution or tumour progression (Mitelman *et al*, 2007). Although

previous studies (Soulier *et al*, 2003;Harewood *et al*, 2003) had failed to detect other consistent chromosomal changes other than dup(21) in patients with iAMP21, it was important to establish whether it represented the primary cytogenetic event.

3.2.8.2   Method

Karyotypes from 36 iAMP21 patients with an abnormal cytogenetic result, for which G-banded slides were available for review, were studied to determine the presence of common chromosomal changes in addition to dup(21). FISH data was also available from routine screening carried out in the UK regional cytogenetics laboratories to indicate the presence of significant abnormalities: namely *ETV6-RUNX1*, *BCR-ABL1* and *MLL* rearrangements, as well as other changes involving these loci (Harrison *et al*, 2005).

3.2.8.3   Results

The karyotypes are displayed in Table 3.5. The chromosomal complement in all patients was near diploid, with a modal number of 45 to 47 chromosomes, apart from a single case in which the modal number was 48 (7829). In patient 3131, a subclone with 51 chromosomes was observed. A pseudodiploid karyotype was seen in 18 patients. In all patients the dup(21) replaced one copy of a normal chromosome 21, which in seven cases was the sole visible chromosomal abnormality. Gain of an X chromosome was observed in nine cases, which was the only recurrent associated abnormality distinguished by conventional G-banding.

The results of breakpoint analysis of both conventional G-banding and routine FISH are displayed in Figure 3.8. No consistent change was found amongst all cases, although breaks at chromosome band 7q22, 12p and 15q2 were detected in five, four and four patients, respectively. FISH with the LSI TEL-AML ES® probe identified five cases with a deletion of one copy of the *ETV6* gene and

six cases had loss of one copy of the *MLL* gene at 11q23. In one patient a constitutional Robertsonian translocation, der(15;21)(q10;q10), was observed.
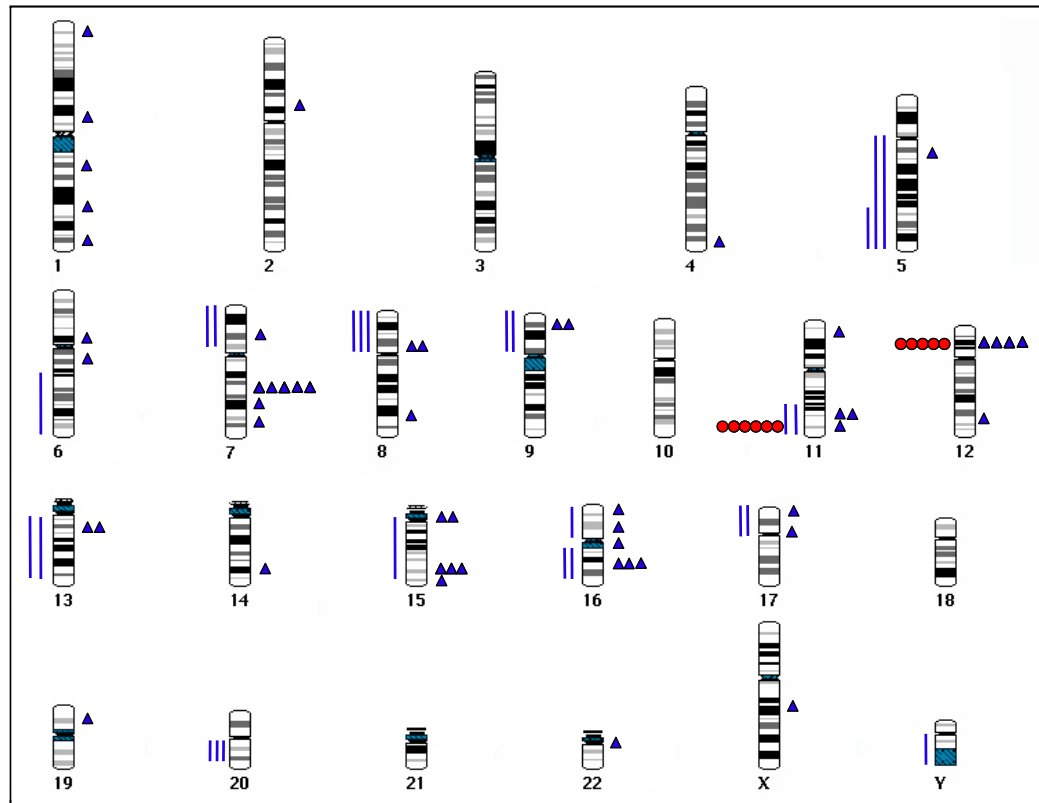
Figure 3.8 Diagrammatic representation of the distribution of breakpoints in iAMP21 patients, as determined from G-banded (blue triangle) and interphase FISH (red spots) screening. Solid blue bars represent arm involvement without defined breakpoint.

3.2.8.4   Conclusion

Review of G-banded metaphases from 36 iAMP21 patients with abnormal karyotypes confirmed that the dup(21) chromosome was present in all patients and in seven cases it was the sole karyotypic change. This suggested that the dup(21) may be the primary cytogenetic event in these patients. Studies using whole genome aCGH (Kuchinskaya *et al*, 2007;Strefford *et al*, 2007) have failed to

detect any common copy number alterations in iAMP21 patients, providing further evidence that the dup(21) may be the primary event.

In the remaining 28 cases, a number of structural and numerical chromosomal abnormalities were observed in addition to dup(21). The majority had a near-diploid chromosome complement, with the 19 having a pseudodiploid karyotype, consistent with previous studies (Harewood *et al*, 2003). None of the known established numerical or structural abnormalities were detected either by cytogenetics or FISH. Gain of one copy of a chromosome X was observed in nine patients, both male and female, an observation noted in a number of previous reports (Heerema *et al*, 2007;Heerema *et al*, 2000;Moorman *et al*, 2003). Deletion of *ETV6* was observed by FISH in five patients with breakpoints of this region being involved in translocations found in four cases, whilst deletion of 11q23 was noted in six patients.

In a single case, 6783, a constitutional Robertsonian translocation, der(15;21), was detected. Although the incidence of Robertsonian translocations in the general population is 1 in 1000 (Jacobs, 1981), der(15;21) are particularly rare, accounting for only 3% of all reported Robertsonian translocations (Gardner & Sutherland, 2004). As follow up studies were not undertaken on this patient, it is not possible to determine if this was a de novo finding or an inherited one.

Patient ID	G- banded Morphology	Karyotype
3131	LM	46,XY,t(1;16)(q23;p13),ider(21)(q10)dup(21)(q?)[3]/ 51,idem,+X,+3,+10,+14,+21[3]
5754	LM	46,XY,ider(21)(q10)dup(21)(q?)[6]
5898	LM	47,XY,+X,del(16)(q13),i(17)(q10),ider(21)(q10)dup(21)(q?)[3]/ 47,idem,add(7)(p1)[3]
6020	LM	46,XY,del(7)(q22q36),ider(21)(q10)dup(21)(q?)[cp3]
6788	LM	46,XY,add(13)(q?),ider(21)(q10)dup(21)(q?)[2]/ 47,idem,+14[1]/ 48,idem,+8,+14[5]
6957	LM	46,XX,ider(21)(q10)dup(21)(q?)[13]
7045	LM	47,XX,+X,del(9)(p?),-10,del(11)(q13),ider(21)(q10)dup(21)(q?),+mar,[cp11]
7829	LM	48,XY,+X,inv(1)(p13q?32),ider(21)(q1)dup(21)(q?),+mar[11]
3956	LA	45,XY,dic(8;16)(p1;p1),del(13)(q?14),dup(21)(q?)[6]/ 46,idem,der(Y)t(Y;13)(q1;q?14),+dic(8;16)(p1;p1),del(13)(q?14)[2]
4134	LA	46,XY,dup(21)(q?)[13]
4178	LA	46,XX,del(7)(q22),t(14;22)(q32;q11),dup(21)(q?)[10]
4623	LA	46,XX,dup(21)(q?)[11]/ 47,idem,+X[1]
6008	LA	46,XY,t(2;8)(p12;q24),del(9)(p?21),?del(13)(q1?),dup(21)(q?)[9]
6783	LA	43-44,XY,del(5)(q11q13),der(15;21)(q10;q10)dup(15;21)(q10;q10),del(16)(q22),-20[cp5]
6937	LA	46,XX,dup(21)(q?)[10]
7219	LA	46,XY,dup(21)(q?),inc[3]
7255	LA	45,XX,-21,+mar,inc[2]
8743	LA	46,XX,t(7;9;17)(q22;p1?,p1?),del(11)(q23q2?5),dup(21)(?)[7]
2776	R	47,XX,+X,der(21)r(21)(q?)dup(21)(q?)[3]
3743	R	45,XX,dup(8)(p?),-11,der(15)t(11;15)(?;q24),der(21)r(21)(q?)dup(21)(q?)[2]
3970	R	47,XX,add(7)(q2),+10,der(21)r(21)(q?)dup(21)(q?)[7]/ 47,idem,del(12)(p13)[4
4405	R	45,Y,t(X;15)(q2?1;q2?4),dic(12;17)(p1;p1),der(21)r(21)(q?)dup(21)(q?)[4]
4444	R	46,XY,der(21)r(21)(q?)dup(21)(q?)[3]
5607	R	46,XY,t(8;11)(p?1;q21),del(11)(q?21),der(21)r(21)(q?)dup(21)(q?)[8]
5674	R	47,XY,+X,dup(21)(q)[7]
5809	R	45,XY,add(1)(p36),-2,add(4)(q35),-7,del(12)(p12),?del(16)(q?2),-19,der(21)r(21)(q?)dup(21)(q?),+4mar,inc[cp6]
7583	R	47,XY,+X,der(21)r(21)(q?)dup(21)(q?)[4]
7650	R	47,XY,+9,der(21)r(21)(q?)dup(21)(q?)

Table 3.5. G-banded karyotypes of 36 iAMP21 patients.

Patient ID	G- banded Morphology	Karyotype
3527	SA	45,XX,-7,del(12)(p12),dup(21)(q?)[5]
4780	SA	45,XY,-11,del(12)(p1?2),der(20)t(11;20)(q?;q?),dup(21)(q?)[21]
3745	SM	46,XY,der(21)dup(21)(q?)[4]/ 46,idem,del(5)(q?),der(15)t(5;15)(q?;q?)[3]/ 47,XY,-18,+21,+22[1]
4135	SM	46,XX,t(12;16)(q24;p11),del(15)(q24q26),t(17;20)(p1?3;q11),der(21)dup(21)(q?)[6]
4237	SM	46,XX,der(21)dup(21)(q?)[3]/ 46,idem,del(16)(q1?)[7]
4279	SM	46-47,XY,der(21)dup(21)(q?)inc[12]
5655	SM	46,XX,del(1)(q4?),del(6)(q1?5),del(7)(q2?2q3?1),der(21)dup(21)(q)[3]/ 46,idem,add(6)(q2?)[12]
6868	SM	47,XY,+X,-5,-9,add(20)(q),+21,der(21)dup(21)(q),+mar,inc[7]
4316	n/a	46,XX[24]
7828	n/a	46,XY[20]
6009	n/a	50,XY,+X,+4,+21,+21[10]
6899	n/a	46,XY[20]

Table 3.5. (continued) G-banded karyotypes of 36 iAMP21 patients. Karyotypes for control patients 6009 (High hyperdiploid) and 6899 (normal) are also included.

3.3   iAMP21- a distinctive genetic subgroup?

3.3.1 Cryptic iAMP21

3.3.1.1   Introduction

With the advent of new technologies to detect copy number change, oncogene amplification is becoming increasingly evident in a number of haematological disorders. In addition to ALL, a number of reports have observed amplification of regions on chromosome 21 in AML (Baldus *et al*, 2004) and MDS (Papenhausen *et al*, 2005;Andersen *et al*, 2004). In one study carried out in AML, detailed analysis by aCGH showed that this amplification did not include the *RUNX1* gene but occurred at two different positions. One location was downstream of *RUNX1* (38.7-39.1Mb) in a region that harbours the transcription factors *ERG* and *ETS2*, whilst the second target was located upstream, to a region

that harbours the *APP* gene (25-30Mb). Expression studies confirmed overexpression of both *ERG*, *ETS2* and *APP* in these patients (Baldus *et al*, 2004). In more recent studies, it was noted that there was high expression of *ERG* in AML with cytogenetically normal karyotypes, which was associated with adverse risk (Marcucci *et al*, 2007). Over expression of *APP*, has however been found in a number of AML patients irrespective of their chromosome 21 involvement.

As the majority of iAMP21 were identified by chance during FISH screening for the *ETV6-RUNX1* fusion, it cannot be ruled out that we have selected a group of patients which may have a secondary rearrangement of chromosome 21 which has arisen from a smaller cryptic abnormality which may involve the over representation of *ERG*, similar to the one reported in AML. In a number of haematological disorders, variant translocations have been identified which occur as a secondary chromosomal change and at a lower incidence than the primary translocation. If this were so in iAMP21 patients, it is probable that the primary abnormality from which the dup(21) was derived would locate to chromosome 21 and would involve a cryptic copy number change. Using the information gained from studies described in the previous sections, a FISH study was designed to test this hypothesis, which was based on a number of assumptions:

- The incidence of the primary abnormality would be higher than the 1.5 % incidence reported for iAMP21 (Harewood *et al*, 2003;Soulier *et al*, 2003)
- No other prognostically significant abnormalities, such as the *BCR-ABL1*, *ETV6-RUNX1* fusions, or *MLL* rearrangements would be present
- The region involved would be adjacent to the *RUNX1* locus, and would involve gain/amplification

- The karyotypic features would be similar in both groups namely: a modal chromosome number of between 40–50, with an abnormal karyotype but no obvious involvement of chromosome 21
- Clinical features such as immunophenotype would be similar in both groups

3.3.1.2 Methods

A four probe FISH screen was designed (Figure 3.9) to cover a ~10Mb region of chromosome 21 comprising two probes upstream (RP11-12M14 and RP11-8P19) of *RUNX1* and two (RP1195I21 and RP110N12) downstream. In addition, the commercial chromosome 21 subtelomere probe was included to determine the status of this region in these patients, as well as the LSI TEL-AML ES®, (Vysis, UK) probe. The downstream probes spanned *ERG* and *ETS2*, to provide a direct comparison to the amplicon found in AML patients.
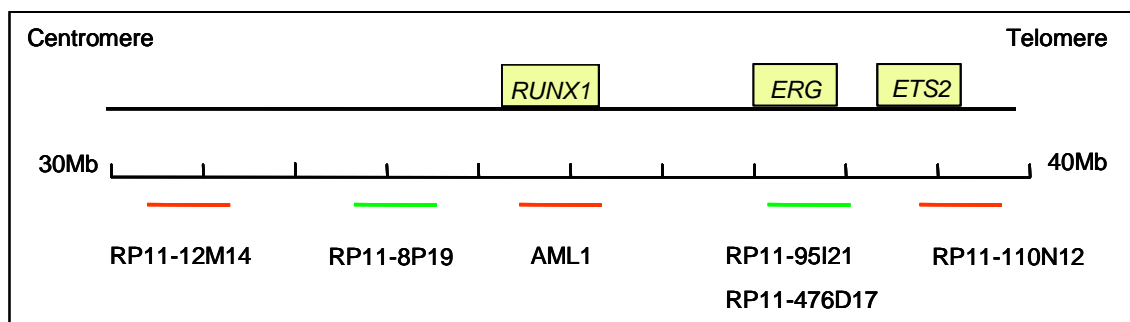
Figure 3.9 Genomic positions on chromosome 21 of FISH probes used to screen patients for copy number changes in regions adjacent to *RUNX1*. The red and green lines indicate the labelling of the probes with either Spectrum red or green, respectively. The TEL-AML ES® for AML1 (*RUNX1*) is shown in red. Probes run from left to right in a centromere to telomere direction.

A series of 30 childhood BCP-ALL patients with an abnormal karyotype with no evidence of *MLL* rearrangements, *ETV6-RUNX1* or *BCR-ABL1* fusions were selected from a search of the LRUKD karyotype database. The additional selection criteria were that the patients had a modal number of 40-50

chromosomes and no visible chromosome 21 abnormalities (Appendix 3, Table A3.6). These patients were screened using the probes described above using standard FISH procedures as outlined in section 2.3.2.

3.3.1.3 Results

FISH was successful with at least four probes for all patients. In all cases tested a copy number of two was obtained for each of the probes employed (Appendix 3, Table A3.6). For each patient, the copy number at each probe location was the same. The results for all patients were consistent with their G-banded karyotype (Appendix 3, Table A3.7).

3.3.1.4 Conclusion

A small group of BCP-ALL cases, with no cytogenetic or *RUNX1* FISH evidence of iAMP21, were screened by FISH to look for cryptic abnormalities of chromosome 21, particularly duplications/amplifications involving regions adjacent to the *RUNX1* gene. No copy number changes were detected in these regions. From this data it was concluded that the iAMP21 abnormality does not represent a variant that has arisen from a cryptic duplication of chromosome 21. In addition no patients were identified with amplicons similar to those described in AML.

3.3.2 Variant iAMP21

3.3.2.1 Introduction

Screening of BCP-ALL patients using a combination of FISH and conventional cytogenetics to detect cases of iAMP21 (as outlined in section 3.1.) resulted in the discovery of two cases (4746, 5047) (Table 3.1) which were negative for the *ETV6-RUNX1* fusion, with ≥ 5 copies of the *RUNX1* gene. These cases did not strictly conform to the definition of iAMP21, and the additional *RUNX1* signals detected did not correlate with gain of intact copies of

chromosome 21. As the studies previously undertaken in this project had established that *RUNX1* was always present within the amplicon, it was important to characterise these two cases and determine whether they represented hidden or variant iAMP21.

It is possible that iAMP21 may haven arisen from further rearrangement of a structurally rearranged chromosome 21, such as i(21)(q10) , or that it may represent a secondary abnormality to i(21)(q10). If this were so, it is possible that there may be evidence of a cryptic copy number imbalance along the length of an apparently unrearranged i(21)(q10) chromosome.

To investigate this theory, as well as to establish whether the two cases outlined above represented hidden iAMP21, six patients previously identified as having an i(21)(q10) together with the above two cases with five *RUNX1* signals, were screened with the same probes as outlined in section 3.2.1 and the results compared to those obtained from verified iAMP21 cases.

3.3.2.2 Methods

Interphase FISH screening was undertaken on all eight cases following the method outlined in Section 3.2.1.

3.3.2.3 Results

Patient	dup(21)	24.1	29.8	32.3	*RUNX1*	40	43.7	46.9
		13J15	30N6	147H1	*RUNX1*	AF121782	88N2	21qTel
4676	i(21)	4	5	5	5	5	4	4
5003	i(21)	6.5	6.5	6.5	6.5	6.5	6.5	6.5
5586	i(21)	4.5	4.5	4.5	4.5	4.5	4.5	4.5
5612	i(21)	3	3	3	3	3	3	3
7015	i(21)	4	4	4	4	4	4	4
9410	i(21)	4.5	4.5	4.5	4.5	4.5	4.5	4.5
4746	rea(21)	7.5	7.5	5	7	5.5	7	6.5
5047	add(21)	Fail	4	4	5	Fail	1	1

Table 3.6 Interphase FISH screening of six cases with i(21)(q10) and two potential iAMP21 variants. Columns represent probes and rows represent patients. The mean numbers of signals are given.

The results of interphase FISH screening undertaken in all eight cases are displayed in Table 3.6. Successful results were obtained from all probes in six cases. Two probes failed in case 5047. In five of the cases with i(21)(q10), the copy number recorded for each probe was the same. In three patients (5003, 5586 and 9410) two abnormal cell populations were noted, which indicated the presence of clonal evolution. For each of these cases, the number of signals in any one cell was the same for each of the dual probes employed, suggesting that a duplication of the isochromosome had occurred (Appendix 3, TableA3.8). In a single patient (4676) with an i(21)(q10), the number of signals observed for each probe, was variable with the average copy number for probes RP11-30N6, RP11-147H1 ,*RUNX1* and AF121782 being one single signal higher than the other probes. G-banded analysis (Appendix 3, Table A3.9) indicated that in addition to the i(21)(q10) a duplicated chromosome 21 was also present. G-banded review showed that the morphology of this dup(21) was not consistent with that of the dup(21) seen with iAMP21 patients.

3.3.2.4 Conclusion

Six patients with i(21)(q10) were investigated by FISH using probes located along 21q to determine whether copy number variation may be associated with this abnormality. No evidence of duplications or losses along 21q was found. In a number of cases two populations of cells were present and within each clone the copy number for all probes was the same and consistent with the number of 21q arms observed by cytogenetics. These findings suggest that i(21)(q10) chromosomes are distinct from the dup(21) seen in iAMP21 patients. Had iAMP21 arisen from an isochromosome 21 it would have been expected that the observed copy number gain along the whole length of the dup(21) chromosome would have been two prior to amplification, thus in any one interphase cell the normal copy number would be three (the third signal represents the normal 21). Following amplification of the isochromosome, it would be expected that those regions not amplified or deleted would still have a copy number of two giving a total copy number in the interphase cell of three. BAC aCGH and iFISH (section 3.2) showed that the copy number in the regions proximal to *RUNX1* (genomic position 15.1 – 20.0Mb) was consistent with a normal copy number namely two copies. Assuming that one copy represents the normal 21, and the other located on the dup(21) chromosome, it seems unlikely that all patients would lose a single copy in every one of these regions.

The FISH profiles obtained for patients 4746 and 5047 are similar to those reported for iAMP21 patients. It is noteworthy that patient 5047 showed loss of the subtelomeric region similar to the majority of iAMP21 patients. In both patients the karyotypes revealed the presence of a number of small marker chromosomes, which were composed of chromosome 21 material as confirmed by WCP 21. It is possible that these patients represent variant iAMP21 cases with an amplification of chromosome 21 which has arisen by a different mechanism.

3.3.3 Amplified der(15;21)

3.3.3.1 Introduction

The results of interphase FISH and aCGH outlined in sections 3.2. revealed that patient 6783, had the smallest chromosome 21 amplicon. However, the cytogenetic morphology had shown that the dup(21) chromosome in this case (Figure 3.5) was amongst one of the largest in the study. This warranted further investigation.

3.3.3.2 Method

A second, more detailed cytogenetic G-banded review was carried out on patient 6783, including both the diagnostic and remission sample. The findings from the remission sample prompted studies of stimulated peripheral blood to determine the constitutional origin of the chromosomal abnormalities observed. This was carried out by the regional cytogenetics laboratory. Chromosome painting with WCP 15 and 21 was carried out to confirm the cytogenetic findings and determine the chromosomal origin of the dup(21).

Prospective screening of new ALL patients for the presence of iAMP21 identified a second case (11005) in which there were additional copies of the *RUNX1* gene located on two copies of a dup(21) chromosome. Cytogenetic analysis revealed, that in addition to the clone with the dup(21) chromosomes, a second clone existed also with a Robertsonian der(15;21) as the only karyotypic change. As the clone with the two copies of dup(21) did not show this der(15;21), FISH was undertaken on both cases using WCP 15 and 21, to determine whether these dup(21) chromosomes were composed of material from both chromosomes 15 and 21.

Oligonucleotide aCGH using the Agilent Human Genome CGH, Microarray Kits 185A and 244A was performed patients 6783 and 11005, respectively, following the protocol outlined in section 2.5. The profiles of chromosomes 15 and 21 were compared for both patients.

3.3.3.3 Results

An additional cytogenetic review of 50 metaphases from case 6783 showed no evidence of a normal diploid population, but a single metaphase was observed with a der(15;21)(q10;q10) as the sole karyotypic change. Review of a follow up bone marrow sample, taken when the patient was in complete remission, showed that der(15;21)(q10;q10) was present in all cells examined. Cytogenetic analysis of stimulated peripheral blood, undertaken by the regional cytogenetics laboratory confirmed this abnormality to be a constitutional Robertsonian translocation.

Metaphase FISH with WCP 15 and 21 carried out on the diagnostic sample, identified that the dup(21) was composed of both chromosome 15 and 21 material (Figure 3.10). As the karyotype showed only one copy each of the normal chromosomes 15 and 21, it was assumed that the dup(21) must have arisen from the Robertsonian der(15;21) chromosome, and thus was described as der(15;21)dup(15;21).
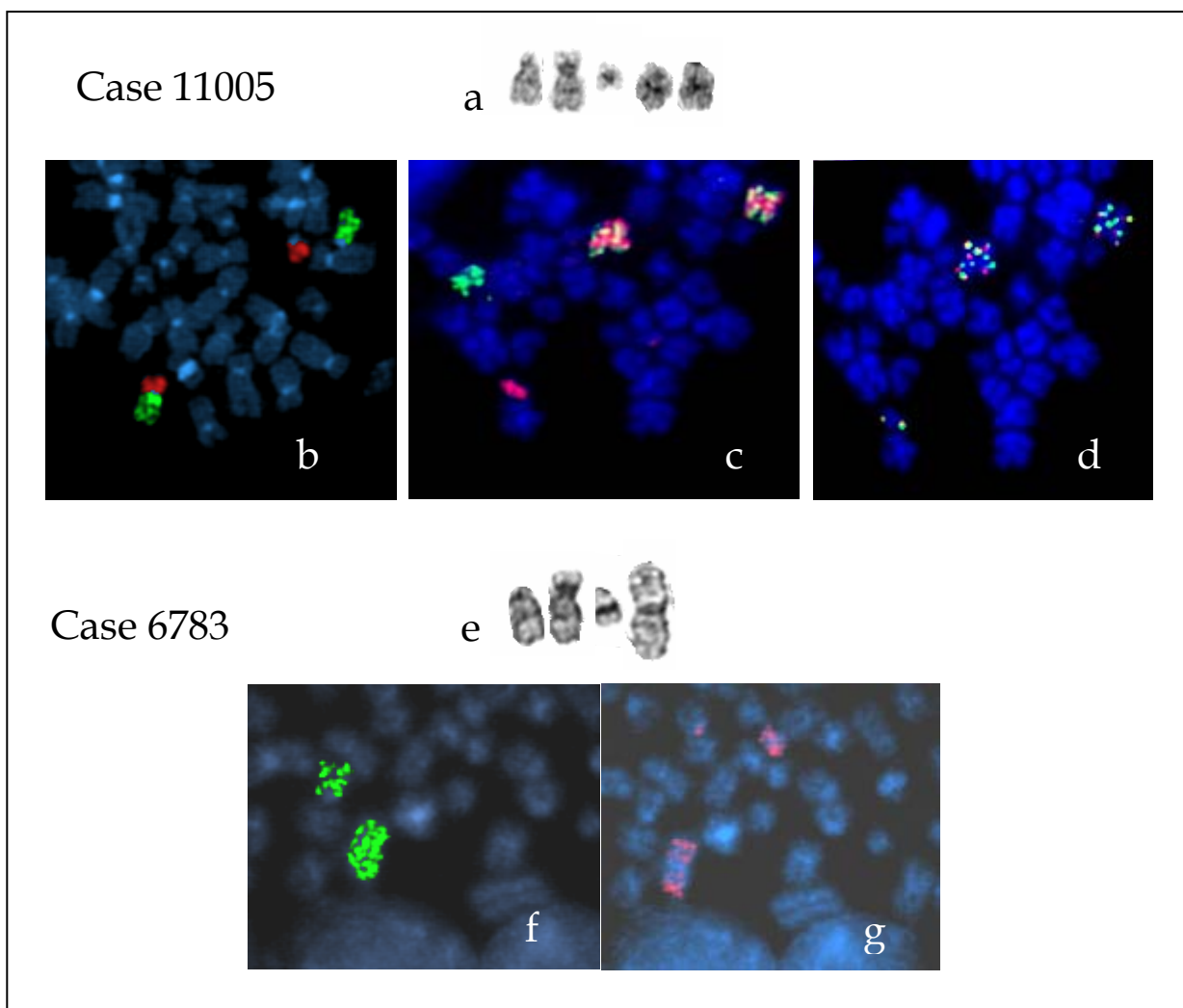
Figure 3.10 Combined FISH and G-banding from patients with der(15;21)dup(15;21). a) and e) G-banded form of chromosome 15, chromosome 21 and der(15;21)dup(15;21) from patients 11005 and 6783. WCP 15 (green) and 21 (red) on b) der(15;21) and c), f) and g) der(15;21)dup(15;21). d) *RUNX1* exon probes from patient 11005 on the der(15;21)dup(15;21) chromosomes.

Metaphase FISH on case 11005 with WCP 15 and 21 (Figure 3.10), showed that the dup(21) chromosome was composed of both 15 and 21, implicating that in both of these cases (6783 and 11005) the dup(21) chromosomes had arisen from the der(15;21).

The array profiles for chromosome 21 and 15 are displayed in Figure 3.11. Both patients showed copy number imbalances along the lengths of both

chromosomes, comprising deletions, gains and amplifications. However the genomic profiles differed between the two patients. This is demonstrated by superimposing the two profiles in Figure 3.11.

The same 6.6Mb minimal CRA of chromosome 21 as defined in other iAMP21 patients (Section 3.2.3.) was also present in patient 6783, whilst the size of the amplicon in patient 11005 was larger at ~20Mb, extending from genomic position 19Mb to 40Mb. A deletion of the subtelomeric region ~ 6Mb in size was found in patient 11005. It extended from genomic position ~ 40Mb through to the telomere.

The array profiles of chromosome 15 for both patients were highly complex with numerous regions of deletion, gain and amplification. A minimal CRA ~ 9Mb in size, located between genomic positions 60.0 and 69.0Mb (bands 15q21-q22), was common to both patients. Two common regions of deletion were recorded on chromosome 15. The first (~7Mb in size) was positioned between 36.0 and 43.0Mb (band 15q13); whilst the second (also ~7Mb in size) was located between 51 and 57Mb (band 15q15-q21) (Appendix 3, Table A3.10). Patient 11005 had a deletion which spanned from ~84Mb through to the telomeric region, whilst the same region in patient 6783 was gained.
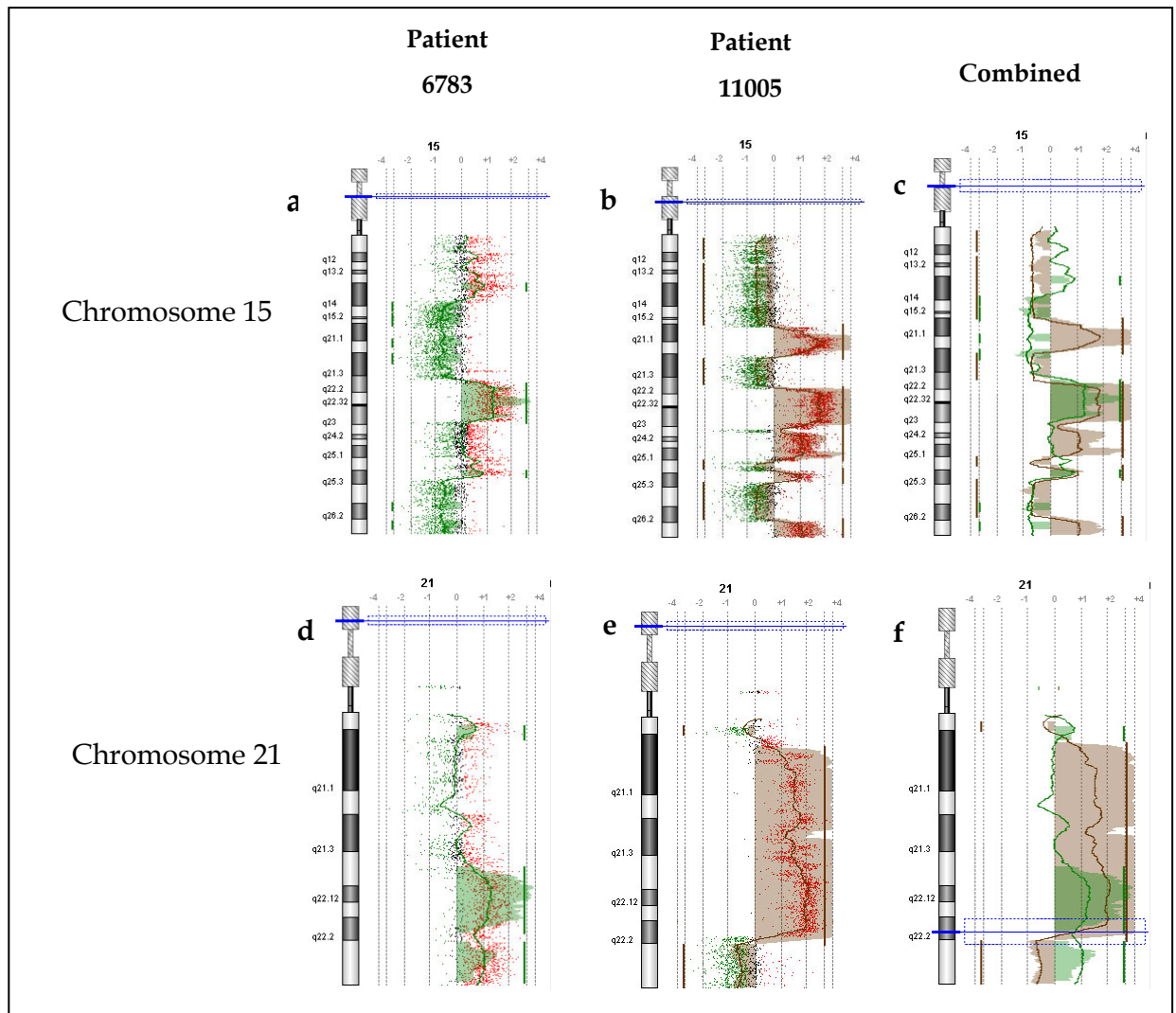
Figure 3.11 Oligonucleotide a CGH profiles of chromosome 15 and chromosome 21 from patients 6783 and 11005. a) b) Chromosome 15 profiles for 6783 and 11005, respectively and c) combined. d) e) Chromosome 21 profiles for 6783 and 11005, respectively and f) combined. Combined profiles illustrate common regions of deletion and amplification.
Key Green = 6783; Brown = 11005.

3.3.3.4   Conclusion

Two cases were identified with der(15;21)dup(15;21). Cytogenetic analysis of both cases determined that this abnormality was derived from a Robertsonian translocation, der(15;21)(q10;q10). In one patient this der(15;21) was confirmed to be constitutional in origin. This particular Robertsonian translocation is

extremely rare (Gardner & Sutherland, 2004), therefore the finding of two cases is extremely interesting.

High resolution aCGH carried out on these two cases confirmed the extent of involvement of both chromosomes 15 and 21 within the dup(21) marker. For each patient, unique profiles were obtained for both chromosomes with areas of deletion, amplification and gain being detected. The minimal CRA of chromosome 21 seen in iAMP21 patients was observed in patient 11005 and this region was contained within the amplicon of patient 6783. Patient 11005 also had a deletion of the subtelomeric region. Collectively, these results were consistent with the definition of iAMP21 for these patients.

The chromosome 15 profiles were also different between the two patients, with some common regions of deletion and amplification. Despite these differences, it is possible that the duplicated marker chromosomes had arisen via a common mechanism from a der(15;21) translocation. It was not possible to establish whether the der(15;21)dup(15;21) chromosome in patient 11005 had arisen from an acquired or a constitutional der(15;21). However, as only a single cell examined by both cytogenetic analysis and FISH was found with a normal karyotype it cannot be ruled out that the der(15;21) is a constitutional mosaic in this patient. Further studies are required to confirm this finding.

3.4 Diagnostic Test

3.4.1 Introduction

Treatment success rates in childhood ALL have progressively improved with time. Currently, five year event-free survival rates of >80% are achieved on a number of treatment protocols throughout the world (Pui & Evans, 2006;Borowitz *et al*, 2008). The detection of genetic abnormalities associated with a poor prognosis is however essential in order to maintain the success of current risk adapted therapy by ensuring that high risk patients are treated appropriately. Moorman *et al* (2007b) established that patients diagnosed as

iAMP21 treated on the MRCALL97 treatment trial had a significantly inferior event free and overall survival compared with other ALL patients on the same trial. As a result patients diagnosed with this abnormality in the UK are now treated on the high risk arm of the current ALL2003 childhood treatment trial. In a recent study by Cooley *et al* (2007), it was noted that patients with loss of chromosome 21 have a poorer outcome than those with normal copy number for chromosome 21. This was a cytogenetic study only, but based on the karyotypes published in this paper, it is likely that patients with iAMP21 were included, hence having an impact on the overall outcome of the patient group.

To date, characterisation of iAMP21 using classical cytogenetics and FISH (as outlined in previous sections) as well as other molecular methods to look for copy number changes and gene expression profiling (Strefford *et al*, 2006;Kuchinskaya *et al*, 2007), have failed to identify a putative target gene or gene fusion initiating leukaemogenesis in these patients. Consequently, the only methods for detection of iAMP21 patients are those that accurately detect their distinctive genomic profiles. Although aCGH could potentially fulfil this role, it is an expensive option as a routine diagnostic test. Thus, FISH, using probes directed to the *RUNX1* locus, remains the most reliable method. Although iAMP21 may be reliably defined by this method, it depends on the presence of metaphases for the definitive diagnosis. A significant number of ALL samples fail cytogenetic analysis (Harrison *et al*, 2005), which is frequently a reflection of the lack of metaphases. In interphase it is particularly difficult to distinguish iAMP21 patients from those having gain of chromosome 21 or i(21)(q10). The best way to differentiate between the different abnormalities when no metaphases are present would be to use a test that precisely detects the copy number of chromosome 21; for example a combined FISH test consisting of a *RUNX1* probe together with a chromosome 21 centromeric and telomeric probe. However, the centromeric region of chromosome 21 is problematic as it has repetitive sequences in common with chromosome 13. This results in cross

hybridisation when using FISH probes, making accurate enumeration difficult. Although these tests would be definitive for the detection of chromosome 21 copy number, they would not provide an unequivocal test for the detection of iAMP21.

Coupled with this dilemma is the fact that a number of centres outside the UK do not employ FISH for the detection of chromosomal abnormalities, but rely on molecular based techniques, for example using RT-PCR for the detection of the *ETV6-RUNX1* fusion will fail to find iAMP21. It is thus paramount to design a diagnostic test which will accurately identify iAMP21 patients using either a complementary FISH or molecular technique.

Based on the FISH and aCGH data (section 3.2) (Kuchinskaya *et al*, 2007;Strefford *et al*, 2007), a diagnostic test was designed making the following assumptions:

- *RUNX1* would define the level of amplification within the CRA
- DNA copy number distal to the CRA at the subtelomere will always be lower than *RUNX1*
- DNA copy number proximal to the CRA will be normal, gained or deleted but never amplified to the same extent as *RUNX1*

Thus by quantifying the DNA copy number as a ratio difference between three targets, one either side of the CRA and one within, it should be possible to definitively diagnose iAMP21, as these patients would be the only group with the highest copy number within the CRA.

Two quantitative molecular techniques, Q-PCR and MLPA, in addition to a diagnostic FISH test were designed and evaluated in order to establish their relative abilities to accurately identify iAMP21 and distinguish these patients from those with other abnormalities involving chromosome 21.

3.4.2 Methods

3.4.2.1 FISH

All patients involved in the evaluation of the FISH procedure had been previously screened with the commercial LSI TEL-AML ES® probe to:

- exclude the presence of the *ETV6-RUNX1* fusion
- determine the *RUNX1* copy number

From this screen, patients were selected who had been identified as *ETV6-RUNX1* negative with ≥ 5 *RUNX1* signals. Two dual colour FISH tests, one with an upstream probe located close to the centromere and one with a 21q subtelomere probe, in association with *RUNX1* provided the second part of the diagnostic test. A comparison of the copy number obtained for all three probes was then undertaken and the ratio of the upstream probe compared to *RUNX1* and the down stream probe compared to *RUNX1* was calculated. It was hypothesised that those patients who were iAMP21 positive would have a ratio of < 1 for each site. In order to validate the test, the FISH procedure and scoring was carried out blind by an independent technician.

3.4.2.1.1 Probe selection

Two BAC probes RP11-213G23 (H) (genomic position 15.3Mb) and Probe RP11-135B17 (I) (genomic position 46.8Mb) were chosen to represent the proximal and distal probes to the *RUNX1* target. (Probe I is a new subtelomeric probe, selected to ensure consistency, because the exact genomic location of the commercial subtelomeric probe used in previous studies is not fully known). Probe RP11-17O20 (J) (genomic position 35.3Mb) was selected as the *RUNX1* target probe. Previous screening of fixed cell suspensions from 20 iAMP21 patients had established that both probes H and I were not amplified.

3.4.2.1.2 FISH experiment

Two, dual colour, dual probe experiments were undertaken with the *RUNX1* probe, (labelled with Spectrum green) being combined with one of each of the other probes (labelled with Spectrum red). Copy number was determined in 50 abnormal cells for each probe and the modal number of signals found for each probe used to calculate the ratio. This FISH analysis was undertaken by Kerry Barber, LRCG.

3.4.2.1.3 Patients

FISH was performed blind on a total of 30 patients including iAMP21 patients (n=8), gain of chromosome 21 as the sole abnormality (n=6), high hyperdiploidy (n=5), tetraploidy (n=1), isochromosome 21 (n=4), possible variants of iAMP21 (n=3), normal (n=1) ALL patients with no detectable chromosome 21 abnormalities (n=1).

3.4.2.1.4 Results

The results of FISH screening are displayed in Table 3.6. In a single patient (7588), FISH failed, as the distribution and quality of the signals were such that it was not possible to accurately count the number of signals at each probe location. Seven of the eight iAMP21 patients were correctly identified based on the ratio assessment.

Patient	H	*RUNX1*	I	Ratio A H:*RUNX1*	Ratio B I:*RUNX1*	iAMP21	Chromosome 21 Abnormality
4894	3	3	3	1	1	No	21
7214	3	3	3	1	1	No	21
8274	3	3	3	1	1	No	21
11463	3	3	3	1	1	No	21
11734	3	3	3	1	1	No	21
7251	4	4	4	1	1	No	Tetraploid
6786	4	4	4	1	1	No	Heh
9180	4	4	4	1	1	No	Heh
9453	4	4	4	1	1	No	Heh
9488	4	4	4	1	1	No	Heh
10192	4	4	4	1	1	No	Heh
5047	2	4	1	0.5	0.3	Yes	iAMP21
5754	3	7	1	0.4	0.1	Yes	iAMP21
10444	1	7	1	0.1	0.1	Yes	iAMP21
10542	1	7	1	0.1	0.1	Yes	iAMP21
11056	2	5	1	0.4	0.2	Yes	iAMP21
11061	2	7	1	0.3	0.1	Yes	iAMP21
11116	1	5	5	0.2	1	No	iAMP21
11158	3	6	1	0.5	0.2	Yes	iAMP21
5612	3	3	3	1	1	No	iso(21)
4247	2	3	3	0.7	1	No	iso(21)
11200	3	3	3	1	1	No	iso(21)
7558	Fail	Fail	Fail	Fail	Fail	Fail	iso(21)
5586	5	5	5	1	1	No	iso(21)
9859	2	2	2	1	1	No	Normal
4676	5	5	5	1	1	No	Unknown
4746	1	6	6	0.2	1	?	Unknown
9010	1	3	1	0.3	0.3	?	der(9)ins(21)

Table 3.6 Interphase FISH screen of ALL patients with probes designed to detect iAMP21. Columns represent probes and rows represent patients.
H = RP11-213G23 clone, genomic position 15.3 Mb (proximal to *RUNX*1),
I = RP11-135B17, genomic position 46.8 Mb (distal to *RUNX*1).
Patients are ordered according to chromosome 21 abnormality. Modal copy number is recorded in the boxes. The interpretation is recorded in the iAMP21 column, with Yes = iAMP21 and No= non iAMP21. The true abnormality is given in the final column.
21= Gain of chromosome 21; Heh= high hyperdiploid; iso(21) = i(21)(q10)
iAMP21= intrachromosomal amplification of chromosome 21

In one iAMP21 case (11116) the observed ratio did not reach the expected, thus it was recorded as iAMP21 negative. A review of the *RUNX1* signal distribution in interphase in this patient, was however consistent with the clusters of signals associated with iAMP21.

In another case (9010) the ratios of the proximal and distal probes were consistent with that of iAMP21. However, enumeration of signals with the commercial TEL-AML1 probe had shown that the modal copy number for *RUNX1* was 3, (range 3-4). Metaphase FISH demonstrated that two of the signals were on a single chromosome, confirmed to be a der(9)t(9;21)(p1;q?)dup(21)(?) chromosome. This patient had been included in the blind test to highlight the importance of having ≥ 5 signals to indicate the presence of iAMP21. The scorer had noted that, although the ratio fulfilled the criteria for diagnosis of iAMP21, the overall number of *RUNX1* signals was too low.

Two patients (4247, 4746) showed ratios similar to those of the iAMP21 patient (11116). These results were discrepant with the expected ratios in patient 4247 for the upstream probe. In case 4676, the karyotypic origin of chromosome 21 had not been established. For the other cases the ratios of both A and B were recorded as one. This highlighted that the copy number in these areas is equal along the length of the chromosome.

3.4.2.1.5 Conclusion

Screening 30 ALL cases with a probe set specifically designed to detect iAMP21 patients, demonstrated that in the majority of cases results were concordant with the expected outcome. Seven of eight iAMP21patients were correctly identified. A discrepant result was noted in a single case, in which the number of signals in the subtelomeric region was the same as the *RUNX1* probe. Although a previous case of iAMP21 (6788, section 3.2.3.) had been noted with

amplification of the subtelomeric region, the level of amplification in that case was lower than that recorded for *RUNX1*. Patient 11116 had a failed cytogenetic result, thus it cannot be ruled out that additional copies of chromosome 21 may account for some of the additional *RUNX1* signals. In a single patient the ratios were neither consistent with iAMP21 nor with the karyotype. This case may represent a variant iAMP21. In all cases where the chromosome 21 status was known, the results were as expected, consistent with the predicted outcome. This demonstrated that, using this approach, it was possible to distinguish iAMP21 patients and differentiate them from patients with high hyperdiploidy and i(21)(q10).

3.4.2.2 Polymerase chain reaction (PCR)

In a non peer reviewed abstract Haas *et al* (2005) designed a DNA- based real-time polymerase chain reaction test to identify iAMP21 patients. The test was based on the comparative quantification of three regions, using two probes located to chromosome 21 and one to chromosome 11. By comparing the level at each region they were able to delineate and discriminate between patients with iAMP21 and those with gain of chromosome 21, due to either having an isochromosome 21, trisomy 21 or a high hyperdiploid karyotype with additional copies of 21. In order to test this model on the patients in this study, a quantitative DNA based RT-PCR (Q-PCR) test was designed. Using the hypothesis outlined in section 3.4.1, three target genes were selected on chromosome 21. *STCH* located at genomic position ~14.6Mb was selected as the centromeric upstream target, *RUNX1* as the target within the amplicon and *PRMT2* located at genomic position ~46.8Mb as the telomeric target. *CYP27C1* on chromosome 2, genomic position ~12.7Mb was selected as the reference gene/ house keeping gene that the relative ratios would be obtained from. This gene was chosen as karyotype analysis of iAMP21 and high hyperdiploid karyotypes

(Robinson *et al*, 2007;Heerema *et al*, 2007) have shown that it is not involved in copy number changes in ALL.

By comparing the relative ratios of these genes in our samples to those of normal DNA, it should be possible to distinguish iAMP21 patients from those with gain of chromosome 21 as they would show a different pattern of gain along the length of chromosome 21 in a similar manner to the diagnostic FISH test (Section 3.4.2).

3.4.2.2.1 Methods

The Multiplex Q-PCR test was conducted as described in section 2.6. Genomic DNA from three iAMP21 patients (6996, 6788 and 7045), three with high hyperdiploidy and 3 or 4 copies of chromosome 21 (7290, 4073, 11002) and a single ALL patient with gain of chromosome 21 as the sole abnormality (4381) were initially investigated. Genomic DNA from six normal individuals was also tested.

3.4.2.2.2 Results
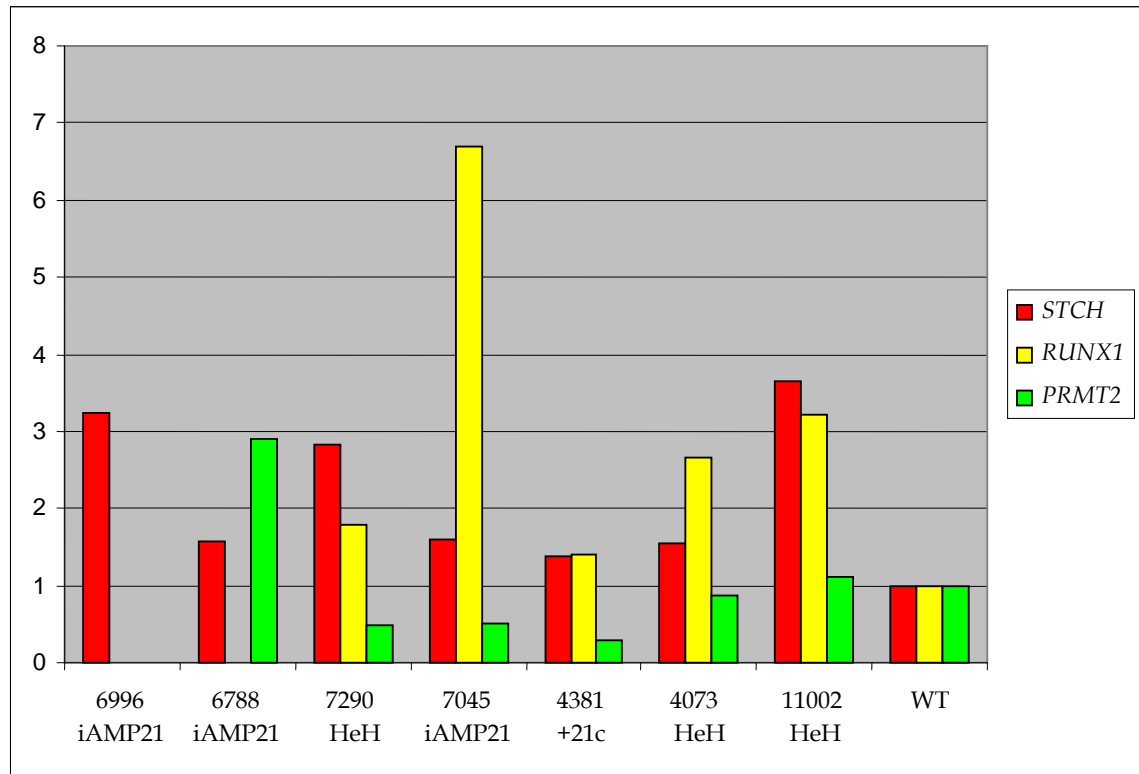
Figure 3.12 Q-PCR of DNA levels for *STCH*, *RUNX1* and *PRMT2* in seven ALL patients. 2^-DDCt recorded for each DNA target in each patient are plotted adjacent to each other.

The fold change (2^-DDCt) obtained for each gene from all seven patients are displayed in Figure 3.12 (Appendix 3, Tables A3.11–A3.13). In two patients (6788 and 6996) no fluorescence was detected following 40 cycles of amplification for the *RUNX1* locus. In addition patient 6996 failed to give a result for the *PRMT2* downstream target gene. Thus no interpretation of the results for this patient was possible.

The results obtained from the three high hyperdiploid cases and the patient with a constitutional gain of chromosome 21 (+21c) was unexpected. Fold

change differences indicated that in all four patients there was a lower level of the downstream target gene *PRMT2* in comparison to *RUNX1* and *STCH*.

The level of *RUNX1* and *STCH* was higher in all four cases compared to that of the wild type, consistent with the cytogenetics, however it was expected that the level of all three genes was the same. Patient 7045 showed the expected pattern, with a higher level of *RUNX1* in comparison to both the upstream target *STCH* and the downstream target *PRMT2*.

An assessment was made of six normal individuals to investigate whether the unexpected results were due to an error in the design of the PCR reaction or a true reflection of copy number change in these patients. These results are displayed in Figure 3.13. As with the previous experiment, unexpected results were obtained from all cases. Fold change differences indicated that the relative levels for all three genes were different in all samples. In particular the level of *RUNX1* appeared to be lower in all patients than either *STCH* or *PRMT2*.

3.4.2.2.3 Conclusion

Results obtained from both the normal control and test samples appeared to be inaccurate. This suggested that the PCR reaction was not sufficiently optimised to detect the copy number changes with the sensitivity required for the test. Primer and probe design is crucial to the success of any Q-PCR reaction. Our results indicated that there were problems with the test design. Initial calculations had assumed that the PCR efficiency for all primers was equal and 100%. In order to eliminate this error the primer efficiency for each target gene was adjusted using the Light Cycle Q Software.
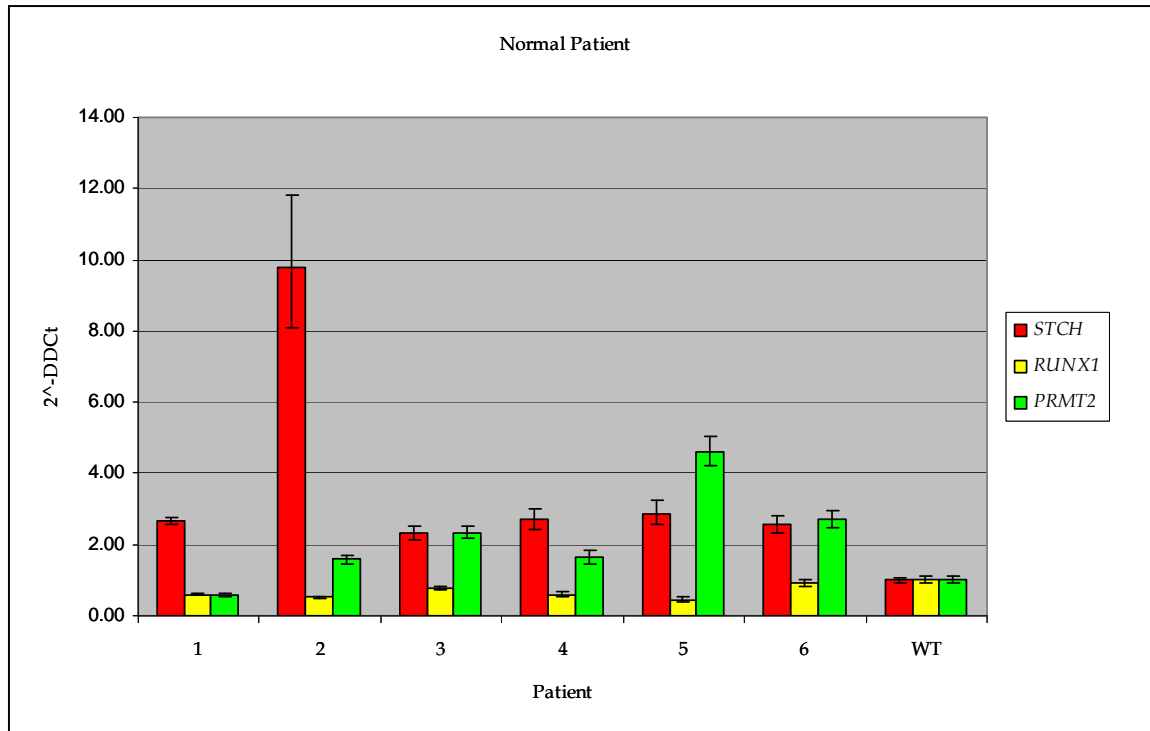
Figure 3.13 Q-PCR of DNA levels for *STCH*, *RUNX1* and *PRMT2* in six normal controls. 2^-DDCt recorded for each DNA target in each control are plotted adjacent to each other. For each target the standard deviation is shown by the vertical line.

The results obtained (Figure 3.13) (Appendix 3, Tables A3.14–A3.16) did not correct any of the differences seen initially. This indicated that the primer efficiencies were too different between the target genes to make the relative quantification compatible. To demonstrate this further, a comparison was made between *STCH* and *PRMT* using *RUNX1* as the calibrator (Appendix 3, Figure A3.3). In theory, as each sample has the same copy number for chromosome 21 at the start of the reaction, they should have equal concentration at the end. The results clearly indicated that both *STCH* and *PRMT2* were lower than *RUNX1*. This implied that the *RUNX1* primers did not have the same PCR efficiency as the other target genes. Hence, this explained the low levels of *RUNX1* seen in the normal samples. In the only other previously reported RQ-PCR test for iAMP21

(Haas *et al*, 2005), the primer design has not been published; thus it was not possible to compare results.

In addition to primer design, the test must be robust enough to deal with differences in DNA quality. Discrepancies were noted between the control patient and wild type DNA indicating that both the quantity and quality of the patient genomic DNA may have been poor. Overall this test failed to generate a robust result that was able to detect genomic DNA levels of *STCH*, *RUNX1*, *PRMT2* and *CYP27C1* accurately. Further work is required to optimise the PCR reaction in order to ensure that the reactions are run at optimal conditions with equal primer efficiency. Due to time constraints this was not possible and further work on the development of a Q-PCR diagnostic test has ceased.

3.4.2.3 Multiplex ligation dependent probe amplification

3.4.2.3.1 Introduction

Multiplex ligation dependent probe amplification (MLPA) is a recently described method for detecting gross deletions and duplications of DNA sequences (Schouten *et al*, 2002). The technique allows for the simultaneous detection of different nucleic acid sequences in a single PCR reaction (section 2.7), which can then be quantified. Designing an MLPA assay with a selection of target sites along the length of chromosome 21, including areas either side of the CRA as well as within would allow for the identification of iAMP21 due to their distinct chromosome 21 profiles, as highlighted in section 3.2.

To evaluate the efficiency of MLPA in the identification of iAMP21 patients, a test was developed using two MLPA probe pairs targeting *RUNX1* and *PRSS7* (an upstream gene located at 18.5MB) which were combined with the commercially available telomere probe mix (P036B, MRC Holland, Amsterdam) as outlined in section 2.7.1. By comparing the relative amounts of DNA at each site, iAMP21 patients were accurately identified.

3.4.2.3.2 Methods

MLPA was performed on genomic DNA from a total of 33 patients including iAMP21 (n=16), gain of chromosome 21 as the sole abnormality (n=4), high hyperdiploidy (n=6), hypodiploidy (n=1), isochromosome 21 (n=1), variant iAMP21 (n=3), ALL patients with no detectable abnormalities (n=2).

The MLPA work was performed blind by Dr D Bunyan, Wessex Regional Cytogenetic Unit. The results obtained were compared to the karyotype and *RUNX1* FISH.

3.4.2.3.3 Results

The MLPA screening results for the four locations on chromosome 21, from all 33 patients are displayed in Table 3.7. Patients defined as iAMP21 showed variable copy number at each of the four sites. For all 16 iAMP21 cases the highest level was recorded at the *RUNX1* locus. In 12 of these cases a deletion of the 21q subtelomere was found, consistent with the results from the FISH diagnostic test (section 3.5.5.3.1). In three patients (6783, 4279 and 6788) the results were discrepant with the FISH findings. In patient 6783, FISH had shown the presence of two copies of the 21q subtelomere in comparison to the three observed by MLPA. In patient 4279, only a single copy had been recorded for this location by FISH compared to the two copies seen with MLPA (a normal copy number for chromosome 21 was observed by conventional cytogenetics). In patient 6788, four copies of the 21q subtelomere had been detected by FISH, whilst MLPA had only detected three copies. Of the 11 cases with high hyperdiploidy, hypodiploidy and sole gain of chromosome 21, the copy number in the majority of cases was consistent with the cytogenetics. As expected the level was the same at all four locations. One exception to this was case 4073 in which only two copies of the 21q subtelomere was detected instead of the expected three (one on each of the three chromosomes 21). As no FISH with

subtelomeric probes had been carried out, it was not possible to confirm this unexpected gain. In two high hyperdiploid cases (12025 and 7558), the copy number recorded for *RUNX1* was lower and higher (3 and 6), respectively, than that recorded for both the subtelomeric region and *PRSS7*.

A comparison between the *RUNX1* copy number detected by FISH and MLPA illustrated that there were a number of discrepant results between the two techniques.

In fourteen of the 16 iAMP21 cases the results were higher with FISH than MLPA. In the majority of cases this differed by only one or two copies with most of the FISH results being higher than those from MLPA.

Abnormalities detected in patients for subtelomeric regions other than chromosome 21 are shown in Appendix 3, Tables A3.17-A3.18. Cases with gain of chromosomes due to the presence of a high hyperdiploid karyotype or gain of single chromosomes were successfully detected by subtelomeric MLPA. In the majority of cases these gains were consistent with the cytogenetics. A small number of cases had discrepant results, when compared to the cytogenetics. As no FISH with the relevant subtelomeric probes had been carried out, it was not possible to determine if the unexpected gains or losses were true.

In the iAMP21 patients, no consistent gain or loss of any subtelomeric region, other than chromosome 21, was observed. Screening with 21p subtelomeric probes showed a gain in five patients (6783, 6996, 7219, 8983,11706), whilst in one patient (4405) a deletion had occurred.

Patient ID	Copy Number						
	21p	*PRSS7*	*RUNX1* (FISH)	*RUNX1*	21q	21qFISH	Code
3043	3	3	3	3	3	NK	21
4073	3	3	3	3	2	NK	21
4184	3	3	ND	3	3	NK	21
4318	3	3	ND	3	3	NK	21
7653	3	3	3	3	3	NK	Ho
4642	3	3	ND	3	3	NK	HeH
11102	3	3	4	3	3	NK	HeH
7290	4	4	4	4	4	NK	HeH
9525	4	4	4	4	4	NK	HeH
12025	4	3	4	3	4	NK	HeH
7558	5	6	4	6	5	NK	HeH i(21)
4405	1	3	8	7	1	1	iAMP21
6783	3	2	5	4	3	2	iAMP21
6788	2	2	4.5	5	3	4	iAMP21
6996	4	5	10.5	6	1	1	iAMP21
7045	2	2	6.5	5	1	1	iAMP21
7093	2	3	7	5	1	1	iAMP21
7219	3	3	7	6	1	1	iAMP21
7619	4	4	8	7	1	NK	iAMP21
7732	2	3	5	4	1	1	iAMP21
7774	2	2	5	3	2	NK	iAMP21
8743	2	2	5	4	1	1	iAMP21
8983	3	3	7	5	1	1	iAMP21
9028	2	3	8	6	1	1	iAMP21
11005	2	3	7	7	1	1	iAMP21
11706	3	3	9.5	6	1	1	iAMP21
4279	2	2	5	3	2	2	iAMP21
10958	2	2	2	2	2	NK	Normal
12377	2	2	2	2	2	NK	Normal
4676	4	5	5	5	4	5	i(21)
4247	2	2	3	3	3	3	NK
4746	1	4	7	4	6	6	NK
9101	1	1	4	3	1	1	NK
Key	Del	Nor	Gain	Amp			

Table 3.7 MLPA and FISH data measuring the copy number of the p and q subtelomeric regions and *PRSS7* and *RUNX1* on chromosome 21. iAMP21= iAMP21, 1= Gain of chromosome 21 as the sole abnormality, HeH = High hyperdiploidy, Ho= Hypodiploidy, i(21)= Isochromosome 21, NK= undefined abnormality in chromosome 21. MLPA copy number changes are recorded in coloured columns whilst the FISH data recorded as the mean is shown in clear columns.

Key: D=deletion (1 copy); N= Normal (2 copies), G=Gain (3-4 copies); A= Amplification (> 5 copies).

3.4.2.3.4 Conclusion

The results obtained from screening a number of ALL patients to look for copy number changes along the length of chromosome 21, clearly demonstrate the power of MLPA in detecting copy number change. In all 16 iAMP21 patients the profiles obtained were consistent with those previously described for iAMP21 patients and distinct from those seen in the other groups. The test carried out blind, clearly validated the test design and illustrated that this technique was able to differentiate between those cases defined as iAMP21 and those which were not.

Unlike the other studies outlined in this thesis, this technique provided data on the status of the 21p subtelomere in iAMP21 patients. In 31% (5/16) there was gain of the 21p subtelomere. Previous studies to characterise iAMP21 using a variety of techniques (section 3.2) had not investigated 21p. In four of these cases a direct comparison with the karyotype was not possible, as conventional cytogenetics had either failed or the result was normal. In one case with der(15;21)dup(15;21) (6783) (Section 3.3.3.), there was no evidence of an additional chromosome 21 in the karyotype. Thus, it was concluded that the gains of both the 21p and 21q subtelomeres were located within the der(15;21)dup(15;21) chromosome in this case. These results provided further evidence for the complexity of this abnormality.

Discrepant results were noted between FISH and MLPA data regarding accuracy of copy number change. This was probably due to comparing results from genomic DNA and interphase FISH. The interphase FISH scoring excluded the normal cell population. DNA from the normal cell population is included within the total genomic DNA used in the MLPA assay and will have the effect of reducing the relative copy number gain in some cases.

Chapter Four – Discussion

4 Discussion

Genetic aberrations are a key feature of malignancy where they result in the altered expression and function of genes residing within those regions of the genome where they occur. In haematological malignancies abnormalities comprise:

- Chromosomal translocations or other structural rearrangements which result in the formation and overexpression of oncogenic fusion genes
- Copy number changes including deletions /monosomy which can result in loss of tumour suppressor genes or duplications /trisomy which lead to overexpression of oncogenes

These aberrations contribute to the development of leukaemia by altering the regulatory processes that control cellular function, which in turn results in changes in proliferation, differentiation and resistance to apoptosis, as described in the introduction (Section1.1). Individual genetic abnormalities alone are usually insufficient to drive the leukaemic phenotype but require the co-operation of additional aberrations, for example in genes encoding the principal regulators of B lymphocyte development and differentiation, such as mutations in *PAX 5* present in 40% of pre-B -ALL (Mullighan *et al*, 2007).

Current treatment protocols are based on a risk-adapted strategy, whereby the intensification of therapy is tailored to risk of relapse as indicated by certain clinical features including age, WBC at diagnosis, gender, immunophenotype, as well as the presence of specific genetic abnormalities. This approach has resulted in overall survival rates of over 80% in childhood ALL and 40% in adults (Pui & Evans, 2006). Increased intensification of such treatments is unlikely to effect higher rates of cure, but will increase treatment

related toxicity both in the short and long term. In order to achieve further improvements in response to treatment, it is thus important to develop new treatment strategies based on targeted therapies which will act against the specific genetic abnormalities that are crucial to the survival of the leukaemic clones. A number of recurrent genetic subtypes have been described in ALL, accounting for approximately 75% of cases (Johansson *et al*, 2004). With the development of new technologies, novel genetic subgroups are being identified. The accurate characterisation of these novel abnormalities is essential in order to further increase our understanding of the mechanisms involved in the disease biology as well as providing the basis for improved clinical management and the identification of therapeutic targets.

4.1   iAMP21 Characterisation

The application of a combination of cytogenetic techniques, including G-banding, FISH and aCGH has successfully enhanced our understanding of the iAMP21 abnormality. From the results of initial investigations using aCGH and FISH, it was apparent that this abnormality, previously described as *RUNX1* amplification (Harewood *et al*, 2003;Soulier *et al*, 2003;Strefford *et al*, 2006), spanned a large region of 21q. In all patients gain, amplification and deletion of chromosome 21 was established. Detailed analysis of the results illustrated that the abnormality was highly complex, with each patient having a unique genomic profile, with regards to the extent of 21q involvement, the level of amplification and the size of the amplicon. Despite this variability, a minimum CRA located between genomic positions 32.3 and 40.0Mb (21q22.1-21q22.2), which included the *RUNX1* gene, was identified in 100% (10/10) of cases. Studies with high resolution oligonucleotide aCGH refined the minimal CRA to a region of ~6Mb in size between genomic positions 33.2-39.8Mb and demonstrated that there was a 'step wise profile' of duplication, gain, amplification and deletion running in a centromeric to telomeric direction (Strefford *et al*, 2006;Kuchinskaya *et al*,

2007;Strefford *et al*, 2007). These findings were confirmed in another recent study by Kuchinskaya *et al* (2008), where a similar pattern of gain, amplification and deletion using similar techniques was observed. However, they were, unable to confirm the CRA. Instead, they identified an amplicon that was 15~30Mb in size located between genomic positions 14.5 and 46.5Mb, spanning a large region of chromosome 21.

FISH analysis of a larger group of iAMP21 patients, established that the highest copy number for all patients occurred at the *RUNX1* locus, confirming the aCGH data. As patients were selected for study based on their increased *RUNX1* copy number, it could be argued that this result was not unexpected and was a reflection of selection bias. The extent of involvement of chromosome 21 in iAMP21 became apparent following BAC aCGH analysis. Although *RUNX1* copy number gain was known prior to the onset of this study, its involvement within the CRA was unknown. The results obtained from the oligonucleotide aCGH (a more sensitive technique than BAC aCGH) illustrated that the level of amplification was similar over the length of the amplicon. As *RUNX1* was located within the amplicon, this justified the choice of *RUNX1* as representative of the CRA.

FISH studies, carried out on both interphase and metaphase cells, provided further evidence that the abnormality was highly complex, involving large regions of 21q, with each patient having a unique chromosome 21 profile in relation to the level of amplification and size of amplicon. The variability seen at this level supported the differences observed between patients in the G-banded morphology of the dup(21). An unexpected result from the initial investigations was the detection of a minimum CRD observed in 70% (7/10) of patients. This CRD was ~ 3.5Mb in size and included the subtelomeric region of chromosome 21. Further work demonstrated that this CRD occurred in a larger proportion of cases at an incidence of 76% (35/45).

The amplification of a genomic region is thought to represent selection of a region where the expression of gene(s) promotes growth of the tumour. Albertson *et al* (2006) emphasised that mapping of amplicons should identify candidate oncogenes within them. However, proving that a gene is the important target within an amplicon is problematic, as several genes map to the amplified region. In order to identify the significant genes, studies are usually undertaken to determine whether the candidate oncogene is expressed in the tumour and whether expression is enhanced when the gene is amplified. Gene expression analysis carried out on eight of the iAMP21 patients in a separate study, demonstrated that 10% of the top 150 significantly overexpressed genes were located within the CRA. However, analysis was unable to identify any one gene, including *RUNX1*, which was significantly differentially expressed in these patients (Strefford *et al*, 2006). It was noted that *RUNX1* was equally overexpressed in *ETV6-RUNX1* fusion positive and iAMP21 patients. This may be due to the failure of the expression profiling platform to distinguish these two groups or to the gain of chromosome 21, which is often seen as a secondary change in *ETV6-RUNX1* positive ALL. Mikhail *et al* (2002) also found increased *RUNX1* expression in four cases with iAMP21. However, this overexpression was not exclusive to patients with this abnormality. As reviewed by Myllykangas and Knuutila (2006) the overexpression of genes within amplified regions is variable in different cancers and frequently it is difficult to separate those driving genes (amplified and overexpressed) from bystander genes. In a number of studies it has been suggested that the co-amplification of genes within an amplicon is responsible for driving the disease, for example the co amplification of activated genes associated with *HER2* amplification in breast cancer (Kauraniemi & Kallioniemi, 2006;Arriola *et al*, 2008). It is possible that it is the co-amplification of a number of genes within the iAMP21 amplicon that is important in this subgroup of patients, rather than any one single gene within the amplicon.

The minimum size of the CRA in iAMP21 was established from the results of BAC aCGH and FISH data of a single patient. Subsequent investigations revealed that in this patient the abnormal chromosome 21, later described as a variant iAMP21, had arisen from a Robertsonian t(15;21) translocation. Although the amplification of 21q in this patient was verified, it is uncertain whether it should have been regarded as a typical iAMP21 and thus used to define the CRA of the entire patient group. If this patient is excluded then the size of the CRA becomes ~10Mb in size. Thus it is possible that the lack of identification of over expression of a single gene in the CRA is a reflection of defining the amplicon based on the results from a single patient. By removal of this patient from the expression analysis, it may be possible that the overexpression of other genes within this region would be identified. To the contrary, as the size becomes relatively large, it may emerge that the co- expression of a number of genes becomes important.

In the same study, high resolution array analysis of single-nucleotide polymorphisms (SNP) was undertaken on samples from three iAMP21 patients from the same series. The results confirmed the regions of copy number change and showed loss of heterozygosity (LOH) within the minimal CRA. As gain in copy number may mask LOH, no conclusions could be drawn as to whether the LOH was due to copy number neutral LOH (CNNLOH), otherwise known as acquired isodisomy or acquired uniparental disomy (UPD). This phenomenon has been seen in 20% of AML (Raghavan *et al*, 2005), where it is frequently associated with gene mutations such as *FLT3* (Griffiths *et al*, 2005). A recent study of 399 childhood ALL patients using high resolution 50K SNP chip analysis failed to detect any cases of CNNLOH involving copy number changes along chromosome 21, from which it was concluded that it is a rare event in childhood ALL (Kawamata *et al*, 2008). Thus, the presence of LOH as found in the three cases of iAMP21 should be further investigated.

4.2 Breakage–Fusion -Bridge

The combined technical approach employed to characterise iAMP21 provided evidence to imply that this abnormality had arisen from a distinct mechanism. A disadvantage of aCGH and interphase FISH is that neither technique is able to provide any information on the location *in situ* of the copy number alterations detected. The results obtained from the detailed characterisation of metaphases, using mBAND and BAC probe FISH mapping, provided evidence of inversions, duplications, amplification and deletions. These findings combined with the observation that each patient had a distinct genomic profile suggest that the dup(21) may have arisen from a series of chromatid breaks and reunions, such as those found in the Breakage-Fusion-Bridge (BFB) model. This mechanism was first described in maize by McClintock in 1941 (1941). It proposes that, after an initiating event, a double stranded DNA break (DSB) occurs, generating an unstable chromosome with two broken sister chromatids. Following replication of this chromosome, the sister chromatids, which are in close proximity, fuse together at their ends to form a dicentric chromosome. As a result of this fusion, the two sister chromatids cannot easily separate from one another in the subsequent anaphase. Thus as the two centromeres pull apart to opposite poles, a chromatin bridge is produced which eventually ruptures under tension. This leads to the generation of another unstable chromosome which contains an inverted repeat. This process defines the BFB cycle. Subsequent to DNA replication in the next cell cycle, this BFB cycle is repeated. These "chromosome end-to-end fusion" cycles may continue for generations and, as the fused chromosomes do not always break exactly at the site of fusion, it follows that one daughter cell will receive a chromosome with an inverted repeat while the other chromosome will have a terminal deletion. In this way it is possible to generate complex chromosomes with extensive intrachromosomal gains, amplifications and deletions organised as inverted repeats (Figure 4.1). The process is repeated until the chromosome

becomes stabilised by the gain of a teleomere. In this way it is possible to generate a chromosome with highly complex intrachromosomal rearrangements.
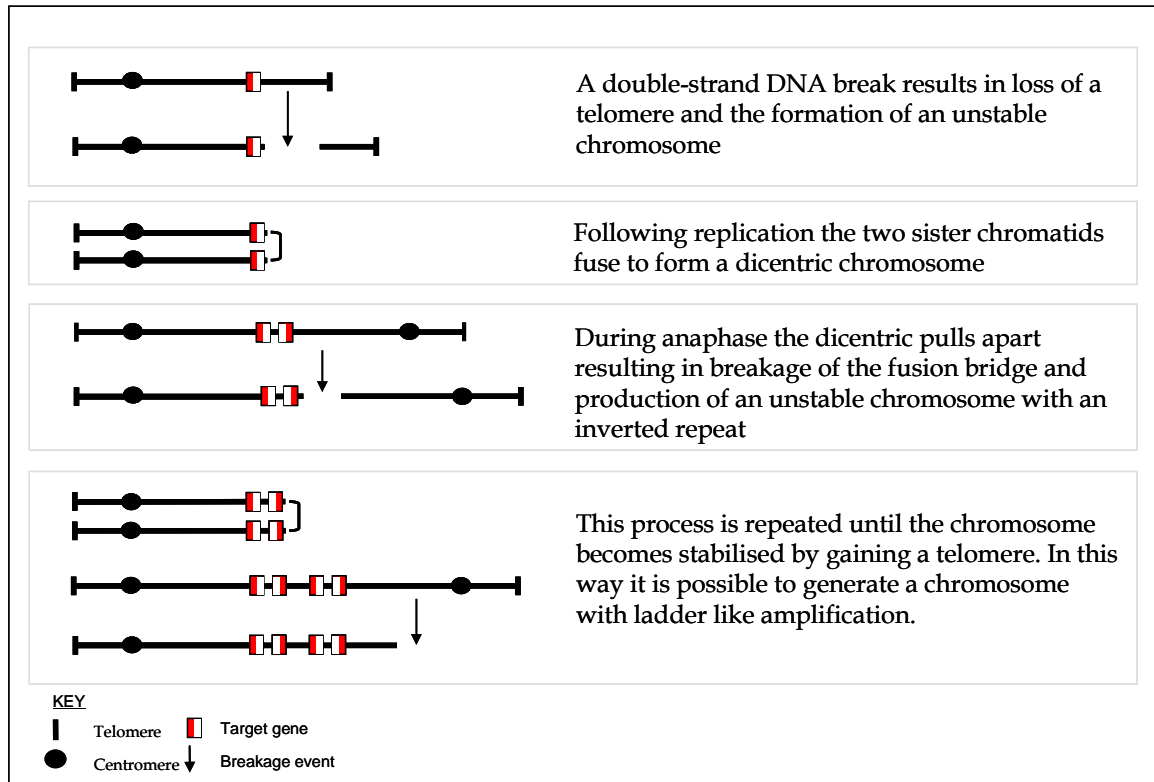
Figure 4.1 The Breakage Fusion Bridge Cycle. Adapted from Robinson *et al* (2007).

The variation in the size of the amplicon found in the iAMP21 patients using both aCGH and FISH, together with the ladder like distribution of *RUNX1,* and the varied morphology of the dup(21) between patients are consistent with this abnormality having arisen through a BFB mechanism. Although no evidence of anaphase bridges were found in this study due to the lack of visible anaphase cells, the work carried out by Kuchinskya *et al* (2007) demonstrated the presence of anaphase bridges containing chromosome 21 material, thus providing confirmation of the hypothesis.

In the review by Albertson (2006) it was described that amplified DNA can be visualised cytogenetically in three main ways, all of which may arise from the BFB mechanism:

1. Homogeneous staining regions, defined as an area on a chromosome with uniform staining frequently harbouring multiple copies of amplified DNA, often organised in a head–to–tail or inverted repeat fashion
2. Insertions, where the amplified region is inserted into other chromosomes throughout the genome
3. Double minutes defined as extra chromosomal amplified DNA visualised as acentric chromosomal fragments

In iAMP21 patients the amplified DNA was located on the dup(21), defining this abnormality as intrachromosomal amplification. Usually, this type of amplification is associated with the presence of HSR. However, both the morphology and staining pattern was extremely heterogeneous and a more appropriate description of the amplified regions would be an "abnormal staining region". This may reflect the complexity of the mechanisms involved in the generation of such regions or that the chromosomes may have been generated from ring chromosomes. Gisselsson *et al* (2000) observed that ring chromosomes may successfully undergo cell division utilising a BFB type of mechanism. As a ring chromosome may break at any point between the centromeres, it can give rise to daughter cells which differ from each other as well as from the mother cell.

A frequent observation throughout this study was the variability in copy number noted by FISH at those locations where amplification may have occurred. This range in copy number may have been a reflection of difficulties encountered in enumerating signals or it may have been a true reflection of inter-

cell differences. It is possible that a number of populations exist within the same patient samples, each with distinct amplicons.

The BFB model requires, as an initiating event, a DNA DSB (Gisselsson *et al*, 2000;Murnane, 2006). A number of mechanisms have been proposed, including errors in DNA repair and replication, loss or dysfunction of telomeres (Murnane, 2006;Bailey & Murnane, 2006) and breaks within regions of homology such as fragile sites (Arlt *et al*, 2006). The results from this study indicated that the most likely mechanism was loss of telomere.

4.2.1 Loss of Telomere

Telomere loss is a known initiating event of the BFB mechanism (Gisselsson *et al*, 2001;Lo *et al*, 2002;Murnane & Sabatier, 2004;Sabatier *et al*, 2005;). Telomeres are DNA-protein complexes that contain short repeat sequences added onto the ends of chromosomes by telomerase. They have a number of functions including protecting the ends of chromosomes and so preventing chromosome end to end fusion. The telomeric DNA sequences consists of tandem 5'-TTAGGG-3' repeats with a single-stranded G-rich 3' overhang of about 50-210 bases (Maser & Depinho, 2004). The single-stranded 3'-end overhang invades the duplex telomeric DNA repeats to form a large duplex telomere loop (T-loop) and a smaller single-stranded displacement loop (D-loop) (Maser & Depinho, 2004;Cheung & Deng, 2008). This configuration, together with a number of telomere-associated proteins, creates the telomere cap which in addition to protecting the chromosome end, distinguishes it from a DSB.

Loss or dysfunction of telomeres can occur in a number of different ways. Studies into these mechanisms, as reviewed by (Murnane, 2006) have shown that changes in expression of the proteins involved in the regulation of telomerase (an enzyme that controls telomere length by adding the TTAGGG sequence repeats to the 3' end of DNA in the telomere), including the Mre-11-Rad50-Nbs1 complex, have resulted in increased chromosome fusions. Equally the loss of

'capping function' has been found in cells with disrupted expression of telomere-associated proteins such as TRAF2, Ku and DNAs-PKcs (Murnane, 2006). DSB can result in the indirect loss of a telomere by deleting regions upstream of the telomere, or direct loss as a result of breaks within the telomeres themselves. As telomeres are similar to fragile sites, in that they have repetitive DNA, they are prone to DSB due to stalled replication forks (Murnane, 2006).

In this current study, loss of the chromosome 21q subtelomeric region was demonstrated in 77% of iAMP21cases. As the FISH probe used to detect specific subtelomeric sequences are designed to hybridise to regions adjacent to the repetitive telomeric sequence present on all chromosomes, it was hypothesised that in the iAMP21 patients, the 21q telomere had been deleted and that this loss initiated the BFB cycles observed in these patients.

FISH screening and oligonucleotide aCGH (Strefford *et al*, 2006) analysis of these cases demonstrated that the subtelomeric deletions were always adjacent to the amplicon. This finding is consistent with the loss of material near to the point of chromosome breakage, followed by the concomitant amplification of sequence centromeric to the breakpoint. This provides further evidence that BFB is initiated in iAMP21 patients by loss of telomere. In those cases with no subtelomeric probe deletion, it is possible that deletion may have occurred in a region distal to the subtelomeric probe. One patient (6788) demonstrated that there was an amplification of subtelomeric DNA, consistent with breakage occurring in the adjacent region, followed by amplification in a fashion similar to that observed in mouse embryonic stem cells (Lo *et al*, 2002). Similarly in patient 3131, detailed mapping showed the telomeric probe to be located to an unexpected region, indicating that a break had occurred in a region distal to this probe. In another four patients (7255, 3743, 3527, 4780), a normal copy number was observed for the subtelomeric probe. However, in these cases it was not possible to confirm the location of this probe in metaphase, thus it cannot be ruled out that an additional copy of chromosome 21, with an intact telomeric

region was present (as seen by conventional cytogenetics in patients 3131 and 3743) or that the deletion was distal to this probe.

Although the data indicated that the loss of a telomere may be the initiating event in the majority of iAMP21 patients, it is possible that in those patients with no evidence of subtelomeric loss that the BFB cycles may have alternatively arisen from defects in telomere function, or that the process may have been initiated by other events.

Previous studies have demonstrated amplification of genes at a distance from the telomere, indicating that alternative mechanisms do exist. Ciullo *et al* (2002) noted that overexpression of the *PIP* gene in breast cancer was initiated by activation of the fragile site, FRA7, on chromosome 7. Similarly, Miller *et al* (2006) found evidence that *MET*, which is up-regulated in oesophageal cancer, maps to the fragile site, FRA7G. Although no fragile sites have been detected on chromosome 21, Hattori *et al* (2000) found evidence of duplications of sequences of chromosome 21 which may be susceptible to DSB. Tanaka *et al* (2005;2007) noted that a critical event in the initiation of gene amplification was the formation of a large DNA palindrome, following the initial DBS break. They showed that DNA inverted repeats marked the borders between those regions which were amplified and those which are not. This indicated that the sites of such repeats may be important for the initiation of amplification. Similarly, Kolomietz *et al* (2002) highlighted that *Alu* repeat clusters, which have a high density of repetitive DNA, may be hot spots for DSB, and subsequent amplification.

Despite having no direct evidence that BFB initiated by loss of a telomere resulted in the generation of iAMP, the circumstantial evidence from this study indicated that this was the most plausible mechanism.

4.2.2 Termination of BFB

The BFB cycle ends, primarily, when the unstable chromosome stabilises by acquiring a new telomere. Acquisition of a new telomere, as reviewed by Murnane and Sabatier (2004), has been proposed to occur through a number of possible mechanisms including direct addition by telomerase, a recombination-based mechanism of alternative lengthening of telomeres, non reciprocal-translocations, break-induced replication, and the formation of dicentric, isochromosome or ring chromosomes.

The 'de novo' addition of repeat telomere sequences by telomerase has been observed in humans with genetic diseases that result from terminal deletions (Varley *et al*, 2000) as well as in tumour cells (Murnane & Sabatier, 2004). In childhood ALL, raised levels of telomerase (*hTERT*) (Cogulu *et al*, 2008) has been detected in pre-treatment samples compared to remission ones, indicating an increase in telomere synthesis associated with disease. A further mechanism of telomere acquisition is breakage-induced-replication (BIR) (Watanabe & Horiuchi, 2005), where the broken end of a chromosome with telomere loss invades a region of homology and initiates replication at that point by duplication. Telomeres can also be acquired in mammalian cells through the capture of the ends of other chromosomes as a result of nonreciprocal translocations.

The mechanism by which the telomeres are restored has an impact on the stability of the genome as a whole. Sabatier *et al* (2005) found that one of the most common methods of acquisition is through translocation, which can be either reciprocal or nonreciprocal (NRT), with loss of DNA from a donor chromosome, or through duplication, where DNA is retained on the donor chromosome. NRT result in the stabilisation of the recipient chromosome at the expense of the donor chromosome, which will now become unstable due to loss of its telomere. As a consequence, this chromosome undergoes further translocations with other chromosomes, resulting in the generation of complex karyotypes with numerous

translocations, amplifications and dicentric chromosomes. This chain of events will progress until there is acquisition of telomere through some mechanism other than non reciprocal translocation. In contrast, duplications do not result in further instability as the donor chromosome does not lose its telomere, but this mechanism will generate allelic imbalance. Thus, partial duplication of chromosome arms is observed in the karyotype.

Both complex and simple karyotypes were detected in the iAMP21 patients in this study. The finding of complex karyotypes in some patients has provided further evidence of the BFB mechanism being initiated by of loss of telomere. However, in a number of patients dup(21) was the sole visible abnormality. Gisselsson *et al* (2000) suggested that complex karyotypes (≥ 5 chromosomal aberrations) arise following BFB events in highly malignant tumours, whilst in less malignant tumours BFB events can give rise to chromosomal abnormalities that may be limited to ring chromosomes and telomeric associations. In a number of patients in this study (ten), a ring chromosome 21 with duplicated regions was present, consistent with this observation.

It is noteworthy that the level of *RUNX1* amplification in the iAMP21 patients ranged from 5 to 14 copies, with a median of 9. This may be an indication that the abnormality becomes stabilised relatively quickly. The results observed by conventional cytogenetic analysis and PNA telomere FISH demonstrated that in those iAMP21 cases examined, telomeres were present on the dup(21) chromosomes. It is possible to hypothesise that in these patients either a non-reciprocal translocation involving the telomere of another chromosome or a translocation involving duplication has occurred. In the iAMP21 cases it appears that the dup(21) has stabilised, although how this occurs remains unresolved.

4.2.3 Cell Cycle Checkpoint

Until a chromosome is able to stabilise via acquisition of a telomere, it follows that cells undergoing BFB cycles enter into their next mitosis with a chromosome lacking a telomere. In normal cells this would initiate cell cycle arrest via the ATM/p53 signalling pathway. Therefore it seems likely that cells undergoing BFB cycles will have abnormalities of the genes involved in these pathways. Studies in AML and MDS with amplification of *MLL* and *RUNX1* have linked these findings to mutations in *p53* (Andersen *et al*, 2004;Andersen *et al*, 2001). Similar studies have not been undertaken in patients with iAMP21 to investigate the presence and mutation status of genes such as *ATM* or *p53*. High density oligonucleotide aCGH of patients with iAMP21 did not highlight a particular association with deletions of these genes, thus the presence of mutations cannot be excluded. It is of note that in a number of patients, deletions of the long arm of chromosome 11 were observed by cytogenetics, indicating a possible link with loss of the *ATM* gene, which is located at 11q21. Further studies need to be conducted in order to establish the involvement of these two genes in iAMP21 patients.

4.3   iAMP21-a distinct genetic subgroup

Recurrent abnormalities of chromosome 21 are frequently found in a number of haematological malignancies. The two largest genetic subgroups in childhood ALL (high hyperdiploidy and those with the *ETV6-RUNX1* fusion) contain either numerical and/or structural rearrangements of this chromosome, which together have an estimated frequency of approximately 50% (Pui, 2000).

In childhood ALL, iAMP21 has been observed as a rare cytogenetic subgroup in 1.5 -2% of patients. This abnormality is associated with distinct clinical features including a higher incidence in older children, a low presenting WBC count, a pre-B immunophenotype and a poor prognosis (Robinson *et al*, 2003;Moorman *et al*, 2007b). As this abnormality was originally identified by

chance it was important to establish that it represented a primary genetic aberration rather than a secondary one, to an as yet, unidentified abnormality.

Whole genome analysis using aCGH and conventional cytogenetics failed to detect any other consistent genetic aberrations in these patients, providing evidence that the dup(21) was the primary event. These results however do not rule out the possibility that the dup(21) chromosome may have arisen as a secondary event to a cryptic abnormality on chromosome 21. Kempski *et al* (1997;1998) noted cryptic chromosomal rearrangements including deletions and inversions of chromosome 21 in myeloid disorders, whilst Mikhail *et al* (2002) showed *RUNX1* amplification on an apparently normal chromosome 21. Coupled with these observations, evidence of the intrachromosomal amplification of chromosome 21 (outlined in section 3.3.1) has been reported in both AML and in MDS (Viguie *et al,*2002;Baldus *et al*, 2004;Papenhausen *et al*, 2005;Herry *et al*, 2006). Studies of *de novo* AML found that in these myeloid disorders, the amplification was linked to the transcription factors *ERG* and *EST2* (Baldus *et al*, 2004). Although no evidence of overexpression of these genes was found in iAMP21 patients (Strefford *et al*, 2006), their CRA included both of these genes. In an attempt to establish whether iAMP21 had arisen from a cryptic abnormality of chromosome 21 involving these genes or other genes in regions neighbouring *RUNX1,* an investigation was undertaken on a group of patients with karyotypic features similar to the iAMP21 cases but without any visible abnormalities of chromosome 21. As there was no evidence of abnormalities in these regions, it was concluded that iAMP21 had not arisen as a secondary change to a cryptic abnormality on chromosome 21.

In AML, amplification of chromosome 21 appears to be distinct from that of iAMP21 found in ALL. The amplified genes in AML have been identified as *ERG* and *ETS*, not *RUNX1* (Baldus *et al*, 2004). A comparison of the dup(21) morphology between the two diseases also provides evidence that it is different. The morphology of dup(21) in the AML appears uniform and more recognisable

as a rearranged chromosome 21 (Viguie *et al*, 2002;Fisher *et al*, 2003;Podgornik *et al*, 2007). Although, it is possible that in both disorders the dup(21) may have arisen by similar mechanisms, the initiating event may be different, resulting in the generation of different amplicons.

Having established that iAMP21 was not secondary to a cryptic chromosome 21 abnormality, it was important to exclude that it had not arisen from a visible structural abnormality of chromosome 21. The discovery that in two cases iAMP21 had arisen from a Robertsonian der(15;21) translocation raised the question as to whether the dup(21) may have arisen from an i(21)(q10). Screening a small group of i(21)(q10) patients failed to identify any unexpected copy number changes along the length of either chromosome arm, indicating that they were distinct from iAMP21.

The results from all studies point to iAMP21 representing a distinct genetic subgroup in ALL. However, two reports have linked *RUNX1* amplification to the *ETV6-RUNX1* fusion. In one report, the clone of cells with amplification of *RUNX1* was separate from the one with *ETV6-RUNX1* fusion (Ma *et al*, 2001). The additional *RUNX1* signals were not present on a single abnormal dup(21), but located to a number of marker chromosomes. In the second case, in addition to the *RUNX1* amplified cells being a distinct *ETV6-RUNX1* negative population, 5.5% of the *ETV6-RUNX1* positive cells also had *RUNX1* amplification (Niini *et al*, 2000). Gain of additional copies of *RUNX1* is a frequent secondary finding in *ETV6-RUNX1* positive ALL, with the additional copies usually corresponding to either gain of chromosome 21, gain of the derivative chromosome 21, or gain of the derivative chromosome 12. Although both reports clearly provide evidence of amplification similar to iAMP21in interphase cells, the G-banded morphology is different from iAMP21. Without screening cells from these reported patients with the probes used in this study, it is not possible to determine whether the amplification is similar to that described in this study or different. It is of note, that in both cases the majority of cells with

amplification occurred in a population distinct from the one with *ETV6-RUNX1* fusion, suggesting that the amplification had arisen independently, rather than as a secondary event to the *ETV6-RUNX1* fusion. Further studies are required to establish whether these cases can be linked in any way to the iAMP21 genetic subgroup.

4.4   Variant iAMP21

A number of variant translocations, in which one gene characteristically involved in a common translocation is fused to a different partner gene, have been described in haematological malignancies. The fusion proteins resulting from these variant translocations have a similar structure and function to those from the common translocation and so exert the same effect at a molecular level. Four cases were identified in this study with copy number changes characteristic of iAMP21, but which could not be strictly defined as such. Detailed analysis revealed that two of these cases had arisen from a Robertsonian der(15;21) translocation. In both cases the der(15;21) chromosomes had features consistent with having arisen as a result of BFB, with the derivative chromosome containing both chromosomes 15 and 21 material distributed along the length of the der(15;21). As iAMP21, there was evidence that the initiating event may have been loss of a telomere, with one case (11005) having loss of a 21q subtelomere whilst the other (6783) had loss of a 15q subtelomere. These two cases may represent variant iAMP21 which have arisen by a common mechanism to generate a derivative chromosome with features consistent with the iAMP21 abnormality. Niini *et al* (2000) described *RUNX1* amplification in one case in which copy number changes on the long arm of chromosome 15 were also observed using comparative genomic hybridisation. In the study by Cooley *et al* (2002), two cases with a missing chromosome 21 also had loss of chromosome 15 and a further case with an add(21) had a clone with a dic(15;21). It is possible that chromosome 15 may be involved in leukemogenesis in iAMP 21 patients.

Heerema *et al* (Heerema *et al*, 2002) noted that 1% of childhood ALL had breakpoints in 15q13~15, a finding consistent with the CRD seen on chromosome 15 in the two patients with der(15;21)dup(15;21). The *RAD51* gene is located in this region, which is known to be involved in homologous recombination and repair of DNA. It is possible that in these cases deletion of *RAD51* has contributed to the abnormality. Further studies are required to determine whether this chromosome and/or gene are involved in iAMP21 patients.

In the remaining two cases, chromosome 21 material was found in locations other than on the dup(21). In one case (4746), a t(20;21) translocation had been detected by both G-banding and FISH, together with three copies of a rearranged chromosome 21. It is possible that in this case the additional copies arose from a duplication of the reciprocal partner chromosome from this translocation. Alternatively, amplification may have been generated by BFB cycles followed by stabilisation of the abnormal chromosome 21 by insertion into other chromosomes (Albertson, 2006). Lastly, in patient 5047, the distribution of *RUNX1* signals was not consistent with iAMP21, as four marker chromosomes, each containing chromosome 21 material were identified. In these cases it is possible that because they have a genomic profile similar to that of iAMP21, that they represent variant or masked cases. However, as it has not yet been established at the molecular level that these cases are linked, it is not appropriate to definitively define them as iAMP21, thus they remain a diagnostic dilemma.

4.5   Diagnostic Test

The success of risk adapted therapy relies on the accurate detection of patients with features associated with a poor prognosis. Moorman *et al* (2007b), established that the iAMP21 subgroup was linked to a poor prognosis and patients on the UKALL97 treatment trial, had a significantly inferior 5 year overall survival compared to other groups on the same treatment trial. To date, there is no supporting evidence from alternative treatment protocols with long

term follow up, of the association between iAMP21 and a poor prognosis, as for the most part these patients have remained undetected. The majority of other groups do not routinely use FISH techniques, but rely instead on other molecular techniques to identify the significant genetic subgroups.

As outlined in section 3.1.1, currently FISH provides the only reliable method to identify these patients. Although this was the original method used to define the subgroup, in the absence of metaphases it can be difficult to distinguish them from ALL patients with other numerical abnormalities of chromosome 21. It was thus of paramount importance to design a test which would accurately diagnose iAMP21 patients using complementary FISH or molecular based techniques.

The results from this study have illustrated that iAMP21 has a distinct profile in relation to copy number changes along the length of chromosome 21. These differences were exploited to design a diagnostic test based on the comparative quantification of three regions along the length of chromosome 21 (section 3.2). Blind testing validated that in principal this technique (MLPA) was equally effective distinguishing cases of iAMP21 from those with numerical abnormalities of chromosome 21. Ideally a diagnostic test should identify all individuals with the particular abnormality without any risk of false positive or false negative results. In this study, although no false negative cases were identified, cases with copy number changes involving *RUNX1* were difficult to distinguish from those with iAMP21, and so might be classified as false positive. The selection of only a single location within the CRA may have been responsible for this limitation. By using alternative as well as additional probes within this region, it should be possible to improve this test to accurately distinguish iAMP21 cases from those with numerical abnormalities of chromosome 21. However one other limitation of this test is its inability to detect other genetic rearrangements arising from balanced translocations, such as *BCR-ABL1* or *ETV6-RUNX1* fusions, thus it cannot be described as a definitive test.

4.6   Future Studies

The current definition of iAMP21 requires the presence of ≥ 5 copies of the *RUNX1* gene. Although the results of this study validated that this was an appropriate selection criteria, it is biased against those cases where the copy number is ≤ 4. It is possible that cases with similar profiles exist which have a lower *RUNX1* copy number than that currently used to define the abnormality. FISH screening with the TEL-AML1 ES® probe (Vysis, UK) in large series of patients, have identified a number of *ETV6-RUNX1* negative cases, with 3 – 4 copies of the *RUNX1* gene (personal communication: Professor CJ Harrison, LRCG). Conventional cytogenetic analysis did not always establish in these cases, if this was due to the presence of an additional copy of chromosome 21, a rearrangement of the *RUNX1* locus or copy number changes within the chromosome 21. Screening these patients with an improved iAMP21 FISH diagnostic test (Section 3.4.2.1) should establish whether they have similar genomic profiles to those seen in iAMP21. Any cases identified in this way to have low level copy number changes along chromosome 21 would undergo further studies similar to the ones outlined in the characterisation of iAMP21 (Section 3.2), in an attempt to precisely define this abnormality.

4.6.1 *RUNX1*

Since the first description of iAMP21 in which Le Coniat *et al* (Le Coniat *et al*, 1995) linked this abnormality to *RUNX1*, there has been speculation about the involvement of this gene in the abnormality. Mutations of *RUNX1* have been found in a number of cases of AML and MDS (Busson-Le Coniat *et al*, 2001;Penther *et al*, 2002;Owen *et al*, 2008;Niebuhr *et al*, 2008), however sequence analysis failed to detect such mutations in the significant regions of the gene in childhood ALL patients with amplification of *RUNX1* (Greaves *et al*, 2003;Hong *et al*, 2008). It has been hypothesised that mutations and translocations in this gene are the initiating event in the leukaemias in which they occur. Evidence

supporting this theory in ALL comes from studies which have demonstrated that the *ETV6-RUNX1* fusion occurs in a pre-leukaemic clone which requires a second hit to bring about overt disease (Pui & Evans, 2006). This gene remains a potential candidate for leukaemogenesis in these cases, due to its essential role in haematopoiesis, therefore further studies are required to determine its mutation status in a larger group of patients, as well as to exclude the presence of any fusion gene involving *RUNX1*. Currently FISH has been the only technique used to exclude a fusion and it may be possible that a break has occurred within a region that is too small to be detected by FISH. An investigation into exon copy number with MLPA may provide a means to further investigate this.

4.6.2 *SLC19A1*

Recent studies in the pharamacogenetics of ALL (Cheok & Evans, 2006) have provided evidence of potential mechanisms for the development of drug resistance. By identifying the genetic determinants of such drug resistance it may be possible in the future to tailor treatment to individuals and so reduce the toxicity and increase the efficacy of treatment in ALL. One of the potential causes of the development of drug resistance in ALL is alterations in the genes involved in metabolism, such as drug transporters or drug targets (Ganapathy *et al*, 2004).

Folate is an essential co-factor in purine and pyridine synthesis and methotrexate its structural analogue inhibits a number of specific steps in DNA synthesis (Figure 4.2). The main mechanism by which methotrexate and natural folate enter cells is through the reduced folate gene or *SLCA19I* located on chromosome 21 (Pui & Evans, 2006).

In high hyperdiploid ALL with gain of chromosome 21, increased expression of *SLC19A1* has been shown in association with greater accumulation of methotrexate polyglutamates (Chango *et al*, 2000). This increase in expression is associated with an improved outcome in those children treated with low dose methotrexate and it has been proposed as a mechanism to explain the good

prognosis associated with this specific subgroup. Mutations in this gene have been found in tumour cell lines leading to disrupted methotrexate transport and subsequent drug resistance (Laverdiere *et al*, 2002). Although genetic mutations have not been identified in primary ALL cells, a common polymorphism of this gene has been associated with increased relapse in ALL. In a study of childhood ALL patients homozygous for the 80A polymorphism (Kager *et al*, 2005;Ge *et al*, 2007) it was noted that the methotrexate levels in plasma were higher than those patients without the polymorphism and that their prognosis was worse. The authors suggested that this was a direct consequence of decreased uptake of methotrexate.

The *SLC19A1*gene is located on chromosome 21 at genomic position ~45.7 Mb. In a number of iAMP21 patients this region was located within the CRD identified from the aCGH and FISH studies. As studies in folate pathway gene expression have noted that expression differs in different subtypes of ALL (Cheok & Evans, 2006) it is possible to hypothesise that the poor outcome observed in these patients may be a direct consequence of either deletions and/or mutations of this gene. Further studies should be undertaken in iAMP21 patients to investigate the expression level of *SLC19A1*as well as the presence or absence of the G80A polymorphism.
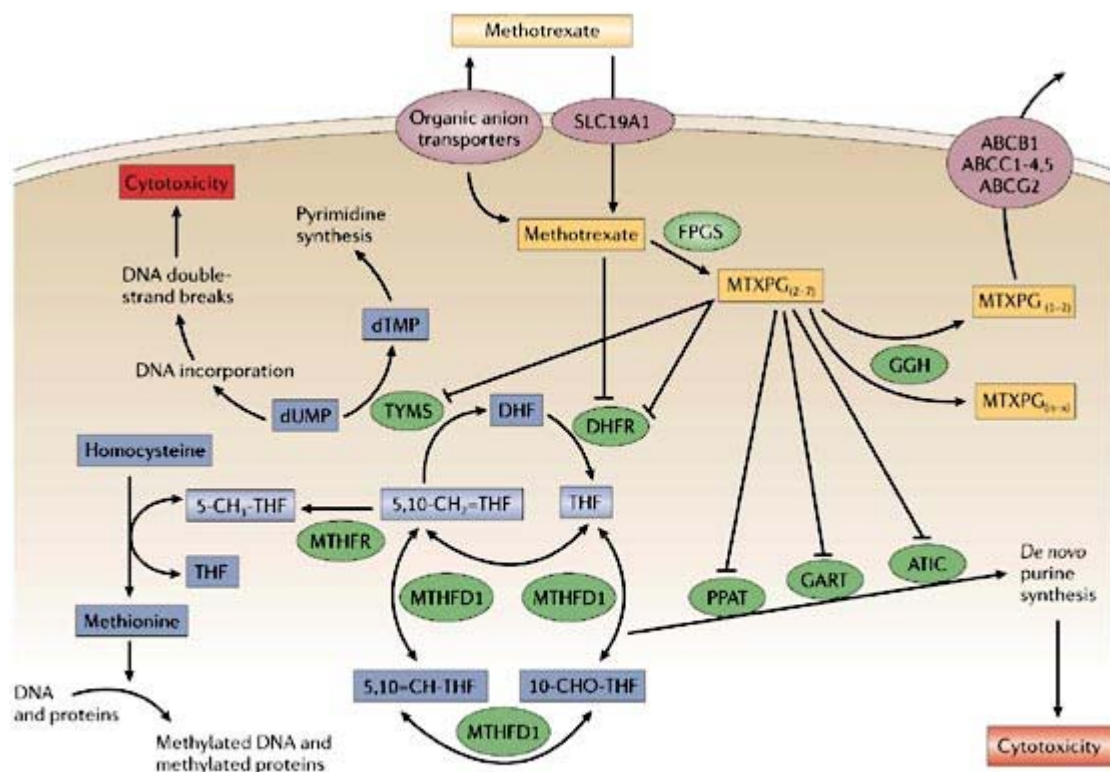
Figure 4.2 The folate pathway. Methotrexate enters the cell via *SLC19A1*, and inhibits the dihydrofolate reductase, which results in the depletion of cellular folates. Adapted from Cheok (2006).

Currently there have been no reports of relapse in the iAMP21 patients being treated on regimen C of the UK treatment trial ALL2003 (personal communication: Dr AV Moorman, LRCG). Similarly the initial results from the Berlin-Frankfurt-Münster (BFM) ALL treatment trials, indicate that iAMP21 patients fare better (personal communication: Dr AV Moorman, LRCG). Although these are preliminary results it is possible that it may be due to the more intensified therapy which includes methotrexate given in both of these trials which may over come the deleterious effect of the deletions / mutations in *SLC19A1*. Further studies into the efficacy of these treatment trials may provide evidence in support of this hypothesis.

4.6.3 Screening of relapse samples

The results from this study have identified a small CRA in all iAMP21 patients. However, despite extensive studies, no putative target gene has been identified, located within this region or elsewhere in the genome, to be the causal event driving leukaemogenesis in these patients. Detailed analysis of patient karyotypes coupled with high resolution genome aCGH also failed to identify any single common abnormality, other than dup(21) that may be the driving mechanism. A direct comparison between diagnostic and relapse samples from iAMP21 patients may confirm whether the dup(21) is the primary change in these patients. In addition to this a comparison between the two samples would determine if the dup(21) chromosome has remained stable or continued to evolve. It is proposed that a study be undertaken on relapse samples using a combination of techniques including, interphase FISH, conventional cytogenetics and oligonucleotide aCGH and the results compared to those of the diagnostic samples.

4.7 Conclusions

- Investigations using FISH, aCGH and G-banding have established that iAMP21 is a highly complex genetic abnormality involving large regions of chromosome 21

- It is characterised by the presence of a highly complex rearrangements along the duplicated chromosome 21, involving numerous chromosomal breaks, giving rise to a chromosome with deleted, duplicated, inverted and amplified regions

- iAMP21 appears to be a primary cytogenetic change and not a secondary abnormality

- The abnormality can be distinguished from other numerical abnormalities of chromosome 21 by exploiting the unique pattern of gain, amplification and deletion seen in these patients

- Variant cases may exist, however further work is required to characterise them more fully
- The abnormality may be driven by a BFB mechanism, potentially initiated by loss of a telomere: an unusual mechanism in ALL
- Patients with iAMP21 appear to be distinct from other genetic subgroups associated with ALL
- The initiating mechanism has not yet been elucidated. This discovery would assist in more accurate diagnosis and provide further insight into the understanding of other rare subgroups of ALL

5 Appendices

Appendix 1

Table A1.1 Karyotypes and clinical details of previously reported patients with iAMP21.

Case No in study	Sex /Age (years)	WBC 10⁹/L	Karyotypes	Number of *RUNX1* signals by FISH	
3	F/11	NA	46,XX,-21,+mar	5	1
1	M/15	4.3	46,X,-Y,add(21)(q22),+mar1 [8]/46,XY[12]	4–5	1
2	M/6	4.9	53,XY,+X,+Y,inv(3),add(4),+9,+17,+21,+21,+add(21)(q22)	4–5	1
1	F/10	1.4	46,XX,der(21)[2]	4–5	2
2	M/11	5.9	47,X,+X,inv(Y)(p11.2q12),+10,-20,der(21)[20]	6	2
1	F/15	NA	46,XX,add(1)(p?),del(6)(q25)	>4	3
38	M/2.9	NA	46,XY	4–5	3
39	F /3.4	NA	46,XY	>4	3
10	F/12	7.1	48,XX,+X,+10,del(11)(q23),qdp(21)(q11q22)[13]/46,XX[7]	5	4
9	F/8	0.9	47,XX,+X,del(21)(q22),der(21)[12]/46,XX[4]	5-10	5
1	M/12	4.3	46,XY,del(18)(p11),der(21)	10–15	6
2	F/5.6	26.3	48,XX,-20,+der(21),+2mar	6	6
44	M/13	7.6	46,XY,i(9)(q10),-16,+mar (trp 21q using SKY)	4	7
64	M/14	14.5	46,XY	6–15	7
3	M/17	1	46,XY,add(1)(q25),add(21)(q21) [6]/46,XY[14]	8	8
4	F/19	10.1	46,XX,del(7)(p14p21),-21,+mar[10]/46,XX[2]	6–8	8
1	F/11	18	46,XX,del(8)(q?),+13,-19,add(21)(p)[5]	>10	9

Table A1.1 Karyotypes and clinical details of previously reported patients with iAMP21 (continued).

Case No in study	Sex /Age (years)	WBC 10⁹/L	Karyotypes	Number of *RUNX1* signals by FISH	
11	F/13	2.8	46,XX,-21,+mar[9]/46,XX[2]	5–10	9
5	M/14	2.2	46,XY,inv(7)(p?15q?21),-21,+mar[2]/46,XY[4]	5–7	9
6	M/12	15.1	46,XY,-21,+mar[8]	5–7	9
7	F/13	3.8	46,XX,del(7)(q22q35),del(11)(p12),add(21)(p11.2) [9]/46,XX[5]	5	9
8	F/15	9.9	46,XX,trp(21)(q11.2q22)[13]/46,XX[7]	4	9
11	F/13	6.6	47,XX,?add(4)(q31),del(7)(q3?2),i(21),+mar[5]/46,XX[10]	5	9
12	M/5	7.2	56,XY,+X,+Y,+6,+10,+14,+17,-19,+21,+22,+mar1,+mar2, +mar3[5]/46,XY[18]	5–10	9
13	F/6	3,1	54,XX,+X,+6,+9,+14,+17,+18,+2mar[12]	4–10	9
14	M/11	NA	46,XY[30]	3–10	9
15	F/11	1.6	Failure	>10	9
16	M/7	NA	Failure	4–10	9
1	F/15	NA	46,X [20]	15–20	9
65	F/8	2	Failure	6–15	9
2423	M/10	2	48,XY,+X,+14,ider(21)(q10)dup(21)(q?)	6+	10
2776	F/7	17	47,XX,+X,der(21)r(21)(q?)dup(21)(q?)	4-6	10
3131	M/11	11	46,XY,t(1;16)(q23;p13),ider(21)(q10)dup(21)(q?)/51,idem,+X,+3,+10,+14,+21	6+	10
3368	M/20	6	46,XY,del(7)(p1?5),t(8;22)(q1?1;q13),dup(21)(q?)	5+	10
3527	F/13	3	45,XX,-7,del(12)(p12),dup(21)(q?)	5+	10

Table A1.1 Karyotypes and clinical details of previously reported patients with iAMP21 (continued).

Case No in study	Sex/ Age (years)	WBC 10⁹/L	Karyotypes	Number of *RUNX1* signals by FISH	Ref
3956	M/7	3	45,XY,dic(8;16)(p1;p1),del(13)(q1?4),dup(21)(q?)/46,idem,t(Y;13)(q1;q1?4),+dic(8;16)(p1;p1)*	4-7	10
3970	F/12	2	47,XX,add(7)(q2?),+10,der(21)r(21)(q?)dup(21)(q?)/47,idem,del(12)(p13)	6-10	10
4134	M/8	4	46,XY,dup(21)(q?)	5+	10
4135	F/14	1	46,XX,t(12;16)(q24;p11),del(15)(q24q26),t(17;20)(p1?3;q11),der(21)dup(21)(q?)	6+	10
4178	F/14	3	46,XX,del(7)(q22),t(14;22)(q32;q11),dup(21)(q?)*	7+	10
4237	F/13	3	46,XX,der(21)dup(21)(q?)/46,idem,del(16)(q1?)	6-8	10
4279	M/5	8	47,XY,-12,der(21)dup(21)(q?),+mar1,+mar2	4-9	10
4405	M/8	3	45,Y,t(X;15)(q2?1;q2?4),dic(12;17)(p1;p1),der(21)r(21)(q?)dup(21)(q?)	5-8	10
4444	M/9	2	46,XY,der(21)r(21)(q?)dup(21)(q?)	6+	10
4623	F/6	14	46,XX,dup(21)(q?)/47,idem,+X	4-7	10
5601	F/14	1	46,XX,del(9)(p22),dup(21)(q?)	4-6	10
5607	M/8	4	46,XY,t(8;11)(p2?1;q21),der(21)r(21)(q?)dup(21)(q?)/47,idem,+X*	4-6	10
5754	M/9	2	46,XY,ider(21)(q10)dup(21)(q?)*	4-6	10
2848	M/5	2	46,XY, dup(21)(q?)	5-7	10
3382	M/11	6	46,XY,i(9)(q10),del(11)(q2?1),der(21)dup(21)(q?)	5	11
3767	F/10	1.1	46,XX,dup(21)(q?)	5	11

Table A1.1 Karyotypes and clinical details of previously reported patients with iAMP21 (continued).

Case No in study	Sex/Age (years)	WBC 10⁹/L	Karyotypes	Number of *RUNX1* signals by FISH	
4414	M/7	9	45,XY,t(6;19)(p21;p13),der(7)t(7;15)(p1;q1),del(11)(p13), -15,del(16)(q2),ider(21)(q10)dup(21)(q?)	4-6	[11]
1	M/8	29.8	44~46,XY,del(1)(q32),-5,-9,-21,-21,add(21)(q22),+mar1,inc[7]/46,XY[3]	4	[12]
2	F/9	2.6	46,XX,del(6)(q24),add(21)(q22)[4]/46,XX[7]	4-5	[12]
3	M/10	1.9	46,XY,add(21)(q22)[9]/46,XY[1]	3-6	[12]
4	F/8	2.4	46,XX,add(21)(q22)[18]/46,XX[2]	4-7	[12]
5	F/10	11.6	45,XX,t(3;12)(q21;q24),-7,add(21)(q22)[11]	4-5	[12]
6	M/11	4.2	46,XY,add(21)(q22)[11]/46,XY[4]	4-5	[12]
8	F/12	11.7	46,XX,t(5;9)(q35;q22), -7,ins(8;7)(p11;q11q32),der(11)t(7;11)(q32;p15),add(21)(q22),+mar[5]/ 45,XX,t(5;9)(q35;q22),-7,add(21)(q22)[4]/46,XX[3]	3-4	[12]
9	M/12	69.9	46,XY,add(21)(q22)[8]	4	[12]
10	F/12	2.3	46,XX[20]	4	[12]
11	F/2	68	47,XX,t(1;19)(q23;p13),+mar[20]	3-4	[12]
12	F/5	32.8	53-57,XX,+4,+5,+6,+17,+21,+r(21)(q?)dup(21)(q22.13)inc[12]	4-5	[12]
13	M/10	4.2	46,XY,add(4)(q31),add(21)(q22)[21]	5	[12]
14	F/9	33.9	47,XX,del(7)(p11.1),add(21)(q22),+mar[6]/46,XX[8]	5	[12]

Reference List

1. Busson-Le CM, Nguyen KF, Daniel MT, Bernard OA, Berger R. Chromosome 21 abnormalities with AML1 amplification in acute lymphoblastic leukemia. Genes Chromosomes.Cancer 2001;32:244-249.

2. Dal CP, Atkins L, Ford C et al. Amplification of AML1 in childhood acute lymphoblastic leukemias. Genes Chromosomes.Cancer 2001;30:407-409.

3. Martinez-Ramirez A, Urioste M, Contra T et al. Fluorescence in situ hybridization study of TEL/AML1 fusion and other abnormalities involving TEL and AML1 genes. Correlation with cytogenetic findings and prognostic value in children with acute lymphocytic leukemia. Haematologica 2001;86:1245-1253.

4. Mathew S, Rao PH, Dalton J, Downing JR, Raimondi SC. Multicolor spectral karyotyping identifies novel translocations in childhood acute lymphoblastic leukemia. Leukemia 2001;15:468-472.

5. Morel F, Herry A, Le Bris MJ et al. AML1 amplification in a case of childhood acute lymphoblastic leukemia. Cancer Genet.Cytogenet. 2002;137:142-145.

6. Niini T, Kanerva J, Vettenranta K, Saarinen-Pihkala UM, Knuutila S. AML1 gene amplification: a novel finding in childhood acute lymphoblastic leukemia. Haematologica 2000;85:362-366.

7. Nordgren A, Heyman M, Sahlen S et al. Spectral karyotyping and interphase FISH reveal abnormalities not detected by conventional G-banding. Implications for treatment stratification of childhood acute lymphoblastic leukaemia: detailed analysis of 70 cases
30. Eur.J.Haematol. 2002;68:31-41.

8. Penther D, Preudhomme C, Talmant P et al. Amplification of AML1 gene is present in childhood acute lymphoblastic leukemia but not in adult, and is not associated with AML1 gene mutation
6. Leukemia 2002;16:1131-1134.

9. Soulier J, Trakhtenbrot L, Najfeld V et al. Amplification of band q22 of chromosome 21, including AML1, in older children with acute lymphoblastic leukemia: an emerging molecular cytogenetic subgroup. Leukemia 2003;17:1679-1682.

10. Harewood L, Robinson H, Harris R et al. Amplification of AML1 on a duplicated chromosome 21 in acute lymphoblastic leukemia: a study of 20 cases. Leukemia 2003;17:547-553.

11. Robinson HM, Broadfield ZJ, Cheung KL et al. Amplification of AML1 in acute lymphoblastic leukemia is associated with a poor outcome. Leukemia 2003;17:2249-2250.

12. Perez-Vera P, Montero-Ruiz O, Frias S et al. Multiple copies of RUNX1: description of 14 new patients, follow-up, and a review of the literature. Cancer Genet Cytogenet 2008;180:129-134.

Appendix 2

Reagents

<u>Luria-Bertani (LB) plates.</u>

10g Tryptone (Sigma,UK)
5g Yeast extract (Sigma,UK)
10g $NaCL_2$ (Sigma,UK)
15g Agar (Sigma,UK)
Make up to 1 litre with distilled water, autoclave, allow to cool to below
50 °C, add Chloramphenicol (Sigma,UK) or Kanamycin (Sigma,UK), pour into
sterile Petri-dishes and store at 4 °C for up to 1 month.

<u>Luria-Bertani (LB) broth</u>
10g Tryptone (Sigma, UK)
5g Yeast extract (Sigma, UK)
10g $NaCL_2$ (Sigma, UK
Make up to 1 litre with distilled water and autoclave.
Store at room temperature for up to 1 month.

<u>Tris EDTA TE buffer pH 7.4</u>
10ml 1M TrisCL pH 7.4 (Sigma, UK)
2ml 0.5M EDTA pH8 (Sigma, UK)
Make up to 1 litre with distilled water and autoclave.
Store at room temperature for up to 1 month.

<u>Tris-Borate-EDTA buffer (TBE) Buffer</u>

108gms Tris-Base (Sigma, UK)
55gms Boric acid (Sigma, UK)
9.3gms Na_2 EDTA (Sigma, UK)
Make up to 1 litre with distilled water.
Store at room temperature for up to 1 month.

<u>2x SSC</u>
50mls 20xSSC (Sigma, UK)
450mls purified H_2O

<u>Block</u>
1gm dried milk powder (Marvel) in 10mls purified H_2O

PCR Primers

RUNX1 (Forward) 5 '-GGCCTCATAAACAACCACAG- 3' Tm (57.3 ºC)
RUNX1 (Reverse) 5 '-CATTCAGTGTGATTCGTCCTG- 3'   Tm (57.9 ºC)

*STCH (*Forward) 5 '- TTGACTCTCCTGTTGGCCG - 3'   Tm (57.3 ºC)
STCH (Reverse) 5 '- CCCAACAGAACAATAGGTGG - 3'   Tm (58.8 ºC)

PRMT2 (Forward) 5 '- GACAAACCACTGCAGATTGG - 3'   Tm (57.3 ºC)
PRMT2 (Reverse) 5 '- CTCTTCATCCTGCCACGTG- 3'   Tm (58.8 ºC)

CYP27C1 (Forward) 5 '- AGTGGCCACCATCCTTTATG - 3' Tm (57.3 ºC)
CYP27C1 (Reverse) 5 '- CTGCATACATGGAGGTCTTG - 3' Tm (57.3 ºC)

Appendix 3

Table A3. 1 Karyotypes of cases identified from G-banding review as being possible iAMP21 patients.

Patient ID	Chromosome 21 morphology following review	Karyotype
2647	iAMP21	47,XY,+X,dup(21)(q11q22),+dup(21)(q11q22)[7]/46,XY[2]
2848	iAMP21	46,XY,add(21)(q11)[7]/46,XY[4]
2879	Loss of 21	48,XX,+X,der(1)t(1;?13)(p34;q14),der(13)t(1;?;13)(p34;?;q14),+14,-15,+17,der(18)t(18;21)(q22;q21),-21,+mar[11]/46,XX[3]
3137	duplicated 21	46,XX,add(7)(p),add(21)(q)[4]/46,idem,add(3)(q2)[3]/46,XX[3]
3230	No slides for review	46,XX,add(21)(q22)[9]/46,XX[2]
3767	iAMP21	46,XX,dup(21)(q?)[2]/46,XX[5]
2752	iAMP21	46,XX,?add(9)(q34),del(11)(q23),der(18)?t(18;20)(q25;p1?1),der(20)t(11;20)(q?;p?), add(21)(q22)[3]
2904	iAMP21	46,XX,del(7)(q22q32),add(21)(q22)[16]/46,XX[9]
5661	iAMP21	47,XX,+X,?del(11)(q?),?add(17?)(q),add(21)(q?),inc[cp10]
5632	duplicated 21	47,XX,t(14;20)(q32;q1?),add(21)(p1),+add(21)(p1)[9]/46,XX[1]
4343	duplicated 21	45,XX,der(1)t(1;4)(p36;?)dup(1)(q32),del(2)(p2?),der(3)t(3;6)(p?;p?),der(4)t(4;5;2),der(5)t(4;5)(q?;q?),der(7)t(7;20)(p22;?), der(10)t(10;2)(p;?),der(10)(6;10)(?;q),inv(11)(p15q23),-13,del(16)(q21),der(16)t(16;17)(q13;p13),der(18)t(18;20)(q;?), der(20)t(9;20),der(20)t(9;20;?17;14),dup(21)(q21)[cp4]
5897	Loss of 21	45,XY,t(1;2)(p?22;q3?6),del(4)(q2?5),del(6)(p2?2),-6,?idic(9)(p2),add(14)(q32),+16, add(16)(q2?4),-20,-21,+mar[cp3]/46,XY[7]

Table A3.2. BAC clone name and position for chromosome 21. Clones run from top to bottom in centromere to telomere direction.

BAC clone	Clone Position Mb	Clone Start position	Clone End position	Chromosome 21 band
AF127936	15.1	14988775	15138458	21q21.1
RP11-15E10	18.7	18595720	18774434	21q21.1
RP11-375O2	19.3	19211405	19376024	21q21.1
RP11-49B5	20.3	20224514	20390557	21q21.1
RP11-64I12	22.1	22059729	22195086	21q21.1
RP11-97F14	22.9	22783095	22943367	21q21.2
RP11-80N20	23.8	23885285	24051118	21q21.2
RP11-13J15	24.1	24047487	24200441	21q21.2
RP11-88D18	25.5	25400597	25568509	21q21.2
RP11-15H6	26.7	26666311	26816805	21q21.3
RP11-90A17	27.7	27718668	27867189	21q21.3
RP11-79G23	29.3	29260483	29449549	21q21.3
RP11-30N6	29.7	29766105	29836744	21q21.3
RP11-191I6	31.4	31453691	31454003	21q22.1
RP11-147H1	32.3	32372362	32372918	21q22.1
RP11-79D9	33.2	33204657	33369197	21q22.1
RP11-79A12	34.7	34660659	34819795	21q22.1
RUNX1	35.3	35229245	35371851	21q22.1
AF121782	40.0	40015038	40157799	21q22.2
RP11-114H1	41.2	41110821	41272864	21q22.2
RP11-120C17	41.7	41630603	41780323	21q22.3
RP11-88N2	43.7	43556394	43769964	21q22.3
21qtel D21S1575	46.9	46144350	46311763	21q22.3

Table A3.3 Copy number changes detected by interphase FISH screening along the length of chromosome 21 in ten iAMP21 patients and two control patients (6899, 6009). Probes run from top to bottom, centromeric to telomeric direction. Copy number is recorded as the range of signals detected at each location.

Bac Probe	iAMP21 Patients											Control patients	
	4405	4134	4279	5898	6092	6783	6788	6957	7219	7255		6009	6899
AF127936	2	2-4	2-3	1-2	2	2-5	2	2	2-5	2-3		2-4	2
RP11-15E10	2-3	2.6	Fail	1-2	2	2	2-3	2	2-5	1-2		2-4	2
RP11-375O2	2-3	2-5	2-3	1-2	2	2	2	2	2-6	1-2		2-4	2
RP11-49B5	2-4	2-5	2-4	1-2	2	2-3	2-3	2	2-5	2-4		2-4	2
RP11-64I12	2-6	2-5	2-4	2-3	2-4	2-3	2-3	2-3	2-3	2-4		2-4	2
RP11-97F14	2-6	2-5	2-4	2-3	2-7	2	2-3	2-3	2-3	2-4		2-4	2
RP11-80N20	2-9	2-8	2-4	2-3	2-6	2-3	2-5	2-5	2-7	2-7		2-4	2
RP11-13J15	2-8	2-8	2-4	2-3	2-6	2-3	2-5	2-5	2-7	2-8		2-4	2
RP11-88D18	2-9	2-5	2-5	2-3	2-6	2	2-5	2-5	2-7	2-5		2-4	2
RP11-15H6	2-11	2-7	2-4	2-3	2-6	2-4	2-5	2-5	2-7	2-9		2-4	2
RP11-90A17	2-12	2-8	2-6	2-4	2-6	2-4	2-8	2-7	2-9	2-7		2-4	2
RP11-79G23	2-10	2-6	2-5	2-5	2-5	2-5	2-5	2-5	2-8	2-8		2-4	2
RP11-30N6	2-9	2-6	2-5	2-5	2-4	2	2-5	2-6	2-7	2-8		2-4	2
RP11-191I6	2-11	2-5	2-7	2-5	2-7	2	2-5	2-5	2-8	2-9		2-4	2
RP11-147H1	2-14	2-6	2-6	2-5	2-8	2-6	2-5	2-5	2-7	2-9		2-4	2
RP11-79D9	2-14	2-7	2-5	2-5	2-7	2-5	2-5	2-7	2-8	2-8		2-4	2
RP11-79A12	2-7	2-10	2-5	2-5	2-7	2-6	2-6	2-7	2-7	2-8		2-4	2
RUNX1	2-8	2-7	2-9	2-6	5-8	2-6	2-5	2-9	2-9	2-9		2-4	2
AF121782	2-11	2-3	2-5	2-5	2-6	2-3	2-6	2-5	2-6	2-8		2-4	2
RP11-114H1	1-2	1-2	2-6	2-5	2	2-5	2-6	2-5	1-3	2-3		2-4	2
RP11-120C17	1-2	2-6	2-6	2-5	2	2-5	2-5	2-6	1-3	2-4		2-4	2
RP11-88N2	1-2	1-2	1-2	1-2	2	2-5	2-5	2-6	1-3	2-4		2-4	2
21qtel D21S1575	1-2	1-2	1-2	1-2	2	1-3	2-5	1-2	1-3	2-3		2-4	2

Figure A3.1 BAC aCGH profiles of seven iAMP21 patients (5898, 6788, 6957, 6783, 7219, 7255, 4279) and control patient (6899).
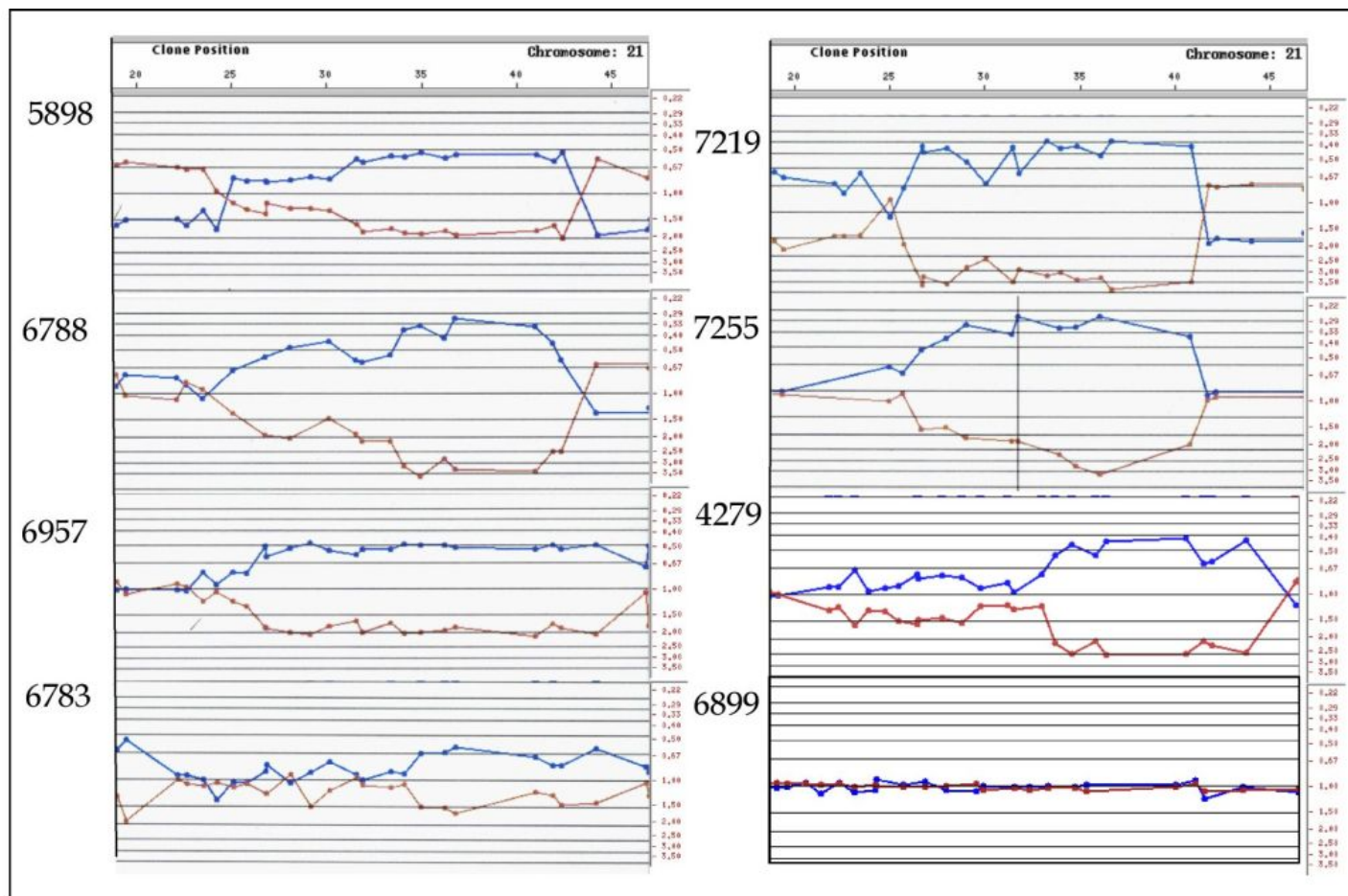
Table A3.4 Copy number changes detected by interphase FISH screening along the length of chromosome 21 in 48 iAMP21. Probes run from top to bottom, centromeric to telomeric direction. Copy number is recorded as the range of signals detected at each location.

Patients	dup(21)	BAC Clone and genomic position Mb											
		24.1		29.8		32.3		35.5		40.0		43.7		46.9
		RP11-13J15		RP11-30N6		RP11-147H1		RUNX1		AF121782		RP11-88N2		21qtel
3131	LM	4-6		3-4		6-7		4-7		4-5		5		3-4
5754	LM	3		5-8		4-7		4-7		4-6		5-8		1
5898	LM	3		3-6		3-6		4-6		3-5		1		1
6020	LM	3		4-5		5-6		5-7		3-5		1		1
6788	LM	4-5		3-5		4-5		3-5		4-6		4-5		3-5
6957	LM	3-5		4-5		4-6		4-9		4-6		4-6		1
7045	LM	4-6		4-8		5-8		5-8		4-8		4-8		1
7829	LM	FAIL		6-7		FAIL		6-9		6-9		1		1
3956	LA	5		5-8		5-8		6-10		6-8		5-7		1
4134	LA	5-8		3-7		4-6		4-7		3-4		3		1
4178	LA	4-5		6-7		6-8		6-8		7-8		1		1
4623	LA	2		4		5-9		5-6		6-9		1		1
6008	LA	5		5		4-6		5-10		5-8		1		1
6783	LA	3		2		3-6		4-6		3		3-5		1-3
6937	LA	2		4-5		7-8		7-10		7-9		1		1
7219	LA	5-7		5-7		5-7		5-9		4-5		1		1
7255	LA	5-7		3-4		4-14		5-11		5-8		3		2
8743	LA	3-5		4-6		3-5		3-5		4-5		4-5		1
2776	R	3		3		3		4-6		6-8		5-8		1
3743	R	2		2		4-5		4-7		4-5		5		3
3970	R	FAIL		3-4		FAIL		4-5		6-7		1		1
4405	R	4-8		6-10		6-10		5-8		5-8		1		1
4444	R	4-6		4-6		4-6		4-7		6-8		5-8		1
5607	R	5-7		2-3		5-7		4-6		FAIL		4-7		FAIL
5674	R	1		4-6		FAIL		6-8		5-8		1		1
5809	R	3		4		5-8		6-8		5-7		1		1
7583	R	3		3		4-5		4-6		4		4-5		1
7650	R	4-5		5		6-8		5-9		5-7		1		1
3527	SA	3		3-4		4-5		4-5		3		2		2
4780	SA	2		4		4-5		5		2-3		2		2
3745	SM	5-8		4-5		6-8		6-8		5		5-7		1

Table A3.4 (continued) Copy number changes detected by interphase FISH screening along the length of chromosome 21 in 48 iAMP21. Probes run from top to bottom, centromeric to telomeric direction. Copy number is recorded as the range of signals detected at each location.

Patients	dup(21)	BAC Clone and genomic position Mb						
		24.1	29.8	32.3	35.5	40.0	43.7	46.9
		RP11-13J15	RP11-30N6	RP11-147H1	*RUNX1*	AF121782	RP11-88N2	21qtel
4135	SM	5-6	5-7	5-7	6-9	6-7	4-5	1
4237	SM	5-6	5-7	5-8	4-9	5-8	5-7	1
4279	SM	3-4	4-5	4-7	4-9	3-5	1	1
5655	SM	5	3	1	4-7	4-5	1	1
6868	SM	FAIL	5-6	FAIL	5-6	FAIL	5-6	FAIL
4316	n/a	FAIL	3	FAIL	3-5	4-5	3	3
5858	n/a	3-4	5-7	5-7	4-8	6-7	4	4
6092	n/a	4-6	3-4	4-8	5-8	3-7	2	2
6111	n/a	FAIL	FAIL	FAIL	4-11	FAIL	FAIL	1
6996	n/a	5-9	FAIL	8-10	8-14	8-9	1	1
7024	n/a	3-4	1	4-5	4-8	6-9	1	1
7093	n/a	4	5-7	5-7	6-8	5-7	1	1
7100	n/a	3	3-4	4-5	3-7	3	3	2
7732	n/a	3	3-5	FAIL	4-7	5-7	4-6	1
7828	n/a	4-6	5-8	7-9	3-9	5-8	1	1
8767	n/a	3	4-6	4-6	4-7	5-7	1	1
8983	n/a	3-9	1	FAIL	4-9	FAIL	1	1

Table A3.5 Amplicon size as defined as a continuous area of amplification in iAMP21 patients. Patients are ordered according to G-banded morphology
Key : LM=Large metacentric; LA= Large acrocentric; R= Ring; SA= small acrocentric, SM= submetacentric; n/a= Not applicable

Patient ID	G-Banded morphology	Amplicon size Mb
3131	LM	> 11.4
5754	LM	>13.9
5898	LM	>10.2
6020	LM	>10.2
6788	LM	>22.8
6957	LM	>19.6
7045	LM	>19.6
3956	LA	>19.6
4134	LA	>11.4
4178	LA	>15.9
4623	LA	>7.7
6008	LA	>15.9
6783	LA	>7.7
6937	LA	>10.2
7219	LA	>10.2
7255	LA	>7.7
8743	LA	>19.6
2776	R	>8.2
3743	R	>11.4
4405	R	>15.9
4444	R	>19.6
5809	R	>7.7
7583	R	>3.2
7650	R	>15.9
3527	SA	>3.2
4780	SA	>3.2
3745	SM	>19.6
4135	SM	>19.6
4237	SM	>19.6
4279	SM	>10.2
5655	SM	>4.5
5858	n/a	>10.2
6092	n/a	>7.7
7024	n/a	>7.7
7093	n/a	>10.2
7100	n/a	>3.2
7828	n/a	>15.9
8767	n/a	>7.7

Figure A3.2 FISH with PAN telomeric probes (red) on patient 4623 (a) followed by (b) sequential WCP21 (green). WCP21 highlights normal chromosome 21 (small chromosome) and dup(21) (large green chromosome).
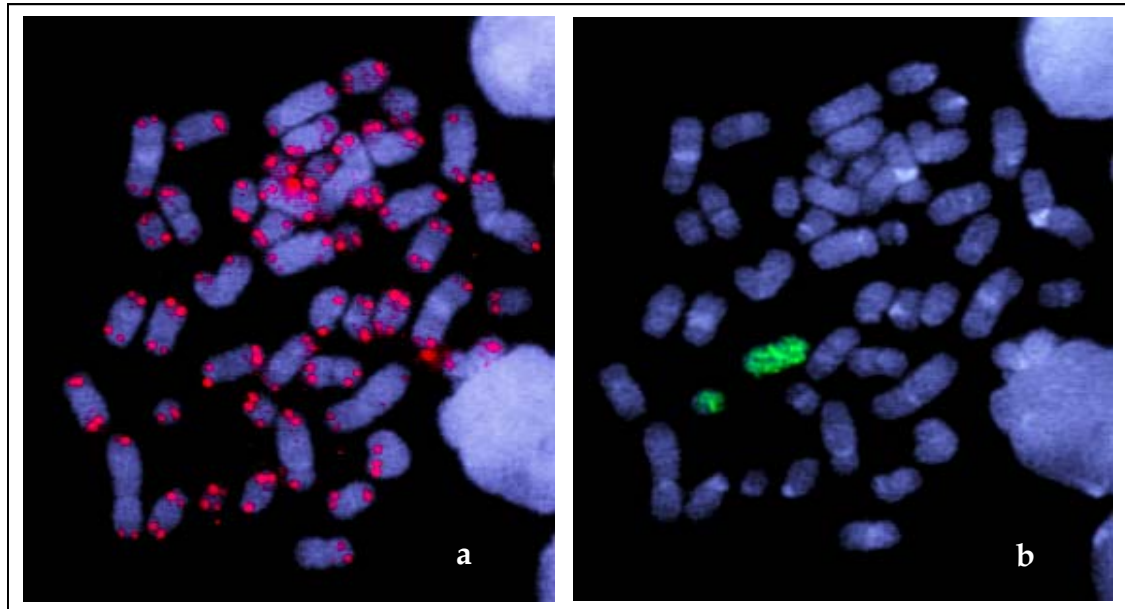
Table A3.6 Karyotypes of patients selected to screen for cryptic abnormalities of chromosome 21.

Patient ID	Age at diagnosis	Immnophonotype	Karyotype
3209	14	BCP-ALL	46,X,-Y,+5[6]/46,XY[8]
3335	3	BCP-ALL	46-47,XX,del(1p),?add(9)(p11),del(9)(p11),del(9)(p13),-10,add(11)(p11),-12,del(17)(q21),-18,+3-4mar[cp19]
3403	7	BCP-ALL	46,XY,del(7)(q22)[7] 46,XY,r(7)[8]/46,XY[5]
3836	6	BCP-ALL	47,XX,+X[13]/46,XX[7]
3854	10	BCP-ALL	46,XX,der(20)t(8;20)(q13;q13)[4]/46,XX[36]
3867	1	BCP-ALL	45,X,der(X)t(X;3)(p22;p21),der(3)t(3;9)(q2?;p2?),der(3;9)(q10;q10)[17]/46,XX[3]
3895	3	BCP-ALL	46,XY,del(7)(q32)[2]/ 46,XY[28]
3939	14	BCP-ALL	46,XY,del(9)(p1?2p2?4)[4]/46,XY[1]
3993	1	BCP-ALL	47,XY,+X,?inv(11)(q13q23)[11]
4021	8	BCP-ALL	45,X,-Y,add(9)(p11)[5]/47,idem,+X,?+Y[1]/46,XY[2]
4088	9	BCP-ALL	46,XY,del(13)(q14q32)[7]/47,Y,add(X)(p?2),+4,add(9)(p?)[4]
4206	2	BCP-ALL	46,XY,del(9)(p22)[4]/46,XY[20]
4335	12	BCP-ALL	46,XX,del(11)(q13q23)[11]/46,XX[4]
4400	3	BCP-ALL	46,XX,del(12)(p11.2p13),del(13)(q22q32),add(20)(q13)[6]/46,XX[11]
4461	12	BCP-ALL	46,XX,t(2;16)(p1?1;p1?1),del(9)(q1?1;q22)[16]/46,XX[13]
4509	2	BCP-ALL	46,XY,del(9)(p11)[20]
4521	13	BCP-ALL	46,XY,add(2)(q?1)[5]/46,XY[19]
4557	12	BCP-ALL	47,XY,+12[2]/46,XY[28]
4730	2	BCP-ALL	45,XY,del(7)(q22),del(7)(q22),-9,add(9)(p12),der(16)t(9;16)(q1?3;q1?3)[8]/46,XY[26]
4821	1	BCP-ALL	45,XY,t(1;18)(p2?2;q11),-7,der(9)t(7;9)(p1?;p2?),t(14;22)(q11;q1?2)[4]

Table A3.6 Karyotypes of patients selected to screen for cryptic abnormalities of chromosome 21 (contd).

Patient ID	Age at diagnosis	Immnophonotype	Karyotype
4964	5	BCP-ALL	46,XX,?t(8;20)(q2?3;q1?3.1),del(14)(q11q1?3)[10]
4970	11	BCP-ALL	46,XX,+8,?dic(8;18)(p11;p11)[7]/47,idem,+?dic(8;18)(p11;p11)[7]/46,XX[1]
4972	10	BCP-ALL	46,XX,?dup(14)(?q32?q32)[17]/46,XX[8]
4984	5	BCP-ALL	46,XY,i(9)(q10)[8]
4990	16	BCP-ALL	46,XX,t(7;17)(q22;p11.2),del(11)(q13q21),t(12;22)(p13q1?3)[5]/46,idem,del(7)(q22q?34)[13]/46,XX[2]
5069	4	BCP-ALL	46,XX,der(7)t(7;17)(p22;q21),t(7;15)(q22;q15)[20]/46,XX,t(7;15)(q22;q15),der(12)t(12;17)(p13;q21)[3]/46,XX[7]
5578	9	BCP-ALL	48,X,t(Y;20)(q?11.2;p?)ins(Y;3)(q?11.2;?q?q),+13,+18[10]
5630	12	BCP-ALL	46,XX,der(3,13,16)t(3;13)(q1?;q1)t(13;16)(q2;p1)del(3)(p?q?),t(3;8)(q2?;q2?)/46,XX[2]
5644	2	BCP-ALL	46,XX,del(9)(p1?),der(12)t(11;?;12)[3]/46,XX[8]
5666	7	BCP-ALL	45,XX,der(7)t(7;9)(q3?;q3?),-9[6]/46,XX[4]

Table A3.7 Interphase FISH screen of ALL patients with probes adjacent to *RUNX1*.
Columns represent probes and rows represent patients.

.

Clone Position Mb	31.1	34.6	35.5 (RUNX1)	38.6 (ERG)	39.1 (ETS2)	46
Band	21q22.1	21q22.1	21q22	21q22.3	21q22.2	21q22.3
Patient ID	Copy Number					
3209	2	2	2	2	Fail	Fail
3335	2	2	2	2	2	Fail
3403	2	2	2	2	2	2
3836	Fail	Fail	2	2	2	2
3854	2	2	2	2	2	2
3867	2	2	2	2	2	2
3895	2	2	2	2	2	2
3939	2	2	2	2	Fail	2
3993	2	2	2	2	2	2
4021	2	2	2	2	2	2
4088	2	2	2	2	2	2
4206	2	2	2	2	2	2
4335	2	2	2	2	2	2
4400	2	2	2	2	2	2
4461	2	2	2	2	2	2
4509	2	2	2	2	2	2
4521	2	2	2	2	2	2
4557	2	2	2	2	2	2
4730	2	2	2	2	2	2
4821	2	2	2	2	2	2
4964	2	2	2	2	2	2
4970	2	2	2	2	2	2
4972	2	2	2	2	2	2
4984	2	2	2	2	2	2
4990	2	2	2	2	2	2
5069	2	2	2	2	2	2
5578	2	2	2	2	2	2
5630	2	2	2	2	2	2
5644	2	2	Fail	2	2	2
5666	2	2	2	2	2	2

Table A3.8 Interphase FISH screen of i(21)(q10) ALL patients with probes adjacent to *RUNX1.* Columns represent probes and rows represent patients.

Patient ID	dup(21)	Bac clone and genomic position (Mb)						
		24.1	29.8	32.3	35.5	40.0	43.7	46.9
		RP11-13J15	RP11-30N6	RP11-147H1	*RUNX1*	AF121782	RP11-88N2	21qtel
5612	3	3	3	3	3	3	3	3
9410	4	4	4	4	4	4	4	4
9410	5	5	5	5	5	5	5	5
5586	4	4	4	4	4	4	4	4
5586	5	5	5	5	5	5	5	5
5586	6	6	6	6	6	6	6	6
5003	6	6	6	6	6	6	6	6
5003	7	7	7	7	7	7	7	7

Table A3.9 G-banded karyotypes of i(21) i(21)(q10) ALL patients.

Patient ID	Karyotype
5003	49,XX,idic(21)(p11),+idic(21)(p11)x2,+mar1,+mar2[cp4]
5586	56,XX,+X,+X,+4,+6,+10,+14,+17,+18,+21,+21[4]/ 55,idem,-21,-21,+i(21)(q10)[4]/ 56,idem,-21,-21,+i(21)(q10),+i(21)(q10)[6]/46,XX[1]
5612	52-53,XY,+X,+4,+8,+14,+17,+18,idic(21)(p11),inc[cp5]/46,XY[13]
7015	47,XX,+X,t(2;14)(p1?1;q11),-7,i(21)(q10)x2,+mar[5]/46,XX[5]
9410	56,XY,+X,+Y,+6,+10,+14,+14,+15,+17,+21,+21,idic(21)(p1)[15]
4676	47,XY,del(9)?(p11p13),i(21)(q10),+dup(21)(q?21q22)[15]/46,XY[5]

Table A3.10 Olignucleotide aCGH data for patients with dup(15;21) der(15;21)

Patient 6783

Diminished(5)(60.37[q12.1]-80.84[q14.1]), Diminished(9)(21.89[p21.3]-21.99[p21.3]),

Enhanced(15)(23.23[q11.1]-25.78[q11.1]), Enhanced(15)(28.52[q11.2]-35.23[q13.1]),

Diminished(15)(36.37[q13.1]-36.57[q13.1]), Diminished(15)(36.84[q13.2]-57.75[q21.1]),

Amplified(15)(57.75[q21.1]-69.55[q22.31]), Diminished(15)(78.93[q24.1]-79.18[q24.2]),

Enhanced(15)(79.19[q24.2]-84.29[q25.2]), Diminished(15)(84.29[q25.2]-100.32[q26.3]),

Diminished(16)(48.09[q12.1]-60.27[q21.1]), Diminished(20),

Diminished(21)(9.89[p11.2]-13.96[p11.2]), Enhanced(21)(14.48[p11.2]-15.96[p11.1]),

Diminished(21)(24.28[q21.1]-25.69[q21.1]), Enhanced(21)(25.71[q21.1]-28.14[q21.1]),

Enhanced(21)(31.19[q21.2]-32.33[q21.3]), Amplified(21)(32.86[q21.3]-39.48[q22.13]),

Enhanced(21)(39.48[q22.13]-41.57[q22.2]), Amplified(21)(41.57[q22.3]-46.92[q22.3]),

Diminished(X)(87.78[q21.31]-91.89[q21.31]), Diminished(Y)(2.98[p11.32]-6.50[p11.2])

Patient 11005

Diminished(1)(20.59[1q32]-245.3[qter])Enhanced(2)(41.18[p22]-4.15)Diminished(2)

Diminished(13)(36.99[q13.3]-96.32)Diminished(15)(18.36[q10]-43.36[q21.1])

Enhanced(15)(43.36[q21.1]-46.19[q21.1])Amplified(15)(46.19[q21.1]-49.04[q21.2])

Enhanced(15)(49.04[q21.2]-51.02[q21.2])Diminished(15)(51.02[q21.2]-60.04[q22.2])

Amplified(15)(60.04[q22.2]-69.32[q23.0])Enhanced(15)(69.32[q23.0]-71.06)

Diminished(15)(71.06[q23]-71.93[q24.1])Enhanced(15)(71.94[71941196]-79.65[q25.1])

Diminished(15)(79.71[q25.1]-82.37[q25.2])Enhanced(15)(82.37[q25.2]-85.3[q25.3])

Enhanced(15)(85.3[q25.3]-85.97[q26.2])Enhanced(15)

Diminished(21)(14.4-15.4)Enhanced(21)(1.54[q21.1]-17.67[q21.1])

Amplified(21)(17.67[q21.1]-18.4[q21.1])Enhanced(21)(18.41[q21.1]-18.99[q21.1])

Amplified(21)(18.0[q21.1]-40.51)Diminished(21)

Table A3.11 Q-PCR fold change data from iAMP21 patients for *RUNX1*

Patient ID	House Ct	Average Ct	std dev	*RUNX1*	Average Ct	std dev	D Ct	std dev	DD Ct	2^-DDCt	Range	Range	Error	Error
6996	28.28			>35.00										
	27.58			>35.00										
	26.95			26.49										
		27.6	0.67		26.49		-1.11		-0.25	1.19				
6788	>35.00			26.21										
	>35.00			26.3										
	34.26			25.51										
		34.26			26.01	0.43	-8.25		-7.39	167.73				
7290	26.57			25.46										
	26.7			25.14										
	26.7			25.04										
		26.66	0.08		25.21	0.22	-1.44	0.23	-0.58	1.49	1.8	1.3	0.26	0.22
7045	26.91			23.16										
	25.78			23.52										
	25.6			23.06										
		26.1	0.71		23.25	0.24	-2.85	0.75	-1.99	3.96	6.7	2.4	2.7	1.61
4381	25.34			25.36										
	25.46			24.57										
	25.4			24.1										
		25.4	0.06		24.68	0.64	-0.72	0.64	0.14	0.91	1.4	0.6	0.51	0.32
WT	25.83			25.13										
	25.66			24.57										
	25.2			24.4										
		25.56	0.33		24.7	0.38	-0.86	0.5	0	1	1.4	0.7	0.42	0.29

Table A3.11 Q-PCR fold change data from iAMP21 patients for *RUNX1* (contd).

Patient ID	House Ct	AverageCt	std dev	*RUNX1*	AverageCt	std dev	D Ct	std dev	DD Ct	2^-DDCt	Range	Range	Error	Error
11002	28.21			26.72										
	28.66			26.79										
	28.6			26.9										
		28.49	0.24		26.8	0.09	-1.69	0.26	-1.69	3.22	3.9	2.7	0.64	0.53
4073	27.34			25.87										
	27.4			25.82										
	26.96			25.8										
		27.23	0.24		25.83	0.04	-1.4	0.24	-1.4	2.65	3.1	2.2	0.48	0.41
WT	25.83			25.13										
	25.66			24.57										
	25.2			24.4										
		25.56	0.33		24.7	0.38	-0.86	0.5	0	1	1.4	0.7	0.42	0.29

Table A3.12 Q-PCR fold change data from iAMP21 patients for *STCH*

Patient ID	House Ct	Average Ct	std dev	*STCH*	AverageCt	std dev	D Ct	std dev	DD Ct	2^-DDCt	Range	Range	Error	Error
6996	22.95			20.96										
	23.04			21.07										
	23.06			21.1										
		23.02	0.06		21.04	0.07	-1.97	0.09	-1.7	3.25	3.5	3	0.22	0.21
6788	25.92			24.94										
	26.04			25.08										
	25.85			25.04										
		25.94	0.1		25.02	0.07	-0.92	0.12	-0.64	1.56	1.7	1.4	0.14	0.12
7290	25.75			24.19										
	25.85			23.97										
	25.91			24.02										
		25.84	0.08		24.06	0.12	-1.78	0.14	-1.5	2.83	3.1	2.6	0.29	0.26
7045	25.17			24.3										
	25.23			24.35										
	25.24			24.17										
		25.21	0.04		24.27	0.09	-0.94	0.1	-0.67	1.59	1.7	1.5	0.11	0.11
4381	25.34			25.36										
	25.46			24.57										
	25.4			24.1										
		25.4	0.06		24.68	0.64	-0.72	0.64	-0.45	1.37	2.1	0.9	0.76	0.49
WT	25.23			24.3										
	25.18			26.19										
	25.25			24.35										
		25.22	0.04		24.95	1.08	-0.27	1.08	0	1	2.1	0.5	1.11	0.53

Table A3.12 Q-PCR fold change data from iAMP21 patients for *STCH* (contd).

Patient ID	House Ct	AverageCt	std dev	*STCH*	AverageCt	std dev	D Ct	std dev	DD Ct	2^-DDCt	Range	Range	Error	Error
11002	25.58			23.85										
	25.66			23.72										
	25.73			23.81										
		25.66	0.08		23.79	0.07	-1.86	0.1	-1.86	3.64	3.9	3.4	0.26	0.24
4073	27.29			27.91										
	27.32			26.16										
	27.32			26										
		27.31	0.02		26.69	1.06	-0.62	1.06	-0.62	1.54	3.2	0.7	1.67	0.8
WT	23.82			22.91										
	23.75			23.09										
	23.85			23.18										
		23.81	0.05		23.06	0.14	-0.75	0.15	0	1	1.1	0.9	0.11	0.1

Table A3.13 Q-PCR fold change data from iAMP21 patients for *PRMT2*

Patient ID	House Ct	Average Ct	std dev	PRMT2	Average Ct	std dev	D Ct	std dev	DD Ct	2^-DDCt	Range	Range	Error	Error
6996	22.95													
	23.04													
	23.06													
		23.02	0.06											
6788	25.92			25.95										
	26.04			26.02										
	25.85			26										
		25.94	0.1		25.99	0.04	0.05	0.1	-1.53	2.89	3.1	2.7	0.21	0.2
7290	25.75			29.1										
	25.85			28.79										
	25.91			27.46										
		25.84	0.08		28.45	0.87	2.61	0.88	1.03	0.49	0.9	0.3	0.41	0.22
7045	25.17			27.68										
	25.23			27.83										
	25.24			27.8										
		25.21	0.04		27.77	0.08	2.56	0.09	0.97	0.51	0.5	0.5	0.03	0.03
4381	25.34			28.76										
	25.46			28.87										
	25.4			28.83										
		25.4	0.06		28.82	0.06	3.42	0.08	1.84	0.28	0.3	0.3	0.02	0.02
WT	25.23			26.72										
	25.18			26.79										
	25.25			26.9										
		25.22	0.04		26.8	0.09	1.58	0.1	0	1	1.1	0.9	0.07	0.07

Table A3.13 Q-PCR fold change data from iAMP21 patients for *PRMT2* (contd).

Patient ID	House Ct	Average Ct	std dev	PRMT2	Average Ct	std dev	D Ct	std dev	DD Ct	2^-DDCt	Range	Range	Error	Error
	25.66			25.55										
	25.73			25.5										
		25.66	0.08		25.51	0.04	-0.15	0.08	-0.15	1.11	1.2	1	0.07	0.06
4073	27.29			27.55										
	27.32			27.61										
	27.32			27.33										
		27.31	0.02		27.5	0.15	0.19	0.15	0.19	0.88	1	0.8	0.1	0.09
WT	23.82			25.58										
	23.75			25.66										
	23.85			25.73										
		23.81	0.05		25.66	0.08	1.85	0.09	0	1	1.1	0.9	0.07	0.06

Table A3.14 Q-PCR fold change data from six normal DNA samples for *RUNX1*

cDNA	House	Average Ct	std dev	*RUNX1*	Average Ct	std dev	D Ct	std dev	DD Ct	2^-DDCt	Range	Range	Error	Error
A1	25.89			25.92										
A2	25.84			25.92										
A3	25.87			25.78										
		25.87	0.03		25.87	0.08	0.01	0.08	0.73	0.6	0.6	0.6	0.04	0.03
A4	25.92			26.08										
A5	25.71			26.01										
A6	25.72			26.04										
		25.78	0.12		26.04	0.04	0.26	0.12	0.98	0.51	0.6	0.5	0.05	0.04
A7	23.76			23.39										
A8	23.67			23.36										
A9	23.82			23.45										
		23.75	0.08		23.4	0.05	-0.35	0.09	0.37	0.77	0.8	0.7	0.05	0.05
A10	25.72			26.01										
A11	25.93			25.94										
A12	26.02			25.85										
		25.89	0.15		25.93	0.08	0.04	0.17	0.76	0.59	0.7	0.5	0.08	0.07
B1	26.96			27.71										
B2	27.4			27.62										
B3	27.23			27.48										
		27.2	0.12		27.6	0.12	0.41	0.17	1.13	0.46	0.5	0.4	0.06	0.05
B4	24.88			24.38										
B5	25.14			24.35										
B6	25.01			24.49										
		25.01	0.13		24.41	0.07	-0.6	0.15	0.12	0.92	1	0.8	0.1	0.09
B10	23.26			22.41										
B11	23.14			22.55										
B12	23.59			23.11										
		23.2	0.08		22.48	0.1	-0.72	0.13	0	1	1.1	0.9	0.09	0.09

Table A3.15 Q-PCR fold change data from six normal DNA samples for *STCH*

cDNA	House	Average Ct	std dev	*STCH*	Average Ct	Std dev	D Ct	std dev	DD Ct	2^-DDCt	Range	Range	Error	Error
A1	25.89			24.51										
A2	25.84			24.01										
A3	25.87			24.57										
		25.87	0.03		24.54	0.04	-1.33	0.05	-1.42	2.67	2.8	2.6	0.09	0.09
A4	25.92			23.28										
A5	25.71			22.76										
A6	25.72			22.41										
		25.78	0.12		22.59	0.25	-3.2	0.27	-3.29	9.77	11.8	8.1	2.05	1.69
A7	23.76			22.51										
A8	23.67			22.71										
A9	23.82			22.63										
		23.75	0.08		22.62	0.1	-1.13	0.13	-1.22	2.33	2.5	2.1	0.21	0.2
A10	25.72			24.58										
A11	25.93			24.58										
A12	26.02			24.48										
		25.89	0.15		24.55	0.06	-1.34	0.16	-1.43	2.7	3	2.4	0.33	0.29
B1	26.96			26.02										
B2	27.4			25.83										
B3	27.23			25.78										
		27.32	0.12		25.88	0.13	-1.44	0.17	-1.53	2.88	3.3	2.6	0.37	0.33
B4	24.88			23.76										
B5	25.14			23.76										
B6	25.01			23.73										
		25.01	0.13		23.75	0.02	-1.26	0.13	-1.35	2.55	2.8	2.3	0.24	0.22
B10	23.26			23.29										
B11	23.14			23.3										
B12	23.59			23.28										
		23.2	0.08		23.29	0.01	0.09	0.09	0	1	1.1	0.9	0.06	0.06

Table A3.16 Q-PCR fold change data from six normal DNA samples for *PRMT2*

cDNA	House	Average Ct	std dev	*PRMT2*	Average Ct	std dev	D Ct	std dev	DD Ct	2^-DDCt	Range	Range	Error	Error
A1	25.89			28.6										
A2	25.84			28.39										
A3	25.87			28.68										
		25.87	0.03		28.56	0.15	2.69	0.15	0.81	0.57	0.6	0.5	0.06	0.06
A4	25.92			27										
A5	25.71			27.02										
A6	25.72			27										
		25.78	0.12		27.01	0.01	1.22	0.12	-0.66	1.58	1.7	1.5	0.14	0.12
A7	23.76			24.38										
A8	23.67			24.36										
A9	23.82			24.48										
		23.75	0.08		24.41	0.06	0.66	0.1	-1.22	2.33	2.5	2.2	0.17	0.16
A10	25.72			27.06										
A11	25.93			27.08										
A12	26.02			27.03										
		25.89	0.15		27.06	0.03	1.17	0.16	-0.71	1.64	1.8	1.5	0.19	0.17
B1	26.96			27.01										
B2	27.4			26.94										
B3	27.23			27.01										
		27.32	0.12		26.99	0.04	-0.33	0.13	-2.21	4.62	5	4.2	0.42	0.39
B4	24.88			25.41										
B5	25.14			25.47										
B6	25.01			25.47										
		25.01	0.13		25.45	0.03	0.44	0.13	-1.44	2.71	3	2.5	0.27	0.24
B10	23.26			25.11										
B11	23.14			24.97										
B12	23.59			25.16										
		23.2	0.08		25.08	0.1	1.88	0.13	0	1	1.1	0.9	0.09	0.09

Figure A3.3 Comparison of 'Ct' ratios between *STCH* and *PRMT2* using *RUNX1* as the calibrator.
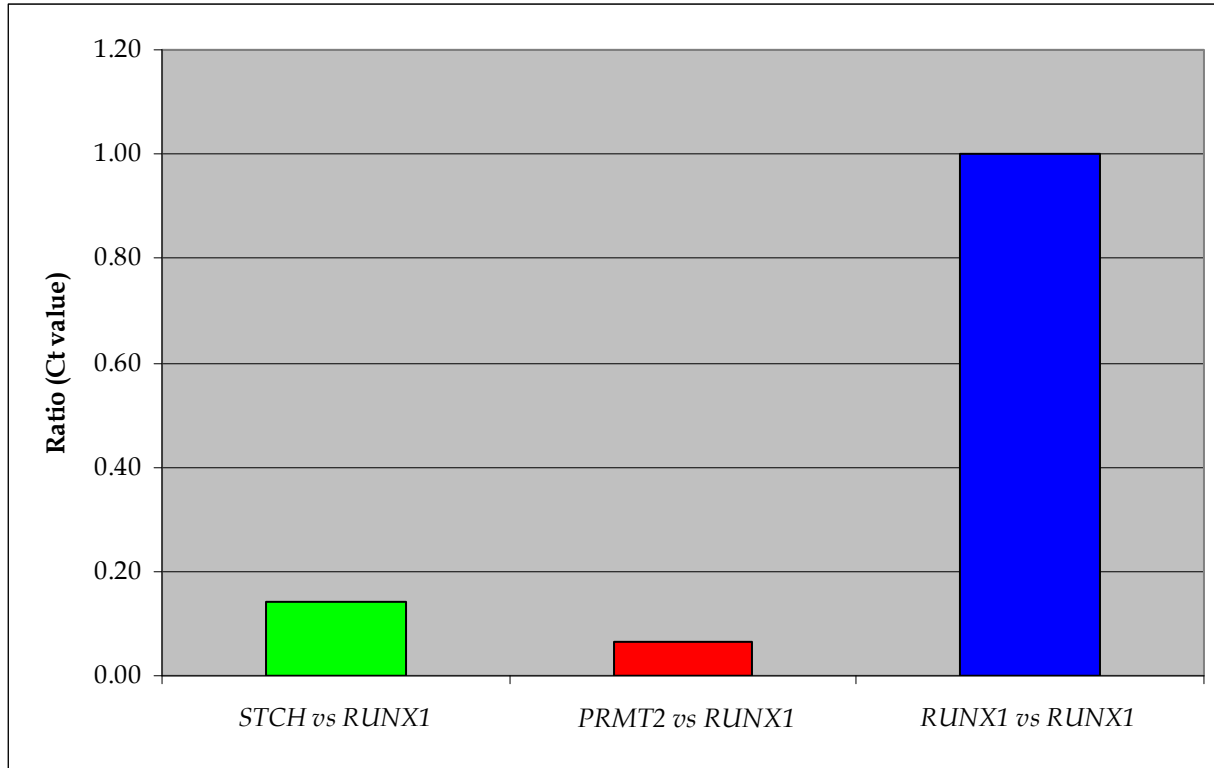
Table A3.17 Gains and Losses of telomeric regions detected by MLPA.

Code: 21= gain of a single chromosome 21, Ho =Hypodiploid karyotype, HeH= Hyperdiplio, Nor =Normal, NK = chromosome 21 abnormality not known.

Patient ID	Code	PRSS7	RUNX1	1p	1q	2p	2q	3p	3q	4p	4q	5p	5q	6p	6q	7p	7q	8p	8q	9p	9q	10p	10q	11p	11q	12p	12q	13p	13q	14p	14q	15p	15q	16p	16q	17p	17q	18p	18q	19p	19q	20p	20q	21p	21q	22p	22q	XYp	XYq
3043	21	3	3	2	2	2	2	2	2	2	2	2	2	2	2	2	2	2	2	2	2	2	2	2	2	2	2	2	2	2	2	2	2	2	2	2	2	2	2	2	2	2	2	3	3	2	2	2	2
4073	21	3	3	2	2	2	2	2	2	2	2	2	2	2	2	2	2	2	2	2	2	2	2	2	2	2	2	2	2	2	2	2	2	2	2	2	2	2	2	2	2	2	2	3	2	2	2	3	2
4184	21	3	3	2	2	2	2	2	2	2	2	2	2	2	2	2	2	2	2	2	2	2	2	2	2	2	2	2	2	2	2	2	2	2	2	2	2	2	2	2	2	2	2	3	3	2	2	3	3
4318	21	3	3	2	2	2	2	2	2	2	2	2	2	2	2	2	2	2	2	2	2	2	2	2	2	2	2	2	2	2	2	2	2	2	2	2	2	2	2	2	2	2	2	3	3	2	2	2	2
7653	Ho	3	3	2	2	2	2	2	2	2	2	2	2	2	2	2	2	4	4	2	2	4	2	2	2	2	2	2	2	2	2	2	2	2	2	2	2	3	3	2	2	2	2	3	3	2	2	3	3
4642	HeH	3	3	2	2	2	2	2	2	3	3	2	2	3	3	2	2	3	3	2	2	3	3	2	2	2	2	2	2	3	3	2	2	2	3	3	3	2	2	2	2	3	3	3	3	2	2	3	3
11102	HeH	3	3	2	2	2	2	2	2	3	3	2	2	2	2	2	2	3	3	3	3	2	2	2	2	2	2	2	2	3	3	2	2	2	2	3	3	3	3	2	2	2	2	3	3	2	2	3	3
7290	HeH	4	4	2	2	2	2	2	2	3	3	2	2	2	3	2	2	3	3	2	2	3	2	2	2	2	2	2	2	3	3	2	2	2	2	2	3	3	3	2	2	2	2	4	4	2	2	3	3
9525	HeH	4	4	2	2	2	2	2	2	2	2	2	2	2	2	2	2	2	2	2	2	1	2	2	2	2	2	2	2	1	2	2	2	2	1	2	2	2	2	2	2	2	3	1	1	4	4	3	3
12025	HeH	3	3	2	3	2	2	2	3	2	2	3	3	2	2	2	2	3	3	3	2	3	2	2	2	2	2	2	2	3	3	2	2	2	3	2	2	4	2	2	2	4	4	2	2	2	2	3	3
7558	HeH Iso	6	6	2	2	1	2	2	2	3	3	2	2	3	3	2	2	3	3	2	2	3	3	2	1	2	2	2	2	3	3	2	2	2	3	3	3	2	2	2	3	2	2	5	5	2	2	3	3
4405	iAMP21	3	7	2	1	2	1	2	2	2	2	2	2	2	2	2	2	2	2	2	2	2	2	2	2	2	2	2	2	2	2	2	2	1	4	2	2	2	2	2	2	1	1	3	3	3	3
6783	iAMP21	2	4	2	2	2	2	2	2	2	2	2	2	2	2	2	2	2	2	2	2	2	2	2	2	2	2	2	2	2	2	1	2	2	2	2	2	2	2	1	1	3	3	2	2	2	2
6788	iAMP21	2	5	2	2	2	2	2	2	2	2	2	2	2	2	2	2	2	2	2	2	2	2	2	2	2	2	2	2	2	2	2	2	2	2	2	2	2	2	2	2	2	2	3	2	2	2
6996	iAMP21	5	6	2	2	2	2	2	2	2	2	2	2	2	2	3	2	2	2	2	2	2	1	2	2	2	2	1	2	2	2	2	2	2	2	2	2	2	2	2	2	4	1	2	2	2	2
7045	iAMP21	2	5	2	2	2	2	2	2	2	2	2	2	2	2	2	2	2	2	2	2	2	2	2	2	2	2	2	2	2	2	2	2	2	2	2	2	2	2	2	2	1	2	2	2	2	2
7093	iAMP21	3	5	2	3	2	2	2	2	2	2	2	2	2	2	2	3	2	2	2	2	2	2	2	2	2	2	2	2	2	2	2	2	2	2	2	2	2	2	2	2	2	2	2	2	2	2
7219	iAMP21	3	6	2	2	2	2	2	2	2	2	2	2	2	2	2	2	2	3	1	2	2	2	2	2	2	2	2	2	2	2	2	2	2	2	2	2	2	2	2	2	3	1	2	2	2	2
7619	iAMP21	4	7	2	2	2	2	2	2	2	2	2	2	2	2	2	2	2	3	2	2	2	2	2	2	2	2	2	2	2	2	2	2	2	2	2	2	2	2	2	2	4	1	2	2	2	2
7732	iAMP21	3	4	2	2	2	2	2	2	2	2	2	2	2	2	2	2	2	2	2	2	2	2	2	2	2	2	2	2	2	2	2	2	2	2	2	2	2	2	2	2	1	2	2	2	3	1
7774	iAMP21	2	3	2	2	2	2	2	2	2	2	2	2	2	2	2	2	2	2	2	2	2	2	2	2	2	2	2	2	2	2	2	2	2	2	2	2	2	2	2	2	2	2	2	2	2	2
8743	iAMP21	2	4	2	2	2	2	2	2	2	2	2	2	2	2	2	2	2	2	2	2	2	2	1	2	2	2	2	2	2	2	2	2	2	2	2	2	2	2	2	2	1	2	2	2	3	2
8983	iAMP21	3	5	2	2	2	2	2	2	1	2	1	2	2	2	2	1	2	1	1	1	1	2	2	2	2	2	1	1	1	2	2	2	2	2	2	2	2	2	2	2	1	1	3	1	2	2
9028	iAMP21	3	6	2	2	1	2	2	2	2	2	2	2	2	2	2	2	1	2	2	2	2	2	1	2	2	2	2	2	2	2	2	2	2	2	2	2	2	2	2	2	1	2	2	2	3	3
11005	iAMP21	3	7	2	1	2	1	2	2	2	2	2	2	2	2	2	2	2	2	2	2	2	2	2	2	2	2	2	2	2	2	1	2	2	4	2	2	2	2	2	2	2	1	3	2	3	2
11706	iAMP21	3	6	2	2	2	2	2	2	2	2	2	2	2	2	2	2	2	2	2	2	2	2	2	2	2	2	2	2	2	2	2	2	2	2	2	2	2	2	2	2	3	1	2	2	2	2
4279	iAMP21	2	3	2	2	2	2	2	2	2	2	2	2	2	2	2	2	2	2	2	2	2	2	2	2	2	2	2	2	2	2	2	2	2	2	2	2	2	2	2	2	2	2	2	2	2	2
10958	iAMP21	2	2	2	2	2	2	2	2	2	2	2	2	2	2	2	2	2	2	2	2	2	2	2	2	2	2	2	2	2	2	2	2	2	2	2	2	2	2	2	2	2	2	2	2	2	2
12377	Normal	2	2	2	2	2	2	2	2	2	2	2	2	2	2	2	2	2	2	2	2	2	2	2	2	2	2	2	2	2	2	2	2	2	2	2	2	2	2	2	2	2	2	2	2	2	2
4676	i(21)	5	5	2	2	2	2	2	2	2	2	2	2	2	2	2	2	2	2	2	2	2	2	2	2	2	2	2	2	2	2	2	2	2	2	2	2	2	2	2	2	4	4	2	2	2	2
4247	NK	2	3	2	2	2	2	2	2	2	2	2	2	2	2	2	2	2	2	2	2	2	2	2	2	2	2	2	2	2	2	2	2	2	2	2	2	2	2	2	2	2	2	3	2	2	2
4746	NK	4	4	2	2	2	1	2	2	2	2	2	2	2	2	2	2	2	2	2	2	2	2	2	2	2	2	2	3	2	2	2	2	2	3	2	2	2	2	2	2	1	1	6	2	2	3
9101	NK	1	3	2	2	2	2	2	2	2	2	2	2	2	2	2	2	2	2	1	3	2	2	2	2	2	2	2	2	2	2	2	1	2	2	2	2	2	2	2	2	1	1	2	2	2	2

Table A3.18 Gains and Losses of telomeric regions detected by MLPA and G-banding. +21= gain of a single chromosome 21. Ho =Hypodiploid karyotype HeH= Hyperdipliod Nor =Normal

Patient ID	Gains/Losses detected by MLPA	Code	Karyotype
3043	+21p,+*PRSS7*, +*RUNX1*,+21q	+21	47,XY,+21/46,XY[5]
4073	+21p,+*PRSS7*,+*RUNX1*, +Xp	+21	47,XX,+21c[10]/48,idem,+X [10]
4184	+21p,+*PRSS7*,+*RUNX1*, +21q,+Xp,+Xq	Ho	25,XY,+21[9]/50,XY,+X,+Y,+21,+21 [3]/46,XY[2]
4318	+21p,+*PRSS7*,+*RUNX1*, +21q	+21	47,XY,del(9)(p22p24),+21c[20]
7290	+4p,+4q,+6p,+6q,+8p,+8q, +10p,+10q, +14p,+14q,+17p,+17q,+18q, +21px2,+*PRSS7* x2,+*RUNX1* x2,+21qx2, +X/Yp,+X/Yq	HeH	57,XX,+X,+4,+6,+8,+10,+14,+17,+18,+ 21,+21,+21[18]/56,idem,dup(1)(q1q4),-21[2]
7558	-2p, +4p,+4q,+6p,+6q,+8p,+8q, +10p,+10q ,-11q, +14p,+14q,-16q, +17p,+17q,+19q,+21px3, +*PRSS7* x4,+*RUNX1* x4,+21qx3, +X/Yp,+X/Yq	HeH i(21)	50-53,XY,+X,+4,+6,+?17,+i(21)(q10),+i(2 1)(q10),inc[cp5]/46,XY[4]
9525	-13q,-16q,19q+,-20p,-20q, +21px2,+PRSS7x2, +*RUNX1*x2,+21qx2, +X/Yp,+X/Yq	+21	47,XY,+X,-13,-16,+21,+21[10]/46,XY[5]
10958	No change	Nor	46,XY[20]
11102	+4p,+4q,+9p,+9q,+10p,+10q , +14p,+14q,+17p,+17q,+18q, +21p,+*PRSS7*,+*RUNX1*,+21 q, +X/Yp,+X/Yq	HeH	53~55,XY,+X,+4,+9,+10,+18,+21c,+21 ,+2~3mar[cp12]
12025	+1q,+4p,+4q,+6p,+6q, +9p,+9q,+10p,+10q,+14p,+1 4q,+17p,+18p,+18qx2 +21px2,+*PRSS7*,+*RUNX1*,+ 21qx2, +X/Yp,+X/Yq	HeH	56~59,XX,+X,+4,+6,+8,+9,+10,+14,+1 5,+17,+18,+19,+21,+21,+mar[8]/46,X X[2]

6 References

(1986) Morphologic, immunologic, and cytogenetic (MIC) working classification of acute lymphoblastic leukemias. Report of the workshop held in Leuven, Belgium, April 22-23, 1985. First MIC Cooperative Study Group. *Cancer genetics and cytogenetics*, **23**, 189-197.

(2001) *Pathology and Genetics of Tumours of Haematopoietic and Lymphoid Tissues*, IARC, Lyon.

(1981) Third International Workshop on Chromosomes in Leukemia (1980): Clinical significance of chromosomal abnormalities in acute lymphoblastic leukemia. *Cancer Genet Cytogenet*, **4**, 111-137.

Albertson,D.G. (2006) Gene amplification in cancer. *Trends Genet.*, **22**, 447-455.

Albertson,D.G., Snijders,A.M., Fridlyand,J., Jordan,R., Pinkel,D., & Schmidt,B.L. (2006) Genomic analysis of tumors by array comparative genomic hybridization: more is better. *Cancer Res.*, **66**, 3955-3956.

Andersen,M.K., Christiansen,D.H., Kirchhoff,M., & Pedersen-Bjergaard,J. (2001) Duplication or amplification of chromosome band 11q23, including the unrearranged MLL gene, is a recurrent abnormality in therapy-related MDS and AML, and is closely related to mutation of the TP53 gene and to previous therapy with alkylating agents. *Genes Chromosomes.Cancer*, **31**, 33-41.

Andersen,M.K., Christiansen,D.H., & Pedersen-Bjergaard,J. (2004) Amplification or duplication of chromosome band 21q22 with multiple copies of the AML1 gene and mutation of the TP53 gene in therapy-related MDS and AML. *Leukemia*, **19**, 197-200.

Andreasson,P., Hoglund,M., Bekassy,A.N., Garwicz,S., Heldrup,J., Mitelman,F., & Johansson,B. (2000) Cytogenetic and FISH studies of a single center consecutive series of 152 childhood acute lymphoblastic leukemias. *European Journal of Haematology*, **65**, 40-51.

Arlt,M.F., Durkin,S.G., Ragland,R.L., & Glover,T.W. (2006) Common fragile sites as targets for chromosome rearrangements. *DNA Repair (Amst)*, **5**, 1126-1135.

Arriola,E., Marchio,C., Tan,D.S., Drury,S.C., Lambros,M.B., Natrajan,R., Rodriguez-Pinilla,S.M., Mackay,A., Tamber,N., Fenwick,K., Jones,C., Dowsett,M., Ashworth,A., & Reis-Filho,J.S. (2008) Genomic analysis of the HER2//TOP2A amplicon in breast cancer and breast cancer cell lines. *Lab Invest*.

Bailey,S.M. & Murnane,J.P. (2006) Telomeres, chromosome instability and cancer. *Nucleic Acids Res.*, **34**, 2408-2417.

Bain,B. (1999) *Leukaemia Diagnosis,* Second edition edn, Blackwell Science.

Bain,B.J. (1998) Classification of acute leukaemia: the need to incorporate cytogenetic and molecular genetic information. *J.Clin.Pathol.*, **51**, 420-423.

Baldus,C.D., Liyanarachchi,S., Mrozek,K., Auer,H., Tanner,S.M., Guimond,M., Ruppert,A.S., Mohamed,N., Davuluri,R.V., Caligiuri,M.A., Bloomfield,C.D., & de la,C.A. (2004) Acute myeloid leukemia with complex karyotypes and abnormal chromosome 21: Amplification discloses overexpression of APP, ETS2, and ERG genes. *Proc.Natl.Acad.Sci.U.S.A*, **101**, 3915-3920.

Barber,K.E., Martineau,M., Harewood,L., Stewart,M., Cameron,E., Strefford,J.C., Rutherford,S., Allen,T.D., Broadfield,Z.J., Cheung,K.L., Harris,R.L., Jalali,G.R., Moorman,A.V., Robinson,H.M., & Harrison,C.J. (2004) Amplification of the ABL gene in T-cell acute lymphoblastic leukemia. *Leukemia*, **18**, 1153-1156.

Bennett,J.M., Catovsky,D., Daniel,M.T., Flandrin,G., Galton,D.A., Gralnick,H.R., & Sultan,C. (1976) Proposals for the classification of the acute leukaemias. French-American-British (FAB) co-operative group. *Br.J.Haematol.*, **33**, 451-458.

Bennett,J.M., Catovsky,D., Daniel,M.T., Flandrin,G., Galton,D.A., Gralnick,H.R., & Sultan,C. (1981) The morphological classification of acute lymphoblastic leukaemia: concordance among observers and clinical correlations. *Br.J.Haematol.*, **47**, 553-561.

Borkhardt,A., Cazzaniga,G., Viehmann,S., Valsecchi,M.G., Ludwig,W.D., Burci,L., Mangioni,S., Schrappe,M., Riehm,H., Lampert,F., Basso,G., Masera,G., Harbott,J., & Biondi,A. (1997) Incidence and clinical relevance of TEL/AML1 fusion genes in children with acute lymphoblastic leukemia enrolled in the German and Italian multicenter therapy trials. Associazione Italiana Ematologia Oncologia Pediatrica and the Berlin-Frankfurt-Munster Study Group. *Blood*, **90**, 571-577.

Borowitz,M.J., Devidas,M., Hunger,S.P., Bowman,W.P., Carroll,A.J., Carroll,W.L., Linda,S., Martin,P.L., Pullen,D.J., Viswanatha,D., Willman,C.L., Winick,N., Camitta,B.M., & for the Children's Oncology Group (2008) Clinical significance of minimal residual disease in childhood acute lymphoblastic leukemia and its relationship to other prognostic factors: a Children's Oncology Group study. *Blood*, **111**, 5477-5485.

Busson-Le Coniat,M., Nguyen,K.F., Daniel,M.T., Bernard,O.A., & Berger,R. (2001) Chromosome 21 abnormalities with AML1 amplification in acute lymphoblastic leukemia. *Genes Chromosomes.Cancer*, **32**, 244-249.

Byrne,J. & Russell,N. (2005) Haemopoietic growth factors. Postgradutate Haematology. (ed. by A. V. Hoffbrand, D. Catovsky, & E. G. D. Tuddenham), pp. 303-317. Blackwell Publishing.

Cameron,E.R. & Neil,J.C. (2004) The Runx genes: lineage-specific oncogenes and tumor suppressors. *Oncogene*, **23**, 4308-4314.

Chango,A., Emery-Fillon,N., de Courcy,G.P., Lambert,D., Pfister,M., Rosenblatt,D.S., & Nicolas,J.P. (2000) A Polymorphism (80G->A) in the Reduced Folate Carrier Gene and Its Associations with Folate Status and Homocysteinemia. *Molecular Genetics and Metabolism*, **70**, 310-315.

Cheok,M.H. & Evans,W.E. (2006) Acute lymphoblastic leukaemia: a model for the pharmacogenomics of cancer therapy. *Nat.Rev.Cancer*, **6**, 117-129.

Cheung,A.L. & Deng,W. (2008) Telomere dysfunction, genome instability and cancer. *Front Biosci.*, **13**, 2075-2090.

Chim,C.S., Tam,C.Y., Liang,R., & Kwong,Y.L. (2001) Methylation of p15 and p16 genes in adult acute leukemia: lack of prognostic significance. *Cancer*, **91**, 2222-2229.

Ciullo,M., Debily,M.A., Rozier,L., Autiero,M., Billault,A., Mayau,V., El,M.S., Guardiola,J., Bernheim,A., Coullin,P., Piatier-Tonneau,D., & Debatisse,M. (2002) Initiation of the breakage-fusion-bridge mechanism through common fragile site activation in human breast cancer cells: the model of PIP gene duplication from a break at FRA7I. *Hum.Mol Genet.*, **11**, 2887-2894.

Cogulu,O., Kosova,B., Gunduz,C., Karaca,E., Aksoylar,S., Erbay,A., Karapinar,D., Vergin,C., Vural,F., Tombuloglu,M., Cetingul,N., & Ozkinay,F. (2008) The evaluation of hTERT mRNA expression in acute

leukemia children and 2 years follow-up of 40 cases. *Int.J.Hematol.*, **87**, 276-283.

Cooley,L.D., Chenevert,S., Shuster,J.J., Johnston,D.A., Mahoney,D.H., Carroll,A.J., Devidas,M., Linda,S.B., Lauer,S.J., & Camitta,B.M. (2007) Prognostic significance of cytogenetically detected chromosome 21 anomalies in childhood acute lymphoblastic leukemia: a Pediatric Oncology Group study
1. *Cancer Genet.Cytogenet.*, **175**, 117-124.

CTSU. UKALL 2003. Clinical Trial Service Unit & Epidemiological Studies Unit, Oxford . 2008.
Ref Type: Electronic Citation

Cuthbert,G., Thompson,K., McCullough,S., Watmore,A., Dickinson,H., Telford,N., Mugneret,F., Harrison,C., Griffiths,M., & Bown,N. (2000) MLL amplification in acute leukaemia: a United Kingdom Cancer Cytogenetics Group (UKCCG) study. *Leukemia*, **14**, 1885-1891.

Czepulkowski,B. (2001) *Analyzing chromosomes,* BIOS Scientific Publishers Ltd, Oxford.

Deininger,M., Buchdunger,E., & Druker,B.J. (2005) The development of imatinib as a therapeutic agent for chronic myeloid leukemia. *Blood*, **105**, 2640-2653.

Deininger,M.W., Goldman,J.M., & Melo,J.V. (2000) The molecular biology of chronic myeloid leukemia. *Blood*, **96**, 3343-3356.

Downing,J.R. & Mullighan,C.G. (2006) Tumor-specific genetic lesions and their influence on therapy in pediatric acute lymphoblastic leukemia. *Hematology.Am.Soc.Hematol.Educ.Program.*, 118-22, 508.

Druker,B.J., Guilhot,F., O'Brien,S.G., Gathmann,I., Kantarjian,H., Gattermann,N., Deininger,M.W., Silver,R.T., Goldman,J.M., Stone,R.M., Cervantes,F., Hochhaus,A., Powell,B.L., Gabrilove,J.L., Rousselot,P., Reiffers,J., Cornelissen,J.J., Hughes,T., Agis,H., Fischer,T., Verhoef,G., Shepherd,J., Saglio,G., Gratwohl,A., Nielsen,J.L., Radich,J.P., Simonsson,B., Taylor,K., Baccarani,M., So,C., Letvak,L., & Larson,R.A. (2006) Five-year follow-up of patients receiving imatinib for chronic myeloid leukemia. *N.Engl.J.Med.*, **355**, 2408-2417.

Evan,G.I. & Vousden,K.H. (2001) Proliferation, cell cycle and apoptosis in cancer. *Nature*, **411**, 342-348.

Ferrando,A.A. & Look,A.T. (2003) Gene expression profiling in T-cell acute lymphoblastic leukemia
14. *Semin.Hematol.*, **40**, 274-280.

Fisher,A., Tyreman,C., Cullis,J., & Ross,F.M. (2003) Five cases of myeloid neoplasia with idic(21)(q22); a possible novel mechanism of chromosome 21 amplification. *Journal of Medical Genetics*, **40**, S50.

Ford,A.M., Bennett,C.A., Price,C.M., Bruin,M.C., Van Wering,E.R., & Greaves,M. (1998) Fetal origins of the TEL-AML1 fusion gene in identical twins with leukemia
39. *Proc.Natl.Acad.Sci.U.S.A*, **95**, 4584-4588.

Gale,K.B., Ford,A.M., Repp,R., Borkhardt,A., Keller,C., Eden,O.B., & Greaves,M.F. (1997) Backtracking leukemia to birth: identification of clonotypic gene fusion sequences in neonatal blood spots. *Proc.Natl.Acad.Sci.U.S.A*, **94**, 13950-13954.

Ganapathy,V., Smith,S.B., & Prasad,P.D. (2004) SLC19: the folate/thiamine transporter family. *Pflugers Arch.*, **447**, 641-646.

Garcia-Casado,Z., Cervera,J., Verdeguer,A., Tasso,M., Valencia,A., Pajuelo,J.C., Mena-Duran,A.V., Barragan,E., Blanes,M., Bolufer,P., & Sanz,M.A. (2006) High-level amplification of the RUNX1 gene in two cases of childhood acute lymphoblastic leukemia. *Cancer Genet.Cytogenet.*, **170**, 171-174.

Gardner,R. & Sutherland,G. (2004) *Chromosome Abnormalities and Genetic Counseling,* Third Edition edn, Oxford University Press, New York.

Ge,Y., Haska,C.L., LaFiura,K., Devidas,M., Linda,S.B., Liu,M., Thomas,R., Taub,J.W., & Matherly,L.H. (2007) Prognostic role of the reduced folate carrier, the major membrane transporter for methotrexate, in childhood acute lymphoblastic leukemia: a report from the Children's Oncology Group. *Clin.Cancer Res.*, **13**, 451-457.

Gisselsson,D., Jonson,T., Petersen,A., Strombeck,B., Dal,C.P., Hoglund,M., Mitelman,F., Mertens,F., & Mandahl,N. (2001) Telomere dysfunction triggers extensive DNA fragmentation and evolution of complex chromosome abnormalities in human malignant tumors. *Proc.Natl.Acad.Sci.U.S.A*, **98**, 12683-12688.

Gisselsson,D., Pettersson,L., Hoglund,M., Heidenblad,M., Gorunova,L., Wiegant,J., Mertens,F., Dal,C.P., Mitelman,F., & Mandahl,N. (2000) Chromosomal breakage-fusion-bridge events cause genetic intratumor heterogeneity. *Proc.Natl.Acad.Sci.U.S.A*, **97**, 5357-5362.

Graux,C., Cools,J., Melotte,C., Quentmeier,H., Ferrando,A., Levine,R., Vermeesch,J.R., Stul,M., Dutta,B., Boeckx,N., Bosly,A., Heimann,P., Uyttebroeck,A., Mentens,N., Somers,R., MacLeod,R.A., Drexler,H.G., Look,A.T., Gilliland,D.G., Michaux,L., Vandenberghe,P., Wlodarska,I., Marynen,P., & Hagemeijer,A. (2004) Fusion of NUP214 to ABL1 on amplified episomes in T-cell acute lymphoblastic leukemia. *Nat.Genet.*, **36**, 1084-1089.

Graux,C., Cools,J., Michaux,L., Vandenberghe,P., & Hagemeijer,A. (2006) Cytogenetics and molecular genetics of T-cell acute lymphoblastic leukemia: from thymocyte to lymphoblast. *Leukemia*, **20**, 1496-1510.

Greaves,M. (2002) Childhood leukaemia. *British Medical Journal*, **324**, 283-287.

Greaves,M.F., Maia,A.T., Wiemels,J.L., & Ford,A.M. (2003) Leukemia in twins: lessons in natural history
22. *Blood*, **102**, 2321-2333.

Griffiths,M., Mason,J., Rindl,M., Akiki,S., McMullan,D., Stinton,V., Powell,H., Curtis,A., Bown,N., & Craddock,C. (2005) Acquired isodisomy for chromosome 13 is common in AML, and associated with FLT3-itd mutations. *Leukemia*, **19**, 2355-2358.

Gruszka-Westwood,A.M., Horsley,S.W., Martinez-Ramirez,A., Harrison,C.J., Kempski,H., Moorman,A.V., Ross,F.M., Griffiths,M., Greaves,M.F., & Kearney,L. (2004) Comparative expressed sequence hybridization studies of high-hyperdiploid childhood acute lymphoblastic leukemia
3. *Genes Chromosomes.Cancer*, **41**, 191-202.

Haas,O.A., Moritz,A., Stanulla,M., Koenig,M., Roettgers,S., Reichelt,C., Harbott,J., Strehl,S., & Schrappe,M. (2005) A DNA-based RQ-PCR screening assay for the identification of cases with RUNX1 copy number changes in childhood B cell precursor acute lymphoblastic leukemia (BCP-ALL). *Blood*, **106**.

Hann,I., Vora,A., Harrison,G., Harrison,C., Martineau,M., Moorman,A.V., Secker Walker,L.M., Eden,O., Hill,F., Gibson,B., & Richards,S. (2001) Determinants of outcome after intensified therapy of childhood lymphoblastic leukaemia: results from Medical Research Council United Kingdom acute lymphoblastic leukaemia XI protocol. *Br J Haematol*, **113**, 103-114.

Harbott,J., Viehmann,S., Borkhardt,A., Henze,G., & Lampert,F. (1997) Incidence of TEL/AML1 fusion gene analyzed consecutively in children with acute lymphoblastic leukemia in relapse. *Blood*, **90**, 4933-4937.

Harewood,L., Robinson,H., Harris,R., Al-Obaidi,M.J., Jalali,G.R., Martineau,M., Moorman,A.V., Sumption,N., Richards,S., Mitchell,C., & Harrison,C.J. (2003) Amplification of AML1 on a duplicated chromosome 21 in acute lymphoblastic leukemia: a study of 20 cases. *Leukemia*, **17**, 547-553.

Harris,N.L., Jaffe,E.S., Diebold,J., Flandrin,G., Muller-Hermelink,H.K., Vardiman,J., Lister,T.A., & Bloomfield,C.D. (1999) The World Health Organization classification of neoplastic diseases of the hematopoietic and lymphoid tissues. Report of the Clinical Advisory Committee meeting, Airlie House, Virginia, November, 1997. *Annals of Oncology*, **10**, 1419-1432.

Harrison,C.J. (2000) The genetics of childhood acute lymphoblastic leukaemia. *Baillieres Best.Pract.Res.Clin.Haematol.*, **13**, 427-439.

Harrison,C.J. (2001) The detection and significance of chromosomal abnormalities in childhood acute lymphoblastic leukaemia. *Blood Rev.*, **15**, 49-59.

Harrison,C.J., Martineau,M., & Secker-Walker,L.M. (2001) The Leukaemia Research Fund/United Kingdom Cancer Cytogenetics Group Karyotype Database in acute lymphoblastic leukaemia: a valuable resource for patient management. *Br.J.Haematol.*, **113**, 3-10.

Harrison,C.J., Moorman,A.V., Barber,K.E., Broadfield,Z.J., Cheung,K.L., Harris,R.L., Jalali,G.R., Robinson,H.M., Strefford,J.C., Stewart,A., Wright,S., Griffiths,M., Ross,F.M., Harewood,L., & Martineau,M. (2005) Interphase molecular cytogenetic screening for chromosomal abnormalities of prognostic significance in childhood acute lymphoblastic leukaemia: a UK Cancer Cytogenetics Group Study. *Br.J.Haematol.*, **129**, 520-530.

Harrison,C.J., Moorman,A.V., Broadfield,Z.J., Cheung,K.L., Harris,R.L., Reza,J.G., Robinson,H.M., Barber,K.E., Richards,S.M., Mitchell,C.D., Eden,T.O., Hann,I.M., Hill,F.G., Kinsey,S.E., Gibson,B.E., Lilleyman,J., Vora,A., Goldstone,A.H., Franklin,I.M., Durrant,J., & Martineau,M. (2004) Three distinct subgroups of hypodiploidy in acute lymphoblastic leukaemia. *Br.J.Haematol.*, **125**, 552-559.

Hattori,M., Fujiyama,A., Taylor,T.D., Watanabe,H., Yada,T., Park,H.S., Toyoda,A., Ishii,K., Totoki,Y., Choi,D.K., Groner,Y., Soeda,E., Ohki,M., Takagi,T., Sakaki,Y., Taudien,S., Blechschmidt,K., Polley,A., Menzel,U., Delabar,J., Kumpf,K., Lehmann,R., Patterson,D., Reichwald,K., Rump,A., Schillhabel,M., Schudy,A., Zimmermann,W., Rosenthal,A., Kudoh,J., Schibuya,K., Kawasaki,K., Asakawa,S., Shintani,A., Sasaki,T.,

Nagamine,K., Mitsuyama,S., Antonarakis,S.E., Minoshima,S., Shimizu,N., Nordsiek,G., Hornischer,K., Brant,P., Scharfe,M., Schon,O., Desario,A., Reichelt,J., Kauer,G., Blocker,H., Ramser,J., Beck,A., Klages,S., Hennig,S., Riesselmann,L., Dagand,E., Haaf,T., Wehrmeyer,S., Borzym,K., Gardiner,K., Nizetic,D., Francis,F., Lehrach,H., Reinhardt,R., & Yaspo,M.L. (2000) The DNA sequence of human chromosome 21. *Nature*, **405**, 311-319.

Hecht,J.L. & Aster,J.C. (2000) Molecular Biology of Burkitt's Lymphoma. *Journal of Clinical Oncology*, **18**, 3707-3721.

Heerema,N.A., Nachman,J.B., Sather,H.N., Sensel,M.G., Lee,M.K., Hutchinson,R., Lange,B.J., Steinherz,P.G., Bostrom,B., Gaynon,P.S., & Uckun,F. (1999a) Hypodiploidy with less than 45 chromosomes confers adverse risk in childhood acute lymphoblastic leukemia: a report from the children's cancer group. *Blood*, **94**, 4036-4045.

Heerema,N.A., Raimondi,S.C., Anderson,J.R., Biegel,J., Camitta,B.M., Cooley,L.D., Gaynon,P.S., Hirsch,B., Magenis,R.E., McGavran,L., Patil,S., Pettenati,M.J., Pullen,J., Rao,K., Roulston,D., Schneider,N.R., Shuster,J.J., Sanger,W., Sutcliffe,M.J., van,T.P., Watson,M.S., & Carroll,A.J. (2007) Specific extra chromosomes occur in a modal number dependent pattern in pediatric acute lymphoblastic leukemia. *Genes Chromosomes.Cancer*, **46**, 684-693.

Heerema,N.A., Sather,H.N., Sensel,M.G., La,M.K., Hutchinson,R.J., Nachman,J.B., Reaman,G.H., Lange,B.J., Steinherz,P.G., Bostrom,B.C., Gaynon,P.S., & Uckun,F.M. (2002) Abnormalities of chromosome bands 15q13-15 in childhood acute lymphoblastic leukemia 49. *Cancer*, **94**, 1102-1110.

Heerema,N.A., Sather,H.N., Sensel,M.G., Liu-Mares,W., Lange,B.J., Bostrom,B.C., Nachman,J.B., Steinherz,P.G., Hutchinson,R., Gaynon,P.S., Arthur,D.C., & Uckun,F.M. (1999b) Association of chromosome arm 9p abnormalities with adverse risk in childhood acute lymphoblastic leukemia: A report from the Children's Cancer Group. *Blood*, **94**, 1537-1544.

Heerema,N.A., Sather,H.N., Sensel,M.G., Zhang,T., Hutchinson,R.J., Nachman,J.B., Lange,B.J., Steinherz,P.G., Bostrom,B.C., Reaman,G.H., Gaynon,P.S., & Uckun,F.M. (2000) Prognostic impact of trisomies of chromosomes 10, 17, and 5 among children with acute lymphoblastic leukemia and high hyperdiploidy (> 50 chromosomes). *J.Clin.Oncol.*, **18**, 1876-1887.

Herry,A., Douet-Guilbert,N., Gueganic,N., Morel,F., Le Bris,M.J., Berthou,C., & De,B.M. (2006) Del(5q) and MLL amplification in homogeneously staining region in acute myeloblastic leukemia: a recurrent cytogenetic association. *Ann.Hematol.*, **85**, 244-249.

Hoffbrand,A.V., Catovsky,D., & Tuddenham,E.G.D. (2005) *Postgraduate Haematology,* Fith edn.

Hoffbrand,A.V. & Pettit,J.E. (1993) *Essential Haematology,* Third Edition edn, Blackwell Scientific Publications.

Hogervorst,F.B.L., Nederlof,P.M., Gille,J.J.P., McElgunn,C.J., Grippeling,M., Pruntel,R., Regnerus,R., van Welsem,T., van Spaendonk,R., Menko,F.H., Kluijt,I., Dommering,C., Verhoef,S., Schouten,J.P., van't Veer,L.J., & Pals,G. (2003) Large Genomic Deletions and Duplications in the BRCA1 Gene Identified by a Novel Quantitative Method. *Cancer Research*, **63**, 1449-1453.

Hong,D., Gupta,R., Ancliff,P., Atzberger,A., Brown,J., Soneji,S., Green,J., Colman,S., Piacibello,W., Buckle,V., Tsuzuki,S., Greaves,M., & Enver,T. (2008) Initiating and cancer-propagating cells in TEL-AML1-associated childhood leukemia
7. *Science*, **319**, 336-339.

ISCN (2005) *An International System for Human Cytogenetic Nomenclature,* 1 edn, S.Karger, Basel.

Jabber Al-Obaidi,M.S., Martineau,M., Bennett,C.F., Franklin,I.M., Goldstone,A.H., Harewood,L., Jalali,G.R., Prentice,H.G., Richards,S.M., Roberts,K., & Harrison,C.J. (2002) ETV6/AML1 fusion by FISH in adult acute lymphoblastic leukemia
1. *Leukemia*, **16**, 669-674.

Jacobs,P.A. (1981) Mutation rates of structural chromosome rearrangements in man
23. *Am.J.Hum.Genet.*, **33**, 44-54.

Jeandidier,E., Dastugue,N., Mugneret,F., Lafage-Pochitaloff,M., Mozziconacci,M.J., Herens,C., Michaux,L., Verellen-Dumoulin,C., Talmant,P., Cornillet-Lefebvre,P., Luquet,I., Charrin,C., Barin,C., Collonge-Rame,M.A., Perot,C., Van den,A.J., Gregoire,M.J., Jonveaux,P., Baranger,L., Eclache-Saudreau,V., Pages,M.P., Cabrol,C., Terre,C., & Berger,R. (2006) Abnormalities of the long arm of chromosome 21 in 107 patients with hematopoietic disorders: a collaborative retrospective study

of the Groupe Francais de Cytogenetique Hematologique 10. *Cancer Genet.Cytogenet.*, **166**, 1-11.

Johansson,B., Mertens,F., & Mitelman,F. (2004) Clinical and biological importance of cytogenetic abnormalities in childhood and adult acute lymphoblastic leukemia. *Annals of Medicine*, **36**, 492-503.

Kager,L., Cheok,M., Yang,W., Zaza,G., Cheng,Q., Panetta,J.C., Pui,C.H., Downing,J.R., Relling,M.V., & Evans,W.E. (2005) Folate pathway gene expression differs in subtypes of acute lymphoblastic leukemia and influences methotrexate pharmacodynamics. *J.Clin.Invest*, **115**, 110-117.

Kauraniemi,P. & Kallioniemi,A. (2006) Activation of multiple cancer-associated genes at the ERBB2 amplicon in breast cancer. *Endocrine-Related Cancer*, **13**, 39-49.

Kawamata,N., Ogawa,S., Zimmermann,M., Kato,M., Sanada,M., Hemminki,K., Yamatomo,G., Nannya,Y., Koehler,R., Flohr,T., Miller,C.W., Harbott,J., Ludwig,W.D., Stanulla,M., Schrappe,M., Bartram,C.R., & Koeffler,H.P. (2008) Molecular allelokaryotyping of pediatric acute lymphoblastic leukemias by high-resolution single nucleotide polymorphism oligonucleotide genomic microarray. *Blood*, **111**, 776-784.

Kempski,H.M., Chessells,J.M., & Reeves,B.R. (1997) Deletions of chromosome 21 restricted to the leukemic cells of children with Down syndrome and leukemia. *Leukemia*, **11**, 1973-1977.

Kempski,H.M., Craze,J.L., Chessells,J.M., & Reeves,B.R. (1998) Cryptic deletions and inversions of chromosome 21 in a phenotypically normal infant with transient abnormal myelopoiesis: a molecular cytogenetic study. *Br.J.Haematol.*, **103**, 473-479.

Kolomietz,E., Meyn,M.S., Pandita,A., & Squire,J.A. (2002) The role of Alu repeat clusters as mediators of recurrent chromosomal aberrations in tumors. *Genes Chromosomes.Cancer*, **35**, 97-112.

Kuchinskaya,E., Heyman,M., Nordgren,A., Schoumans,J., Staaf,J., Borg,A., Soderhall,S., Grander,D., Nordenskjold,M., & Blennow,E. (2008) Array-CGH reveals hidden gene dose changes in children with acute lymphoblastic leukaemia and a normal or failed karyotype by G-banding. *Br.J.Haematol.*, **140**, 572-577.

Kuchinskaya,E., Nordgren,A., Heyman,M., Schoumans,J., Corcoran,M., Staaf,J., Borg,A., Soderhall,S., Grander,D., Nordenskjold,M., & Blennow,E. (2007) Tiling-resolution array-CGH reveals the pattern of DNA copy number

alterations in acute lymphoblastic leukemia with 21q amplification: the result of telomere dysfunction and breakage/fusion/breakage cycles? *Leukemia*, **21**, 1327-1330.

Laverdiere,C., Chiasson,S., Costea,I., Moghrabi,A., & Krajinovic,M. (2002) Polymorphism G80A in the reduced folate carrier gene and its relationship to methotrexate plasma levels and outcome of childhood acute lymphoblastic leukemia. *Blood*, **100**, 3832-3834.

Le Coniat,M., Della Valle,V., Marynen,P., & Berger,R. (1997) A new breakpoint, telomeric to TEL/ETV6, on the short arm of chromosome 12 in T cell acute lymphoblastic leukemia. *Leukemia*, **11**, 1360-1363.

Le Coniat,M., Romana,S.P., & Berger,R. (1995) Partial chromosome 21 amplification in a child with acute lymphoblastic leukemia. *Genes Chromosomes.Cancer*, **14**, 204-209.

Leukaemia Research. (2008a). Adult acute myeloid leukaemia. Available from: http://www.lrf.org.uk/en/1/disaamhome.html

Leukaemia Research. (2008b)Childhood acute lymphoblastic leukaemia. Available from: http://www.lrf.org.uk/en/1/discalhome.html

Lo,A.W., Sprung,C.N., Fouladi,B., Pedram,M., Sabatier,L., Ricoul,M., Reynolds,G.E., & Murnane,J.P. (2002) Chromosome instability as a result of double-strand breaks near telomeres in mouse embryonic stem cells. *Mol Cell Biol.*, **22**, 4836-4850.

Ma,S.K., Wan,T.S., Cheuk,A.T., Fung,L.F., Chan,G.C., Chan,S.Y., Ha,S.Y., & Chan,L.C. (2001) Characterization of additional genetic events in childhood acute lymphoblastic leukemia with TEL/AML1 gene fusion: a molecular cytogenetics study. *Leukemia*, **15**, 1442-1447.

Marcucci,G., Maharry,K., Whitman,S.P., Vukosavljevic,T., Paschka,P., Langer,C., Mrozek,K., Baldus,C.D., Carroll,A.J., Powell,B.L., Kolitz,J.E., Larson,R.A., & Bloomfield,C.D. (2007) High expression levels of the ETS-related gene, ERG, predict adverse outcome and improve molecular risk-based classification of cytogenetically normal acute myeloid leukemia: a Cancer and Leukemia Group B Study. *J.Clin.Oncol.*, **25**, 3337-3343.

Martineau,M., Clark,R., Farrell,D.M., Hawkins,J.M., Moorman,A.V., & Secker-Walker,L.M. (1996) Isochromosomes in Acute Lymphoblastic Leukaemia: i(21q) is a Significant Finding. *Genes Chromosomes Cancer*, **17**, 21-30.

Maser,R.S. & Depinho,R.A. (2004) Telomeres and the DNA damage response: why the fox is guarding the henhouse. *DNA Repair (Amst)*, **3**, 979-988.

McClintock,B. The Stability of broken ends of chromosomes in Zea Mays. Genetics 26, 234-282. 1941.
Ref Type: Generic

Mikhail,F.M., Serry,K.A., Hatem,N., Mourad,Z.I., Farawela,H.M., El Kaffash,D.M., Coignet,L., & Nucifora,G. (2002) AML1 gene over-expression in childhood acute lymphoblastic leukemia. *Leukemia*, **16**, 658-668.

Mikhail,F.M., Sinha,K.K., Saunthararajah,Y., & Nucifora,G. (2006) Normal and transforming functions of RUNX1: a perspective
5. *J.Cell Physiol*, **207**, 582-593.

Mikhail,F.M., Sinha,K.K., Saunthararajah,Y., & Nucifora,G. (2005) Normal and transforming functions of RUNX1: A perspective. *J.Cell Physiol*.

Miller,C.T., Lin,L., Casper,A.M., Lim,J., Thomas,D.G., Orringer,M.B., Chang,A.C., Chambers,A.F., Giordano,T.J., Glover,T.W., & Beer,D.G. (2006) Genomic amplification of MET with boundaries within fragile site FRA7G and upregulation of MET pathways in esophageal adenocarcinoma. *Oncogene*, **25**, 409-418.

Mitelman Database of Chromosomal Abnormlaities in Cancer. Mitelman Database of Chromosome Aberrations in Cancer. Mitelman Database of Chromosome Aberrations in Cancer . 2008.
Ref Type: Electronic Citation

Mitelman,F., Johansson,B., & Mertens,F. (2007) The impact of translocations and gene fusions on cancer causation
1. *Nat.Rev.Cancer*, **7**, 233-245.

Miyoshi,H., Shimizu,K., Kozu,T., Maseki,N., Kaneko,Y., & Ohki,M. (1991) t(8;21) Breakpoints on Chromosome 21 in Acute Myeloid Leukemia are Clustered within a Limited Region of a Single Gene, AML1. *Proceedings of the National Academy of Sciences*, **88**, 10431-10434.

Moorman,A.V., Clark,R., Farrell,D.M., Hawkins,J.M., Martineau,M., & Secker-Walker,L.M. (1996) Probes for hidden hyperdiploidy in acute lymphoblastic leukaemia. *Genes Chromosomes and Cancer*, **16**, 40-45.

Moorman,A.V., Harrison,C.J., Buck,G.A., Richards,S.M., Secker-Walker,L.M., Martineau,M., Vance,G.H., Cherry,A.M., Higgins,R.R., Fielding,A.K.,

Foroni,L., Paietta,E., Tallman,M.S., Litzow,M.R., Wiernik,P.H., Rowe,J.M., Goldstone,A.H., & Dewald,G.W. (2007a) Karyotype is an independent prognostic factor in adult acute lymphoblastic leukemia (ALL): analysis of cytogenetic data from patients treated on the Medical Research Council (MRC) UKALLXII/Eastern Cooperative Oncology Group (ECOG) 2993 trial. *Blood*, **109**, 3189-3197.

Moorman,A.V., Richards,S.M., Martineau,M., Cheung,K.L., Robinson,H.M., Jalali,G.R., Broadfield,Z.J., Harris,R.L., Taylor,K.E., Gibson,B.E., Hann,I.M., Hill,F.G., Kinsey,S.E., Eden,T.O., Mitchell,C.D., & Harrison,C.J. (2003) Outcome heterogeneity in childhood high-hyperdiploid acute lymphoblastic leukemia. *Blood*, **102**, 2756-2762.

Moorman,A.V., Richards,S.M., Robinson,H.M., Strefford,J.C., Gibson,B.E., Kinsey,S.E., Eden,T.O., Vora,A.J., Mitchell,C.D., & Harrison,C.J. (2007b) Prognosis of children with acute lymphoblastic leukemia (ALL) and intrachromosomal amplification of chromosome 21 (iAMP21) 8. *Blood*, **109**, 2327-2330.

Morison,I.M., Ellis,L.M., Teague,L.R., & Reeve,A.E. (2002) Preferential loss of maternal 9p alleles in childhood acute lymphoblastic leukemia 1. *Blood*, **99**, 375-377.

Mullighan,C.G., Goorha,S., Radtke,I., Miller,C.B., Coustan-Smith,E., Dalton,J.D., Girtman,K., Mathew,S., Ma,J., Pounds,S.B., Su,X., Pui,C.H., Relling,M.V., Evans,W.E., Shurtleff,S.A., & Downing,J.R. (2007) Genome-wide analysis of genetic alterations in acute lymphoblastic leukaemia. *Nature*, **446**, 758-764.

Murnane,J.P. (2006) Telomeres and chromosome instability. *DNA Repair (Amst)*, **5**, 1082-1092.

Murnane,J.P. & Sabatier,L. (2004) Chromosome rearrangements resulting from telomere dysfunction and their role in cancer. *Bioessays*, **26**, 1164-1174.

Myllykangas,S. & Knuutila,S. (2006) Manifestation, mechanisms and mysteries of gene amplifications. *Cancer Lett.*, **232**, 79-89.

Najfeld,V., Lai,J., Scalise,A., Guarini,L., & Lipton,J.M. (1998) Amplification of q22 chromosomal region of chromosome 21, including AML-1 gene, is a clonal marker in pediatric patients with acute lymphoblastic leukemia (ALL). *Blood*, **92**, 396A.

Niebuhr,B., Fischer,M., Tager,M., Cammenga,J., & Stocking,C. (2008) Gatekeeper function of the RUNX1 transcription factor in acute leukemia 2. *Blood Cells Mol.Dis.*, **40**, 211-218.

Niini,T., Kanerva,J., Vettenranta,K., Saarinen-Pihkala,U.M., & Knuutila,S. (2000) AML1 gene amplification: a novel finding in childhood acute lymphoblastic leukemia. *Haematologica*, **85**, 362-366.

Nowell,P.C. & Hungerford,D.A. (1961) Chromosome studies in human leukemia. II. Chronic granulocytic leukemia. *J.Natl.Cancer Inst.*, **27**, 1013-1035.

Nucifora,G., Begy,C.R., Erickson,P., Drabkin,H.A., & Rowley,J.D. (1993) The 3;21 translocation in myelodysplasia results in a fusion transcript between the AML1 gene and the gene for EAP, a highly conserved protein associated with the Epstein-Barr virus small RNA EBER 1. *Proc.Natl.Acad.Sci.U.S.A*, **90**, 7784-7788.

Osato,M., Asou,N., Abdalla,E., Hoshino,K., Yamasaki,H., Okubo,T., Suzushima,H., Takatsuki,K., Kanno,T., Shigesada,K., & Ito,Y. (1999) Biallelic and heterozygous point mutations in the runt domain of the AML1/PEBP2alphaB gene associated with myeloblastic leukemias. *Blood*, **93**, 1817-1824.

Ottmann,O.G., Druker,B.J., Sawyers,C.L., Goldman,J.M., Reiffers,J., Silver,R.T., Tura,S., Fischer,T., Deininger,M.W., Schiffer,C.A., Baccarani,M., Gratwohl,A., Hochhaus,A., Hoelzer,D., Fernandes-Reese,S., Gathmann,I., Capdeville,R., & O'Brien,S.G. (2002) A phase 2 study of imatinib in patients with relapsed or refractory Philadelphia chromosome-positive acute lymphoid leukemias. *Blood*, **100**, 1965-1971.

Owen,C., Barnett,M., & Fitzgibbon,J. (2008) Familial myelodysplasia and acute myeloid leukaemia--a review 5. *Br.J.Haematol.*, **140**, 123-132.

Papenhausen,P.R., Griffin,S., & Tepperberg,J. (2005) Oncogene amplification in transforming myelodysplasia. *Exp.Mol.Pathol.*, **79**, 168-175.

Parker,H., Cheung,K.L., Robinson,H.M., Harrison,C.J., & Strefford,J.C. (2008) Cytogenetic and genomic characterization of cell line ARH77 1. *Cancer Genet.Cytogenet.*, **181**, 40-45.

Penther,D., Preudhomme,C., Talmant,P., Roumier,C., Godon,A., Mechinaud,F., Milpied,N., Bataille,R., & vet-Loiseau,H. (2002) Amplification of AML1 gene is present in childhood acute lymphoblastic leukemia but not in

adult, and is not associated with AML1 gene mutation 6. *Leukemia*, **16**, 1131-1134.

Perez-Vera,P., Montero-Ruiz,O., Frias,S., Rivera-Luna,R., Valladares,A., Arenas,D., Paredes-Aguilera,R., & Carnevale,A. (2008) Multiple copies of RUNX1: description of 14 new patients, follow-up, and a review of the literature. *Cancer genetics and cytogenetics*, **180**, 129-134.

Pierotti,M., Sozzi,G., & Croce,C. (2003) Oncogenes. **Cancer Medicine** (ed. by D. W. Kufe, R. E. Pollock, R. R. Weichselbaum, R. C. Bast, Jr., T. S. Gansler, & J. F. Holland) BC Decker Inc, Hamilton.

Pinkel,D. & Albertson,D.G. (2005) Array comparative genomic hybridization and its applications in cancer. *Nat.Genet.*, **37 Suppl**, S11-S17.

Pinkel,D., Segraves,R., Sudar,D., Clark,S., Poole,I., Kowbel,D., Collins,C., Kuo,W.L., Chen,C., Zhai,Y., Dairkee,S.H., Ljung,B.M., Gray,J.W., & Albertson,D.G. (1998) High resolution analysis of DNA copy number variation using comparative genomic hybridization to microarrays. *Nat.Genet.*, **20**, 207-211.

Pinson,M.P., Martineau,M., Jabbar,M.S., Kilby,A.M., Walker,H., & Harrison,C.J. (2000) Sequential FISH reveals an abnormal karyotype involving 14 chromosomes in a child with acute lymphoblastic leukemia 1. *Leukemia*, **14**, 1705-1707.

Podgornik,H., Debeljak,M., Zontar,D., Cernelc,P., Prestor,V.V., & Jazbec,J. (2007) RUNX1 amplification in lineage conversion of childhood B-cell acute lymphoblastic leukemia to acute myelogenous leukemia. *Cancer genetics and cytogenetics*, **178**, 77-81.

Pui,C.H. (2000) Acute lymphoblastic leukemia in children. *Curr.Opin.Oncol.*, **12**, 3-12.

Pui,C.H. & Evans,W.E. (2006) Treatment of acute lymphoblastic leukemia. *N.Engl J Med*, **354**, 166-178.

Pui,C.H. & Evans,W.E. (1998) Acute lymphoblastic leukemia. *N.Engl.J.Med.*, **339**, 605-615.

Pui,C.H., Relling,M.V., & Downing,J.R. (2004) Acute lymphoblastic leukemia. *N.Engl.J.Med.*, **350**, 1535-1548.

Raghavan,M., Lillington,D.M., Skoulakis,S., Debernardi,S., Chaplin,T., Foot,N.J., Lister,T.A., & Young,B.D. (2005) Genome-Wide Single Nucleotide

Polymorphism Analysis Reveals Frequent Partial Uniparental Disomy Due to Somatic Recombination in Acute Myeloid Leukemias. *Cancer Research*, **65**, 375-378.

Raimondi,S.C. (2006) Cytogenetics of acute leukemias. Childhood Leukemias (ed. by C. H. Pui), pp. 235-271. Cambridge University Press, Cambridge.

Raimondi,S.C., Pui,C.H., Head,D., Behm,F., Privitera,E., Roberson,P.K., Rivera,G.K., & Williams,D.L. (1992) Trisomy 21 as the sole acquired chromosomal abnormality in children with acute lymphoblastic leukemia. *Leukemia*, **6**, 171-175.

Raimondi,S.C., Zhou,Y., Mathew,S., Shurtleff,S.A., Sandlund,J.T., Rivera,G.K., Behm,F.G., & Pui,C.H. (2003) Reassessment of the prognostic significance of hypodiploidy in pediatric patients with acute lymphoblastic leukemia. *Cancer*, **98**, 2715-2722.

Robinson,H.M., Broadfield,Z.J., Cheung,K.L., Harewood,L., Harris,R.L., Jalali,G.R., Martineau,M., Moorman,A.V., Taylor,K.E., Richards,S., Mitchell,C., & Harrison,C.J. (2003) Amplification of AML1 in acute lymphoblastic leukemia is associated with a poor outcome. *Leukemia*, **17**, 2249-2250.

Robinson,H.M., Harrison,C.J., Moorman,A.V., Chudoba,I., & Strefford,J.C. (2007) Intrachromosomal amplification of chromosome 21 (iAMP21) may arise from a breakage-fusion-bridge cycle. *Genes Chromosomes.Cancer*, **46**, 318-326.

Romana,S.P., Le Coniat,M., & Berger,R. (1994) t(12;21): a new recurrent translocation in acute lymphoblastic leukemia. *Genes Chromosomes.Cancer*, **9**, 186-191.

Romana,S.P., Poirel,H., Leconiat,M., Flexor,M.A., Mauchauffe,M., Jonveaux,P., Macintyre,E.A., Berger,R., & Bernard,O.A. (1995) High frequency of t(12;21) in childhood B-lineage acute lymphoblastic leukemia 31. *Blood*, **86**, 4263-4269.

Roumier,C., Fenaux,P., Lafage,M., Imbert,M., Eclache,V., & Preudhomme,C. (2003) New mechanisms of AML1 gene alteration in hematological malignancies. *Leukemia*, **17**, 9-16.

Rubnitz,J.E., Downing,J.R., Pui,C.H., Shurtleff,S.A., Raimondi,S.C., Evans,W.E., Head,D.R., Crist,W.M., Rivera,G.K., Hancock,M.L., Boyett,J.M., Buijs,A., Grosveld,G., & Behm,F.G. (1997) TEL gene rearrangement in acute

lymphoblastic leukemia: a new genetic marker with prognostic significance. *J.Clin.Oncol.*, **15**, 1150-1157.

Sabatier,L., Ricoul,M., Pottier,G., & Murnane,J.P. (2005) The loss of a single telomere can result in instability of multiple chromosomes in a human tumor cell line. *Mol.Cancer Res.*, **3**, 139-150.

Schouten,J.P., McElgunn,C.J., Waaijer,R., Zwijnenburg,D., Diepvens,F., & Pals,G. (2002) Relative quantification of 40 nucleic acid sequences by multiplex ligation-dependent probe amplification. *Nucleic Acids Res.*, **30**, e57.

Secker-Walker,L.M. (1997) *Chromosomes and Genes in Acute Lymphoblastic Leukemia,* Chapman & Hall, New York.

Secker-Walker,L.M., Lawler,S.D., & Hardisty,R.M. (1978) Prognostic implications of chromosomal findings in acute lymphoblastic leukaemia at diagnosis. *British Medical Journal*, **2**, 1529-1530.

Song,W.J., Sullivan,M.G., Legare,R.D., Hutchings,S., Tan,X., Kufrin,D., Ratajczak,J., Resende,I.C., Haworth,C., Hock,R., Loh,M., Felix,C., Roy,D.C., Busque,L., Kurnit,D., Willman,C., Gewirtz,A.M., Speck,N.A., Bushweller,J.H., Li,F.P., Gardiner,K., Poncz,M., Maris,J.M., & Gilliland,D.G. (1999) Haploinsufficiency of CBFA2 causes familial thrombocytopenia with propensity to develop acute myelogenous leukaemia. *Nat.Genet.*, **23**, 166-175.

Soulier,J., Trakhtenbrot,L., Najfeld,V., Lipton,J.M., Mathew,S., vet-Loiseau,H., De,B.M., Salem,S., Baruchel,A., Raimondi,S.C., & Raynaud,S.D. (2003) Amplification of band q22 of chromosome 21, including AML1, in older children with acute lymphoblastic leukemia: an emerging molecular cytogenetic subgroup. *Leukemia*, **17**, 1679-1682.

Spector,L.G., Ross,J.A., Robinson,L.L., & Bhatia Smita (2006) Epidemiology and etiology. Childhood Leukaemias (ed. by C. H. Pui), pp. 48-66.

Strefford,J.C., van Delft,F.W., Robinson,H.M., Worley,H., Yiannikouris,O., Selzer,R., Richmond,T., Hann,I., Bellotti,T., Raghavan,M., Young,B.D., Saha,V., & Harrison,C.J. (2006) Complex genomic alterations and gene expression in acute lymphoblastic leukemia with intrachromosomal amplification of chromosome 21. *Proc.Natl.Acad.Sci.U.S.A*, **103**, 8167-8172.

Strefford,J.C., Worley,H., Barber,K., Wright,S., Stewart,A.R.M., Robinson,H.M., Bettney,G., van Delft,F.W., Atherton,M.G., Davies,T., Griffiths,M., Hing,S., Ross,F.M., Talley,P., Saha,V., Moorman,A.V., & Harrison,C.J. (2007)

Genome complexity in acute lymphoblastic leukemia is revealed by array-based comparative genomic hybridization. *Oncogene,* **26**, 4306-4318.

Sun,W. & Downing,J.R. (2004) Haploinsufficiency of AML1 results in a decrease in the number of LTR-HSCs while simultaneously inducing an increase in more mature progenitors. *Blood*, **104**, 3565-3572.

Sutcliffe,M.J., Shuster,J.J., Sather,H.N., Camitta,B.M., Pullen,J., Schultz,K.R., Borowitz,M.J., Gaynon,P.S., Carroll,A.J., & Heerema,N.A. (2005) High concordance from independent studies by the Children's Cancer Group (CCG) and Pediatric Oncology Group (POG) associating favorable prognosis with combined trisomies 4, 10, and 17 in children with NCI Standard-Risk B-precursor Acute Lymphoblastic Leukemia: a Children's Oncology Group (COG) initiative. *Leukemia*, **19**, 734-740.

Takeuchi,S., Bartram,C.R., Seriu,T., Miller,C.W., Tobler,A., Janssen,J.W., Reiter,A., Ludwig,W.D., Zimmermann,M., & Schwaller,J. (1995) Analysis of a family of cyclin-dependent kinase inhibitors: p15/MTS2/INK4B, p16/MTS1/INK4A, and p18 genes in acute lymphoblastic leukemia of childhood. *Blood*, **86**, 755-760.

Tanaka,H., Bergstrom,D.A., Yao,M.C., & Tapscott,S.J. (2005) Widespread and nonrandom distribution of DNA palindromes in cancer cells provides a structural platform for subsequent gene amplification. *Nat.Genet.*, **37**, 320-327.

Tanaka,H., Cao,Y., Bergstrom,D.A., Kooperberg,C., Tapscott,S.J., & Yao,M.C. (2007) Intrastrand annealing leads to the formation of a large DNA palindrome and determines the boundaries of genomic amplification in human cancer. *Mol.Cell Biol.*, **27**, 1993-2002.

Varley,H., Di,S., Scherer,S.W., & Royle,N.J. (2000) Characterization of terminal deletions at 7q32 and 22q13.3 healed by De novo telomere addition. *Am.J.Hum.Genet.*, **67**, 610-622.

Viguie,F., Aboura,A., Bouscary,D., Guesnu,M., Baumelou,E., Dreyfus,F., Casadevall,N., & Tachdjian,G. (2002) Isodicentric/pseudoisodicentric chromosome 21 amplification in four cases of acute myelocytic leukemia or myelodysplasia. *Cancer genetics and cytogenetics*, **138**, 80-84.

Watanabe,T. & Horiuchi,T. (2005) A novel gene amplification system in yeast based on double rolling-circle replication. *The EMBO Journal*, **24**, 190-198.

Wood,R.D., Mitchell,M., & Lindahl,T. (2005) Human DNA repair genes, 2005. *Mutation Research/Fundamental and Molecular Mechanisms of Mutagenesis*, **577**, 275-283.

Complex genomic alterations and gene expression in acute lymphoblastic leukemia with intrachromosomal amplification of chromosome 21

Jon C. Strefford*[†‡], Frederik W. van Delft[†§¶], Hazel M. Robinson*, Helen Worley*, Olga Yiannikouris[§¶], Rebecca Selzer[‖], Todd Richmond[‖], Ian Hann**, Tony Bellotti[††], Manoj Raghavan[¶], Bryan D. Young[¶], Vaskar Saha[†§¶], and Christine J. Harrison*[†]

*Leukaemia Research Cytogenetics Group, Cancer Sciences Division, University of Southampton, Southampton SO16 6YD, United Kingdom; [§]Cancer Research UK Children's Cancer Group and [¶]Medical Oncology Unit, Institute of Cancer, Queen Mary University of London, London E1 4NS, United Kingdom; [‖]NimbleGen Systems, Inc., Madison, WI 53711; **Department of Haematology, Great Ormond Street Hospital for Children NHS Trust, London WC1N 3JH, United Kingdom; and [††]Computer Learning Research Centre, Royal Holloway, University of London, Egham, Surrey TW20 0EX, United Kingdom

We have previously identified a unique subtype of acute lymphoblastic leukemia (ALL) associated with a poor outcome and characterized by intrachromosomal amplification of chromosome 21 including the *RUNX1* gene (iAMP21). In this study, array-based comparative genomic hybridization (aCGH) (*n* = 10) detected a common region of amplification (CRA) between 33.192 and 39.796 Mb and a common region of deletion (CRD) between 43.7 and 47 Mb in 100% and 70% of iAMP21 patients, respectively. High-resolution genotypic analysis (*n* = 3) identified allelic imbalances in the CRA. Supervised gene expression analysis showed a distinct signature for eight patients with iAMP21, with 10% of overexpressed genes located within the CRA. The mean expression of these genes was significantly higher in iAMP21 when compared to other ALL samples (*n* = 45). Although genomic copy number correlated with overall gene expression levels within areas of loss or gain, there was considerable individual variation. A unique subset of differentially expressed genes, outside the CRA and CRD, were identified when gene expression signatures of iAMP21 were compared to ALL samples with *ETV6-RUNX1* fusion (*n* = 21) or high hyperdiploidy with additional chromosomes 21 (*n* = 23). From this analysis, *LGMN* was shown to be overexpressed in patients with iAMP21 (*P* = 0.0012). Genomic and expression data has further characterized this ALL subtype, demonstrating high levels of 21q instability in these patients leading to proposals for mechanisms underlying this clinical phenotype and plausible alternative treatments.

array CGH | expression profiling | RUNX1 | iAMP21 | genomic instability

We have recently defined a recurrent chromosomal abnormality at an incidence of 1.5% in childhood B-lineage acute lymphoblastic leukemia (ALL) involving intrachromosomal duplication of chromosome 21 and amplification of the *RUNX1* (*AML1*) gene (iAMP21) (1). These patients have a median age of 9 years, a low presenting white blood cell count, and a poor prognosis (2). Thus, on the current U.K. ALL treatment protocol, ALL 2003, these children are classified as high-risk and receive more intensive treatment. iAMP21 was identified on routine screening of childhood ALL patients for the *ETV6-RUNX1* (*TEL-AML1*) fusion by fluorescence *in situ* hybridization (FISH). Although negative for the fusion, leukemic cells showed multiple *RUNX1* signals, seen as clusters in interphase and in tandem duplication on the long arm of an abnormal chromosome 21 in metaphase. This abnormality cannot be defined by conventional cytogenetic analysis because the abnormal chromosome 21 adopts a range of different morphological forms. FISH with probes directed to the *RUNX1* gene is currently the only detection method, which explains its prior description as "amplification of *RUNX1*." However, there are several reasons why FISH detection, based solely on *RUNX1* copy number, may be inappropriate. First, interpretation may be mis-

leading, particularly in patients with a hidden high hyperdiploid clone comprising several copies of chromosome 21 (3). Second, because the observed increase in *RUNX1* copy number was serendipitous, it may not be the causative mechanism. In view of the high-risk associated with iAMP21, it is important to fully characterize this abnormality to provide accurate diagnosis, particularly for ALL patients without any other high-risk clinical features.

Similar chromosome 21 amplifications have been reported in patients with acute myeloid leukemia (AML) and myelodysplastic syndrome (4–9). The most recent AML study, using BAC array-based comparative genomic hybridization (BAC aCGH), identified two common regions of amplification on 21q in 12 patients. These were at 25–30 Mb and 38.7–39.1 Mb. Oligonucleotide expression analysis revealed that most significantly overexpressed genes were located within these amplicons, implying that the changes in gene expression were entirely related to alterations in copy number (5). Similar gene expression analyses from children with high hyperdiploid ALL (10) and Down syndrome (11) have suggested that additional copies of chromosome 21 lead to overexpression of genes on chromosome 21. By using a variety of classical and innovative molecular techniques, we have been able to characterize the iAMP21 in patients with ALL and, in so doing, provide a plausible alternative therapeutic approach.

Results and Discussion

In this study, we have validated the existence of the chromosomal abnormality iAMP21 in childhood ALL and characterized the rearrangement using whole genome analyses. Genome-wide BAC aCGH showed genomic imbalances in all 10 patients with iAMP21 analyzed. Patterns of imbalance corresponding to over- and under-representation of specific regions of chromosome 21 were unique to each patient (Table 1). Although all BAC clones on chromosome 21 showed gain in at least one patient, these gains most frequently involved clones between genomic positions 22.1 and 27.8 Mb (clones RP11-64I12 to RP11-90A12). The size of the most highly amplified region varied considerably between patients, from 3–8.6 to 24.0–24.1 Mb for patients 6783 and 6788, respectively. However, a common region of amplification (CRA) of ≈8.6 Mb, between clones RP11-191I6 and RP5-206A10 (genomic positions 31.5 and 40.1 Mb, respectively), was identified in all 10 patients, which was accompanied by deletions of 21q in seven patients. With the

MEDICAL SCIENCES

Table 1. BAC aCGH and FISH results for 10 ALL patients with iAMP21

Gene	BAC clone	Clone position, in Mb	3698*	4279*	4414#	5898*#	6111#	6783#	6788*#	6957*	7219*	7255*	6899	6009
STCH	RP5-153I22	15.1		0		-1		+2	0	0	+2	+1	0	+2
USP25	RP11-89M24	15.7												
PRSS7	RP11-15E10	18.7		0		-1		0	0	0	+3	0	0	+2
	RP11-375O2	19.3		+1		-1		0	0	0	+3	-1	0	+2
	RP11-49B5	20.3		0		-1		0	+1			+1	0	+2
	RP11-49J9	21.1												
NCAM2	RP11-64I12	22.1		+1		+1		0	+1	+1	0	+1	0	+2
	RP11-97F14	22.9		2		+1		0	+1	+1	+1	+1	0	+2
	RP11-80N20	24		+1		+1		+1	+3	+3	+5	+4	0	+2
	RP11-13J15	24.1		+1		+1		+1	+3	+3	+4	+5	0	+2
GABPA	RP11-88D18	25.5		+2		+1		0	+3	+3	+4	+3	0	+2
APP	RP11-15H6	26.7		+2		+1		+1	+3	+3	+5	+6	0	+2
	RP11-90A17	27.8		+1				+3	+3	+3	+4	+4	0	+2
N6AMT1	RP11-79G23	29.4		+1		+3		0	+3	+3	+4	+5	0	+2
GRIK1	RP11-30N6	29.8		+1		+3		0	+3	+3	+5	+5	0	+2
TIAM1	RP11-191I6	31.5		+4		+3		+1	+3	+3	+5	+5	0	+2
HUNK:SOD1	RP11-147H1	32.3		+5		+3		+3	+3	+3	+5	+5	0	+2
OLIG2;IFNAR2;IL10RB	RP11-79D9	33.3		+3		+3		+3	+3	+3	+5	+5	0	+2
KCNE2;CLIC6;CRYZL1	RP11-79A12	34.7		+3		+3		+3	+3	+3	+5	+5	0	+2
RUNX1;ERG;TTC3;ETS2	RP11-17O20	35.3											0	+2
PCP4	RP5-206A10	40.1		+3		+3		+1	+4	+3	+2	+2	0	+2
DSCAM	RP11-114H1	41.2		+4		+3		+2	+3	+3	-1	0	0	+2
MX2;MX1	RP11-120C17	41.7		+3		+3		+2	+3	+4	-1	0	0	+2
HSF2BP	RP11-88N2	43.7		-1		-1		+2	+3	+4	-1	+1	0	+2
PCNT2;DIP2	P1-2H14	46.7												
HRMT1L1	RP1-63H24	46.9		-1		-1		0	+3	-1	-1	0	0	+2

DNA copy number changes compared to normal control DNA								
NR	<0.8	<SDL-0.8	within SDL	>SDL-1.2	1.2-1.5	1.5-2.0	2.0-3.0	3.0-4.0

Gains (green) and losses (red) of 21q material detected by BAC aCGH. Yellow regions correspond to those areas exhibiting fluorescent ratios within standard deviation limits (SDL). Ratio values were unavailable on several samples due to a lack of material, and on certain DNA clones due to poor ratio measurements. Where FISH was carried out, results are shown numerically as deviations from a normal copy number of 2. The asterisks indicate cases studied for gene expression by oligonucleotide array. The # indicates those cases used for further genomic profiling with Oligo aCGH array analysis. Cases 6899 and 6009 are ALL patients with an apparently normal and high hyperdiploid (tetrasomy 21) karyotype, respectively.

exception of one within the centromeric region (from 15.1–20.3 Mb in patient 5898), all deletions included a common region of deletion (CRD) of ≈4 Mb close to the telomere. In three patients with iAMP21, imbalances of 21q were the sole genomic changes at 1-Mb resolution. Among the other patients, no recurrent changes involving chromosomes other than 21 were identified. (Table 3, which is published as supporting information on the PNAS web site). To prove the validity of aCGH, the presence of an entire additional copy of chromosome 21 was verified in seven patients with high hyperdiploidy and additional copies of chromosome 21 (HD + 21) (example, patient 6009) (Table 1). Furthermore, no changes in copy number were observed among 50 patients with apparently normal copies of chromosome 21 (example, patient 6899) (Table 1). FISH analysis confirmed the variation in copy number along 21q in the cases analyzed by BAC aCGH (Table 1 and Fig. 1 A and B). FISH identified the same CRA and CRD. The high concordance between the two procedures indicated the accuracy of BAC aCGH in the determination of copy number changes, whereas FISH analysis provided precise quantification. Between three and eight additional copies of the clones within the CRA were demonstrated by FISH, indicating a 2.5–5 fold gain. FISH data on copy number changes in

an additional three patients with iAMP21 provided further confirmation of the BAC aCGH results (data not included). Using tiling-path Oligo aCGH (Fig. 1C), the extent of the CRA was refined to a region of 6.527–6.604 Mb in size (between genomic positions 33.192 and 39.796 Mb) in five patients, whereas the CRD was refined to 3.541 Mb. High-resolution genotype array analysis of single-nucleotide polymorphisms (SNP analysis) was performed on three patients for whom both diagnostic and remission samples were available, permitting comparison of germ-line and tumor genotypes (examples are shown in Fig. 3, which is published as supporting information on the PNAS web site). These analyses identified the same regions of genomic gain and loss of heterozygosity within the CRA and CRD.

Combining the results from these genomic analyses has highlighted regions of variable gain along 21q in patients with iAMP21 and identified a CRA covering a large genomic region of 6 Mb, containing the RUNX1 gene. This CRA was found to be telomeric of the first of the two amplified regions described for AML (25–30 Mb) but overlapping with the second (38.7–39.1 Mb) (5). The majority of patients showed a 3.5-Mb CRD, telomeric of the CRA. The SNP data suggested that the amplification was derived from a
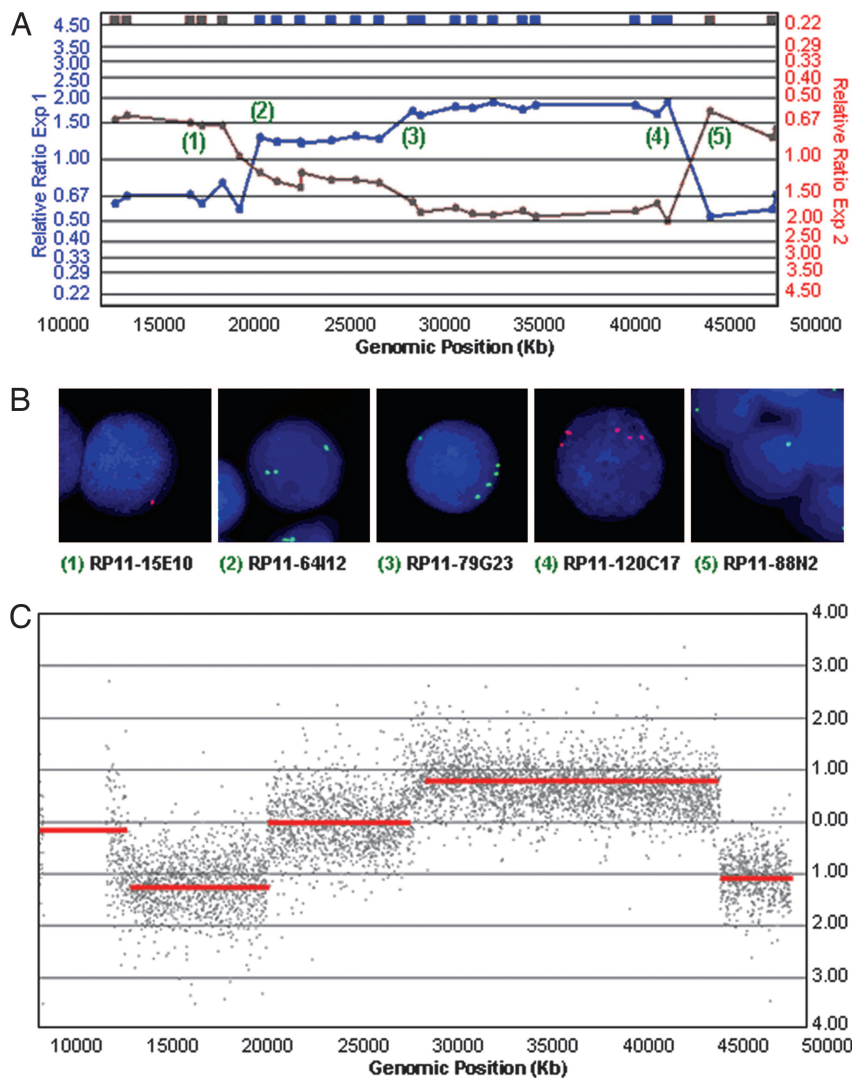
Fig. 1. Genomic analysis of DNA and cell suspension from patient 5989. (*A*) BAC aCGH results: chromosome 21 is positioned horizontally, with the centromeric to telomeric positions running from left to right, respectively. Dye swap experiments 1 and 2 are shown by the blue and red lines, respectively. Double deviation of both these experiments from a normal value of 1.00 demonstrates loss or gain of DNA material. Deviation of the red and blue line >1.00 shows loss or gain of copy number, respectively. (*B*) Examples of the FISH confirmation of aCGH data: each numbered FISH probe corresponds to the same highlighted clone in *A*. (*C*) Oligo aCGH data for this patient. Chromosome 21 is positioned as in *A*. The scatter plot demonstrates mean log intensity ratios at 5,000-bp intervals along chromosome 21. Segmentation analysis is shown as red horizontal lines.

single chromosome. Overall, the results indicated the highly variable nature of this abnormality, reflecting considerable instability of chromosome 21, thus making it difficult to determine the causative event.

Global gene expression profiling, using the Affymetrix U133A oligonucleotide array containing 22,283 probes sets, was performed on eight patients with aCGH results. The CRA was represented on this Affymetrix GeneChip by 96 probe sets in total, including 40 well characterized genes and six ORFs. The genes located within the CRA and CRD are indicated in Tables 4 and 5, which are published as supporting information on the PNAS web site. From a total of 768 probe sets within the CRA, 321 (42%) were present (or marginal) and up-regulated (Fig. 4, which is published as supporting information on the PNAS web site). Of the 46 sequences from the genes and ORF, 13 were up-regulated in at least 75% of patients. The CRD was represented on the GeneChip by 83 probe sets, containing 33 genes, three ORFs, and three ESTs. From a total of 664 probe sets, 462 (70%) were absent. An absent flag was carried in 22 of these 39 gene sequences in at least 75% of patients. When compared to all children with ALL (*n* = 89) from our previously reported analysis (12), 14 (10%) of the top 150 genes significantly overexpressed in patients with iAMP21 were located within the CRA, for which there was a strong correlation with the Taqman data (Table 6, which is published as supporting information on the PNAS web site). As shown in Table 4, 51 (53%) of the 96 probe sets

within the CRA had a 1.5-fold increase in expression. This observation suggested that overexpression of these genes corresponded to the gain of genomic material. However, it was noted that 47% of the probe sets from the CRA were not overexpressed. To examine the effect of the gain of chromosomal material more closely, we calculated the mean and median expression of the genes within the CRA in the eight iAMP21 and six patients with other subtypes of ALL (Fig. 2*A*). The mean expression levels of the genes contained within the CRA was higher in patients with iAMP21 (*t* test, *P* = 0.00903) and those with HD + 21 (*t* test, *P* = 2.02e-7) compared with the other subtypes. These observations support previous reports demonstrating that large-scale genomic alteration does result in changes in expression of genes within these regions (13, 14), but we could not correlate all gene expression changes with alteration at the genomic copy level. There was no linear correlation between the degree of amplification and expression; this may have arisen from heterogeneity of amplification within the region or other regulatory mechanisms influencing gene expression, such as epigenetics and biofeedback regulation. We have recently reported partial acquired isodisomy in patients with AML (15), whereas others have reported disomy of chromosome 21 in cases of Down syndrome and ALL (16). Thus, it is plausible that this type of mechanism may contribute to variations in expression.

Like the AML study (5), our work showed differential expression of genes located outside the CRA, leading to expression variation
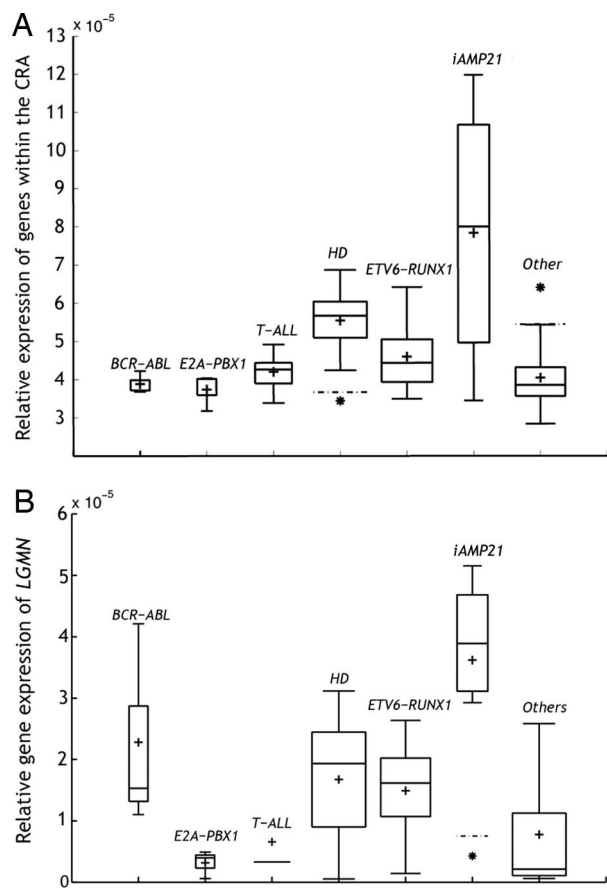
Fig. 2. Box plot diagrams illustrating LGMN expression (*A*) and expression of those genes within the CRA (*B*), compared to other ALL subtypes. On the *x* axis are shown seven ALL subtypes, *BCR-ABL*, *E2A-PBX1*, T-ALL, HD + 21, *ETV6-RUNX1*, iAMP21, and others. The *y* axis represents the relative gene expression level of either *LGMN* or all those genes within the CRA. Each box plot shows the distribution of expression levels from 25th to 75th percentile. The median is shown as a line across the box, whereas the + is the calculated mean expression level for the particular subtype. The dotted line indicates the inner fence, and a value outside the outer fence is shown as an asterisk.

of many genes unassociated with, but flanking genes important in cancer pathogenesis. However, these genes were not consistent between patients. When the expression profiles from patients with iAMP21 were compared to the original cohort of 89 pediatric ALL patients (12) in an unsupervised analysis, the patients with iAMP21 did not cluster together (data not shown). Due to correlation between gene expression and loss or gain of chromosomal material, a supervised cluster analysis was carried out to take into consideration that expression profiles were influenced by ALL samples with rearrangements and gains of chromosome 21. The global gene expression profiling of the eight iAMP21 patients was compared: to the full cohort ($n = 89$); to a subgroup of patients with the *ETV6-RUNX1* fusion ($n = 21$); and to a subgroup of patients with HD + 21 ($n = 23$). When the gene list was compiled in this manner, patients with iAMP21 exhibited a distinctive expression pattern (Fig. 4). Using SAM, with a cutoff level for false discovery rate (FDR) of 10%, the three comparisons yielded 4,174, 4,768, and 5,147 probe sets, respectively. The top 150 probe sets (FDR = 5.3%) were used for comparison against other ALL samples, and the top 100 for comparisons against patients with the *ETV6-RUNX1* fusion (FDR = 0.54%) and HD + 21 (FDR = 0.81%). The gene lists with full annotation are presented in the supplemental data (Tables 7–9, which are published as supporting information on the PNAS web site). Comparison of all three lists identified 11 genes

that were uniquely overexpressed in iAMP21 patients, of which only two, C21orf66 and ATP50, were within the CRA. One of the other overexpressed genes was legumain (*LGMN*). As shown in Fig. 2*B*, *LGMN* expression was significantly elevated in those with iAMP21 when compared to other subtypes of ALL (*t* statistics = 4.38; df = 7; *P* = 0.0012). Using a similar approach, 12 genes outside the CRD were shown to be expressed at significantly lower levels (Table 2).

Unlike the AML report, in which a control cohort of normal karyotype AML patients was used, our report benefited from comparisons with patient groups who had either gained an entire chromosome 21 as part of a high hyperdiploid karyotype or in association with an *ETV6-RUNX1* fusion. By using these subgroups for comparison, it was possible to identify a unique subset of over- and underexpressed genes in patients with iAMP21 relative to those with/without other chromosome 21 aberrations. This finding demonstrated that comparative information on the loss or gain of chromosomal material is essential when interpreting expression data. Curiously, *RUNX1* expression in *ETV6-RUNX1* positive and iAMP21 patients was comparable, which may be due to the inability of the global gene expression profiling platform used in this study to distinguish between wild-type *RUNX1* and *ETV6-RUNX1* fusion transcripts. Additional copies of the *ETV6-RUNX1* fusion and *RUNX1* are common findings in patients with the translocation, t(12;21)(p13;q22) (3), which may contribute to the elevated *RUNX1* expression levels in *ETV6-RUNX1*-positive patients. These observations suggest that there are common processes leading to duplication and translocation, further strengthening the hypothesis that genomic instability of a region on 21q creates a cascade of events leading to or sustaining leukemogenesis.

Although the processes that lead to ALL appear to affect a common genomic region of chromosome 21, there is disparity in the outcome to treatment. HD + 21 and *ETV6-RUNX1* have an excellent survival rate on current chemotherapy protocols, whereas iAMP21 patients have a poor outcome. Recently, two papers have correlated gene expression patterns with *in vitro* chemosensitivity of blast cells and both demonstrated that these patterns were predictive of outcome in childhood ALL (17, 18). Although the expression patterns in our patients did not accurately reflect those associated with poor clinical outcome and chemo-resistance (including Asparaginase), there were a number of similarities including over- (*IGHM*, *CD44*, *IGFBP7*, *RPS9*, and *MAFF*) and underexpression (*TCF4*, *F8A*, and *TAF5*) of a number of genes. Of these, *MAFF* overexpression is known to correlate with steroid resistance and *F8A* down-regulation with insensitivity to asparaginase. We have shown that the gene *LGMN* is overexpressed in ALL samples with iAMP21. *LGMN* is a lysosomal cysteine protease that specifically cleaves after the asparagine residue and participates in antigen processing (19). Cancer cells expressing *LGMN* have been shown to invade extracellular spaces. Overexpression in a number of aggressive cancers correlates with invasiveness, dissemination, and poor outcome (20, 21). We hypothesize that lymphoblasts expressing *LGMN* may enter extravascular spaces. These cells survive because of suboptimal cytotoxic levels, which may lead to subsequent relapse.

We conclude that the CRA on chromosome 21 represents the only detectable recurrent finding in patients with iAMP21. Expression profiling did not show significant overexpression of *RUNX1* in these patients, suggesting that it is unlikely to be the target gene. Overall, the increase of gene expression within the CRA was a result of the genomic copy number gain within this region, suggesting that these genes may be important in leukemogenesis. However, no single causative gene was identified. Outside the CRA, overexpression of *LGMN* was demonstrated. We hypothesize that this gene may contribute to the poor clinical outcome and treatment response observed in iAMP21 patients. In addition to the 6.5–6.6 Mb CRA, there was associated genomic imbalance in patients with iAMP21, in particular deletions affecting the subtelomeric region (CRD) of chromosome 21. These data have pro-

Table 2. Significant differentially expressed genes in patients with iAMP21 ($n = 8$)

Gene	Probe identifier	Gene name	Chromosomal location	UniGene cluster
Up-regulated				
LGMN	201212_at	Legumain	14q32.1	Hs.18069
C1orf54 (FLJ23221)	219506_at	Chromosome 1 open reading frame 54	1q21.2	Hs.91283
STK17B	205214_at	Serine/threonine kinase 17b (apoptosis-inducing)	2q32.3	Hs.88297
BHLHB2	201170_s_at	Basic helix-loop-helix domain containing, Class B, 2	3p26	Hs.171825
ARPC5L	220966_x_at	Actin related protein 2/3 complex, subunit 5-like	9q33.3	Hs.132499
TBCD	211052_s_at	Tubulin-specific chaperone d	17q25.3	Hs.464391
LSM7	204559_s_at	LSM7 homolog, U6 small nuclear RNA associated (*S. cerevisiae*)	19p13.3	Hs.512610
GADD45B	209304_x_at	Growth arrest and DNA-damage-inducible, beta	19p13.3	Hs.110571
C20orf111	209020_at	Chromosome 20 open reading frame 111	20q13.11	Hs.75798
C21orf66	221158_at	Chromosome 21 open reading frame 66	21q21.3	Hs.473635
ATP5O	200818_at	ATP synthase, H+ transporting, mitochondrial F1 complex, O subunit (oligomycin sensitivity conferring protein)	21q22.1-q22	Hs.409140
Down-regulated				
NIPBL	207108_s_at	Nipped-B homolog (*Drosophila*)	5p13.2	Hs.481927
BAT2	208132_x_at	HLA-B associated transcript 2	6p21.3	Hs.436093
CDYL	203100_s_at	Chromodomain protein, Y-like	6p25.1	Hs.269092
GFOD1	219821_s_at	Glucose-fructose-oxidoreductase domain containing 1	6pter-p22.1	Hs.484686
KIAA0265	209256_s_at	KIAA0265 protein	7q32.2	Hs.520710
CAMSAP1	212710_at	Calmodulin regulated spectrin-associated protein 1	9q34.3	Hs.522493
PELI2	219132_at	Pellino homolog 2 (*Drosophila*)	14q21	Hs.105103
KIAA0100	201729_s_at	KIAA0100 gene product	17q11.2	Hs.151761
SS18	216684_s_at	Synovial sarcoma translocation, Chromosome 18	18q11.2	Hs.404263
FEM1B	212367_at	Fem-1 homolog b (C. elegans)	15q22	Hs.362733
RNF146	221430_s_at	Ring finger protein 146	6q22.1-q22.3	Hs.267120
MBD1	208595_s_at	Methyl-CpG binding domain protein 1	18q21	Hs.405610

vided information that will be used to develop an improved diagnostic test. The expansion of this innovative study may uncover other molecular and cellular mechanisms underlying this clinical phenotype, demonstrating a pivotal role of chromosome 21 instability in the initiation of acute leukemia.

Materials and Methods

Patients. In this study, 14 patients with iAMP21, defined in accordance with published cytogenetic and FISH criteria (1), with DNA and/or RNA available were identified among those registered to the U.K. ALL treatment trials: ALL97/99, MRD PILOT, or ALL2003 for children aged 1–18 years, or UKALLXII for adults aged 15–55 years. Genome and expression studies were applied to these patient samples as indicated in Table 3. Each center obtained informed consent from patients or their parents.

Cytogenetic Analysis. Diagnostic bone marrow and/or peripheral blood samples from all patients in this study were analyzed by standard cytogenetic methods in the U.K. regional cytogenetics laboratories. *RUNX1* copy number was determined by using the LSI TEL/AML1 ES Dual Color Translocation FISH probe (Abbott Diagnostics, Maidenhead, U.K.). This information is provided in Table 3.

BAC aCGH and FISH Confirmation. For 10 patients, genomic copy number variation was assessed by using a commercially available BAC aCGH system (Spectral Genomics, Genosystems). The arrays comprised 2,621 genomic clones positioned at ≈1-Mb intervals throughout the genome. Of these, 26 were located along 21q from position 15.1 Mb (centromeric) to 46.9 Mb (telomeric). The positions of genes and BAC clones were determined by using the National Center for Biotechnology Information (NCBI) Map-Viewer for Homo Sapiens, Build 35, version 1 (www.ncbi.nlm.nih.gov/mapview).

Pooled DNA extracted from peripheral blood of 10 healthy donors, sex matched to the test sample, was used as the reference (Promega) and processed according to the manufacturer's in-

structions. On the basis of control experiments, a normal range of 0.8–1.2 was used for the analysis of patients with iAMP21, a range broader than one calculated on the basis of 2× SD for each clone calculated, in the normal-versus-normal hybridizations. In an attempt to improve sensitivity, fluorescence ratio outside the limit of 2× SD (standard deviation limits, SDL), but within standard cutoff values of between 0.8 and 1.2, were also recorded for comparisons with FISH confirmatory data.

For nine patients, DNA copy number changes detected by aCGH were validated by using FISH probes from the same BAC clones as spotted on the array (Genosystems) (Table 1). Where possible, 200 interphase nuclei per probe were analyzed by two independent analysts, and images were recorded by using MACPROBE software (Applied Imaging, Newcastle, U.K.) (further details of aCGH and FISH analysis are given in *Supporting Text*, which is published as supporting information on the PNAS web site).

Genomic Oligonucleotide Arrays. Five patients (all analyzed with BAC aCGH of the same sample) were analyzed with high-density oligonucleotide-based CGH (Oligo aCGH) arrays (NimbleGen Systems, Madison, WI), designed with probes tiled through chromosome 21. Sequences (NCBI build 35.1) were repeat-masked, and oligonucleotides were selected at a minimal spacing distance of 60 bp from both the forward and reverse strands, resulting in ≈190,000 features along the length of the chromosome. The arrays were synthesized as described (22), and standard labeling, hybridization, and image capture was performed in the NimbleGen Systems Service Laboratory, in a similar manner to that described by Selzer *et al.* (23). Data were extracted from scanned images by using NIMBLESCAN extraction software (NimbleGen Systems), which allows automated grid alignment, extraction, and generation of data files. Segmentation analysis of data sets indicated deletion and amplification breakpoints. Corrections for optical noise, background adjustments, and normalization were performed by using BIOCONDUCTOR as described (24). After a loss correction for probe GC content, the $\log_2$ ratios were averaged in windows ranging from

MEDICAL SCIENCES

500 to 5,000 bp to produce the final segmentations (25). Further details are provided *Supporting Text*.

GeneChip Human Mapping 10K Array. The GeneChip mapping assay protocol (Affymetrix) was used to produce the 10,000 SNP array results for three iAMP21 patients as described (26, 27). The protocol was adapted such that the purification of PCR product was performed by using the Ultrafree-MC filtration column (Millipore, Billerica, MA). Signal intensity data were analyzed by the Gene-Chip DNA analysis software (GDAS), which uses a model algorithm to generate SNP calls. Signal values are normalized across each array to the median value, and copy number ratios and changes in SNP calls between leukemia and germ-line remission bone marrow were annotated by using a program written in visual basic. Noise was reduced by zeroing negative signal values, and using mean signal values in a running window of five SNPs.

Global Expression Profiling. *RNA Extraction and probe preparation.* Global expression profiling was carried out on bone marrow aspirates from eight patients (seven with aCGH results). RNA was extracted with TRIzol (Invitrogen) followed by a second ethanol precipitation, before quality assessment using the Agilent 2100 Bioanalyser (Agilent Technologies, Waldbronn, Germany). Fluorescently labeled cRNA probes were synthesized and hybridized to Affymetrix HG-U133A oligonucleotide arrays according to the manufacturer's instructions. The arrays were scanned on a Gene-Array scanner (Agilent Technologies), and the intensities of the fluorescence signals were captured and analyzed with Affymetrix MAS 5.0 software. No scaling was applied. Further detailed descriptions of the procedure and the raw Affymetrix files are given in *Supporting Text*.

Gene expression analysis. GENESPRING 6.0 (Silicon Genetics, Redwood City, CA) was used for raw data normalization. First, the data were normalized to the median per sample, using all genes not marked absent. Each gene was then divided by the median of its measurements in all samples (i.e., across all arrays). If the median of the raw values was <10, then each measurement for that gene was divided by 10. Signal intensities were log transformed for statistical analysis. Genes called absent in all samples were removed to exclude those with minimal variation across the experiments. Probe sets passing the filter were used to find statistically significant differentially expressed genes between the subgroups studied. Significance Analysis of Microarrays (SAM) was applied to the normalized and log-transformed data. We used default settings and selected the significant genes based on the d-score with a maximum FDR of 5.3%. These were compared with a data set of 89 children with ALL, of whom 21 had an *ETV6-RUNX1* fusion, 23 had high hyperdiploidy comprising at least one additional copy of chromosome 21 (HD + 21) and 45 had no abnormality of chromosome 21. For 80 patients, including one patient with a iAMP21, the gene expression pattern has been reported (12).

Both unsupervised and supervised analyses were used and the results visualized in a two-way hierarchical cluster. Normalized gene expression values were used to obtain the mean and median expression values of genes within the defined amplicon. Significance in the differences of expression between the different subgroups was tested by using a *t* test.

Quantitative RT-PCR. Real-Time quantitative RT-PCR (qRT-PCR) was carried out to assess the expression of genes situated within the amplicon (*SOD1, OLIG2, IFNAR2, IL10RB, ITSN1, CRYZL1, RUNX1, TTC3, ERG* and *ETS2*) for six patients, using the Taqman Gene Expression Assays (Applied Biosystems) according to the manufacturer's instructions. Appropriate positive and negative control RNA samples were tested in parallel. The comparative C_t method was used for quantitation of relative gene expression. The average C_t value of the endogenous control gene, *GAPDH*, was subtracted from the average experimental gene C_t value to give the ΔC_t value. Differences between control and test were carried out by using $\Delta\Delta C_t$. Concordance between the qRT-PCR and global expression profile was demonstrated after calculation of the correlation coefficients between the level of expression as quantified by both qRT-PCR and Affymetrix expression arrays.

1. Harewood, L., Robinson, H., Harris, R., Al-Obaidi, M. J., Jalali, G. R., Martineau, M., Moorman, A. V., Sumption, N., Richards, S., Mitchell, C. & Harrison, C. J. (2003) *Leukemia* **17,** 547–553.
2. Robinson, H. M., Broadfield, Z. J., Cheung, K. L., Harewood, L., Harris, R. L., Jalali, G. R., Martineau, M., Moorman, A. V., Taylor, K. E., Richards, S., *et al.* (2003) *Leukemia* **17,** 2249–2250.
3. Harrison, C. J., Moorman, A. V., Barber, K. E., Broadfield, Z. J., Cheung, K. L., Harris, R. L., Jalali, G. R., Robinson, H. M., Strefford, J. C., Stewart, A., *et al.* (2005) *Br. J. Haematol.* **129,** 520–530.
4. Martinez-Ramirez, A., Urioste, M., Melchor, L., Blesa, D., Valle, L., de Andres, S. A., Kok, K., Calasanz, M. J., Cigudosa, J. C. & Benitez, J. (2005) *Genes Chromosomes Cancer* **42,** 287–298.
5. Baldus, C. D., Liyanarachchi, S., Mrozek, K., Auer, H., Tanner, S. M., Guimond, M., Ruppert, A. S., Mohamed, N., Davuluri, R. V., Caligiuri, M. A., *et al.* (2004) *Proc. Natl. Acad. Sci. USA* **101,** 3915–3920.
6. Mrozek, K., Heinonen, K., Theil, K. S. & Bloomfield, C. D. (2002) *Genes Chromosomes Cancer* **34,** 137–153.
7. Hilgenfeld, E., Padilla-Nash, H., McNeil, N., Knutsen, T., Montagna, C., Tchinda, J., Horst, J., Ludwig, W. D., Serve, H., Buchner, T., *et al.* (2001) *Br. J. Haematol.* **113,** 305–317.
8. Andersen, M. K., Christiansen, D. H. & Pedersen-Bjergaard, J. (2005) *Leukemia* **19,** 197–200.
9. Andersen, M. K., Christiansen, D. H. & Pedersen-Bjergaard, J. (2005) *Genes Chromosomes Cancer* **42,** 358–371.
10. Yeoh, E. J., Ross, M. E., Shurtleff, S. A., Williams, W. K., Patel, D., Mahfouz, R., Behm, F. G., Raimondi, S. C., Relling, M. V., Patel, A., *et al.* (2002) *Cancer cell* **1,** 133–143.
11. Mao, R., Zielke, C. L., Zielke, H. R. & Pevsner, J. (2003) *Genomics* **81,** 457–467.
12. van Delft, F. W., Bellotti, T., Luo, Z., Jones, L. K., Patel, N., Yiannikouris, O., Hill, A. S., Hubank, M., Kempski, H., Fletcher, D., *et al.* (2005) *Br. J. Haematol.* **130,** 26–35.
13. Hyman, E., Kauraniemi, P., Hautaniemi, S., Wolf, M., Mousses, S., Rozenblum, E., Ringner, M., Sauter, G., Monni, O., Elkahloun, A., *et al.* (2002) *Cancer Res.* **62,** 6240–6245.
14. Masayesva, B. G., Ha, P., Garrett-Mayer, E., Pilkington, T., Mao, R., Pevsner, J., Speed, T., Benoit, N., Moon, C. S., Sidransky, D., *et al.* (2004) *Proc. Natl. Acad. Sci. USA* **101,** 8715–8720.
15. Raghavan, M., Lillington, D. M., Skoulakis, S., Debernardi, S., Chaplin, T., Foot, N. J., Lister, T. A. & Young, B. D. (2005) *Cancer Res.* **65,** 375–378.
16. Lugthart, S., Cheok, M. H., den Boer, M. L., Yang, W., Holleman, A., Cheng, C., Pui, C. H., Relling, M. V., Janka-Schaub, G. E., Pieters, R. & Evans, W. E. (2005) *Cancer Cell* **7,** 375–386.
17. Holleman, A., Cheok, M. H., den Boer, M. L., Yang, W., Veerman, A. J., Kazemier, K. M., Pei, D., Cheng, C., Pui, C. H., Relling, M. V., *et al.* (2004) *N. Engl. J. Med.* **351,** 533–542.
18. Manoury, B., Hewitt, E. W., Morrice, N., Dando, P. M., Barrett, A. J. & Watts, C. (1998) *Nature* **396,** 695–699.
19. Panosyan, E. H., Seibel, N. L., Martin-Aragon, S., Gaynon, P. S., Avramis, I. A., Sather, H., Franklin, J., Nachman, J., Ettinger, L. J., La, M., *et al.* (2004) *J. Pediatr. Hematol. Oncol.* **26,** 217–226.
20. Murthy, R. V., Arbman, G., Gao, J., Roodman, G. D. & Sun, X. F. (2005) *Clin. Cancer Res.* **11,** 2293–2299.
21. Liu, C., Sun, C., Huang, H., Janda, K. & Edgington, T. (2003) *Cancer Res.* **63,** 2957–2964.
22. Singh-Gasson, S., Green, R. D., Yue, Y., Nelson, C., Blattner, F., Sussman, M. R. & Cerrina, F. (1999) *Nat. Biotechnol.* **17,** 974–978.
23. Selzer, R. R., Richmond, T. A., Pofahl, N. J., Green, R. D., Eis, P. S., Nair, P., Brothman, A. R. & Stallings, R. L. (2005) *Genes Chromosomes Cancer* **44,** 305–319.
24. Gentleman, R. C., Carey, V. J., Bates, D. M., Bolstad, B., Dettling, M., Dudoit, S., Ellis, B., Gautier, L., Ge, Y., Gentry, J., *et al.* (2004) *Genome Biol.* **5,** R80.
25. Olshen, A. B., Venkatraman, E. S., Lucito, R. & Wigler, M. (2004) *Biostatistics* **5,** 557–572.
26. Matsuzaki, H., Loi, H., Dong, S., Tsai, Y. Y., Fang, J., Law, J., Di, X., Liu, W. M., Yang, G., Liu, G., *et al.* (2004) *Genome Res.* **14,** 414–425.
27. Kennedy, G. C., Matsuzaki, H., Dong, S., Liu, W. M., Huang, J., Liu, G., Su, X., Cao, M., Chen, W., Zhang, J., *et al.* (2003) *Nat. Biotechnol.* **21,** 1233–1237.

Intrachromosomal Amplification of Chromosome 21 (iAMP21) May Arise from a Breakage–Fusion–Bridge Cycle

Hazel M. Robinson,[1] **Christine J. Harrison,**[1]* **Anthony V. Moorman,**[1] **Ilse Chudoba,**[2] **and Jonathan C. Strefford**[1]

[1]Leukaemia Research Cytogenetics Group, Cancer Sciences Division, University of Southampton, Southampton, UK
[2]MetaSystems, Altlussheim, Germany

Intrachromosomal amplification of chromosome 21 (iAMP21), involving amplification of the *RUNX1* gene and duplication of chromosome 21, dup(21q), defines a new cytogenetic subgroup in B-lineage acute lymphoblastic leukemia (ALL) with a poor prognosis. Characterization of this abnormality has become vital to ensure that the most accurate detection method is used. We have previously defined common regions of amplification and deletion of chromosome 21 in these patients, although the level and extent of amplification within the amplicon was highly variable. This study, using interphase fluorescence in situ hybridization (FISH) with chromosome 21 locus specific probes, substantiated these findings in a large series of patients and confirmed that the amplicon always included *RUNX1*. Thus, FISH with probes directed to the *RUNX1* gene remains the most reliable detection method. Metaphase FISH, supported by G- and multiple color chromosomal banding (mBAND) revealed the patient specific morphology and genetic profile of the dup(21q) chromosomes, as well as the complexity of the intrachromosomal changes giving rise to them. These findings suggested that iAMP21 had arisen from a breakage–fusion–bridge cycle: a mechanism previously described in tumors, which we report for the first time in ALL.   © 2007 Wiley-Liss, Inc.

INTRODUCTION

Acquired chromosomal abnormalities are important disease-specific markers in hematological malignancies. They have contributed significantly toward the understanding of the mechanisms leading to leukemogenesis. Probably, the most important feature is the independent prognostic significance attributed to a number of them, which form the basis of risk stratification for treatment. Chromosome 21 is often gained in acute myeloid leukemia (AML) (United Kingdom Cancer Cytogenetics Group, 1992) and acute lymphoblastic leukemia (ALL), in which it is the hallmark of the good-risk high hyperdiploid group (Moorman et al., 2003). One gene, *RUNX1* (*AML1*) at 21q22, is frequently involved in chromosomal rearrangements of different, lineage-specific subtypes of leukemia. For example, the translocation, t(8;21)(q22;q22), gives rise to the *RUNX1-RUNX1T1* fusion in AML of favorable risk; t(12;21)(p13;q22) results in the *RUNX1-ETV6* fusion in childhood ALL; while t(3;21)(q26;q22) produces the *RUNX1-MDS1* fusion in myelodysplastic syndrome (MDS) and the blastic phase of chronic myeloid leukemia (Miyoshi et al., 1991; Nucifora and Rowley, 1995; Romana et al., 1995).

In addition to rearrangements of the gene, amplification involving *RUNX1* has been reported in both myeloid and lymphoid leukemia. Although rarely described in AML and MDS (Hilgenfeld et al., 2001; Andersen et al., 2005), there are a number of reports in ALL (Niini et al., 2000; Busson-Le Coniat et al., 2001; Dal Cin et al., 2001; Mikhail et al., 2002; Morel et al., 2002; Penther et al., 2002; Harewood et al., 2003; Robinson et al., 2003; Soulier et al., 2003), from which it has been defined as a rare cytogenetic subgroup (Robinson et al., 2003; Soulier et al., 2003). In these ALL studies, additional copies of the *RUNX1* gene were found while screening for the presence of the *ETV6-RUNX1* fusion by fluorescence in situ hybridization (FISH) (Harrison et al., 2005). Although negative for the fusion, multiple copies of *RUNX1* were found to be arranged in a ladder-like fashion on a single duplicated chromosome 21, dup(21q) (Harewood et al., 2003). The size and morphology of the

dup(21q) was highly variable between patients (Harewood et al., 2003); therefore, it could not be reliably classified by cytogenetics alone. Array-based comparative genomic hybridization (aCGH) defined a common region of amplification (CRA) (genomic position, 33.2–39.8 Mb) and deletion (CRD) (genomic position, 43.7–47 Mb, including subtelomeric sequences) on chromosome 21 (Strefford et al., 2006). This study also demonstrated that, although the CRA always contained *RUNX1*, the amplicon showed considerable variation in extent and level of amplification between patients, as observed in earlier FISH investigations (Le Coniat et al., 1995; Busson-Le Coniat et al., 2001). Thus, the abnormality was renamed to more accurately reflect these features, as intrachromosomal amplification of chromosome 21 (iAMP21) (Strefford et al., 2006). It occurs at an incidence of approximately 2% in childhood ALL, with a higher frequency in older children (Harewood et al., 2003; Soulier et al., 2003). All patients have a common/precursor-B immunophenotype, generally with a low presenting WBC count and, most significantly, an adverse outcome (Robinson et al., 2003; Moorman et al., 2006). In view of these findings, it has been recommended in the United Kingdom that childhood patients are treated as high-risk on current protocols. Thus, characterization of this abnormality has become vital to ensure that the most accurate detection method is applied.

Our recent studies have contributed toward an improved definition. In addition to depicting the genomic features, we have described the gene expression profiles. In eight iAMP21 patients, *RUNX1* was not differentially over expressed when compared to other ALL patients in the cohort described by Van Delft et al. (2005). No putative genes were highlighted within the CRA that might be driving leukemia pathogenesis in these patients (Strefford et al., 2006). Although point mutations in the Runt domain coding exons of *RUNX1* have been detected in AML and MDS (Osato et al., 1999; Roumier et al., 2003; Cameron and Neil, 2004; Mikhail et al., 2006), sequence analysis did not detect such mutations in iAMP21 patients (Busson-Le Coniat et al., 2001; Penther et al., 2002). Therefore, whether *RUNX1*, or any other gene within the CRA, is the target of this chromosomal subgroup has yet to be established.

To increase further our understanding of this abnormality, a combinatorial approach based upon the original aCGH study, using FISH, conventional cytogenetics, and multiple color chromosomal banding (mBAND), has been performed in a large group of iAMP21 patients. Comparison of amplicon size, level of amplification, FISH signal distribution in metaphase, and chromosomal morphology have revealed unexpected findings, pointing to a potentially distinct mechanism giving rise to the formation of iAMP21.

MATERIALS AND METHODS

Patients

A total of 46 ALL patients with iAMP21 entered to one of the United Kingdom treatment trials (ALL97 or ALL2003 for children aged 1–18 years and UKALLXII for adults aged 15–55 years) were included in this study. All patients with metaphases were identified as iAMP21 by FISH and conventional cytogenetics, according to our previous description: patients with three or more extra copies of *RUNX1* on a single abnormal chromosome 21 (Harewood et al., 2003). Patients with no metaphases available were classified according to the definition: within interphase cells, *RUNX1* signals were present as a group, gathered closely together in a cluster, characteristic of amplification on a single chromosome; while a single signal, assumed to represent the normal chromosome 21, was usually located apart.

Cytogenetics

Conventional cytogenetic analysis was undertaken by the United Kingdom regional cytogenetics laboratories on diagnostic bone marrow and/or peripheral blood samples. Chromosomal abnormalities were further characterized by FISH where possible. Karyotypes of the iAMP21 patients were reviewed by the Leukemia Research Cytogenetic Group (Harrison et al., 2001) and described according to the International System of Human Cytogenetic Nomenclature (ISCN, 2005). The abnormal chromosome 21 was classified according to morphology (Harewood et al., 2003).

FISH

FISH was performed on the same fixed cell suspensions as used for cytogenetic analysis. Initial FISH screening, to identify iAMP21 patients, was carried out using the LSI® TEL/AML1 ES Dual Color Translocation probe (Abbott Diagnostics, United Kingdom). *RUNX1* copy number was determined from the number of signals in 200 interphase cells.
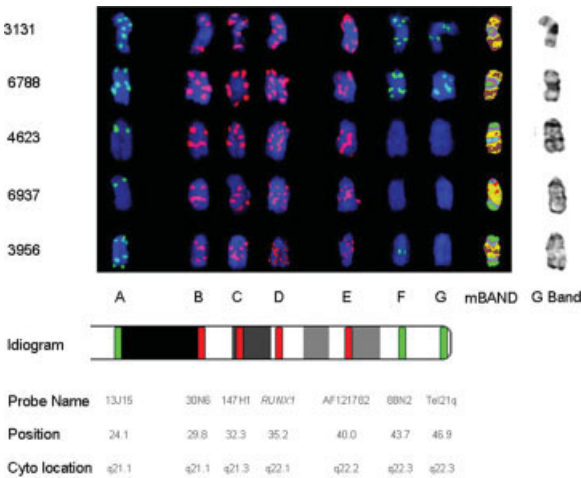
Figure 1. Metaphase FISH, G- and mBAND of five cases of iAMP21. The chromosomal band locations and genomic positions of the seven locus-specific probes, A–G, are shown in the chromosome 21 idiogram. The red and green boxes indicate the labeling of the probes with Spectrum Red and Spectrum Green, repectively. Metaphase FISH results of the seven probes, mBAND and G-banding of dup(21q) (columns) from five patients (3131, 6788, 4623, 6937, and 3956) (rows). In patient 6937, the mBAND classifier assigned the centromeric region brown and the telomeric region green; the opposite of the other four patients. The variable number, size, and intensity of signals are shown. The relative positions of the signals can be deduced by comparison between columns and the differences between patients by comparison of rows. [Color figure can be viewed in the online issue, which is available at www.interscience.wiley.com.]

Further FISH analysis was performed using five chromosome 21 locus-specific probes generated from the same BAC clones as found on the aCGH BAC array (Genosystems, France), as described previously (Strefford et al., 2006), together with a 21q subtelomeric probe (Tel21q) (QBiogene, United Kingdom). The genomic positions of the BAC clones were determined using the National Center for Biotechnology Information (NCBI) MapViewer for Homo Sapiens, Build 35, version 1 (www.ncbi.nlm.nih.gov/mapview). They were selected to represent those regions flanking the CRA, which had been previously shown to be either gained or lost by aCGH (Strefford et al., 2006). These probes, including *RUNX1*, were denoted A to G (A: RP11-13J15; B: RP11-30N6; C: RP11-147H1; D: *RUNX1*; E: AF121782; F: RP11-88N2; G: Tel21q). Their genomic positions and chromosomal localization are provided in Figure 1. Dual probe, dual color experiments were carried out, with the same probe combinations used in all patients. These probes were labeled with either Spectrum Green or Spectrum Red (Abbott Diagnostics), as indicated in Figure 1, and hybridized according to standard methodologies. The copy number for each probe was determined by scoring 100 abnormal interphase cells. The clustering of signals in interphase resulted in their close apposi-

tion, often making accurate enumeration difficult. If a variation in copy number was observed between cells of the same patient, it was recorded as a range. Our previous study (Harewood et al., 2003) identified that the additional signals were usually present on the dup(21q), thus it was assumed that five or more clustered signals (gain of three or more) seen in interphase represented amplification on dup(21q), while three or four signals (gain of one or two) represented a gain or a high level gain, respectively. The close association of the signals in interphase differentiated this abnormality from gain of signals resulting from multiple copies of chromosome 21 as seen, for example, in high hyperdiploidy. The presence of a single signal indicated a deletion.

In samples with available metaphases, the numbers and positions of signals from each probe were mapped to dup(21q) in relation to each other. A peptide nucleic acid (PNA) probe, which hybridizes to the telomeric TTAGGG repeats (Telomere PNA FISH Kit/CY3, Dako Cytomation, Denmark), was used to demonstrate the presence of a telomere on dup(21q). Although it did not identify the chromosomal origin of the telomeric sequences, it hybridized distal to Tel21q. Whole chromosome paint (wcp) 21 (QBiogene) was applied sequentially to metaphases hybridized with the latter two probes to confirm their location to dup(21q). These sequential studies were carried out on five patients (3131, 3956, 4623, 6937, and 6788). The same five patients were studied further with a chromosome 21 mBAND paint (Xcyte 21, MetaSystems, Germany) using different classifiers, as previously described (Chudoba et al., 2004).

RESULTS

Conventional Cytogenetics

Karyotypes of the 37 patients with a successful cytogenetic result are provided in Table 1. In six patients, dup(21q) was the sole chromosomal change. The chromosome number ranged from 45 to 47, with subpopulations of two patients having 48 and 51 chromosomes. Conventional and molecular cytogenetic analysis showed no established chromosomal abnormalities, previously defined as characteristic of certain diagnostic/prognostic subgroups. Apart from the gain of an X chromosome in seven patients, the other associated abnormalities were nonrecurrent. The dup(21q) were classified according to their morphology, as previously described (Harewood et al., 2003): large metacentric (LM), large acrocentric (LA), ring (R), small acrocentric (SA), submetacentric (SM), and normal (N) chromo-

TABLE 1. Karyotypes of 35 iAMP21 Patients

Patient no.	Morphology of dup(21q)	Karyotype
3,131[a]	LM	46,XY,t(1;16)(q23;p13),ider(21)(q10)dup(21)(q?)[3]/51,idem,+X,+3,+10,+14,+21 [3]
5,754[a]	LM	46,XY,ider(21)(q10)dup(21)(q?)[6]
5,898[b,c]	LM	47,XY,+X,del(16)(q13),i(17)(q10),ider(21)(q10)dup(21)(q?)[3]/47,idem,add(7)(p1?)[3]
6,020[c]	LM	46,XY,del(7)(q22q36),ider(21)(q10)dup(21)(q?)[cp3]
6,788[c]	LM	46,XY,add(13)(q?),ider(21)(q10)dup(21)(q?)[2]/48,idem,+8,+14[5]
6,957[c]	LM	46,XX,ider(21)(q10)dup(21)(q?)[13]
7,045	LM	47,XX,+X,del(9)(p?),−10,del(11)(q13),ider(21)(q10)dup(21)(q?),+mar[cp11]
7,829	LM	48,XY,+X,inv(1)(p13q?32),ider(21)(q10)dup(21)(q?),+mar[11]
3,956[a]	LA	45,XY,dic(8;16)(p1?;p1?),del(13)(q1?4),dup(21)(q?)[6]/46,idem,der(Y)t(Y;13)(q1?;q1?4), +dic(8;16)(p1?;p1?),del(13)(q1?4)[2]
4,134[a]	LA	46,XY,dup(21)(q?)[13]
4,178[a]	LA	46,XX,del(7)(q22),t(14;22)(q32;q11),dup(21)(q?)[10]
4,623[a]	LA	46,XX,dup(21)(q?)[11]
6,008	LA	46,XY,t(2;8)(p12;q24),del(9)(p2?1),del(13)(q1?),dup(21)(q?)[9]
6,937	LA	46,XX,dup(21)(q?)[10]
7,219[c]	LA	46,XY,dup(21)(q?),inc[3]
7,255[c]	LA	45,XX,−21,+mar1,inc[2]
8,743	LA	46,XX,t(7;9;17)(q22;p1?;p1?),del(11)(q23q2?5),dup(21)(?)[7]
2,776[a]	R	47,XX,+X,der(21)r(21)(q?)dup(21)(q?)[3]
3,743[a]	R	45,XX,add(8)(p?),−11,der(15)t(11;15)(?;q24),der(21)r(21)(q?)dup(21)(q?)[2]
3,970[a]	R	47,XX,add(7)(q2),+10,der(21)r(21)(q?)dup(21)(q?)[7]/47,idem,del(12)(p13)[4]
4,405[a]	R	45,Y,t(X;15)(q2?1;q2?4),dic(12;17)(p1?;p1?),der(21)r(21)(q?)dup(21)(q?)[4]
4,444[a]	R	46,XY,der(21)r(21)(q?)dup(21)(q?)[3]
5,607[a]	R	46,XY,t(8;11)(p1?;q21),del(11)(q2?1),der(21)r(21)(q?)dup(21)(q?)[8]
5,674[b]	R	47,XY,+X,dup(21)(q?)[7]
5,809	R	45,XY,add(1)(p36),−2,add(4)(q35),−7,del(12)(p12),del(16)(q2?), −19,der(21)r(21)(q?)dup(21)(q?),+4mar,inc[cp6]
7,583	R	47,XY,+X,der(21)r(21)(q?)dup(21)(q?)[4]
7,650	R	47,XY,+9,der(21)r(21)(q?)dup(21)(q?)
3,527[a]	SA	45,XX,−7,del(12)(p12),dup(21)(q?)[5]
4,780[b]	SA	45,XY,−11,del(12)(p1?2),der(20)t(11;20)(q?;q?),dup(21)(q?)[21]
7,45[a]	SM	46,XY,dup(21)(q?)[4]/46,idem,del(5)(q?),der(15)t(5;15)(q?;q?)[3]
4,135[a]	SM	46,XX,t(12;16)(q24;p11),del(15)(q24q26),t(17;20)(p1?3;q11),dup(21)(q?)[6]
4,237[a]	SM	46,XX,dup(21)(q?)[3]/46,idem,del(16)(q1?)[7]
4,279[a,c]	SM	46–47,XY,dup(21)(q?),inc[12]
5,655[b]	SM	46,XX,del(1)(q4?),del(6)(q1?5),del(7)(q2?2q3?1),dup(21)(q?)[3]/46,idem,add(6)(q2?)[12]
6,868	SM	47,XY,+X,−5,−9,add(20)(q),+21,dup(21)(q?),+mar,inc[7]
4,316	N	46,XX[24]
7,828	N	46,XY[20]

LM, large metacentric; LA, large acrocentric; R, ring; SA, small acrocentric; SM, sub-metacentric; N, normal. The normal population has been omitted from the abnormal karyotypes.
[a]Previously reported in Harewood et al. (2003).
[b]Previously reported in Robinson et al. (2003).
[c]Previously reported in Strefford et al. (2006).

somes, as indicated in Tables 1 and 2. Apart from Case 5898, which showed variation from cell to cell, the morphology of the dup(21q) was consistent in all metaphases from the same patient.

Interphase FISH

Interphase FISH results from the 46 iAMP21 patients are shown in Table 2. Results from two or more probes were available for all patients. The number of signals for each probe varied between patients. In all cases the amplicon included the *RUNX1* gene (probe D), for which the copy num-

ber ranged from 4 to 14 signals. The extent of the amplified region was variable, resulting in a unique pattern of imbalance for each patient. On the basis of our aCGH study (Strefford et al., 2006), if amplification of two consecutively positioned probes was observed, it was assumed that the area between them was also amplified. In the majority of patients, the amplicon extended proximally and distally, to include probes C and E, spanning a region of ≥10 Mb. In one patient (6788), the entire length of 21q, including probes A to G, was amplified, while in five patients (3131, 7255, 5607, 5655,

TABLE 2. Interphase FISH Results of the 46 iAMP21 Patients (Rows)

Patients	Morphology of dup(21)	A	B	C	D (RUNX1)	E	F	G
3,131	LM	4–6	3–4	6–7	4–7	4–5	5	3–4
5,754	LM	3	5–8	4–7	4–7	4–6	5–8	1
5,898	LM	3	3–6	3–6	4–6	3–5	1	1
6,020	LM	3	4–5	5–6	5–7	3–5	1	1
6,788	LM	4–5	3–5	4–5	3–5	4–6	4–5	3–5
6,957	LM	3–5	4–5	4–6	4–9	4–6	4–6	1
7,045	LM	4–6	4–8	5–8	5–8	4–8	4–8	1
7,829	LM	FAIL	6–7	FAIL	6–9	6–9	1	1
3,956	LA	5	5–8	5–8	6–10	6–8	5–7	1
4,134	LA	5–8	3–7	4–6	4–7	3–4	3	1
4,178	LA	4–5	6–7	6–8	6–8	7–8	1	1
4,623	LA	2	4	5–9	5–6	6–9	1	1
6,008	LA	5	5	4–6	5–10	5–8	1	1
6,937	LA	2	4–5	7–8	7–10	7–9	1	1
7,255	LA	5–7	3–4	4–14	5–11	5–8	3	2
8,743	LA	3–5	4–6	3–5	3–5	4–5	4–5	1
7,219	LA	5–7	5–7	5–7	5–9	4–5	1	1
2,776	R	3	3	3	4–6	6–8	5–8	1
3,743	R	2	2	4–5	4–7	4–5	5	3
3,970	R	FAIL	3–4	FAIL	4–5	6–7	1	1
4,405	R	4–8	6–10	6–10	5–8	5–8	1	1
4,444	R	4–6	4–6	4–6	4–7	6–8	5–8	1
5,607	R	5–7	2–3	5–7	4–6	FAIL	4–7	FAIL
5,674	R	1	4–6	FAIL	6–8	5–8	1	1
5,809	R	3	4	5–8	6–8	5–7	1	1
7,583	R	3	3	4–5	4–6	4	4–5	1
7,650	R	4–5	5	6–8	5–9	5–7	1	1
3,527	SA	3	3–4	4–5	4–5	3	2	2
4,780	SA	2	4	4–5	5	2–3	2	2
3,745	SM	5–8	4–5	6–8	6–8	5	5–7	1
4,135	SM	5–6	5–7	5–7	6–9	6–7	4–5	1
4,237	SM	5–6	5–7	5–8	4–9	5–8	5–7	1
4,279	SM	3–4	4–5	4–7	4–9	3–5	1	1
5,655	SM	5	3	1	4–7	4–5	1	1
6,868	SM	FAIL	5–6	FAIL	5–6	FAIL	5–6	FAIL
4,316	N	FAIL	3	FAIL	3–5	4–5	3	3
7,828	N	4–6	5–8	7–9	3–9	5–8	1	1
5,858	F	3–4	5–7	5–7	4–8	6–7	4	4
6,092	F	4–6	3–4	4–8	5–8	3–7	2	2
6,111	F	FAIL	FAIL	FAIL	4–11	FAIL	FAIL	1
6,996	F	5–9	FAIL	8–10	8–14	8–9	1	1
7,024	F	3–4	1	4–5	4–8	6–9	1	1
7,093	F	4	5–7	5–7	6–8	5–7	1	1
7,100	F	3	3–4	4–5	3–7	3	3	2
7,732	F	3	3–5	FAIL	4–7	5–7	4–6	1
8,767	F	3	4–6	4–6	4–7	5–7	1	1

Key to colour codes	Deletion= 1 signal	Normal= 2 signals	Gain= 3 signals	High-level gain= 4 signals	Amplification= 5 or more signals	Fail

Results for each patient are given in rows. The chromosomal morphology of the dup(21q) is indicated in column 2: LM, large metacentric; LA, large acrocentric; R, ring; SA, small acrocentric; SM, small metacentric; N, normal; F, failed cytogenetics. The results are grouped according to the morphology of the dup(21 q). The boxes relate to the results from individual probe hybridizations for each patient (columns A–G). The number inside the boxes indicates the copy number for each probe; FAIL, FISH failed to produce a result. [Color table can be viewed in the online issue, which is available at www.interscience.wiley.com.]

and 6092), the level of amplification was variable within the amplicon. In two patients (6996 and 5858), interphase FISH showed two clusters of signals, with a single signal apart, indicating that, in addition to the normal chromosome 21, two copies of dup(21q) were present. Unfortunately, no metaphases were available to confirm these findings.

Deletions of probe G, covering the subtelomeric region, were observed in 34/44 (77%) patients. In 20 (59%) of them, the deletion extended proximally to include probe F, defining a deleted region of up to ~3.5 Mb. Probe G was gained in six patients (3131, 6788, 3743, 4316, 5858, and 5809) and showed a normal copy number in five (7255, 3527, 4780, 6092, and 7100). In three patients (5674, 5655, and 7024), deletions were observed at sites proximal to *RUNX1*.

Comparison of dup(21q) and Amplicon Size

Comparison of the dup(21q) morphology with the FISH data (Table 2) provided the opportunity to determine the relationship between the level and extent of amplification and the size and form of the abnormal chromosome. The two patients (3527 and 4780) with the smallest dup(21q) chromosomes were the only ones to have SA morphology. They had the smallest amplified regions, covering probes C and D only, with the lowest level of gain indicated by three additional signals. They showed no deletion of the subtelomeric region by FISH. In the remaining 33 cases, dup(21q) was larger, which corresponded to an increased amplicon size by FISH. However, the different patterns of imbalance did not correlate with a particular morphological type. In view of the level and extent of the amplified regions in the two cases with normal chromosomes 21 and the lack of abnormal metaphases seen by FISH, it is likely that the abnormal population was nondividing.

Metaphase FISH Analysis

In five cases (3131, 6788, 4623, 6937, and 3956), metaphase FISH was successful with the seven locus-specific probes. The signals were located to the normal and dup(21q) chromosome, as shown in Figure 1. There was a high level of heterogeneity in number, size, and intensity of signals between probes on the dup(21q) chromosomes, with considerable variation between patients. Signals frequently appeared larger and brighter, suggesting amplification of the regions spanned by the probes. Most significantly, signals were often in unex-
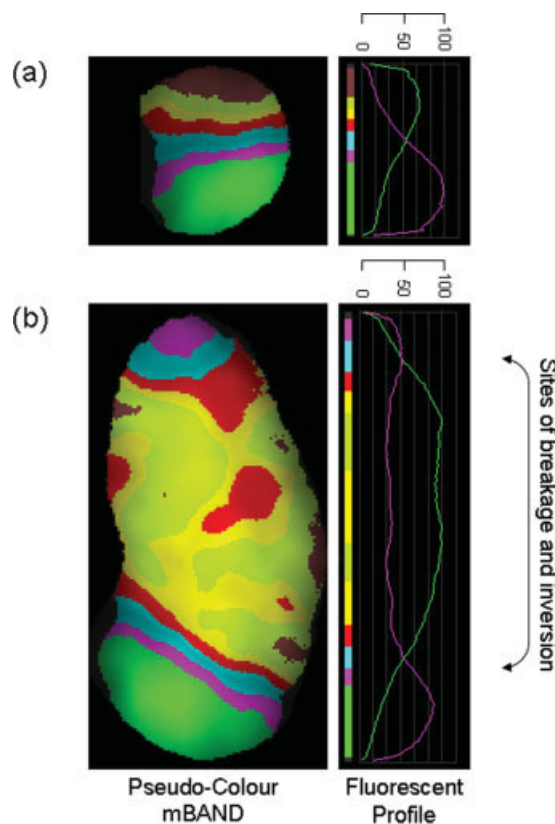

Figure 2.   High resolution mBAND image of a normal chromosome 21 (a) compared to the dup(21q) from patient 6937 (b). The duplicated and inverted regions are clearly shown. [Color figure can be viewed in the online issue, which is available at www.interscience.wiley.com.]

pected locations in relation to each other, indicating that a series of complex intrachromosomal rearrangements had occurred. For example, patient 3131 showed four signals for probe A and two for probe B. The orientation of these probes relative to each other provided evidence of an inversion in each arm. The multiple signals of probes C, D, and E were distributed in a ladder-like fashion along dup(21q), consistent with a high level of chromosomal breakage within these regions. The subtelomeric signals (probe G) were located to the center of each chromosome arm. As the signals for probe F appeared to be located distal to the subtelomeric ones, this provided additional evidence of an inversion. In Case 6788, the signals were distributed unevenly between the two arms. Patients 4623 and 6937 showed loss of signals for probes F and G, while 3956 showed loss of the probe G signal only, indicating variability in the extent of the subtelomeric deletion. Signals from the probe localized to the highly amplified region (D) were distributed along the length of the dup(21q), indicating multiple breaks and inversions. The mBAND and G-

banding images confirmed the complexity of the rearrangements giving rise to dup(21q), as well as the variability between patients, even when classified into the same morphological group (LM, patients 3131 and 6788; LA, patients 4623, 6937, and 3956). Figure 2 shows a higher resolution mBAND image from patient 6937, which indicates the duplicated and inverted segments in comparison to the normal chromosome 21. Although the origin of the telomere was unknown, pantelomeric probes indicated the presence of telomeric sequences on the dup(21q) chromosomes of three patients with loss of their subtelomeres (3956, 4623, and 6937).

DISCUSSION

This study reports detailed analysis of a large group of ALL patients with iAMP21 by FISH and conventional cytogenetics, from which a clearer understanding of the mechanisms giving rise to the dup(21q) have emerged. This approach provided conclusive evidence that the abnormality is highly complex, with each patient having a unique dup(21q) genomic profile. This was further supported by the range of morphological forms observed at the chromosomal level. It demonstrated that the amplicon was usually large, with considerable variability in the level of amplification, both within the amplicon and between patients. FISH confirmed that the highly amplified region of 21q always included the *RUNX1* gene, which corresponded to the CRA indicated in our previous study. In 77% of patients, an accompanying deletion of variable size around the subtelomeric region was present, corresponding to the previously identified CRD (Strefford et al., 2006).

The distribution of signals from the individual locus-specific probes observed in metaphase indicated that the dup(21q) was formed as a result of multiple breaks and reunions, leading to complex intrachromosomal rearrangements, including deletions, duplications, inversions, and amplifications. The complexity of the rearrangements was highlighted by the variable mBAND and G-banding patterns. There was some evidence from interphase FISH that the dup(21q) chromosome may be duplicated in some patients, but it was not possible to confirm this in metaphase.

From solid tumor studies, there is increasing evidence that gene amplification may arise from a breakage–fusion–bridge (BFB) cycle. This mechanism, first described by McClintock (1941), proposed that, following an initiating event, a double-stranded DNA break (DSB) occurs (Fig. 3a),
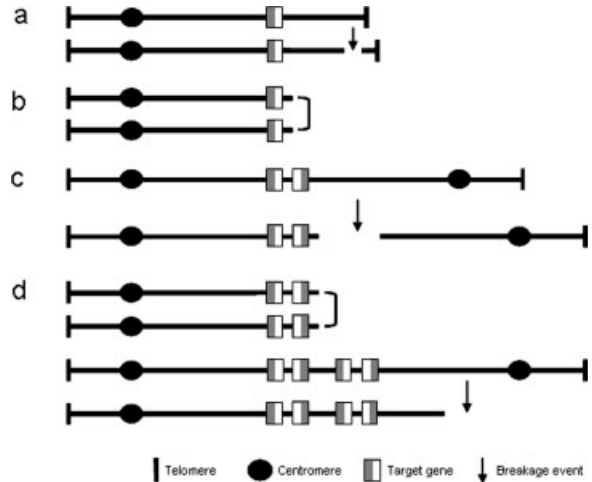

Figure 3. Diagrammatic representation of BFB cycle. (a) DSB occurs, leading to loss of the telomere; (b) Two broken sister chromatids form a dicentric chromosome; (c) Breakage leads to a chromosome with an inverted repeat; (d) Multiple BFB cycles produce a series of inverted repeats.

resulting in the formation of a chromosome with two broken sister chromatids (Fig. 3b). Subsequent to replication, the chromatids fuse to form a dicentric chromosome (Fig. 3c). Mitotic segregation of the centromeres to opposite poles at anaphase results in breakage at a site close to the original one, leading to generation of a chromosome with an inverted repeat (Fig. 3c). Following multiple cycles of BFB it is possible to produce a chromosome with accumulated additional copies of intrachromosomal regions organized as inverted repeats (palindromic amplification) (Fig. 3d). It is likely that the dup(21q), with the characteristic ladder-like distribution of *RUNX1* signals, has arisen through a BFB mechanism. As the size of the CRA is relatively large, it is probable that other regions are coamplified along with *RUNX1*, supported by the spatial distribution of signals.

Loss of a telomere has been proposed as an initiating event of the BFB cycle (Gisselsson et al., 2001; Lo et al., 2002; Murnane and Sabatier, 2004; Sabatier et al., 2005). In this study, we have shown deletion of the subtelomeric region in the majority of cases, indicative of telomeric disruption. These deletions were always located adjacent to the amplicon. This observation is consistent with the loss of chromosomal material from the region close to the point of chromosomal breakage, followed by amplification of sequences centromeric to the breakpoint. In those cases with no subtelomeric loss, it is possible that a deletion may have occurred within the region distal to that covered by the subtelomeric probe. In one patient (6788),

amplification of the subtelomeric region was observed, consistent with breakage in the adjacent distally located region, in a manner similar to that reported for mouse embryonic stem cells (Lo et al., 2002). Further support comes from the dup(21q) of patient (3131), in whom the subtelomeric signal was found in an unexpected location, indicating that a break must have occurred within a region distal to this probe. In five patients with no subtelomeric deletion and three with gain of probe G, it was not possible to confirm the location of these signals in metaphase. Thus, it cannot be ruled out that an additional copy(ies) of a chromosome 21 intact telomeric region was present, as observed in two patients (3131 and 3745) with subpopulations including an extra copy of chromosome 21 seen by conventional cytogenetics.

Although loss or dysfunction of the telomeric region may prove to be the initiating event, the complexity of the dup(21q) indicated that breakage must also have occurred in other regions of the chromosome. Previous studies have indicated that amplification of genes may result from breakage within locations in close proximity to fragile sites (Ciullo et al., 2002). Although there are no reports of fragile sites located to chromosome 21, Hattori et al. (2000) reported duplicated sequences on chromosome 21, which may be susceptible to DSB (Kolomietz et al., 2002).

The BFB cycle usually ends when the unstable chromosome acquires a new telomere. Acquisition of a new telomere may result from a number of mechanisms including: nonreciprocal translocations, breakage induced replication, direct addition by telomerase, the formation of a dicentric or ring chromosome (Murnane and Sabatier, 2004). Thus, the loss of one telomere may directly affect the stability of the whole genome (Hattori et al., 2000; Ciullo et al., 2002; Gisselsson, 2005; Sabatier et al., 2005). It is likely that the more efficient the cell is at telomere acquisition the less complex the karyotype and the lower the level of amplification. It was of note that the level of amplification in the iAMP21 patients was relatively low (5–14 copies), raising the possibility that stabilization of this abnormality occurs early, thus inhibiting high level amplification.

Firm evidence to support this hypothesis of a BFB cycle giving rise to iAMP21 would be convincingly supported by the observation of anaphase bridges in bone marrow smears or biopsies. Although no such material was available for these patients, it is unlikely that bridges would have been seen because, apart from a single case, all dup(21q) chromosomes were identical between cells of the same

patient. This implicates that the cycle may have terminated and the chromosome become stable by the time the diagnostic sample had been taken.

In this study, we have used a FISH approach in an attempt to define further the mechanism giving rise to iAMP21. A high level of chromosomal instability and subsequent karyotype complexity of the dup(21q) chromosome has indicated that it has arisen from a BFB cycle. The initiating event giving rise to this mechanism remains, as yet, unresolved. This study has confirmed that *RUNX1* is always located within the amplicon. Therefore, FISH with probes directed to the *RUNX1* gene remains the most reliable detection method for this high-risk abnormality: iAMP21.

ACKNOWLEDGMENTS

REFERENCES

Andersen MK, Christiansen DH, Pedersen-Bjergaard J. 2005. Amplification or duplication of chromosome band 21q22 with multiple copies of the AML1 gene and mutation of the TP53 gene in therapy-related MDS and AML. Leukemia 19:197–200.

Busson-Le Coniat M, Nguyen KF, Daniel MT, Bernard OA, Berger R. 2001. Chromosome 21 abnormalities with AML1 amplification in acute lymphoblastic leukemia. Genes Chromosomes Cancer 32:244–249.

Cameron ER, Neil JC. 2004. The Runx genes: Lineage-specific oncogenes and tumor suppressors. Oncogene 23:4308–4314.

Chudoba I, Hickmann G, Friedrich T, Jauch A, Kozlowski P, Senger G. 2004. mBAND: A high resolution multicolor banding technique for the detection of complex intrachromosomal aberrations. Cytogenet Genome Res 104:390–393.

Ciullo M, Debily MA, Rozier L, Autiero M, Billault A, Mayau V, El Marhomy S, Guardiola J, Bernheim A, Coullin P, Piatie-Tonneau D, Debatisse M. 2002. Initiation of the breakage-fusion-bridge mechanism through common fragile site activation in human breast cancer cells: The model of PIP gene duplication from a break at FRA7I. Hum Mol Genet 11:2887–2894.

Dal Cin P, Atkins L, Ford C, Ariyanayagam S, Armstrong SA, George R, Cleary A, Morton CC. 2001. Amplification of AML1 in childhood acute lymphoblastic leukemias. Genes Chromosomes Cancer 30:407–409.

Gisselsson D. 2005. Mitotic instability in cancer: Is there method in the madness? Cell Cycle 4:1007–1010.

Gisselsson D, Jonson T, Petersen A, Strombeck B, Dal Cin P, Hoglund M, Mitelman F, Mertens F, Mandahl N. 2001. Telomere dysfunction triggers extensive DNA fragmentation and evolution of complex chromosome abnormalities in human malignant tumors. Proc Natl Acad Sci USA 98:12683–12688.

Harewood L, Robinson H, Harris R, Al Obaidi MJ, Jalali GR, Martineau M, Moorman AV, Sumption N, Richards S, Mitchell C, Harrison CJ. 2003. Amplification of AML1 on a duplicated chromosome 21 in acute lymphoblastic leukemia: A study of 20 cases. Leukemia 17:547–553.

Harrison CJ, Martineau M, Secker-Walker LM. 2001. The Leukaemia Research Fund/United Kingdom Cancer Cytogenetics Group Karyotype Database in acute lymphoblastic leukaemia: A valuable resource for patient management. Br J Haematol 113:3–10.

Harrison CJ, Moorman AV, Barber KE, Broadfield ZJ, Cheung KL, Harris RL, Jalali GR, Robinson HM, Strefford JC, Stewart A, Wright S, Griffiths M, Ross FM, Harewood L, Martineau M. 2005. Interphase molecular cytogenetic screening for chromosomal abnormalities of prognostic significance in childhood acute lymphoblastic leukaemia: A UK Cancer Cytogenetics Group Study. Br J Haematol 129:520–530.

Hattori M, Fujiyama A, Taylor TD, Watanabe H, Yada T, Park HS, Toyoda A, Ishii K, Totoki Y, Choi DK, Groner Y, Soeda E, Ohki M, Takagi T, Sakaki Y, Taudien S, Blechschmidt K, Polley A, Menzel U, Delabar J, Kumpf K, Lehmann R, Patterson D, Reichwald K, Rump A, Schillhabel M, Schudy A, Zimmermann W, Rosenthal A, Kudoh J, Schibuya K, Kawasaki K, Asakawa S, Shintani A, Sasaki T, Nagamine K, Mitsuyama S, Antonarakis SE, Minoshima S, Shimizu N, Nordsiek G, Hornischer K, Brant P, Scharfe M, Schon O, Desario A, Reichelt J, Kauer G, Blocker H, Ramser J, Beck A, Klages S, Hennig S, Riesselmann L, Dagand E, Haaf T, Wehrmeyer S, Borzym K, Gardiner K, Nizetic D, Francis F, Lehrach H, Reinhardt R, Yaspo ML. 2000. The DNA sequence of human chromosome 21. Nature 405:311–319.

Hilgenfeld E, Padilla-Nash H, McNeil N, Knutsen T, Montagna C, Tchinda J, Horst J, Ludwig WD, Serve H, Buchner T, Berdel WE, Schrock E, Ried T. 2001. Spectral karyotyping and fluorescence in situ hybridization detect novel chromosomal aberrations, a recurring involvement of chromosome 21 and amplification of the MYC oncogene in acute myeloid leukaemia M2. Br J Haematol 113:305–317.

ISCN. 2005. An International System for Human Cytogenetic Nomenclature. Basel, Switzerland: Karger, pp. 1–130.

Kolomietz E, Meyn MS, Pandita A, Squire JA. 2002. The role of Alu repeat clusters as mediators of recurrent chromosomal aberrations in tumors. Genes Chromosomes Cancer 35:97–112.

Le Coniat M, Romana SP, Berger R. 1995. Partial chromosome 21 amplification in a child with acute lymphoblastic leukemia. Genes Chromosomes Cancer 14:204–209.

Lo AW, Sprung CN, Fouladi B, Pedram M, Sabatier L, Ricoul M, Reynolds GE, Murnane JP. 2002. Chromosome instability as a result of double-strand breaks near telomeres in mouse embryonic stem cells. Mol Cell Biol 22:4836–4850.

McClintock B. 1941. The stability of broken ends of chromosomes in Zea mays. Genetics 41:234–282.

Mikhail FM, Serry KA, Hatem N, Mourad ZI, Farawela HM, El Kaffash DM, Coignet L, Nucifora G. 2002. AML1 gene overexpression in childhood acute lymphoblastic leukemia. Leukemia 16:658–668.

Mikhail FM, Sinha KK, Saunthararajah Y, Nucifora G. 2006. Normal and transforming functions of RUNX1: A perspective. J Cell Physiol 207:582–593.

Miyoshi H, Shimizu K, Kozu T, Maseki N, Kaneko Y, Ohki M. 1991. t(8;21) breakpoints on chromosome 21 in acute myeloid leukemia are clustered within a limited region of a single gene, AML1. Proc Natl Acad Sci USA 88:10431–10434.

Moorman AV, Richards SM, Martineau M, Cheung KL, Robinson HM, Jalali GR, Broadfield ZJ, Harris RL, Taylor KE, Gibson BE, Hann IM, Hill FG, Kinsey SE, Eden TO, Mitchell CD, Harrison CJ. 2003. Outcome heterogeneity in childhood high-hyperdiploid acute lymphoblastic leukemia. Blood 102:2756–2762.

Moorman AV, Richards SM, Robinson HM, Strefford JC, Gibson BE, Kinsey SE, Eden OB, Vora AJ, Mitchell CD, Harrison CJ. Prognosis of children with acute lymphoblastic leukaemia (ALL)

and intra-chromosomal amplification of chromosome 21 (iAMP21). DOI: 10.1182/BLOOD-2006-08-040436 (online advance publication).

Morel F, Herry A, Le Bris M-J, Douet-Guilbert N, Le Calvez G, Marion V, Berthou C, De Braekeeler M. 2002. AML1 amplification in a case of childhood acute lymphoblastic leukemia. Cancer Genet Cytogenet 137:142–145.

Murnane JP, Sabatier L. 2004. Chromosome rearrangements resulting from telomere dysfunction and their role in cancer. Bioessays 26:1164–1174.

Niini T, Kanerva J, Vettenranta K, Saarinen-Pihkala UM, Knuutila S. 2000. AML1 gene amplification: A novel finding in childhood acute lymphoblastic leukemia. Haematologica 85:362–366.

Nucifora G, Rowley JD. 1995. AML1 and the 8;21 and 3;21 translocations in acute and chronic myeloid leukemia. Blood 86:1–14.

Osato M, Asou N, Abdalla E, Hoshino K, Yamasaki H, Okubo T, Suzushima H, Takatsuki K, Kanno T, Shigesada K, Ito Y. 1999. Biallelic and heterozygous point mutations in the runt domain of the AML1/PEBP2αB gene associated with myeloblastic leukemias. Blood 93:1817–1824.

Penther D, Preudhomme C, Talmant P, Roumier C, Godon A, Mechinaud F, Milpied N, Bataille R, Avet-Loiseau H. 2002. Amplification of AML1 gene is present in childhood acute lymphoblastic leukemia but not in adult, and is not associated with AML1 gene mutation. Leukemia 16:1131–1134.

Robinson HM, Broadfield ZJ, Cheung KL, Harewood L, Harris RL, Jalali GR, Martineau M, Moorman AV, Taylor KE, Richards S, Mitchell C, Harrison CJ. 2003. Amplification of AML1 in acute lymphoblastic leukemia is associated with a poor outcome. Leukemia 17:2249–2250.

Romana SP, Poirel H, Leconiat M, Flexor MA, Mauchauffe M, Jonveaux P, Berger R, Bernard OA. 1995. High frequency of t(12;21) in childhood B-lineage acute lymphoblastic leukemia. Blood 86:4263–4269.

Roumier C, Fenaux P, Lafage M, Imbert M, Eclache V, Preudhomme C. 2003. New mechanisms of AML1 gene alteration in hematological malignancies. Leukemia 17:9–16.

Sabatier L, Ricoul M, Pottier G, Murnane JP. 2005. The loss of a single telomere can result in instability of multiple chromosomes in a human tumor cell line. Mol Cancer Res 3:139–150.

Soulier J, Trakhtenbrot L, Najfeld V, Lipton JM, Mathew S, Avet-Loiseau H, De Braekeleer M, Salem S, Baruchel A, Raimondi SC, Raynaud SD. 2003. Amplification of band q22 of chromosome 21, including AML1, in older children with acute lymphoblastic leukemia: An emerging molecular cytogenetic subgroup. Leukemia 17:1679–1682.

Strefford JC, Van Delft FW, Robinson HM, Worley H, Yiannikouris O, Selzer R, Richmond T, Hann I, Bellotti T, Raghavan M, Young BD, Saha V, Harrison CJ. 2006. Complex genomic alterations and gene expression in acute lymphoblastic leukemia with intrachromosomal amplification of chromosome 21. Proc Natl Acad Sci USA 103:8167–8172.

United Kingdom Cancer Cytogenetics Group. 1992. Primary, single, autosomal trisomies associated with haematological disorders. United Kingdom Cancer Cytogenetics Group (UKCCG). Leuk Res 16:841–851.

Van Delft FW, Bellotti T, Luo Z, Jones LK, Patel N, Yiannikouris O, Hill AS, Hubank M, Kempski H, Fletcher D, Chaplin T, Foot N, Young BD, Hann IM, Gammerman A, Saha V. 2005. Prospective gene expression analysis accurately subtypes acute leukaemia in children and establishes a commonality between hyperdiploidy and t(12;21) in acute lymphoblastic leukaemia. Br J Haematol 130:26–35.